Movement-Related Pathogenesis of Rotator Cuff Disease in Persons with Shoulder Pain: Effects of Decreased Scapulothoracic Upward Rotation

A Dissertation
SUBMITTED TO THE FACULTY OF THE
UNIVERSITY OF MINESOTA
BY

Rebekah Lynne Lawrence

IN PARTIAL FULFILLMENT OF THE REQUIREMENTS
FOR THE DEGREE OF
DOCTOR OF PHILOSOPHY

Advisor: Paula M. Ludewig, PT, PhD

May 2018

Acknowledgements

I would like to express sincere gratitude to my mentor, Paula Ludewig, for the abundant opportunities, guidance, patience, and compassion she has provided throughout this journey. The example you set as a researcher, educator, and person will forever challenge me to improve so that I may help others as you have me. Thank you especially for helping me understand what it means to be fully alive.

Thank you to my committee (Jon Braman, Ward Glasoe, Andrew Hansen, Dan Keefe, Kristin Zhao) for sharing your time and expertise to help me craft this project into what I hope will become impactful work. I would like to particularly thank Dr. Keefe for his generosity, wisdom, and allowing me to become part of his impressive team.

The past six years have blessed me with the opportunity to work with and learn from a truly remarkable group of individuals including Rich Adamczak, Conrad Lindquist, Arin Ellingson, Dawn Lowe, Cathy Carson, and Denis Clohisy, among countless others. I'd would especially like to thank Justin Staker who has been an invaluable source of friendship and laughs. You are a rare combination of vision, talent, and character and I look forward to seeing how you use it to transform our profession.

I would not be on this journey had it not been for the friendship and mentorship of Kevin Farrell and other members of the St. Ambrose University Physical Therapy faculty. Anything I contribute to our profession will be a reflection of your dedication.

Thank you to the participants of this study and the radiology technologists who assisted in data collection. This thesis could not have been completed without their time and dedication.

Finally, I would like to acknowledge the sources of funding that made this work possible: National Institutes of Health (F31-HD087069, L30-HD089226, T32-AR050938), Foundation for Physical Therapy, University of Minnesota Department of Orthopaedic Surgery, University of Minnesota Clinical and Translational Science Institute, and Minnesota Partnership for Biotechnology and Medical Genomics.

"Isn't it astonishing that all these secrets have been preserved for so many years just so we could discover them!" – Orville Wright

"The light shines in the darkness, and the darkness has not overcome it." – John 1:5

Dedication

To my family
For the endless love and support
and for teaching me the joy found in working hard on work worth doing.

In Memoriam

Sally K. Ride
1951-2012
No spark shines brighter or lasts longer
than one that inspires a child to dream.
She was mine.

Abstract

Background: Shoulder pain is a common musculoskeletal complaint that is often associated with rotator cuff injury and abnormal scapular movement. In particular, decreased scapulothoracic upward rotation has been theorized to increase an individual's risk for subacromial rotator cuff compression. However, the effect of abnormal shoulder motion on mechanisms of rotator cuff injury remains unclear. Further, the ability to accurately and non-invasively quantify shoulder complex kinematics is limited.

Objectives: The objectives of this thesis are: 1) Develop and validate a protocol for using single-plane fluoroscopy and 2D/3D shape-matching to quantify shoulder complex kinematics; 2) Determine the impact of decreased scapulothoracic upward rotation on subacromial proximities; and 3) Identify the kinematic mechanisms by which sternoclavicular and acromioclavicular motion contributes to scapulothoracic upward rotation.

Methods: A protocol for using single-plane fluoroscopy and 2D/3D shape-matching to quantify shoulder complex kinematics was validated using radiostereometric analysis in four cadaveric specimens. Shoulder complex kinematics were quantified in 60 participants with and without shoulder pain during scapular plane abduction using the validated protocol. Subject-specific 3D bone models reconstructed from MR images were animated with each participant's glenohumeral kinematics. Subacromial proximities were calculated between the coracoacromial arch and rotator cuff insertion. The effect of decreased scapulothoracic upward rotation on subacromial proximities was assessed. The relative contribution of sternoclavicular and acromioclavicular motion to scapulothoracic upward rotation was calculated using two derived coupling functions.

Results: Single-plane fluoroscopy and 2D/3D shape-matching can accurately quantify static shoulder complex kinematics. Subacromial proximities were generally smallest below 90° humerothoracic elevation. The normalized minimum distance for participants in the low scapulothoracic upward rotation group was significantly smaller (35%) than those in the high scapulothoracic upward rotation group at the minimum position. Scapulothoracic upward rotation can be estimated from acromioclavicular upward rotation, sternoclavicular posterior rotation, and sternoclavicular elevation.

Conclusions: Decreased scapulothoracic upward rotation shifts the range of motion in which normalized minimum distances are smallest to lower angles. Acromioclavicular upward rotation and sternoclavicular posterior rotation are the predominant component motions of scapulothoracic upward rotation.

Table of Contents

List of Tables

List of Figures

List of Abbreviations

AC: acromioclavicular

AT: anterior tilt

BMI: body mass index

CT: computed tomography

DASH: Disabilities of the Arm, Shoulder, and Hand

DR: downward rotation

ER: external rotation

GH: glenohumeral

ICC: intraclass correlation coefficient

IR: internal rotation

ISB: International Society of Biomechanics

MR: magnetic resonance

PT: posterior tilt

RMS: root mean square

RSA: radiostereometric analysis

SAB: scapular plane abduction

SC: sternoclavicular

SEM: standard error of measurement

ST: scapulothoracic

UR: upward rotation

2D: two-dimensional

3D: three-dimensional

Chapter 1: Introduction

The shoulder is a complex structure that is capable of producing a large range of motion in order to accomplish a variety of functional, occupational, and athletic activities. Like all joint systems, the shoulder's anatomical structure not only defines its functional capabilities, but also influences its predisposition to injury. Therefore, a review of shoulder anatomy and biomechanics provides a necessary foundation for the clinical and research questions that are explored in this thesis.

Shoulder Anatomy and Biomechanics

The shoulder consists of three bones (humerus, scapula, and clavicle; **Figure 1**) which, together with the thorax, produce three true joint systems: glenohumeral, sternoclavicular, and acromioclavicular. Although not technically a joint because it lacks articular structure, the scapulothoracic "joint" is also critical to shoulder function.

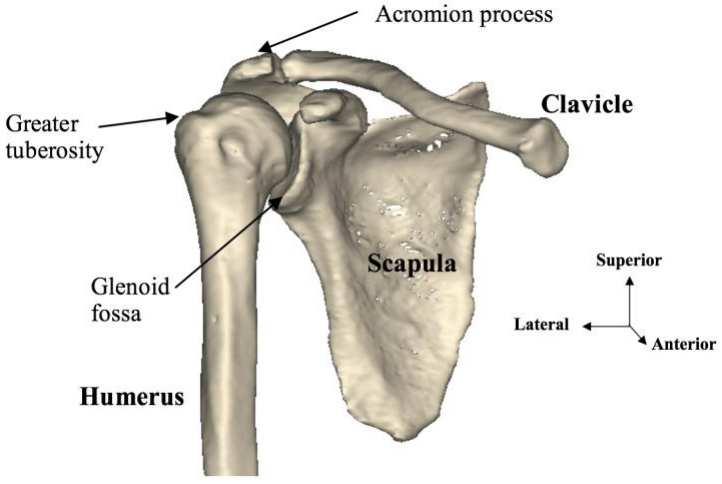

Figure 1: Bony anatomy of the shoulder complex.

Glenohumeral Joint

The glenohumeral joint consists of the humeral head and the glenoid fossa of the scapula (**Figure 1**). Compared to the depth of the glenoid fossa, the size of the humeral head is quite large resulting in substantial range of motion (Ludewig et al., 2009a) but at the cost of structural stability. Glenohumeral joint stability is increased by several inert structures including a cartilaginous labrum that deepens the socket, a fibrous joint capsule, and a network of supporting ligaments. The rotator cuff muscles, however, provide the primary source of joint stability and consist of the supraspinatus (superiorly), subscapularis (anteriorly), and infraspinatus and teres minor (posteriorly) (**Figure 2**). Collectively, the muscles form a "cuff" around the humeral head, produce a compressive force, and help maintain a centered position of the humerus on the glenoid (Inman et al., 1944).

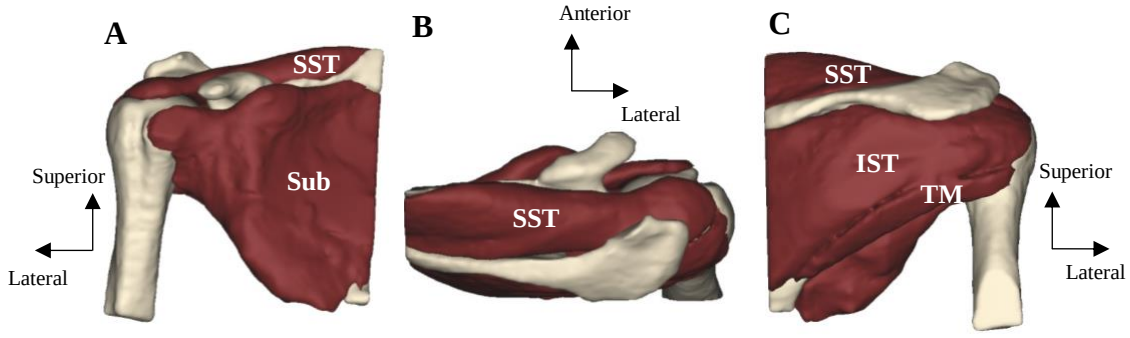

Figure 2: Rotator cuff muscles. **A**) Anterior view; **B**) Superior view; **C**) Posterior view. Abbreviations: SST=supraspinatus, IST=infraspinatus, Sub=subscapularis, TM=teres minor.

The glenohumeral joint is capable of producing substantial motion in six degrees of freedom including the following angular motions: abduction/adduction (i.e. humeral elevation) about an approximately anterior/posterior axis perpendicular to the epicondylar axis, anterior/posterior plane of elevation about the epicondylar axis, and internal/external axial rotation about the humeral long axis (**Figure 3**). During arm raising, the humerus is generally described to elevate and externally rotate relative to the scapula (An et al., 1991; Ludewig et al., 2009a). The amount of glenohumeral plane of elevation depends on the direction of arm motion (Giphart et al., 2013; Ludewig et al., 2009a). The humerus also translates a small amount on the glenoid during functional motion (Giphart et al., 2013; Lawrence et al., 2014b; Ludewig & Cook, 2000).

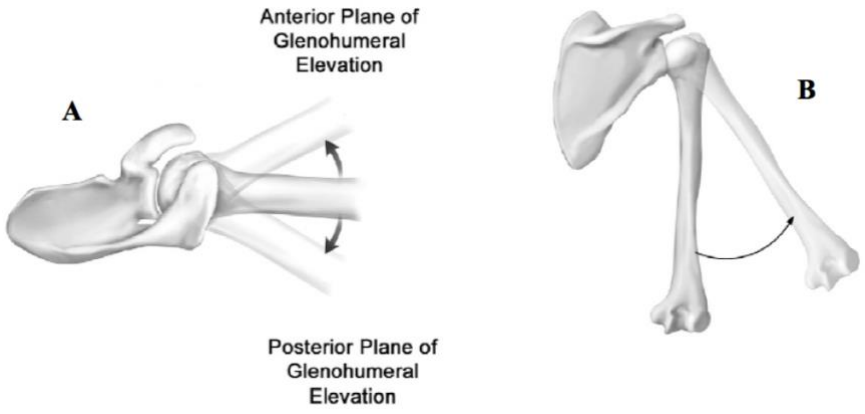

Figure 3: Glenohumeral joint motions. **A**) Anterior/ posterior plane of elevation; **B**) Elevation. Not shown: internal/external axial rotation. Figure adapted from: Ludewig et al. (2009a).

Sternoclavicular Joint

The sternoclavicular joint consists of the medial clavicle and the sternum of the thorax. It is capable of producing motion in six degrees of freedom including the

following angular motions: protraction/retraction about an approximately superior/inferior axis, elevation/depression about an axis perpendicular to the clavicle's long axis, and anterior/posterior rotation about the clavicle's long axis (**Figure 4**). During arm raising, the clavicle is generally described to posteriorly rotate and retract relative to the trunk, with a small amount of elevation (Ludewig et al., 2004; Ludewig et al., 2009a; McClure et al., 2001; Sahara et al., 2007). Importantly, the sternoclavicular joint serves as the only true articulation between the upper extremity and the axial skeleton.

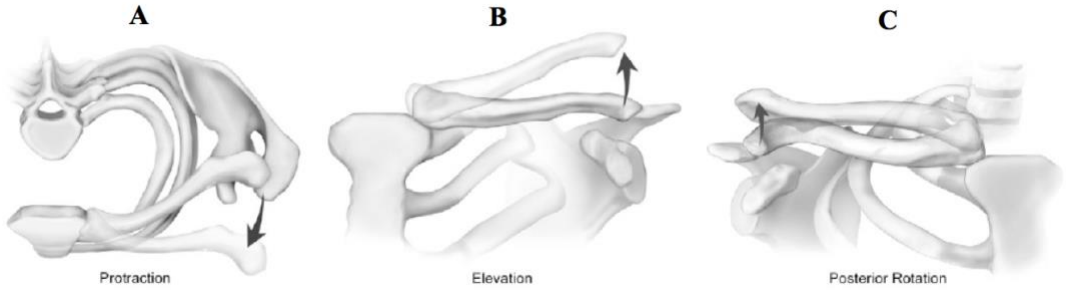

Figure 4: Sternoclavicular joint motions. **A**) Protraction/retraction; **B**) Elevation/ depression; **C**) Posterior/anterior axial rotation. Figure from: Ludewig et al. (2009a).

Acromioclavicular Joint

The acromioclavicular joint consists of the scapular acromion (**Figure 1**) moving relative to the clavicle. The joint plays a crucial role in facilitating glenohumeral motion by orienting the glenoid in the direction of the moving humerus while also creating a "gliding plane" between the scapula and the trunk (Pronk et al., 1993). In order to accomplish this function, the acromioclavicular joint produces the following angular motions: internal/external rotation about an approximately superior/inferior axis, upward/downward rotation about an axis perpendicular to the plane of the scapula, and

anterior/posterior tilt about an approximately medial/lateral axis along the plane of the scapula (**Figure 5**). During arm raising, the acromioclavicular joint is generally described to posteriorly tilt, upwardly rotate, and internally rotate (Ludewig et al., 2009a; Sahara et al., 2007; Teece et al., 2008).

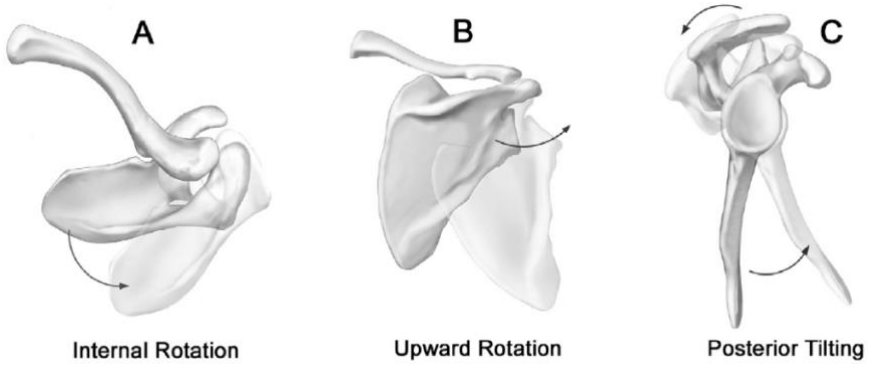

Figure 5: Acromioclavicular and scapulothoracic motions. **A**) Internal/ external rotation; **B**) Upward/downward rotation; **C**) Anterior/ posterior tilt. Figure from: Ludewig et al. (2009a).

The acromioclavicular joint surfaces are not inherently congruent; therefore, the joint is supported by a joint capsule, superior and inferior capsular ligaments, and the coracoclavicular ligaments. The coracoclavicular ligaments (i.e. conoid and trapezoid) extend from the coracoid process of the scapula to the undersurface of the clavicle. Importantly, the coracoclavicular ligaments serve as the only non-contractile link between the upper extremity and the axial skeleton, and facilitate functional shoulder motion by transferring motion between the scapula and clavicle (Dvir & Berme, 1978).

Scapulothoracic "Joint"

The scapulothoracic "joint" is a functional unit describing motion of the scapula relative to the thorax. Because it does not consist of typical joint architecture (e.g. joint capsule, synovial fluid, articular cartilage), it cannot be considered a true joint structure. However, scapulothoracic motion plays several critical roles in shoulder function including orienting the glenoid to promote glenohumeral joint congruency, maintaining muscle length to maximize contractile function, and increasing overall shoulder range of motion (Inman et al., 1944; van der Helm, 1994). Scapulothoracic angular motions include: internal/external rotation about an approximately superior/inferior axis, upward/downward rotation about an axis perpendicular to the plane of the scapula, and anterior/posterior tilt about an approximately medial/lateral axis along the plane of the scapula (**Figure 5**). During arm raising, the scapula generally upwardly rotates and posteriorly tilts relative to the thorax (Ludewig et al., 2009a; McClure et al., 2001). The degree to which the scapula internally/externally rotates during arm elevation is generally small and depends upon the direction (i.e. plane) of movement (Ludewig et al., 2009a; McClure et al., 2001).

Shoulder Complex Coupling

Due to the link-system structure of the shoulder complex, scapulothoracic motion cannot occur in isolation but is the product of sternoclavicular and acromioclavicular joint motion (Dvir et al., 1978; Inman et al., 1944; Teece et al., 2008). This interaction between sternoclavicular, acromioclavicular, and scapulothoracic motion has been termed "coupling" (Teece et al., 2008). Scapulothoracic upward rotation, for example, is believed to be related to sternoclavicular posterior rotation, sternoclavicular elevation,

and acromioclavicular upward rotation (Teece et al., 2008). In particular, the coupled motion between acromioclavicular upward rotation and sternoclavicular posterior rotation serves a critically important function for maximizing scapulothoracic upward rotation and increasing overall shoulder motion (Inman et al., 1944; Ludewig et al., 2009a). However, few studies have quantified sternoclavicular and acromioclavicular joint motion due to methodological challenges associated with tracking 3D clavicular motion with surface-based motion sensors. Therefore, the relationships between clavicular and scapular motion remain unclear thereby limiting our ability to understand the mechanisms by which normal and abnormal scapulothoracic motion is produced. Ultimately, this gap in the literature challenges our ability to observe, diagnose, and treat movement disorders theorized to cause shoulder pain and pathology.

Shoulder Motion and Rotator Cuff Pathology

Rotator cuff pathology is the most common finding on diagnostic imaging in individuals with shoulder pain (Freygant et al., 2014). Even so, the pathogenesis of rotator cuff disease is widely agreed to be complex and multi-factorial (Braman et al., 2014; Michener et al., 2003; Seitz et al., 2011). Repeated compression or deformation of the rotator cuff tendons during shoulder motion has long been theorized as a potential mechanism for rotator cuff injury (Neer, 1983; Walch et al., 1992) and is generally described in two forms. Compression of the bursal surface of the rotator cuff against the coracoacromial arch has been termed subacromial rotator cuff compression (or "impingement") (**Figure 6**). Although traditionally believed to occur at higher angles of humeral elevation (Neer, 1983), more recent work has found the highest risk for

subacromial rotator cuff compression occurs below 70° humerothoracic elevation (Bey et al., 2007; Giphart et al., 2012; Lawrence et al., 2017). Internal (or posterior) impingement occurs when the articular surface of the rotator cuff becomes entrapped against the glenoid rim (Walch et al., 1992). Although first identified during the combined abduction/external rotation position common to overhead athletes, more recent work has shown it may occur simply with the arm in overhead positions (Gold et al., 2007; Lawrence et al., 2016).

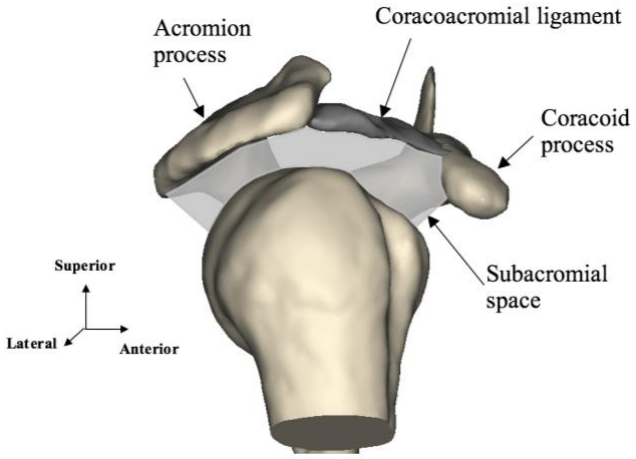

Figure 6: Coracoacromial arch and subacromial space.

Clinical theory often suggests abnormal scapular motion increases an individual's risk for subacromial rotator cuff tendon compression and repeated exposure may lead to subsequent tendon injury (Kibler et al., 2013; Ludewig & Braman, 2011; Ludewig & Reynolds, 2009b; Michener et al., 2003; Seitz et al., 2011). Several studies have found decreased scapulothoracic upward rotation in persons with shoulder pain (Endo et al., 2001; Lawrence et al., 2014a; Ludewig et al., 2000). In particular, Lawrence et al. (2014a) found decreased scapulothoracic upward rotation at humerothoracic elevation

angles lower than 60°. This finding coincides with the range of motion in which subacromial proximities are smallest (Bey et al., 2007; Giphart et al., 2012; Lawrence et al., 2017). Further, since a reduction in scapulothoracic upward rotation is thought to bring the coracoacromial arch into closer proximity with the rotator cuff tendons (**Figure 7**), the lower scapulothoracic upward rotation values found in the symptomatic group may suggest the movement abnormality may be an important mechanism in the movement-based pathogenesis of rotator cuff disease. However, the relationship between decreased scapulothoracic upward rotation and subacromial compression risk remains theoretical, yet addressing abnormal motion is often the focus of rehabilitation (Caldwell et al., 2007; Reinold et al., 2009). As a result, the value of rehabilitation strategies directed at addressing abnormal scapular movement remains unclear leaving clinicians at a significant disadvantage when examining and treating individuals with shoulder pain.

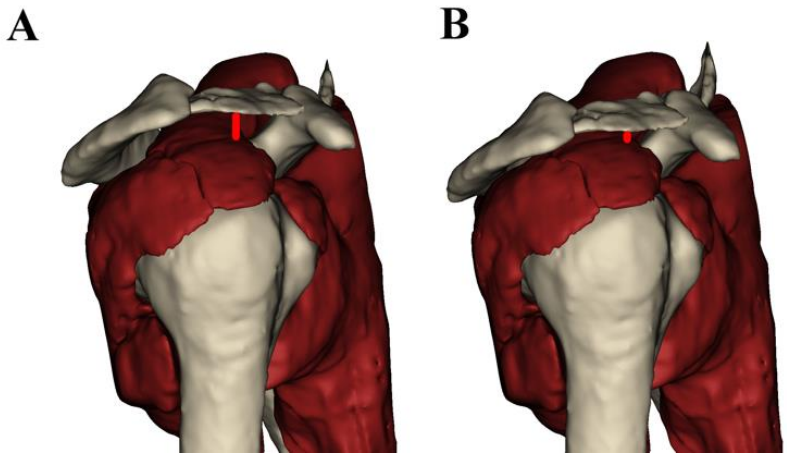

Figure 7: Lateral view of the shoulder showing the potential effect of changing scapulothoracic upward rotation on subacromial space. **A)** Physiologic position; **B)** Decreased scapulothoracic upward rotation. Compared to the length of the red line in A, the shorter line in B illustrates the theorized impact of decreased scapulothoracic upward rotation on subacromial rotator cuff compression.

Challenges to Quantifying Shoulder Complex Kinematics

Subacromial rotator cuff compression risk is often quantified by mapping the proximity between the coracoacromial arch and the rotator cuff insertion sites (i.e. footprints) (Bey et al., 2007; Giphart et al., 2012). Because the distances between these structures are on the order of several millimeters, proximity mapping is highly sensitive to kinematic measurement error associated with conventional methods (e.g. surface-based motion sensors). Further, tracking clavicular kinematics is especially challenging with surface-based sensors due to its shape and primary directions of movement (i.e. posterior axial rotation). Consequently, conventional methods of tracking shoulder complex kinematics prove insufficient to address the underlying clinical and research questions of this thesis.

Recent advancement of kinematic measurement using fluoroscopy and 2D/3D shape-matching has significantly improved non-invasive quantification of glenohumeral joint motion (Bey et al., 2006; Giphart et al., 2012; Zhu et al., 2012). This approach involves collecting joint kinematics using single- or bi-plane fluoroscopy, projecting the image of a 3D bone model onto the 2D imaging plane, and matching the shape of the bone's projection to the fluoroscopic image(s) (You et al., 2001). Once shape-matching is complete, joint kinematics are determined from the position and orientation of the bone model.

The accuracy of 2D/3D shape-matching for quantifying glenohumeral kinematics has been well established using biplane fluoroscopy systems (Bey et al., 2007; Giphart et al., 2012). However, only two studies using single cadaveric shoulder specimens have

reported the accuracy for tracking glenohumeral kinematics using a single fluoroscopic system (Matsuki et al., 2012; Zhu et al., 2012) and both are limited by incomplete description of kinematic errors and only quantifying errors. Further, the use of 2D/3D shape-matching has not been validated for tracking clavicular kinematics. Determining the accuracy of this methodology for quantifying full shoulder complex motion is a critical first step before the technology can be used to address the gap in the literature regarding the impact of decreased scapulothoracic upward rotation on subacromial rotator cuff compression and the kinematic mechanisms by which scapulothoracic upward rotation occurs.

Significance of Research

Musculoskeletal conditions are the leading cause of disability in the United States and account for $950 billion in total costs to society (AHRQ, 1996-2006). The diagnosis of musculoskeletal conditions is often focused on trying to identify the anatomic source of symptoms (i.e. pathoanatomy). However, most physical examination techniques are not sufficiently accurate to identify specific tissue pathologies (Hegedus et al., 2012). Furthermore, the presence of abnormal findings on medical imaging does not necessarily relate to the patient's clinical presentation (Ishimoto et al., 2013) and are often found in asymptomatic individuals (Fukuta et al., 2009; Sher et al., 1995). Randomized clinical trials investigating the effectiveness of rehabilitation interventions prescribed based on pathoanatomic diagnoses typically report average improvements in functional outcomes of only about 50% (Fukuda et al., 2012; Ludewig & Borstad, 2003; Struyf et al., 2013). This suggests focusing the diagnosis of musculoskeletal conditions solely on presumed

pathoanatomic sources of pain may misdirect treatment because it fails to consider the underlying mechanisms from which symptoms develop.

Across all musculoskeletal conditions, shoulder pain is the second most common complaint in the general population (Picavet & Schouten, 2003) and often results in substantial functional loss (Roe et al., 2013). The etiology of shoulder pain is widely agreed to be complex and multi-factorial (Braman et al., 2014; Michener et al., 2003; Seitz et al., 2011), yet the greatest amount of evidence implicates abnormal scapular motion as a potential contributing factor (Endo et al., 2001; Hebert et al., 2002; Lawrence et al., 2014a; Ludewig et al., 2000; Lukasiewicz et al., 1999; McClure et al., 2006; Sousa Cde et al., 2014). As a whole, these studies have identified varying movement abnormalities within the broader patient population. Specifically, the following movement-based subgroups have been identified: decreased scapulothoracic upward rotation (Endo et al., 2001; Lawrence et al., 2014a; Ludewig et al., 2000), increased scapulothoracic upward rotation (McClure et al., 2006; Sousa Cde et al., 2014), decreased scapulothoracic posterior tilt (Ludewig et al., 2000; Lukasiewicz et al., 1999), increased scapulothoracic posterior tilt (McClure et al., 2006; Sousa Cde et al., 2014), and increased glenohumeral translations (Lawrence et al., 2014b). It is expected these subgroups require different treatments to address the abnormal movement(s) associated with the symptoms (Ludewig et al., 2013). However, relatively few studies have investigated the impact of specific movement abnormalities on the development and progression of pain through joint and soft tissue injury. As such, a critical gap exists in the literature linking specific movement impairments to sources of musculoskeletal pain,

which hinders the development of targeted treatments and the refinement of a movement-based diagnostic classification.

This thesis aims to validate the use of single-plane fluoroscopy and 2D/3D shape-matching for quantifying shoulder complex kinematics, identify the impact of decreased scapulothoracic upward rotation on subacromial proximities, and identify the mechanisms by which sternoclavicular and acromioclavicular joint motion contributes to scapulothoracic upward rotation. The contribution of this research will be significant because it can: 1) lead to the development of an accurate and clinically-usefully method of quantifying shoulder kinematics, 2) lead to the development of targeted rehabilitation strategies, and 3) help inform the development of a movement-based diagnostic classification system for patients with shoulder pain.

Aims and Hypotheses

Aim 1: Develop and validate a protocol for using single-plane fluoroscopy and 2D/3D shape-matching to quantify full shoulder complex kinematics.

Hypothesis 1.1: The single-plane fluoroscopy and 2D/3D shape-matching protocol will result in root mean square (RMS) error of less than 3° for rotation about each coordinate axis of the acromioclavicular and glenohumeral joints.

Aim 2: Determine the impact of decreased scapulothoracic upward rotation on subacromial proximities.

Hypothesis 2.1: The difference between groups in the magnitude of the minimum distance and surface area will depend on the angle of humerothoracic elevation.

2.1.a: Compared to the high scapulothoracic upward rotation group, the low scapulothoracic upward rotation group will have significantly decreased minimum distance and significantly increased surface area at rest and 30° humerothoracic elevation.

2.1.b: Compared to the high scapulothoracic upward rotation group, the low scapulothoracic upward rotation group will have significantly increased minimum subacromial distance and significantly decreased surface area at 60° and 90° humerothoracic elevation.

Hypothesis 2.2: The humerothoracic elevation position corresponding to the absolute minimum distance will be significantly lower in the low scapulothoracic upward rotation group compared to the high scapulothoracic upward rotation group.

Hypothesis 2.3: Groups will not differ in the magnitude of the absolute minimum distance.

Hypothesis 2.4: Of the component motions of scapulothoracic upward rotation, acromioclavicular upward rotation will be the strongest predictor of the absolute minimum distance magnitude.

Aim 3: Identify the kinematic mechanisms by which sternoclavicular and acromioclavicular joint motion contributes to scapulothoracic upward rotation

Hypothesis 3.1: Compared to the high scapulothoracic upward rotation group, the low scapulothoracic upward rotation group will be in decreased acromioclavicular upward rotation, sternoclavicular posterior rotation, and sternoclavicular elevation at the same

angles of humerothoracic elevation at which the groups differ in scapulothoracic upward rotation.

Hypothesis 3.2: Acromioclavicular upward rotation and sternoclavicular posterior rotation angular displacement will be the strongest predictors of scapulothoracic upward rotation angular displacement.

Additional Analyses

In addition to the aims and hypotheses stated above, other analyses were also performed to better understand the sources of measurement error associated with the 2D/3D shape-matching validation experiment and the effect of kinematic measurement error on the quantification of subacromial space. The descriptions and results of these additional analyses are provided in the **Appendices**.

Chapter 2: Literature Review

Successfully executing the aims of this thesis requires an understanding of several areas of the literature including proposed mechanisms of rotator cuff pathology, measurement techniques for quantifying 3D shoulder complex kinematics, and descriptions and/or comparisons of shoulder complex kinematics and subacromial proximities in asymptomatic and symptomatic populations. An abundance of studies exists in each of these areas. Therefore, only those considered foundational or of higher methodological quality will be reviewed.

Shoulder Pain and Rotator Cuff Pathology

Shoulder pain is the second most common musculoskeletal complaint with a point prevalence of 21% in the general population (Picavet et al., 2003). Prevalence rates can exceed 50% in persons with disabling conditions such as paraplegia (Pellegrini et al., 2012) and those with high occupational exposure to repetitive activities (Health, 1997). Individuals with shoulder pain often have substantial difficulty performing activities such as reaching, lifting, bathing/dressing, housework, driving, and sport- and work-related tasks (Roe et al., 2013). Randomized controlled trials investigating the efficacy of current standards of practice for treating individuals with shoulder pain typically report average improvements in functional outcomes of only about 50% (Ludewig et al., 2003; Struyf et al., 2013). This suggests a critical need exists to better understand the underlying cause of musculoskeletal pain so that rehabilitation interventions may be more focused in their selection, resulting in improved patient outcomes.

Pathogenesis of Rotator Cuff Pathology

Although numerous theories exist related to the pathogenesis of rotator cuff disease, it is generally agreed that the process is complex and multifactorial. Rotator cuff pathology is believed to follow a progression from early-stage acute tendonitis, to mid-stage tendinosis including partial-thickness tearing, and finally end-stage full-thickness tearing (Neer, 1983). Outside of traumatic injuries, however, the factors that initiate rotator cuff disease remain unclear. In general, the proposed mechanisms of atraumatic rotator cuff pathology can be divided into intrinsic and extrinsic factors (Seitz et al., 2011). Intrinsic mechanisms are defined as those related to the rotator cuff tendons themselves (e.g. tendon properties, vascularity, genetics), while extrinsic mechanisms are defined as factors causing physical deformation of the rotator cuff tendons (e.g. anatomy, biomechanics), which may lead to injury over time.

While there is some evidence for intrinsic mechanisms of rotator cuff pathology (Seitz et al., 2011), the extrinsic mechanisms are often more directly related to orthopaedic medicine and rehabilitation. During shoulder motion the rotator cuff, subacromial bursa, and biceps tendon repeatedly pass in close proximity under the coracoacromial arch and may be susceptible to mechanical compression. This phenomenon has been termed "subacromial impingement". While the concept predated Neer, he refined the clinical phenomenon based on his clinical observations and hypothesized impingement primarily occurred beneath the anterior acromion (Neer, 1972), and that the shape of the acromion was a predisposing factor (Neer, 1983).

Bigliani et al. (1991) expanded on Neer's observations by categorizing the shape of the acromion and theorizing the impact on the subacromial space. From a lateral view,

a Type I acromion is flat and theoretically offers the most clearance for the rotator cuff tendons during motion. A Type II acromion is more curved anteriorly and may result in decreased clearance for the tendons. A Type III acromion is hook shaped, which is believed to reduce the subacromial space the most and cause more severe abrasion of the rotator cuff during contact. Despite the logic of this theory, the association between acromial slope and rotator cuff pathology has been inconsistent in the literature with some studies finding higher rates of pathology in patients with Type III acromions (Balke et al., 2013; Bigliani et al., 1991; Epstein et al., 1993) while other studies found weak or no association (Farley et al., 1994; Pandey et al., 2016).

Based on Neer's observations, techniques to surgically alter the acromial shape have become the standard for the surgical management of shoulder pain over the last 50 years. Indeed, these surgeries (i.e. acromioplasties) are one of the fastest growing surgical interventions in orthopaedic medical practice (Vitale et al., 2010). However, several randomized controlled trials with long-term follow-ups have found outcomes of the procedure are no better than conservative management (Haahr et al., 2005; Ketola et al., 2009) and a recent large randomized controlled trial found no difference in outcomes between acromioplasty and sham surgery (Beard et al., 2017). Together these investigations suggest the shape of the anterior acromion may not be the primary factor driving the development and progression of rotator cuff disease.

In addition to the shape of the acromion, other factors have also been theorized to impact subacromial rotator cuff compression including glenoid inclination, glenoid version, and critical shoulder angle. Glenoid inclination describes the superior/inferior

orientation of the glenoid. Theoretically, an increased glenoid inclination angle may result in a larger superiorly directed force on the humerus during deltoid muscle activity, resulting in increased superior humeral translations and reduced subacromial space (Hughes et al., 2003). This has been supported in cadaveric studies where the force required to produce a given magnitude of superior translation decreased significantly as glenoid inclination angle increased (Wong et al., 2003). However, findings of cross-sectional studies comparing the magnitude of glenoid inclination between individuals with rotator cuff pathology and control subjects have been mixed (Bishop et al., 2009; Hughes et al., 2003; Kandemir et al., 2006). Only two studies investigated the presumed mechanism behind the effect of glenoid inclination and glenohumeral translations *in vivo* and did not find a relationship between inclination angle and the magnitude of glenohumeral translations (Bishop et al., 2009; Peltz et al., 2015). However, it is possible the risk of subacromial compression is more related to the superior/inferior position of the humeral head on the glenoid rather than the magnitude of translation. Nevertheless, these findings suggest the relationship of glenoid inclination on the pathogenesis of shoulder pain is likely complex. For example, it is possible individuals with larger magnitudes of glenoid inclination require more rotator cuff muscle activation to offset the tendency of the humerus to superiorly translate, which may over time lead to tendon degradation and progression to pathology. This would suggest the impact of inclination on the pathogenesis of rotator cuff pathology may be due to an intrinsic mechanism as opposed to the originally hypothesized extrinsic mechanism.

Like inclination, glenoid version describes the orientation of the glenoid but in the anterior/posterior direction. The magnitude of glenoid version is believed to influence the development and progression of rotator cuff pathology by altering the relationship of the humerus within the subacromial space and the mechanical demands on the rotator cuff (Tetreault et al., 2004; Tokgoz et al., 2007). For example, a laterally directed glenoid would theoretically provide the greatest joint stability as any medially directed muscle force would cause joint compression. With an increase in either anteversion or retroversion however, a medially directed muscle force would resolve into medial compressive and anterior or posterior shear forces, depending on the direction of version. Therefore, with increased glenoid version the rotator cuff would need to offset the anterior/posterior shear force similar to its need to offset the superior shear force with inclination. A study by Tétreault (2004) supported this hypothesis by finding the location of the rotator cuff tear was associated with the magnitude and direction of version. Specifically, the mean version was -5° (i.e. retroversion) for patients with an anterior rotator cuff tear involving the supraspinatus and subscapularis, while the mean version was +3° (anteversion) for those with posterior tears of the rotator cuff involving the supraspinatus and infraspinatus. This finding may explain why other studies investigating the relationship between rotator cuff pathology and glenoid version without considering the location of the rotator cuff tear failed to find differences between groups (Dogan et al., 2012; Kandemir et al., 2006).

More recently, the critical shoulder angle has become a focus of study when investigating potential anatomical contributors to rotator cuff disease. The metric is

defined by the angle between vectors representing the superior/inferior orientation of the glenoid and the lateralization of the acromion relative to the inferior margin of the glenoid (Moor et al., 2013). Higher critical shoulder angles have been found in individuals with rotator cuff disease (Moor et al., 2013; Moor et al., 2014; Spiegl et al., 2016), with the relationship potentially explained by both intrinsic and extrinsic mechanisms. Theoretically, a higher critical shoulder angle would result in a larger superiorly directed deltoid force, which may result in subacromial compression if not offset by the inferiorly directed force produced by the subscapularis, infraspinatus, and teres minor. However, if the rotator cuff muscles are able to offset this sheer force, intrinsic degradation of the tendon may occur over time due to the exposure to higher demands. Currently, the extrinsic theory lacks support as one study found no relationship between the magnitude of critical shoulder angle and glenohumeral translations during motion (Peltz et al., 2015). However, like with inclination, the superior/inferior position of the humeral head on the glenoid may be more related to subacromial compression risk than the magnitude of translation.

In general, the inconsistency between studies related to anatomical mechanisms of rotator cuff compression is likely influenced in part by the various methodologies of the studies. In particular, anatomical relationships including acromial slope and glenoid inclination are often measured on 2D radiographic images (Dogan et al., 2012; Hughes et al., 2003; Moor et al., 2013; Moor et al., 2014; Spiegl et al., 2016), which will result in measurement errors due to projection. In addition, measurements in studies utilizing MR or CT images (Tetreault et al., 2004; Tokgoz et al., 2007) are dependent upon the

selection of the image volume slice, which may impact the validity of the measure especially given the complex nature of 3D scapular anatomy. Perhaps more importantly however, the inconsistency between studies suggests the pathogenesis of rotator cuff pathology is multifactorial and only quantifying one potential contributor may not capture the true complexity of the clinical problem. For example, anatomic morphology is an inert and relatively stable factor within an individual over time while biomechanical factors are dynamic and may potentially adjust for reductions in subacromial space caused by anatomy. Therefore, it is likely most valuable to consider anatomical and biomechanical factors in combination when investigating the pathogenesis of rotator cuff disease.

Shoulder Complex Kinematics

Measurement Techniques

Numerous methodologies have been utilized to quantify shoulder complex kinematics including static digitization (Ludewig et al., 1996; Lukasiewicz et al., 1999), radiographs (Endo et al., 2001; Inman et al., 1944; Poppen & Walker, 1976), static MR images (Sahara et al., 2006; Sahara et al., 2007), surface-based electromagnetic sensors (Hebert et al., 2002; Ludewig et al., 2004; Ludewig et al., 2000; McClure et al., 2006; Sousa Cde et al., 2014), bone-fixed electromagnetic sensors (Lawrence et al., 2014a; Lawrence et al., 2014b; Ludewig et al., 2009a; McClure et al., 2001; Teece et al., 2008), biplane radiography (Hallstrom & Karrholm, 2009), and single- (Matsuki et al., 2012) and bi-plane fluoroscopy (Giphart et al., 2013) with 2D/3D shape-matching. Surface-based electromagnetic sensors are the most common method for quantifying dynamic

shoulder kinematics due to their relative ease of use and ability to describe dynamic 3D joint position and orientation. RMS errors for surface-based sensors are generally less than 4°; however, larger errors of 6-11° are described for motion about the long axis of a bone (i.e. scapular internal/external rotation, humeral axial rotation) due to skin motion artifact (Karduna et al., 2001; Ludewig et al., 2002). To prevent such error from confounding description of shoulder motion, several studies have utilized bone-fixed sensors (Lawrence et al., 2014a; Lawrence et al., 2014b; Ludewig et al., 2009a; McClure et al., 2001; Teece et al., 2008). However, the implementation and interpretation of these studies is hindered by the invasive technique and generally small sample sizes.

Recent advances in the quantification of kinematics include the use of fluoroscopy and 2D/3D shape-matching to directly quantify bone motion. The approach utilizes either single- (Matsuki et al., 2012) or bi-plane (Giphart et al., 2013) fluoroscopy systems to collect a series of images representing the 2D projection of the joint's pose during the motion trial. Three-dimensional bone volumes are created from either CT (Bey et al., 2006; Giphart et al., 2012) or MR (Moro-oka et al., 2007; Zhu et al., 2012) scans and 2D renderings of the volumes are then "shape-matched" to the fluoroscopic image by aligning the 3D bones to their 2D projections (You et al., 2001; Zhu et al., 2012). Once matched, clinically-relevant descriptions of joint kinematics can be determined by calculating the relative position and orientation of the bones.

Because 2D/3D shape-matching directly tracks bone motion, the accuracy for quantifying shoulder position and orientation is superior to surface-based methods. Using biplane systems, RMS errors associated with quantifying humeral and scapular position

and orientation are generally <0.5 mm and <1°, respectively (Bey et al., 2006; Giphart et al., 2012; Zhu et al., 2012). Although single-plane systems expose research participants to less overall radiation, they are generally less accurate due to the difficulty matching out-of-plane rotations and translations (You et al., 2001; Zhu et al., 2012). Specifically, maximum in-plane translational bias errors for the humerus and scapula using a single plane system have been reported to be <0.4 mm while maximum out-of-plane bias error was as high as 5.3 mm (Zhu et al., 2012). Further, maximum out-of-plane rotational bias errors were generally <0.6° but could be as high as 2.0° (Zhu et al., 2012). To date, however, no study has described errors associated with tracking clavicular kinematics using either single- or bi-plane fluoroscopy systems, which hinders our ability to explore clinical questions requiring descriptions of full shoulder complex kinematics.

Kinematics in Asymptomatic Individuals

Scapulothoracic kinematics in asymptomatic individuals are well described in the literature (**Table 9**). The magnitudes of scapulothoracic angular positions are highly variable between studies and are influenced by the several factors including methods of data collection, choice of anatomical coordinate systems, and naturally occurring between-subject variability (**Table 9**). The scapula is generally described to upwardly rotate (30-35°) and posteriorly tilt (1-15°) relative to the thorax during humeral elevation to 120° in the scapular plane (Ebaugh et al., 2005; Ludewig et al., 1996; Ludewig et al., 2009a; McClure et al., 2006; McClure et al., 2001). The degree to which the scapula internally or externally rotates relative to the thorax is highly variable between subjects (Lawrence et al., 2014a; Ludewig et al., 1996; Ludewig et al., 2009a; McClure et al.,

2001). From a measurement standpoint, this variability may reflect increased error associated with quantifying rotation about a segment's long axis using surface-based sensors (Karduna et al., 2001). However, it may also be due to differences between individuals in thoracic geometries as the scapula attempts to remain in contact with the thorax. Of the three scapulothoracic angular motions, upward rotation often has the lowest between-subject variability (Ebaugh et al., 2005; Ludewig et al., 2009a; McClure et al., 2006; McClure et al., 2001). This may illustrate the importance of scapular upward rotation to shoulder function and suggests the remaining two motions (anterior/posterior tilt and internal/external rotation) function to maintain contact between the scapula and thorax, and to maximize glenohumeral joint congruency.

Compared to scapulothoracic kinematics, glenohumeral kinematics have been studied less frequently (**Table 10**). As expected, the predominant glenohumeral motion during arm raising is elevation and the magnitude is largely dependent upon the relative magnitudes of humerothoracic elevation and scapulothoracic upward rotation. This concept is termed "scapulohumeral rhythm" and is generally described as an approximately 2:1 ratio of glenohumeral elevation to scapular upward rotation (Inman et al., 1944; Ludewig et al., 2009a). During humeral elevation, the humerus also externally rotates relative to the scapula (5-12°) (An et al., 1991; Giphart et al., 2013; Inman et al., 1944; Ludewig et al., 2009a) which allows the greater tuberosity to clear the acromion and maximum elevation to occur (An et al., 1991; Ludewig et al., 2009a).

Several studies have described sternoclavicular kinematics during humeral elevation (**Table 11**). The clavicle is generally described to retract (8-18°) (Ebaugh et al.,

2005; Lawrence et al., 2014a; Ludewig et al., 2004; Ludewig et al., 2009a; McClure et al., 2006; Sahara et al., 2007; Sousa Cde et al., 2014), elevate (5-13°) (Ebaugh et al., 2005; Lawrence et al., 2014a; Ludewig et al., 2004; Ludewig et al., 2009a; McClure et al., 2006; Sahara et al., 2007; Sousa Cde et al., 2014), and posteriorly rotate (17-22°) (Lawrence et al., 2014a; Ludewig et al., 2004; Ludewig et al., 2009a; Sousa Cde et al., 2014) relative to the thorax during humeral elevation to 120° in the scapular plane. Tracking clavicle motion, and thus quantifying sternoclavicular and acromioclavicular joint motion, proves challenging for several reasons. First, due to its slender, long-bone shape, the clavicle often does not provide an optimal location to place a surface-based motion sensor, which increases the susceptibility for skin motion artifact. Second, the primary motion of the clavicle is about its long axis, which is associated with increased error due to skin motion artifact (Karduna et al., 2001; Ludewig et al., 2002). This is primarily evident in the decreased reliability and increased SEM for sternoclavicular kinematics particularly above 75° humeral elevation (Ludewig et al., 2004). Finally, a third non-collinear point required for constructing orthogonal coordinate systems cannot be found on the clavicle (van der Helm & Pronk, 1995; Wu et al., 2005). Therefore, post-processing of data is required to align the vertical axis of the clavicular coordinate system with that of the thorax (Wu et al., 2005) thereby "zeroing" the anterior/posterior rotation position to a reference position.

Due to these technical challenges, few studies have directly tracked clavicle motion. In 2004, Ludewig et al. (2004) performed a descriptive and reliability study to better understand clavicular motion and determine how reliable surface sensors are in

quantifying the motion. The authors reported the sensor appeared to reasonably follow clavicular motion until 115° humerothoracic elevation and described the resulting sternoclavicular motion as retraction (8°), elevation (9°), and posterior rotation (17°). In general, ICC values were >0.94 and SEM values were less than 2°, suggesting tracking clavicular kinematics with surface-based sensors is reliable within a limited range of motion. Although good reliability statistics are necessary to establish measurement validity, they are not sufficient to conclude the methodology is accurately tracking the underlying bone motion. In particular, the authors reported the values for sternoclavicular posterior rotation values at higher angles of humeral elevation may be underestimated due to the clavicle rotating under the skin.

In response to the challenges of directly tracking clavicular kinematics using surface-based motion sensors, several studies have described sternoclavicular elevation and retraction indirectly by calculating scapular position on the thorax (Ebaugh et al., 2005; Lukasiewicz et al., 1999; McClure et al., 2006; McClure et al., 2001). Lukasiewicz et al. (1999) calculated the superior/inferior location of the scapula as the vertical distance between the C7 spinous process and the centroid of the scapula, and the medial/lateral location of the scapula as the horizontal distance between the C7 spinous process and the centroid of the scapula. These result in crude representations of sternoclavicular elevation/depression and retraction/protraction, respectively, and assume the acromioclavicular joint is a rigid link. This is a considerable assumption that significantly weakens the validity of the results given the magnitude of motion known to occur at the acromioclavicular joint (Ludewig et al., 2009a).

Another approach used to indirectly quantify clavicular kinematics involves tracking the position of the acromioclavicular joint and the sternal notch in 3D space (Ebaugh et al., 2005; McClure et al., 2006; McClure et al., 2001). This method assumes the length of the vector between the sternal notch and the acromioclavicular joint remains constant due to no translation at the sternoclavicular or acromioclavicular joints. However, any change in the orientation of the vector during movement would correspond to changes in sternoclavicular protraction/retraction and elevation/depression. Studies using this approach have found the sternoclavicular joint retracts (10-13°) and elevates (7-13°) during humeral elevation to 120° in the scapular plane (Ebaugh et al., 2005; McClure et al., 2006; McClure et al., 2001). Despite the assumptions inherent in this methodology and the differences in the definition of the trunk coordinate axes, the resulting angular values averaged across subjects are generally consistent with other studies that directly tracked clavicle motion (Ludewig et al., 2004; Ludewig et al., 2009a). However, the degree to which the sternoclavicular joint posteriorly rotates cannot be described as its rotation about the sternal notch-acromioclavicular joint vector cannot be calculated. Given posterior rotation is the predominant motion of the sternoclavicular joint (Ludewig et al., 2009a), this proves to be a critical limitation of this methodology when the goal is to comprehensively describe 3D shoulder complex kinematics.

In an effort to directly track clavicular motion without added skin motion artifact, Sahara et al. (2007) reconstructed the scapula and clavicle from static MR images. Due to the limited field of view of the MR scanner, the coordinate systems of the thorax, scapula, and clavicle were unique and complex. In particular, the apex of the lung was

used to define a thoracic coordinate system. The medial/lateral axis of the clavicle reference frame was then defined through the lateral 80 mm of the clavicle. Due to the crank-shape of the clavicle, defining the lateral axis in this way likely overestimated the description of sternoclavicular retraction when compared to other studies that utilized the entire clavicular anatomy to define the axis. Despite the non-traditional definition of the coordinate axes, the authors described the general pattern of sternoclavicular motion to be retraction, elevation, and posterior rotation. An additional major limitation of this study is assuming the relationship between the sternum and the lung remain constant throughout humeral motion. The likelihood of motion artifact impacting the accuracy of lung reconstruction is high given the need for respiration during the scan, which took approximately 2.5 minutes.

In 2009, Ludewig et al. (2009a) performed the most precise study of sternoclavicular joint motion to date using bone-fixed electromagnetic sensors in 12 asymptomatic subjects. The classic pattern of sternoclavicular retraction (11°), elevation (5°), and posterior rotation (22°) was observed during humeral elevation to 120° in the scapular plane. Of these motions, the magnitude of sternoclavicular posterior rotation was found to be the least variable between subjects. From a systems standpoint, this suggests posterior rotation is the priority motion of the sternoclavicular joint working to facilitate the task of humeral elevation. By comparison, sternoclavicular elevation and retraction were highly variable between individuals. It is believed this variability is due to the need to alter the position of the scapula on the thorax due to varying thoracic curvatures between individuals in order to maintain congruency.

Description of acromioclavicular joint motion is the least studied of the shoulder complex motions (**Table 12**). Inman et al. (1944) were the first to describe acromioclavicular motion by quantifying the angle between the clavicular long axis and the spine of the scapula using radiographs. Although the measure is limited by projection error, the authors reported the acromioclavicular joint upwardly rotates approximately 30° during humeral elevation to 180°. Sahara et al. (2007) also quantified acromioclavicular kinematics and, in addition to the altered clavicular coordinate systems as previously described, utilized a glenoid-based coordinate system to describe scapular orientation. When the orientations of the coordinate axes are compared to the recommended standard (Wu et al., 2005), it is expected the description of acromioclavicular internal rotation position by Sahara et al. will be overestimated. This is due to the overestimation of sternoclavicular retraction position and scapular medial/lateral axis being defined perpendicular to the glenoid as opposed to a vector oriented by the root of the scapular spine and the posterolateral acromion.

In an additional paper performing a secondary analysis of the data (Sahara et al., 2006), Sahara et al. utilized a helical axis approach to describe acromioclavicular motion between the static positions of arm at the side and maximum elevation. Unlike Euler angles where rotations are described about sequential orthogonal axes, the helical axis provides a description of angular displacement about a single axis. As such, the authors describe an axis oriented inferiorly, posteriorly, and medially. Rotation about this axis may be interpreted as a net motion of acromioclavicular upward rotation, posterior tilt, and internal rotation; however, the individual contributions (i.e. helical angles) were not

reported. A small amount of translations (on average 0-2 mm) also occurred at the joint, suggesting the acromioclavicular joint acts as a relatively stationary pivot from which to transfer angular motion from the scapula to the clavicle.

Ludewig et al. (2009a) performed the most accurate and comprehensive study of acromioclavicular joint motion to date. The authors found a pattern of acromioclavicular internal rotation (5°), upward rotation (7°), and posterior tilt (13°) during humeral elevation to 120° in the scapular plane. By comparison to the scapulothoracic and sternoclavicular joint where one rotation tends to emerge as a primary facilitator of humeral elevation, all three acromioclavicular joint rotations tend to have similar between-subject variability. This suggests the joint functions as a critical pivot working to balance the magnitudes of sternoclavicular and scapulothoracic motion, compensate for glenohumeral hyper- and hypo-mobility, and maintain congruency of the scapula on the thorax. This theory is supported by studies showing increased acromioclavicular upward rotation in response to glenohumeral hypomobility (Braman et al., 2010).

In summary, differences between studies in the description of shoulder complex kinematics in asymptomatic individuals are influenced by several factors including the method of motion capture, definition of anatomical coordinate systems, the choice of rotation sequence, and the characteristics of the subject sample. Despite these challenges, a general pattern of motion emerges. During humeral elevation, the primary motions of the shoulder complex consist of sternoclavicular posterior rotation and retraction; acromioclavicular posterior tilt and upward rotation; scapulothoracic upward rotation and posterior tilt; and glenohumeral elevation and external rotation. Additionally, a small

amount of sternoclavicular elevation and acromioclavicular internal rotation occurs. Scapulothoracic internal/external rotation and glenohumeral anterior/posterior plane of elevation also occurs but is dependent upon the direction or plane of humeral motion. However, the patterns described represent group means, which do not always reflect the kinematics patterns observed in individual subjects (Lawrence et al., 2014a; Lawrence et al., 2014b; Ludewig et al., 1996). Clinical theory often suggests deviations from this expected pattern of motion may cause shoulder pain by decreasing the subacromial space (Ludewig et al., 2000; Ludewig et al., 2009b), and studies comparing shoulder complex kinematics in asymptomatic and symptomatic individuals may provide face validity for the theory.

Kinematics in Symptomatic Individuals

Numerous studies have compared shoulder complex kinematics between asymptomatic controls and various subgroups including glenohumeral hypermobility (Ogston & Ludewig, 2007; Struyf et al., 2013), glenohumeral hypomobility (Braman et al., 2010; Fayad et al., 2006; Rundquist, 2007), and in subjects diagnosed with "impingement syndrome" (**Table 13**, **Table 14**, and **Table 15**). Like studies in asymptomatic individuals, study design and methodology are widely variable including both side-to-side comparisons in subjects with unilateral shoulder pain (Endo et al., 2001; Lukasiewicz et al., 1999) and group comparisons between symptomatic and asymptomatic subjects (Lawrence et al., 2014a; Lawrence et al., 2014b; Ludewig et al., 2000; Lukasiewicz et al., 1999; McClure et al., 2006; Sousa Cde et al., 2014).

Collectively, these studies help establish a relationship between abnormal movement and the presence of shoulder pain.

In 1999, Lukasiewicz et al. (1999) compared scapulothoracic kinematics in 20 asymptomatic subjects and 17 subjects with a clinical presentation consistent with unilateral impingement syndrome. Scapular orientation was quantified using projection angles calculated when the arm was statically held in three positions of humeral elevation. The authors found the involved shoulder in the symptomatic subjects had 8° less posterior tilt at higher angles of scapular plane abduction elevation (90° and maximum) compared to their contralateral shoulder and the asymptomatic group. Because posterior tilt is theorized to bring the anterior aspect of the acromion superior and posterior relative to the humeral head, a reduction in this motion was believed to increase the risk for rotator cuff compression.

Endo et al. (2001) sought to also quantify scapular orientation in individuals classified as having shoulder impingement by making comparisons to their asymptomatic contralateral side. Two-dimensional angles were defined using anatomical landmarks on standard anterior/posterior radiographs to quantify scapular orientation relative to the image vertical. However, the validity of this measurement method is impacted by out-of-plane projection error because the radiographs were taken perpendicular to the coronal plane of the trunk and the scapula is consistently internally rotated relative to the trunk during abduction (Ludewig et al., 2009a). Furthermore, it is unknown how much control of trunk and humeral position was employed during data collection to avoid confounding scapular orientation measures when described relative to a fixed image vertical. Despite

these limitations, the authors reported results consistent with Lukasiewicz (1999) in that the symptomatic shoulder had significantly less scapulothoracic posterior tilt at 45° and 90° humerothoracic elevation (3° and 5°, respectively). Furthermore, symptomatic shoulders had 4° less scapulothoracic upward rotation at 90° humerothoracic elevation. These findings further strengthened the theorized causal relationship between abnormal scapulothoracic motion and shoulder pain as a reduction in both posterior tilt and upward rotation are believed to bring the acromion into closer proximity to the rotator cuff tendons (Ludewig et al., 2009b).

Ludewig and Cook (2000) compared shoulder complex kinematics between groups consisting of symptomatic and asymptomatic male construction workers matched to occupational exposure. Using 3D surface-based electromagnetic motion capture, the authors found the symptomatic group had significantly more scapulothoracic internal rotation throughout the range of motion when humeral elevation was performed under an external load. The symptomatic subjects also had significantly less scapulothoracic upward rotation at 60° and less posterior tilt at 120° humerothoracic elevation. These findings are consistent with other studies showing symptomatic subjects have decreased posterior tilt (Endo et al., 2001; Lukasiewicz et al., 1999). Furthermore, the reduction in scapulothoracic upward rotation, posterior tilt, and external rotation suggested impairments in any of the scapular motions considered “normal” may be associated with shoulder pain. However, the unique sample consisting of male construction workers may limit the generalizability of these findings to the broader clinical population.

In 2006, McClure et al. (2006) provided additional evidence for abnormal shoulder kinematics in symptomatic subjects with a clinical presentation consistent with the diagnosis of "impingement syndrome". The authors compared 3D scapular kinematics and scapular position (i.e. sternoclavicular elevation/depression, protraction/retraction) between 45 symptomatic subjects and 45 asymptomatic controls matched for age, gender, and hand dominance. Interestingly, the authors reported symptomatic subjects had 4-5° more scapulothoracic upward rotation and 3° more posterior tilt at higher angles of humerothoracic elevation (90° or 120°). While this is not consistent with previous findings and clinical theory, the authors attributed the findings to a compensatory strategy to increase subacromial space in response to the more chronic nature of the symptomatic group's pain. Furthermore, the authors found the symptomatic group had significantly more sternoclavicular elevation and retraction at higher angles of humerothoracic elevation.

Perhaps the most comprehensive comparison of shoulder complex kinematics between symptomatic and asymptomatic was performed by Lawrence et al. (2014a). The researchers utilized bone-fixed electromagnetic sensors to track sternoclavicular, acromioclavicular, scapulothoracic, and glenohumeral motion in 10 symptomatic and 12 asymptomatic subjects during arm raising and lowering. Consistent with other studies (Endo et al., 2001; Ludewig et al., 2000), the authors reported symptomatic subjects were in less scapulothoracic upward rotation during humeral elevation. Specifically, symptomatic subjects were in 3-5° less scapulothoracic upward rotation at lower angles (30° and 60°) of scapular plane abduction. Likely related to this finding, the authors also

found the symptomatic subjects had 6-7° more glenohumeral elevation at the same angles of humerothoracic elevation. This finding suggests subjects with less upward rotation compensate for the loss of humerothoracic elevation by increasing their glenohumeral elevation. Furthermore, symptomatic subjects demonstrated 5° less sternoclavicular elevation at 30° arm raising and 5° less sternoclavicular posterior rotation throughout the range of motion. The finding of decreased sternoclavicular posterior rotation was perhaps the most intriguing because of the presumed passive mechanism of how sternoclavicular posterior rotation is produced.

More recently, Sousa et al. (2014) compared shoulder kinematics between asymptomatic subjects and symptomatic subjects with acromioclavicular joint arthritis and rotator cuff disease as confirmed by diagnostic ultrasound. The researchers reported several significant differences between groups across all shoulder complex joints. Consistent with McClure et al., (2006) symptomatic subjects were in 4-5° more scapulothoracic upward rotation during both flexion and scapular plane abduction. While McClure et al. theorized an increase in scapulothoracic upward rotation was compensatory to increase subacromial space as a result of chronic symptoms, it is unknown whether the findings of Sousa et al. support this hypothesis as they did not report the mean duration of symptoms.

In addition to differences in scapulothoracic position, Sousa et al. (2014) also reported the symptomatic subjects were in decreased sternoclavicular retraction and increased acromioclavicular posterior tilt during flexion. However, examination of sternoclavicular and acromioclavicular joint upward rotation magnitudes suggest

methodological differences may have confounded the studies description of motion. In particular, it is uncertain how the authors constructed the clavicular coordinate system. The authors report using the methods of Ludewig et al. (2009a); however, inspection of their raw data suggests otherwise. Ludewig et al. (2009a) accounted for the lack of three non-collinear points on the clavicle by aligning the clavicular vertical axis to that of the thorax when the arm was resting at the side, following a recommendation of the International Society of Biomechanics (Wu et al., 2005). This approach should result in a mean and standard deviation sternoclavicular posterior rotation value at rest of approximately 0°. However, the resting values for Sousa et al. (2014) are 6° anterior rotation with a large standard deviation (±15°), suggesting another approach was likely used for setting up the clavicular coordinate system. Uncertainty is also evident in the description of acromioclavicular joint positions. In particular, acromioclavicular joint data suggests subjects were, on average, in downward rotation throughout the range of motion, which is inconsistent with previous studies (Ludewig et al., 2009a; Teece et al., 2008). Collectively, these results challenge the interpretation of absolute magnitudes and group comparisons of sternoclavicular posterior rotation, and subsequently acromioclavicular upward rotation and posterior tilt.

Despite the natural variability in shoulder complex kinematics between individuals and various methodology, this review of comparative kinematic studies shows group differences between asymptomatic and symptomatic subjects are often found during humeral raising. However, the magnitude and direction of group differences are not consistent even when presumably studying the same underlying clinical diagnosis

of “impingement syndrome”. This inconsistency of finding between studies reflects the non-homogeneity of this clinical classification (Braman et al., 2014; Ludewig et al., 2013). Furthermore, the findings suggest subgroups of patients likely exist based on movement-based parameters within the broad clinical population (Ludewig et al., 2017).

Because none of the studies were longitudinal in design, any findings of abnormal kinematics cannot be assumed to be causative in the development of the subject’s symptoms. Collectively however, the studies establish the association between movement and shoulder pain that is critical to proposing mechanistic theories from which future studies can be designed. Interestingly, no study found differences in scapular, humeral, or clavicle position during a relaxed standing position. Therefore, it appears kinematic impairments may only manifest consistently when the shoulder is in elevated positions, emphasizing the importance of observing shoulder movement and not just posture during clinical examinations. Finally, the magnitude of differences between groups is often quite small (<5°) which calls to question the clinical relevance of the difference.

Shoulder Complex Coupling

Studies of shoulder complex kinematics have demonstrated scapulothoracic motion contributes substantially to overall shoulder motion (Ebaugh et al., 2005; Ludewig et al., 1996; Ludewig et al., 2009a; McClure et al., 2001). However, because of the link-system structure of the shoulder complex, scapulothoracic motion cannot occur without concurrent motion at the sternoclavicular and acromioclavicular joints (Dvir et al., 1978; Inman et al., 1944; Pronk et al., 1993; Teece et al., 2008). Therefore, sternoclavicular and acromioclavicular joint motion is “coupled” (Pronk et al., 1993).

Because clavicular and scapular axes are oblique to one another (**Figure 8**), rotation about clavicular axes will have an indirect effect on scapulothoracic motion (and vice versa), with acromioclavicular joint motion acting as an intermediary. The result is a complex relationship between the three joint systems in producing overall functional shoulder motion. Understanding the mechanisms of how this interaction of clavicular and scapular motion occurs is critical to understanding how shoulder motion is produced and how abnormal motion may occur.

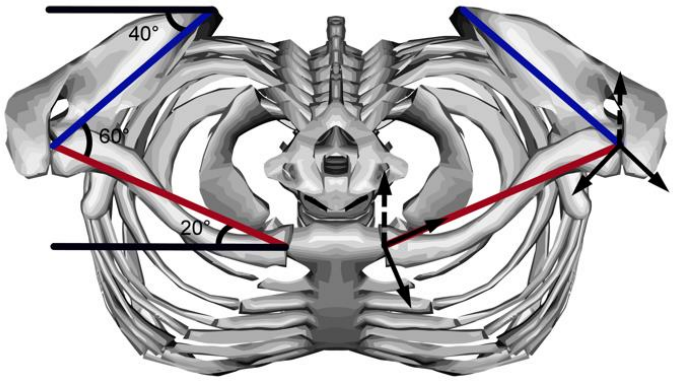

Figure 8: Transverse plane offset between clavicular and scapular coordinate axes proposed to define coupling relationships. Red line: clavicular medial/lateral axis; blue line: scapular medial/lateral axis.

In 1978, Dvir and Berme (1978) used a qualitative kinematic model to explain how shoulder complex motion occurs. Using static anterior/posterior radiographs to visualize shoulder motion, the authors reported the initial phase of motion is defined by the scapula upwardly rotating until the conoid ligament becomes taught. During the second phase, which begins at approximately 60° humeral elevation, scapular motion is transferred to the clavicle through the conoid ligament and the bones move together as a

single “claviscapular” link. Presumably, this initiates the posterior rotation of the sternoclavicular joint that allows for maximal humeral elevation range of motion.

Teece et al. (2008) attempted to build on the theories proposed by Dvir and Berme (1978) by providing a theoretical framework for how clavicular and scapular motions become coupled during humeral motion. The authors proposed the fundamental factor affecting coupled mechanics is the acromioclavicular joint internal rotation angle. This angle is defined by the medial/lateral axes of the clavicular and scapular coordinate systems (**Figure 9**). Because of the obliquity between axes, motion about the clavicular medial/lateral axis is not directly related nor completely independent to the resulting scapular motion. As a result, clavicular and scapular kinematics interact in a complex way and are best understood under two theoretical conditions: if the axes were parallel and if they were perpendicular.

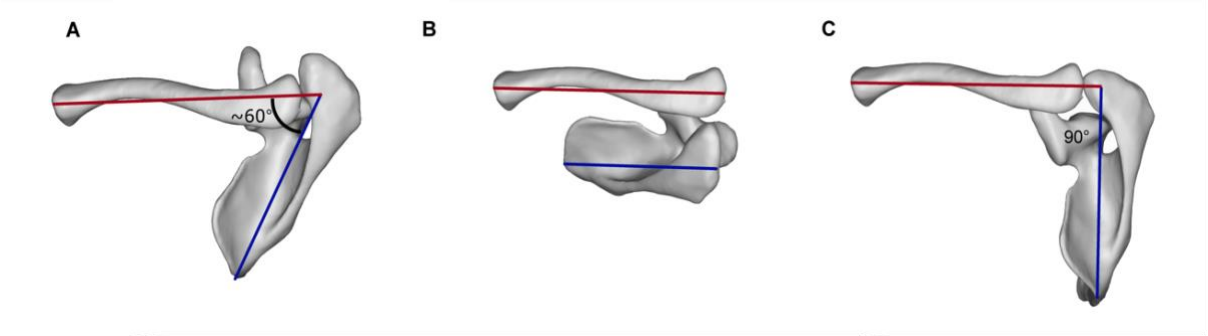

Figure 9: Relationship between the acromioclavicular joint axes and coupled mechanics of the clavicle and scapula. Red line: claviclar medial/lateral axis. Blue line: scapular medial/lateral axis. **A**) Mean physiologic relationship with acromioclavicular internal rotation angle of ~60°. **B**) Theoretical relationship in which the scapular and clavicular medial/lateral axes are parallel (i.e. acromioclavicular internal rotation = 0°). **C**) Theoretical relationship in which the scapular and clavicular medial/lateral axes are perpendicular (i.e. acromioclavicular internal rotation = 90°).

Theoretically, if the acromioclavicular joint internal rotation angle was 0° (i.e. axes parallel) and the acromioclavicular joint was rigidly fixed, sternoclavicular motion would produce scapulothoracic motion in the following ways: sternoclavicular retraction would produce scapulothoracic external rotation; sternoclavicular elevation would produce scapulothoracic upward rotation; and sternoclavicular posterior rotation would produce scapulothoracic posterior tilt. Conversely, if the acromioclavicular joint internal rotation angle was 90° (i.e. axes perpendicular) and the acromioclavicular joint was rigidly fixed, sternoclavicular motion would produce scapulothoracic motion through other relationships: sternoclavicular elevation would produce scapulothoracic anterior tilt, and sternoclavicular posterior rotation would produce scapulothoracic upward rotation. Sternoclavicular retraction would still produce scapulothoracic external rotation as the orientation of the vertical axis has not changed between the two theoretical conditions.

While these two theoretical conditions allow for clavicle motion to dictate resulting scapulothoracic motion, the physiologic alignment between the clavicle and scapula does not allow for such relationships to exist directly. According to Teece et al. (2008), the mean acromioclavicular internal rotation angle is 68° with the arm at the side. This position is approximately 3/4 offset from the theoretical parallel condition, and 1/4 offset from the theoretical perpendicular condition. More recently, Ludewig et al. (2009a) provided a more precise description of acromioclavicular internal rotation angle during a relaxed standing posture (60°) using bone-fixed tracking. Therefore, the relationship is approximately 2/3 offset from the theoretical parallel condition, and 1/3 offset from the theoretical perpendicular condition. As a result, 2/3 of scapulothoracic motion is

produced as though the axes were perpendicular while the remaining 1/3 is produced as though the axes were parallel.

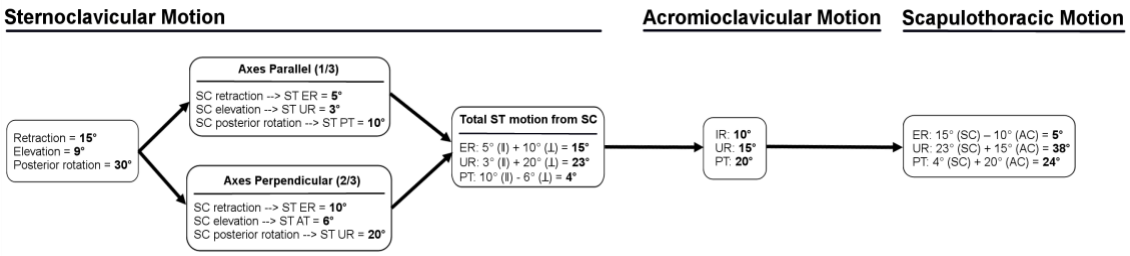

Figure 10: Example of application of the coupling theory as proposed by Teece et al. (2008) using estimated angular values from Ludewig et al. (2009a). Sternoclavicular joint angular displacements are transformed to corresponding scapulothoracic angular displacements according to the coupling theory. Resulting scapulothoracic values from sternoclavicular joint motion is then added to acromioclavicular joint angular displacements resulting in an estimate of total scapulothoracic motion. Abbreviations: SC=sternoclavicular, AC=acromioclavicular, ST=scapulothoracic, ER=external rotation, IR=internal rotation, UR=upward rotation, PT=posterior tilt, AT=anterior tilt.

A worked example of the theory proposed by Teece et al. (2008) is provided in **Figure 10** using estimated angular displacement values from Ludewig et al. (2009a). Estimated angular values of sternoclavicular joint motion are transformed to corresponding scapulothoracic motion using the 2/3 (perpendicular) and 1/3 (parallel) theory. These values are then added to acromioclavicular joint motion resulting in an estimate of total scapulothoracic motion. However, some error is expected in this approach to estimating total scapulothoracic motion for several reasons. First, estimated displacement values represent group means. Inspection of individual subject data is required to fully test the proposed coupling theory. Second, the proposed relationship between sternoclavicular motion and resulting scapulothoracic motion is based on the

magnitude of acromioclavicular internal rotation in a relaxed standing position. This angle increases with increasing angles of humerothoracic elevation (Ludewig et al., 2009a; Sahara et al., 2007; Teece et al., 2008). Therefore, the relationship between sternoclavicular motion and resulting scapulothoracic motion is dynamic and should become more consistent with the theoretical perpendicular condition at higher angles of humerothoracic elevation. Third, the cause and effect relationship between sternoclavicular and scapulothoracic motion suggested by Teece et al. (2008) may not always reflect the true mechanical phenomenon. For example, according to the coupling theory, sternoclavicular posterior rotation could produce both scapulothoracic posterior tilt and upward rotation. However, no muscle is known to produce sternoclavicular posterior rotation and the motion is believed to occur as the result of scapular upward rotation being transferred to the clavicle through tension in the coracoclavicular ligaments (Dvir et al., 1978). Therefore, other factors such as laxity or stiffness in the acromioclavicular joint capsule and ligaments may impact the coupling relationships and resulting motion.

Despite the strong biomechanical rationale for the shoulder coupling relationships, the mechanisms by which this coupling occurs remains unclear. The preponderance of shoulder kinematics literature reports absolute joint angular positions making application of results to coupling difficult given the need to describe joint motion as angular displacements. One past study explored group differences in shoulder complex kinematics within the context of the coupling theory (Lawrence et al., 2014a). In the study of shoulder complex kinematics in individuals with and without shoulder pain,

groups did not differ in scapulothoracic upward rotation in a relaxed standing position, but the symptomatic group was in decreased upward rotation at 30° and 60° humerothoracic elevation. By 90°, the group differences no longer existed. For this to occur, the symptomatic group must have demonstrated increased scapulothoracic upward rotation displacement beyond 60° humerothoracic elevation. Estimates of displacement support this theory with the symptomatic group demonstrating 2° more upward rotation than the asymptomatic group between 60 and 90° humerothoracic elevation, and 3° more upward rotation between 90 and 120° humerothoracic elevation.

The authors proposed three mechanisms by which the symptomatic group "caught up" to the asymptomatic group in terms of scapulothoracic upward rotation. First, between 60° and 90° humerothoracic elevation, the symptomatic group had approximately 3° more sternoclavicular elevation displacement than the asymptomatic group. Similarly, between 90 and 120°, the symptomatic group had 2° more displacement. Both phases of increased sternoclavicular elevation displacement in the symptomatic group likely reduced the differences in scapulothoracic upward rotation between the groups at higher angles of humerothoracic elevation. Second, while the groups did not differ in acromioclavicular upward rotation position across all angles of elevation, the slope of the line for the symptomatic group was descriptively increased beyond 90° humerothoracic elevation compared to the asymptomatic group. Although not statistically significant, this suggests more upward rotation displacement in the symptomatic group during this range of motion which may have further reduced the group differences in scapulothoracic upward rotation. Finally, following an initial period

of sternoclavicular anterior rotation as compared to a resting standing posture, the symptomatic group remained in less posterior rotation throughout the range of motion. The group difference is likely the result of the reduction in scapulothoracic upward rotation in the same ranges since sternoclavicular posterior rotation is presumably a byproduct of scapulothoracic upward rotation (Dvir et al., 1978).

While the explanations presented by Lawrence et al. (2014a) are based on the theory proposed by Teece et al. (2008), the description is based on group data and may not reflect trends in individual subjects. Furthermore, without evidence explaining how shoulder complex motion is produced, mechanisms by which abnormal shoulder motion occurs remain unclear. This critical gap in the literature challenges future work aiming to develop a movement-based diagnostic classification and identify targeted treatment strategies.

Impacts of Shoulder Kinematics on Subacromial Space

Measurement Techniques

Methods for quantifying subacromial space are extremely varied and include both *in vitro* (Brossmann et al., 1996; Burns & Whipple, 1993; Flatow et al., 1994) and *in vivo* (Giphart et al., 2012; Graichen et al., 1999a; Graichen et al., 1999b; Hebert et al., 2003; Seitz et al., 2012b; Silva et al., 2010; Tasaki et al., 2015; Thompson et al., 2011) measures. Two-dimensional methods include photographs (Burns et al., 1993), radiographs (Flatow et al., 1994), single-plane fluoroscopy (Thompson et al., 2011), MR imaging (Brossmann et al., 1996; Hebert et al., 2003; Tasaki et al., 2015), and ultrasonography (Seitz et al., 2012b; Silva et al., 2010); while 3D methods include

biplane fluoroscopy (Bey et al., 2007; Giphart et al., 2012), stereophotogrammetry (Flatow et al., 1994), and image-based modeling (Graichen et al., 1999a; Graichen et al., 1999b). Like studies of shoulder complex kinematics, the choice of study methodology directly impacts both the accuracy and generalizability of results.

The most common description of subacromial space has been acromiohumeral distance, which quantifies the minimum distance between the undersurface of the acromion and the humerus. However, the approach used to calculate the minimum distance may vary between studies and is sometimes not precisely described (Silva et al., 2010). Some researchers report the minimum distance only to the greater tuberosity of the humerus (Bey et al., 2007) to avoid calculation to areas that may not be relevant to the rotator cuff (e.g. lateral humeral shaft), while others quantified the minimum distance directly to the rotator cuff (Tasaki et al., 2015). Generally, the orientation of the minimum distance vector is not constrained (Flatow et al., 1994; Giphart et al., 2012; Graichen et al., 1999a; Graichen et al., 1999b; Hebert et al., 2003; Seitz et al., 2012b); however, some researchers constrained the vector to be oriented vertically (Thompson et al., 2011). These differences in quantification of subacromial space make comparison between studies difficult by impacting the magnitude of the acromiohumeral distances.

Two-dimensional methods of quantifying subacromial space often utilize clinical imaging technologies such as radiographs and MR scans. However, quantifying 3D anatomical relationships using 2D imaging techniques introduces various sources of error. The quantification of acromiohumeral distance using 2D radiographs is affected by magnification and projection error caused by superimposing anatomical structures onto a

single image plane. Further, assessment of anatomical relationships from 2D MR and ultrasonography images is dependent on the orientation and choice of the image from which the measurements are taken. Despite these limitations, 2D methods (radiographs, ultrasonography, MR imaging) are commonly employed because processing 2D data is often much simpler than in 3D studies.

In Vitro Studies

Before the advancement of imaging technologies, cadaveric studies were the primary means to investigate anatomical relationships between the coracoacromial arch and soft tissue during shoulder motion (**Table 16**). Collectively, early *in vitro* studies provided fairly consistent descriptions of the anatomical relationships between the rotator cuff and coracoacromial arch during humeral elevation. Because these studies found contact occurred between 45° and 135° humerothoracic elevation, the clinical theory that pain occurring in mid-range (60-120°) was due to subacromial compression of the rotator cuff tendons seemed to be supported. However, the experimental nature of these studies limited interpretation and application of findings to living human subjects for several reasons. First, the humerus of each specimen was moved relative to a fixed scapula without allowing for axial rotation (Brossmann et al., 1996; Burns et al., 1993; Flatow et al., 1994). Further, Flatow et al. (1994) elevated the humerus using a fixed, specimen-specific glenohumeral axial rotation which did not allow for the replication of multi-axial shoulder motion and may have altered subacromial proximities. Third, dynamic motion was simulated using cables along the line of action of several muscles (Burns et al.,

1993), which likely does not replicate shoulder motion *in vivo*. Fourth, 2D acromiohumeral measurements are subject to errors in describing spatial relationships.

Despite the limitations of early cadaveric studies, two critical advancements were made by Flatow et al. (1994) that helped frame the interpretation of future studies of subacromial proximities. First, the researchers investigated subacromial proximities using both minimum distance and surface area and found that subacromial contact occurred most frequently between 30° and 90° humeral elevation, but surface areas were greatest between 60° and 120° humeral elevation. These differences in results between describing proximity as both a distance and a surface area suggests quantifying mechanical subacromial rotator cuff compression as simply a distance may not adequately reflect the complexity of the phenomenon. A second critical observation involved the need to consider the location of the rotator cuff tendon when interpreting measures of subacromial contact patterns by stating acromiohumeral intervals beyond 90° "no longer accommodated" the rotator cuff tendons. Ultimately, these early *in vitro* studies helped define the mechanical nature of subacromial impingement but remain limited in their ability to represent subacromial relationships during shoulder motion in living subjects.

In Vivo Studies in Asymptomatic Individuals

In vivo studies of subacromial relationships during shoulder motion often utilized similar methodologies to the early *in vitro* studies and were therefore impacted by similar sources of error (**Table 17**), which likely perpetuated the belief that the risk for subacromial rotator cuff compression occurred at mid to higher angles of humeral elevation. For example, Tasaki et al. (2015) utilized open MR imaging to describe the

proximity between the rotator cuff and acromion across multiple humeral positions in 20 asymptomatic subjects and found the minimum distance between the rotator cuff to the acromion occurred at 93.5° humerothoracic elevation. Despite the methodological challenges, the authors made an important observation that contact between the structures occurred in 5 of the 20 subjects, suggesting subacromial rotator cuff compression may not occur in all individuals.

Other *in vivo* studies started to challenge the range of motion that subacromial rotator cuff compression risk was the highest. Thompson et al. (2011) utilized a clinical single-plane fluoroscopy system to quantify acromiohumeral distance during static loaded and unloaded scapular plane abduction in asymptomatic college baseball players. The authors found the minimum distance occurred between 45-60° humerothoracic elevation, suggesting the minimum distance occurs lower in the range of humerothoracic elevation than previous studies suggested (Brossmann et al., 1996; Burns et al., 1993; Flatow et al., 1994). However, the study is limited by the static nature of the motion, the use of 2D measures of acromiohumeral distance, and the use of pixels as the unit of measure making it confounded by the source-to-object distance.

Studies utilizing 3D acromiohumeral distance calculations offer more accurate quantification of the subacromial space by avoiding projection error caused by out-of-plane anatomical relationships. Graichen et al. (1999a) utilized multiple static supine MR images across seven humeral positions to study the effect of humeral abduction and rotation on subacromial space in 12 asymptomatic subjects. Unlike Brossman et al. (1996) and Tasaki et al. (2015), Graichen et al. (1999a) used image processing software

to render 3D models of each subject's shoulder in different glenohumeral positions. Using these models, 3D distances were calculated to quantify the acromiohumeral distance. Consistent with other studies (Brossmann et al., 1996; Flatow et al., 1994; Thompson et al., 2011), the researchers found the acromiohumeral distance decreased with increasing angles of humerothoracic elevation, with the absolute minimum acromiohumeral distance occurring at 120° humerothoracic elevation (3.9 mm). However, the minimum distance vector only passed through the supraspinatus tendon below 90° humerothoracic elevation rendering the absolute minimum acromiohumeral distance at 120° inconsequential relative to mechanisms of rotator cuff injury. In objectively quantifying the acromiohumeral distances, Graichen et al. (1999a) was able to demonstrate a large between-subject variability in acromiohumeral distance (coefficient of variation: 14-46%) suggesting mechanical subacromial impingement is a complex phenomenon likely influenced by several factors. While Graichen et al. (1999a) was the first to quantify 3D distance vectors, they interestingly chose to quantify acromiohumeral distance directly to the humerus despite having created 3D models of the supraspinatus muscle. This decision may have inadvertently perpetuated the assertion that rotator cuff compression continues to occur at angles as high as 120° humerothoracic elevation by failing to describe subacromial relationships directly to the rotator cuff. Further, the supine position for acquiring MR scans may alter scapulohumeral relationships and does not allow for gravity's effect on subacromial anatomical relationships.

In 2012, Giphart et al. (2012) studied acromiohumeral distance in eight healthy male subjects using bi-plane fluoroscopy and 2D/3D shape-matching. The novel

methodology was a significant advancement because it allowed for the precise quantification of dynamic shoulder motion and 3D acromiohumeral distances. The researchers found the minimum distances gradually decreased with increasing angles of humerothoracic elevation with the absolute minimum distance occurring on average at 83° during scapular plane abduction (2.6 mm) and at 97° during flexion (1.8 mm). Because the study was conducted dynamically, data were available throughout the range of motion allowing for a higher resolution of proximity calculations. Further, the location of the acromiohumeral distance vector could be visualized relative to the rotator cuff insertion site providing a means to assess the clinical meaningfulness of the metric. In doing so, the researchers found the minimum distance vector to be located within the supraspinatus footprint between 34-72° during scapular plane abduction and 36-65° during flexion. This description of the range of motion in which rotator cuff compression may occur is lower than previous studies. But given the accuracy and resolution of the kinematic and proximity data, the study provides the best description of subacromial proximity compression risk in asymptomatic subjects to date.

As a whole, these studies of subacromial space in cadaveric specimen and asymptomatic subjects suggest the minimum acromiohumeral distance occurs across a wide range of humerothoracic elevation (45°-120° humerothoracic elevation). However, the rotator cuff has typically passed medially under the acromion by 90° and is no longer in a position of risk (Flatow et al., 1994; Giphart et al., 2012; Graichen et al., 1999a). As such, the interpretation of acromiohumeral distance measures is only truly meaningful when the location of the rotator cuff is accounted for as well. Studies in asymptomatic

subjects also demonstrated how different angles of humeral elevation resulted in statistically significant changes in the subacromial space (Giphart et al., 2012; Graichen et al., 1999a). Given shoulder kinematics have been shown to differ between symptomatic and asymptomatic individuals (Lawrence et al., 2014a; Lawrence et al., 2014b; Ludewig et al., 2000; Lukasiewicz et al., 1999; McClure et al., 2006; Sousa Cde et al., 2014), it is logical to question whether these kinematic differences impact the magnitude of the subacromial space resulting in rotator cuff pathology. However, physical contact between the rotator cuff and coracoacromial arch in asymptomatic subjects (Graichen et al., 1999a; Tasaki et al., 2015) suggests compression alone may not result in symptom provocation in individuals with shoulder pain. Further, no longitudinal study has investigated the cause-and-effect relationship of a reduction in subacromial space on rotator cuff injury. Therefore, the results of studies of subacromial space in symptomatic individuals (**Table 18**) should be interpreted within the proper perspective of association and not causation.

Subacromial Space in Clinical Populations

Studies investigating subacromial proximities in symptomatic individuals have generally taken two approaches to subject recruitment. The first involves recruiting individuals with a diagnosis of "impingement syndrome" which, as previously mentioned, is a broad diagnostic label for shoulder pain often given in the absence of gross instability, hypomobility, or cervicogenic symptoms. The second approach involves recruiting subjects with visible scapular "dyskinesia", which refers to an alteration in the position and/or motion of the scapula (Kibler et al., 2013). Theoretically, the addition of a

movement-based classification to the studies' inclusion criteria may make them more sensitive to detect potential group differences in subacromial proximities between study groups.

Symptomatic Individuals

Several studies have quantified subacromial space in symptomatic subjects presenting with signs and symptoms consistent with "impingement syndrome" (**Table 18**). Hébert et al. (2003) utilized static MR imaging to quantify 2D acromiohumeral distance in subjects classified as having impingement syndrome and compare the results to their contralateral shoulder or asymptomatic controls. While comparing an individual's symptomatic shoulder to both their asymptomatic contralateral shoulder and independent control subjects has merit, the approach requires a mixed-model statistical analysis, which was not performed. Therefore, "group" comparisons are likely confounded by the correlation between the level of the within-subject factor. Nevertheless, the researchers found symptomatic shoulders had 1-1.5 mm smaller acromiohumeral distance at humerothoracic angles above 70° humerothoracic elevation during flexion and 80° humerothoracic elevation during abduction. In both symptomatic and asymptomatic shoulders, the minimum distance occurred at 110° humerothoracic elevation during both flexion and abduction. However, given results of other studies (Bey et al., 2007; Giphart et al., 2012; Graichen et al., 1999a; Graichen et al., 1999b), it is likely the rotator cuff had already cleared the acromion by this angle. Hébert et al. did not provide descriptions of the acromiohumeral vector location relative to the rotator cuff making it difficult to interpret the clinical meaningfulness of their acromiohumeral distances at higher angles.

Further, because glenohumeral kinematics were not quantified in this study, it is difficult to determine potential factors that influenced the difference in acromiohumeral distance between studies.

As previously described, studies using 3D methods provide a more accurate description of the anatomical relationships within the subacromial space. As in their previous study (Graichen et al., 1999a), Graichen et al. (1999b) used bone models reconstructed from MR images to quantify 3D acromiohumeral distance in 10 symptomatic subjects (six classified as having Neer stage I impingement, three with full-thickness rotator cuff tears, one with acromioclavicular osteoarthritis). Acromiohumeral distances were compared between the subjects' symptomatic and asymptomatic sides at 30° and 90° humerothoracic elevation. In all subgroups of subjects, the minimum distance was the smallest at 90° humerothoracic elevation. However, the magnitude of the acromiohumeral distance only differed between the symptomatic and contralateral side in the subjects with full-thickness rotator cuff tears. This finding is consistent with previous studies of subacromial space with the arm at the side in individuals with rotator cuff tears (Cotton & Rideout, 1964; Deutsch et al., 1996). While Graichen et al. (1999b) only studied seven subjects classified with "impingement syndrome" or acromioclavicular arthritis, the lack of differences in minimum distance between shoulders in subjects suggests the presence of shoulder pain may not necessarily relate to the presence of reduced acromiohumeral distance. Furthermore, during isometric abduction at 90° humerothoracic elevation, the acromiohumeral distance in the symptomatic shoulder was 3.0 mm smaller than the asymptomatic contralateral side. This

finding suggests that during muscle contraction, symptomatic individuals may lack the ability to offset the superior component of the deltoid muscle force resulting in superior translation and a reduction in subacromial space. Or conversely, the symptomatic subjects may have an impairment in the function of the middle and lower trapezius muscles to stabilize the scapula during deltoid muscle activity resulting in scapular downward rotation and a reduction in subacromial space. These potential explanations for the group differences during muscle contraction, however, remain theoretical as kinematics were not quantified in the study and the effect of scapular movement on subacromial proximities remains unclear. Nevertheless, the results of the study suggest investigating subacromial proximities during muscle contraction may be more sensitive to identifying group differences than during passive positions.

Using methods similar to Giphart et al. (2012), Bey et al. (2007) compared 3D acromiohumeral distance in 11 subjects 12-16 weeks post acromioplasty and repair of an isolated full-thickness supraspinatus tear. Each subjects' surgical shoulder was compared to their asymptomatic contralateral shoulder during humeral elevation in the coronal plane. As in previous studies, the acromiohumeral distance decreased with increasing angles of humerothoracic elevation (Giphart et al., 2012; Graichen et al., 1999a; Graichen et al., 1999b; Hebert et al., 2003) and the difference between shoulders increased above approximately 75° humerothoracic elevation. Throughout the range of motion, the minimum distance in the symptomatic shoulder was approximately 0.5 mm larger on average than in the asymptomatic shoulder. It is likely this finding is related to the acromioplasty performed at the time of the rotator cuff repair. Further, the angle of

absolute minimum distance occurred at approximately 90° humerothoracic elevation regardless of the shoulder tested. However, the researchers reported the supraspinatus footprint was only under the lateral acromion between approximately 42-54° humerothoracic elevation further strengthening the importance of interpreting the absolute minimum distance in combination with the location of the supraspinatus footprint.

In general, studies investigating subacromial proximities are limited by 2D measures of proximities, bone-to-bone acromiohumeral distances, or both. Further, the use of a minimum distance vector limits the description of subacromial space to a single dimension, and to a pair of points along the surfaces of the acromion undersurface and rotator cuff insertion. In reality, the entirety of both surfaces may be in proximity and reducing the description to a single dimension may likely underrepresent the phenomenon of subacromial rotator cuff compression. As such, expanding descriptions of proximity to multidimensional metrics provide better descriptions of subacromial rotator cuff compression risk throughout a range of motion. In light of these considerations, a modeling study was conducted by Lawrence et al. (2017) to investigate the impact of glenohumeral kinematics on subacromial proximities during a simulated functional reaching task. The authors utilized subject-specific 3D anatomical models reconstructed from MR images acquired from 20 subjects, 10 of whom had a history of shoulder pain consistent with a diagnosis of "impingement syndrome". The anatomical models consisted of the humerus, scapula, coracoacromial ligament, and supraspinatus tendon. Glenohumeral motions were simulated using the mean kinematics of asymptomatic

individuals collected during a functional reaching task (Braman et al., 2009). Among the angles compared statistically, the authors found the supraspinatus tendon was in closest proximity to the coracoacromial arch at 30° humerothoracic elevation (~0.7 mm) and remained in close proximity throughout the range between 0° and 60° humerothoracic elevation (<1.8 mm). Furthermore, 50% of subject models resulted in contact between the supraspinatus tendon and coracoacromial arch during the simulated motion. A history of symptoms did not influence either the magnitude of the minimum distance or the volume of the supraspinatus tendon that intersected with the coracoacromial arch, suggesting any underlying anatomical differences between groups did influence subacromial proximities. By quantifying subacromial proximities directly to the supraspinatus tendon, this study provided a more precise estimate of the range of humerothoracic elevation in which the supraspinatus is at risk for compression.

Scapular Dyskinesia

Silva et al. (2010) compared acromiohumeral distance between junior elite tennis players with and without scapular dyskinesia. Each subject underwent screening for scapular dyskinesia based on a visual screen of active shoulder motion (Kibler & McMullen, 2003). Acromiohumeral distance was quantified using ultrasonography while the arm was at the side and at 60° humerothoracic elevation, both with the humerus positioned in internal rotation. The researchers found that, on average, shoulders with dyskinesia experienced a higher reduction in acromiohumeral distance when the arm was elevated to the 60° position than shoulders without dyskinesia (dyskinesia: 1.9 mm or 21.4%; without dyskinesia: 1.4 mm or 16%). Although this study utilized a 2D measure

of acromiohumeral distance, it establishes scapular movement abnormalities may impact measure of subacromial space. However, because dyskinesia was defined without reference to a specific scapulothoracic motion (e.g. upward rotation), it is difficult to appreciate the impact of specific abnormalities of motion on subacromial proximities.

In a similar study, Seitz et al. (2012b) utilized ultrasonography to investigate the impact of scapular dyskinesia on subacromial space by comparing acromiohumeral distance between asymptomatic controls and asymptomatic subjects classified as having scapular dyskinesia based on a clinical examination (McClure et al., 2009; Tate et al., 2009). For both groups, the minimum acromiohumeral distance occurred at 45° humerothoracic elevation. However, a mean difference between groups of 0.4 mm was not significant at any angle of humerothoracic elevation (rest, 45°, 90°). This lack of group difference in acromiohumeral distance may be due to using "dyskinesia" as an inclusion criterion vs. classifying based on a specific scapular movement abnormality. Indeed, a comparison of scapular orientation between groups did not find significant differences at any angle of scapulothoracic elevation despite group classification based on a common clinical examination technique to detect abnormal scapular motion. The lack of significance does not appear to be due to insufficient statistical power to detect a clinically meaningful difference in kinematics as the largest (non-significant) difference between groups was 2.2° for posterior tilt. In addition, differences between the classification and data collection protocols may potentially confound the study's ability to investigate the effect of dyskinesia on acromiohumeral distances. Specifically, classification of dyskinesia was performed dynamically during loaded and unloaded

flexion and abduction, and data collection involved static assessment of kinematics and acromiohumeral distance during unloaded scapular plane abduction. Therefore, it is possible the scapular dyskinesia during data collection was not elicited to the extent that resulted in the dyskinesia classification thereby nullifying any differences in kinematics and measures of subacromial space.

Conclusion

Despite the volume of research that has investigated both shoulder complex kinematics and subacromial space in individuals with shoulder pain, the fundamental question of whether scapular movement abnormalities impact subacromial rotator cuff compression risk remains unanswered. In addition to methodological differences between studies, the lack of consistent findings likely relates to the non-homogenous nature of the clinical diagnosis of impingement syndrome and not classifying study groups based on particular scapulothoracic movement abnormalities. Evidence suggests several subgroups of patients exist within the broader clinical diagnosis of "impingement syndrome" (Ludewig et al., 2017). Therefore, studying subacromial proximities in these more homogenous patient populations may provide clearer insight on the impact of shoulder kinematics on subacromial rotator cuff compression. Given a reduction in scapulothoracic upward rotation is the most common finding in comparative kinematic studies (Endo et al., 2001; Lawrence et al., 2014a; Ludewig et al., 2000) and is frequently theorized to directly impact subacromial space (Kibler et al., 2013; Ludewig et al., 2011; Ludewig et al., 2009b; Michener et al., 2003; Seitz et al., 2011), investigating this relationship is a logical first step towards understanding the movement-related

mechanisms of rotator cuff pathology. Further, understanding how scapulothoracic motion is produced will provide a foundation from which to develop diagnostic and treatment paradigms in an effort to continually improve patient outcomes.

Chapter 3: Validation of single-plane fluoroscopy and 2D/3D shape-matching for quantifying shoulder complex kinematics (Aim 1)[1]

The investigation of many clinical questions requires precise measurement of human movement. Traditional methods of quantifying kinematics are often subject to errors due to skin motion artifact, which adds irrelevant variability that may confound underlying relationships. Fluoroscopy and 2D/3D shape-matching is an emerging approach to non-invasively quantify human motion. However, data collection and processing protocols are exceedingly complex and require internal validation prior to broad utilization. Therefore, the first aim of this thesis is to develop and validate a protocol for tracking shoulder complex kinematics using single-plane fluoroscopy and 2D/3D shape-matching.

[1] Published in *Medical Engineering and Physics*. 52:69-75. 2018 (PMID: 29229406).
Co-authors: Arin M. Ellingson, PhD and Paula M. Ludewig, PT, PhD

Abstract

Study Design: Laboratory controlled study

Background: Fluoroscopy and 2D/3D shape-matching has emerged as the standard for non-invasively quantifying kinematics. However, its accuracy has not been well established for the shoulder complex when using single-plane fluoroscopy.

Objective: The purpose of this study was to determine the accuracy of single-plane fluoroscopy and 2D/3D shape-matching for quantifying full shoulder complex kinematics.

Methods: Tantalum markers were implanted into the clavicle, humerus, and scapula of four cadaveric shoulders. Biplane radiographs were obtained with the shoulder in five humerothoracic elevation positions (arm at the side, 30°, 60°, 90°, maximum). Images from both systems were used to perform marker tracking, while only those images acquired with the primary fluoroscopy system were used to perform 2D/3D shape-matching. Kinematics errors due to shape-matching were calculated as the difference between marker tracking and 2D/3D shape-matching and expressed as root mean square (RMS) error, bias, and precision.

Results: Overall RMS errors for the glenohumeral joint ranged from 0.7-3.3° and 1.2-4.2 mm, while errors for the acromioclavicular joint ranged from 1.7-3.4°. Errors associated with shape-matching individual bones ranged from 1.2-3.2° for the humerus, 0.5-1.6° for the scapula, and 0.4-3.7° for the clavicle.

Conclusion: The results of the study demonstrate that single-plane fluoroscopy and 2D/3D shape-matching can accurately quantify full shoulder complex kinematics in static positions.

Introduction

Quantifying shoulder kinematics is often fundamental to many clinical questions regarding the development and/or progression of orthopaedic conditions including rotator cuff disease and multidirectional instability. Traditional methods to non-invasively quantify kinematics include optical and electromagnetic motion capture. However, these methods are subject to skin motion artifact (Hamming et al., 2012; Karduna et al., 2001; Ludewig et al., 2002). Other studies quantified kinematics by attaching motion sensors to pins inserted directly into bones (Ludewig et al., 2009a; McClure et al., 2001). While these studies provide a more accurate description of joint motion, they are limited by small sample sizes due to the invasive nature of the methodology. Consequently, larger studies investigating clinically-focused research questions are not feasible.

More recently the use of fluoroscopy and model-based image registration (i.e. 2D/3D shape-matching) has become the standard for non-invasively quantifying joint motion (Bey et al., 2006; Giphart et al., 2012; Miranda et al., 2011; Tashman & Anderst, 2003). Biplane fluoroscopy provides highly precise estimates of glenohumeral motion with errors less than 1.0° and 0.5 mm (Giphart et al., 2012). However, the use of two radiographic systems increases the dose to the subject compared to using a single plane. Further, the use of single plane fluoroscopy does not require specialized biplane radiographic systems but can be employed using common clinical c-arm systems.

In exchange for reduced radiation dose, single plane fluoroscopy generally results in lower kinematic accuracy (You et al., 2001). However, its accuracy for quantifying shoulder kinematics is not well established despite its use in several studies (Kon et al.,

2008; Matsuki et al., 2014; Matsuki et al., 2011; Matsuki et al., 2012; Nishinaka et al., 2008). Only two studies have investigated the accuracy for glenohumeral joint motion (Matsuki et al., 2012; Zhu et al., 2012). Both studies utilized a single shoulder specimen which may limit the generalizability of the results given the substantial variation in shoulder anatomy that exists between individuals, and also between sides within individuals (Auerbach & Raxter, 2008; Daruwalla et al., 2010; Jacobson et al., 2015) and the inherent dependency of shape-matching on anatomical morphologies. Furthermore, no study has investigated the accuracy of tracking clavicular kinematics. This hinders a comprehensive understanding of shoulder complex motion given the clavicle's important role in shoulder complex function (Dvir et al., 1978; Ludewig et al., 2009a; Teece et al., 2008). Therefore, the purpose of this study was to determine the accuracy of single plane fluoroscopy and 2D/3D shape-matching for quantifying full shoulder complex kinematics using biplane marker tracking (i.e. radiostereometric analysis, or RSA) as the criterion reference.

Methods

Instrumentation

The primary imaging system utilized in this study was a Philips BV Pulsera mobile c-arm fluoroscopy unit (99.5 cm source-to-image distance (SID), 30 cm field-of-view (FOV), 1024 × 1024 image resolution). The secondary imaging system was a custom video-radiography system (152 cm SID, 40.6 cm FOV, 1080 × 1080 image resolution). The imaging systems were positioned with an 80° inter-beam angle and with the image intensifier of the primary system 20 cm off the face of the secondary system

(**Figure 11**). This gap allowed for a larger imaging volume without decreasing the source-to-object distance (SOD) of the primary imaging system, and thus preventing unnecessary magnification and reduction of the functional FOV.

Marker Tracking Validation

Prior to the *in vitro* validation experiment, the accuracy of tracking markers within the 3D imaging volume was verified using an acrylic validation object that was precision milled with six 1-mm diameter tantalum markers positioned in two clusters of three markers. The distances between markers and marker clusters were chosen to simulate the approximate distances between markers placed into the clavicle and scapula during the *in vitro* experiments. Two orthogonal coordinate systems were constructed from the two sets of marker clusters using the known 3D marker coordinates.

Images of a distortion grid and calibration cube were acquired using both radiographic systems to correct for image distortion and to define the imaging geometry of the biplane system (Brainerd et al., 2010). The validation object was positioned and imaged in 30 positions and orientations throughout the biplane imaging volume. Image distortion correction, 3D volume calibration, and biplane marker digitization were performed using XMALab 1.3.3 software (Knorlein et al., 2016). Following digitization, the 3D coordinates of each marker were exported for data analysis using custom MATLAB codes (The Mathworks, Inc.; Natick, USA).

The Euclidean distance between marker pairs (i.e. inter-bead distance) was calculated from the 3D marker coordinates. The relative position and orientation of the two marker clusters were also determined. Errors in inter-bead distances and relative

marker cluster position and orientation were determined based on the known marker coordinates and those estimated from digitization. Errors were expressed as RMS error (i.e. the square root of the mean squared error), bias (i.e. the mean error), and precision (i.e. the standard deviation of the error).

Single Plane 2D/3D Shape-Matching Validation

Two cadaveric specimens consisting of the thorax and bilateral upper extremities (4 shoulders total) were acquired (1 male, 1 female; ages at death: 80 and 58 years, respectively). Tantalum markers (1 mm diameter) were inserted into the clavicle, scapula, and humerus through sharp dissection. Resected soft tissue was returned to its anatomical position and sutured following marker placement. The specimens were then secured to a chair in an upright seated position allowing for full shoulder complex motion.

The specimens were oriented in the biplane imaging volume such that the scapula was approximately parallel to the image intensifier of the primary imaging system. The arm was elevated and held passively using a pulley system at five static positions: arm at side (i.e. minimum), 30°, 60°, 90°, and maximum humerothoracic elevation. Humerothoracic elevation angles were verified using a clinical goniometer within ±5° of the target angle. Images were acquired using both radiographic systems with the shoulder at each elevated position. All images acquired with the primary imaging system used high definition fluoroscopy (continuous x-ray mode) and the system's automatic kV/mA function (50-60 kV, 4.0-4.5 mA).

Computed topography (CT) scans of the entire shoulder complex were acquired for each specimen using a Siemens SOMATOM Sensation 64 CT scanner (140 kVp, 0.6

mm slice thickness, 315 mA, 512 × 512 resolution). Three-dimensional bone models of the humerus, scapula, and clavicle were created using Mimics software (Materialise NV; Leuven, Belgium). The tantalum markers were included in the segmented bone masks such that when the 3D bone models were rendered the cortical surface of the bone did not have any evidence of discontinuity from the marker, thus masking bead placements which could create user bias during shape-matching.

Anatomical coordinate systems were constructed by digitizing landmarks on the 3D models per the recommendations of the International Society of Biomechanics (Wu et al., 2005) and expressed relative to the CT coordinate system. Due to the difficulty of consistently identifying three non-collinear points on the clavicle, the third clavicular point was defined 5 cm superior to the center of mass along the clavicle's superior/inferior inertial axis. The geometric center of the humeral head was determined using a least-squares sphere fit to the articular surface. The origins of the humeral and scapular coordinate systems were placed at the geometric center of the humeral head, and the origin of the clavicular coordinate system was placed at the acromioclavicular joint. The locations of marker centroids were digitized on the CT images allowing for the definition of a temporary marker-based coordinate system for each bone. The transformation between the anatomical coordinate system and the temporary marker-based coordinate system was calculated for each bone segment using the CT scanner's coordinate system as the common reference frame.

Radiographic image distortion correction, calibration, and biplane marker digitization were performed using XMALab software (Knorlein et al., 2016) as

previously described. Temporary marker-based coordinate systems were constructed for each segment in each radiographic frame and transformed to anatomical coordinate system using the transformation previously calculated. This process assumes the markers remained rigidly fixed in the bone, which was verified by comparing the precision of the inter-bead distances to those obtained during the marker validation experiment. Model registration was performed using the undistorted images acquired from the primary fluoroscopy system using an open source model-image registration software (JointTrack, available at: https://sourceforge.net/projects/jointtrack/) (**Figure 12**).

A custom MATLAB code was used to process and analyze the kinematic data. Glenohumeral joint position and orientation were described as the humeral anatomical coordinate system relative to the scapular anatomical coordinate system using an X,Z',Y" rotation sequence (Phadke et al., 2011). Acromioclavicular joint orientation was described as the scapular anatomical coordinate system relative to the clavicular anatomical coordinate system using an Y,X',Z" rotation sequence (Wu et al., 2005). The error in joint kinematics due to shape-matching was calculated at each humerothoracic position as the difference between marker tracking and 2D/3D shape-matching. All errors were expressed as RMS error, bias error, and precision. Overall RMS error, bias error, and precision were also calculated by pooling data from all humerothoracic positions. To investigate kinematics errors further, the error due to shape-matching individual bone segments was described by calculating the displacement between the segment's anatomical coordinate systems as defined by marker tracking and 2D/3D shape-matching.

Results

Marker Tracking Validation

The RMS error for the inter-bead distance of the validation object across trials was 0.2 mm with a bias (± precision) of -0.1 mm (± 0.1 mm). This corresponded to relative orientation and position RMS errors between the two marker clusters of 0.2° and 0.3 mm, respectively. The bias error for relative marker cluster orientation and position was 0.0° (± 0.1°) and 0.1 mm (±0.2 mm), respectively.

2D/3D Shape-Matching Validation

One frame was excluded in one specimen due to marker drop-out for the minimum humerothoracic elevation position. The average maximum angle of glenohumeral elevation was 82.3° (±5.0°), which corresponded to an average humerothoracic elevation of 109° ± 6.9°.

For the acromioclavicular joint, the overall RMS errors across all humerothoracic elevation angles was 1.7° for internal rotation, 3.4° for upward rotation, and 2.0° for tilt. RMS error at each angle of humerothoracic elevation are shown in **Figure 13A**, and bias and precision are presented in **Table 1.**

For glenohumeral joint orientation, the overall RMS errors across all humerothoracic elevation angles was 0.7° for elevation, 2.6° for plane of elevation, and 3.3° for axial rotation. RMS error at each angle of humerothoracic elevation are shown in **Figure 13B**, and bias and precision are presented in **Table 1.** The overall RMS error for glenohumeral geometric center position was 4.2 mm along the anterior/posterior axis, 1.2 mm along the superior/inferior axis, and 1.8 mm along the medial/lateral axis. RMS

error, bias, and precision at each angle of humerothoracic elevation are presented in **Table 2**.

RMS errors representing the angular error in shape-matching each individual bone segment are presented in **Figure 14**. RMS errors ranged between 1.2-3.2° for the humerus, 0.5-1.6° for the scapula, and 0.4-3.7° for the clavicle. Corresponding bias and precision values are presented in **Table 3**. Overall RMS errors representing the positional error in shape-matching ranged between 4.2-8.1 mm for the humerus and 1.6-9.3 mm for the scapula. RMS error, bias, and precision at each angle of humerothoracic elevation are presented in **Table 4**.

Discussion

This study provides a comprehensive analysis of the accuracy of using single plane fluoroscopy and 2D/3D shape-matching for quantifying static shoulder complex kinematics. Importantly, the study establishes the methodology as a viable option for quantifying static shoulder complex kinematics. This study also demonstrates the process can be accomplished using clinically available imaging technology, which strengthens the potential to successfully translate this methodology to clinical application of identifying movement disorders. Furthermore, by describing both joint and bone segment accuracy using multiple error metrics, the results of the study can help understand the implications of the errors when the methodology is used to describe shoulder complex kinematics *in vivo*.

Only two previous studies have investigated the accuracy of tracking glenohumeral kinematics using single plane fluoroscopy (Matsuki et al., 2012; Zhu et al.,

2012). In general, the results of these investigations are comparable to the current study. Specifically, Matsuki (2012) found glenohumeral RMS errors of 0.8-3.7° and 0.5-1.5 mm, while Zhu (2012) found bias errors for the humerus and scapula of 0.5-2.0° and 0.2-5.3 mm. However, both studies are limited by the use of only one cadaveric shoulder resulting in errors that may not be generalizable due to the variation in shoulder complex anatomy both between and within individuals (Auerbach et al., 2008; Daruwalla et al., 2010; Jacobson et al., 2015) (**Figure 12**). Additionally, both studies investigated dynamic shoulder motion while static trials were utilized in the current study due to the inability to sync the primary and secondary radiographic systems in the biplane configuration. Although dynamic trials may introduce image blur that may affect shape-matching accuracy, the comparable results between the current study and previous work (Matsuki et al., 2012; Zhu et al., 2012) suggests dynamic motion may not significantly affect shape-matching accuracy compared to the error associated with having a single imaging plane.

Comparison of individual kinematic parameters between fluoroscopy validation studies is often complicated due to the use of "in-plane" and "out-of-plane" terminology. While use of these terms is common and accepted for the primarily uniaxial motion of the knee joint, they are an oversimplification of shoulder complex motion. When the image receptor is positioned parallel to the scapula and the humerus elevates in the scapular plane, glenohumeral elevation is often considered "in-plane". However, the humerus externally rotates considerably as it elevates (Ludewig et al., 2009a) altering the degree to which a motion is considered in- or out-of-plane. Additionally, the complex geometry of

the shoulder girdle makes this terminology even more difficult to interpret. For example, scapular upward/downward rotation could be considered an "in-plane" motion if positioned parallel to the image receptor. However, when it is described relative to the clavicle as is done for acromioclavicular joint motion, scapular upward rotation can no longer be considered "in plane" due to sternoclavicular retraction, which places the clavicle oblique to the imaging plane. These considerations emphasize the need for specific, anatomical descriptions of errors from validation studies.

Importantly, this study demonstrates the clavicle can be accurately tracked using single plane 2D/3D shape-matching. With surface sensors, it is generally recommended to limit tracking to humeral elevation angles lower than 115° due to skin motion artifact affecting axial rotation (Ludewig et al., 2004). Given axial rotation is the primary motion of the clavicle (Ludewig et al., 2009a), accurately quantifying this rotation is critical to understanding the contribution of clavicular motion to overall shoulder complex function. Although it is unknown whether the accuracy for tracking the clavicle found in the current study will be similar for dynamic trials, this methodology looks promising for tracking clavicular motion throughout the range of motion because RMS errors did not appear to be influenced by humerothoracic elevation angle (**Figure 14**).

The current study also offered a more comprehensive analysis of shape-matching errors than previous works that report either bias and precision (Zhu et al., 2012) or RMS error (Matsuki et al., 2012). Although subtle, the differences between these error metrics have very important implications on interpreting validation studies. Specifically, RMS error describes the average magnitude of the error and therefore provides an estimate of

accuracy. In contrast, bias error describes the mean error and can appear artificially small if errors are not consistently positive or negative (i.e. systematic error). For example, glenohumeral axial rotation bias error in the current study is 0.0°, while the RMS is 3.3°. This suggests glenohumeral axial rotation errors are not biased but are on average 3.3° from their true value. In comparison, the similar magnitude of the RMS and bias errors for glenohumeral medial/lateral position indicates a systematic error of approximately 1.5 mm resulting in a more medial position relative to the scapula than its true position. These examples highlight the need to report both metrics when describing the accuracy of measurement systems.

Calculating errors associated with both the joint and individual bone segments allows for investigation into potential sources of error, which has not been possible in reviewing the results of previous studies. For example, acromioclavicular upward rotation was found to have the highest overall rotation RMS error value (3.4°). According to the coupling theory (Teece et al., 2008), this acromioclavicular joint position is related to scapular upward/downward rotation and clavicular elevation/depression and axial rotation. Inspection of the RMS errors for scapular upward rotation error (0.5°) and clavicular elevation (0.6°) and axial rotation (3.7°) suggests the error in acromioclavicular upward rotation is likely due to error in shape-matching clavicle axial rotation. Likewise, the error associated with glenohumeral axial rotation appears to be due to shape-matching errors of humeral internal/external rotation as opposed to scapular internal/external rotation. Interpreting errors in this way is useful when working to

improve the accuracy of shape-matching by identifying the specific bone motion responsible for the resulting description of joint error.

Inspection of the bone data also brings to light the complexities of shape-matching each bone segment. Angular errors for the scapula and clavicle were generally lower than that for the humerus. For the scapula, this is likely a reflection of anatomical uniqueness of the bone as it has many structures that provide valuable information for shape-matching. In comparison, the clavicle does not have as many unique anatomical structures, however obtaining the radiographic image in the scapular plane helps visualize the crank shape of the clavicle (**Figure 12**). This provides information about the degree to which the clavicle is rotated about its long axis, which is difficult to visualize on a more A-P view when the clavicle appears more cylindrical. In contrast, the humerus offers less anatomical information to assist in shape-matching due to its long symmetrical shape, which results in higher shape-matching errors (**Figure 14**).

The preliminary experiment validating marker tracking is critical when using RSA to validate 2D/3D shape-matching as it determines how accurately markers can be tracked in 3D space. The current study found higher errors relative to the results of previous studies (Anderst et al., 2009; Brainerd et al., 2010; Tashman et al., 2003). These studies reported inter-bead distance bias errors up to ±0.02 mm and precision values up to 0.05 mm. However, expressing marker tracking accuracy in terms of inter-bead distance may be less meaningful because the metric is not in the units of our primary dependent variable (i.e. relative position and orientation). Developing coordinate systems from the marker clusters allowed marker tracking errors to be described in terms of relative

orientation (degrees) and position (mm). This analysis demonstrated that the errors associated with the orientation/position of the marker clusters are very small and within an acceptable tolerance, despite higher inter-bead distance errors.

This study has limitations that should be considered. First, the use of RSA to validate shape-matching has inherent limitations. The same images are used for marker tracking and shape-matching. As such, they are subject to the same distortion correction and calibration and any inaccuracies with these processes will not be known. While the results of the marker validation experiment provide an estimate of the magnitude of this error, an optimal validation experiment would have separate sources of error. However, the use of other systems such as electromagnetic sensors or optical markers would introduce additional differences associated with the unique definition of the coordinate systems from two different methodologies. Second, the accuracy of RSA as the gold standard in describing rotations about anatomical axes is limited by the resolution of the CT scan and metal artifact from the tantalum markers. This is because error in identifying the marker centroids on the CT scan will result in errors in defining the "true" orientation/position of the temporary marker-based coordinate system. This error will affect the transformation between the temporary marker-based coordinate system and the anatomical coordinate system, resulting in a systematic error in describing anatomical bone orientation/position. Therefore, it is possible the errors in defining the marker centroids increased the errors attributed to the 2D/3D shape-matching. Finally, although the study included more specimens than previous validation studies using single plane

fluoroscopy, additional specimens would likely improve the estimate of the error associated with shape-matching.

Overall, the results of the study demonstrate that single-plane fluoroscopy and 2D/3D shape-matching can accurately quantify shoulder complex motion. Furthermore, the methodology can be performed using clinically available technology. Future research is needed to quantify how the errors affect the result of kinematic models used to estimate parameters such as acromiohumeral distance, cartilage deformation, and joint forces and net muscle moments.

Table 1: Bias ± precision for Acromioclavicular and Glenohumeral Joint Orientations

	Acromioclavicular Joint			Glenohumeral Joint		
Position	**IR/ER**	**UR/DR**	**Tilt**	**Elevation**	**Plane of Elevation**	**Axial Rotation**
Min	0.3 ± 1.7	-0.3 ± 4.1	-0.9 ± 0.5	-0.3 ± 1.0	-0.5 ± 0.9	-0.3 ± 1.2
30°	1.1 ± 1.4	1.5 ± 3.2	-1.7 ± 2.1	-0.3 ± 0.2	-0.9 ± 2.4	1.0 ± 3.7
60°	0.0 ± 1.6	1.2 ± 3.7	-1.2 ± 0.7	0.1 ± 0.2	-1.4 ± 3.5	1.2 ± 3.0
90°	0.6 ± 1.8	0.5 ± 5.4	-0.2 ± 3.2	-0.4 ± 0.8	-1.7 ± 2.4	-1.3 ± 4.8
Max	0.1 ± 2.8	0.3 ± 1.9	-0.8 ± 1.9	0.0 ± 1.0	-0.9 ± 2.8	-0.8 ± 4.1
Overall	0.4 ± 1.7	0.7 ± 3.4	-0.9 ± 1.9	-0.2 ± 0.7	-1.1 ± 2.4	0.0 ± 3.4

Notes: All magnitudes in degrees. Positive bias values for the acromioclavicular joint indicates shape-matching overestimated external rotation, upward rotation, and anterior tilt as compared to marker tracking, or underestimated internal rotation, downward rotation, and posterior tilt. Positive bias values for the glenohumeral joint indicates shape-matching overestimated abduction, posterior plane of elevation, and external rotation as compared to marker tracking, or underestimated adduction, anterior plane of elevation, and internal rotation. Abbreviations: IR = internal rotation, ER = external rotation, UR = upward rotation, DR = downward rotation. Bias represents systematic errors or offsets.

Table 2: RMS Error (bias ± precision) for Glenohumeral Joint Position

Position	Anterior/ Posterior	Superior/ Inferior	Medial/ Lateral
Min	3.0 (1.0 ± 3.4)	1.4 (1.2 ± 1.0)	1.2 (-0.9 ± 0.9)
30°	3.8 (0.4 ± 4.4)	1.2 (0.3 ± 1.3)	1.7 (-1.5 ± 1.0)
60°	2.8 (2.2 ± 1.9)	0.9 (0.1 ± 1.0)	1.5 (-1.5 ± 0.3)
90°	5.6 (4.2 ± 4.3)	1.1 (0.2 ± 1.3)	2.1 (-1.7 ± 1.4)
Max	4.8 (3.7 ± 3.6)	1.2 (0.0 ± 1.3)	2.1 (-1.8 ± 1.2)
Overall	4.2 (2.4 ± 3.5)	1.2 (0.3 ± 1.1)	1.8 (-1.5 ± 1.0)

Notes: All magnitudes in mm. Positive bias indicates shape-matching resulted in a more posterior, inferior, and/or medial position of the humerus relative to the scapula as compared to marker tracking.

Table 3: Bias ± Precision for Humeral, Scapular, and Clavicular Bone Angular Error

Humerus			
	Elevation	**Plane**	**Axial Rotation**
Min	0.5 ± 0.7	0.1 ± 0.4	-0.4 ± 1.6
30°	0.8 ± 2.1	-0.2 ± 1.1	-1.4 ± 2.8
60°	1.3 ± 3.4	0.4 ± 0.7	-1.1 ± 3.4
90°	1.5 ± 1.3	0.4 ± 0.7	1.2 ± 5.0
Max	1.4 ± 2.4	0.0 ± 2.5	0.6 ± 3.8
Overall	1.1 ± 2.0	0.1 ± 1.2	-0.2 ± 3.3
Scapula			
	IR/ER	**UR/DR**	**Tilt**
Min	-0.3 ± 1.9	0.2 ± 0.3	0.5 ± 1.3
30°	-0.5 ± 1.4	-0.1 ± 0.4	0.0 ± 0.3
60°	0.1 ± 1.6	0.2 ± 0.3	0.1 ± 1.0
90°	-0.3 ± 1.7	-0.1 ± 0.3	-0.1 ± 1.1
Max	0.0 ± 2.3	0.6 ± 0.6	0.3 ± 0.3
Overall	-0.2 ± 1.6	0.2 ± 0.4	0.2 ± 0.8
Clavicle			
	Retraction	**Elevation**	**Axial Rotation**
Min	0.0 ± 0.1	-0.2 ± 1.0	-0.3 ± 3.8
30°	0.3 ± 0.6	-0.2 ± 0.6	-2.2 ± 3.5
60°	0.0 ± 0.2	0.0 ± 0.7	-1.8 ± 3.3
90°	0.4 ± 0.5	0.1 ± 0.5	-0.6 ± 6.0
Max	0.2 ± 0.4	0.2 ± 0.5	-1.0 ± 2.3
Overall	0.2 ± 0.4	0.0 ± 0.6	-1.2 ± 3.6

Notes: All magnitudes in degrees. Positive bias values for the humerus indicates shape-matching overestimated abduction, posterior plane of elevation, and external rotation as compared to marker tracking, or underestimated adduction, anterior plane of elevation, and internal rotation. Positive bias values for the scapula indicates shape-matching overestimated external rotation, upward rotation, and anterior tilt as compared to marker tracking, or underestimated internal rotation, downward rotation, and posterior tilt. Positive bias values for the clavicle indicates shape-matching overestimated retraction, elevation, and anterior axial rotation as compared to marker tracking, or underestimated protraction, depression, and posterior axial rotation. Abbreviations: IR = internal rotation, ER = external rotation, UR = upward rotation, DR = downward rotation.

Table 4: RMS Error (bias ± precision) for Humeral and Scapular Bone Position Error

	Anterior/Posterior	Superior/Inferior	Medial/Lateral
Humerus			
Min	2.7 (1.2 ± 3.0)	1.2 (0.6 ± 1.3)	4.8 (-3.4 ± 4.2)
30°	4.3 (-3.5 ± 3.0)	4.0 (-2.5 ± 3.6)	11.6 (9.8 ± 7.2)
60°	3.2 (-1.8 ± 3.1)	4.1 (-2.7 ± 3.6)	9.0 (7.1 ± 6.5)
90°	4.4 (-2.5 ± 4.1)	3.2 (-2.6 ± 2.2)	6.8 (5.6 ± 4.3)
Max	5.5 (-2.3 ± 5.8)	3.6 (-2.5 ± 2.9)	5.7 (4.4 ± 4.2)
Overall	4.2 (-1.9 ± 3.9)	3.5 (-2.1 ± 2.9)	8.1 (5.1 ± 6.4)
Scapula			
Min	5.9 (4.5 ± 4.7)	2.9 (2.4 ± 2.0)	1.9 (-1.6 ± 1.3)
30°	12.9 (-9.9 ± 9.5)	3.8 (-1.3 ± 4.2)	1.6 (0.0 ± 1.9)
60°	9.5 (-5.5 ± 9.0)	2.8 (-0.5 ± 3.1)	0.9 (-0.3 ± 1.0)
90°	7.2 (-2.5 ± 7.8)	2.6 (0.0 ± 3.0)	1.3 (-0.2 ± 1.4)
Max	8.6 (-1.2 ± 9.9)	3.5 (-0.2 ± 4.1)	2.2 (-0.1 ± 2.6)
Overall	9.3 (-3.3 ± 8.9)	3.2 (0.0 ± 3.3)	1.6 (-0.4 ± 1.6)

Notes: All magnitudes in mm. Positive bias indicates shape-matching resulted in a more posterior, inferior, and/or medial position of the bone segment compared to marker tracking.

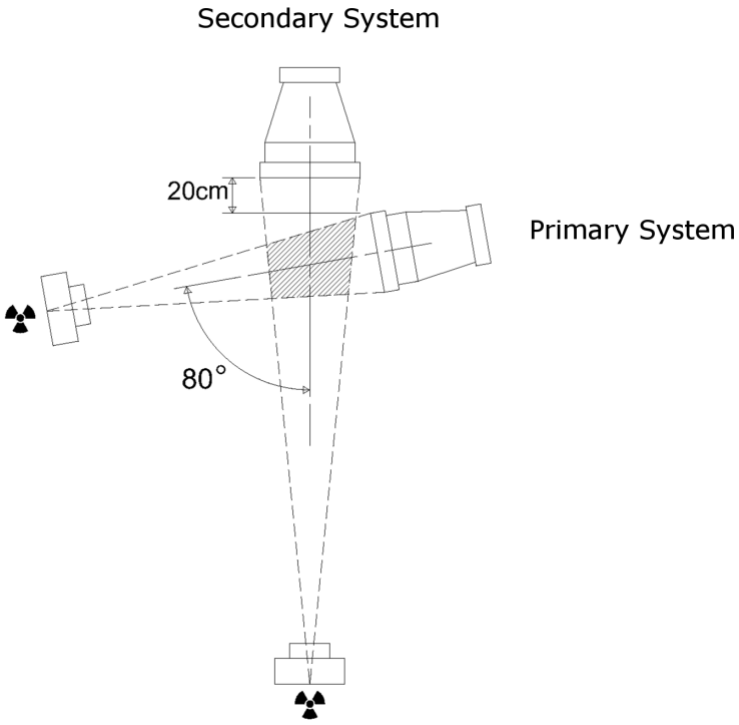

Figure 11: Configuration of the biplane radiographic setup (top view). Marker tracking was performed using images acquired from both the primary and secondary systems in the biplane configuration, while 2D/3D shape-matching utilized images only from the primary fluoroscopy system.

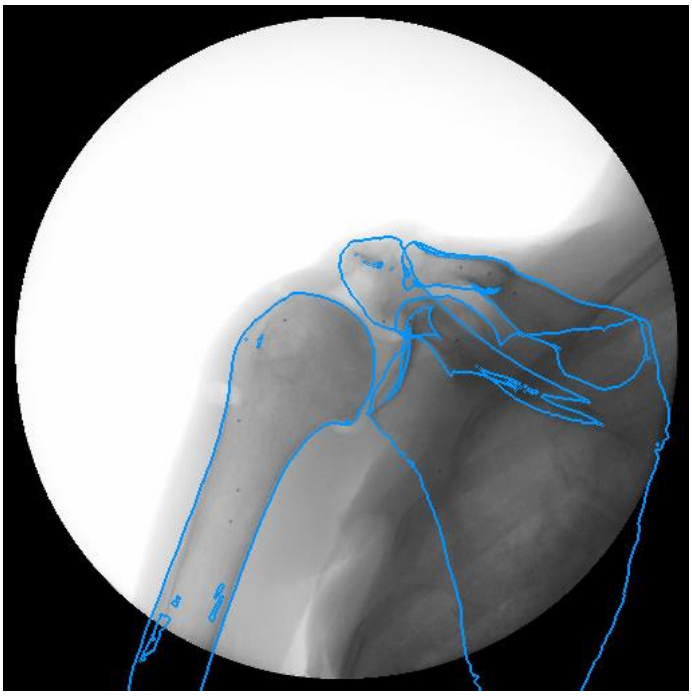

Figure 12: Example of shape-matched humerus, scapula, and clavicle at the minimum position of humerothoracic elevation. Figure demonstrates the crank shape of the clavicle can be visualized when the subject is placed such that the scapula is approximately parallel to the image intensifier. The image also shows an example of anatomical variability in that the specimen has an extremely sloped humeral greater tuberosity compared to the expected relatively flat superior surface.

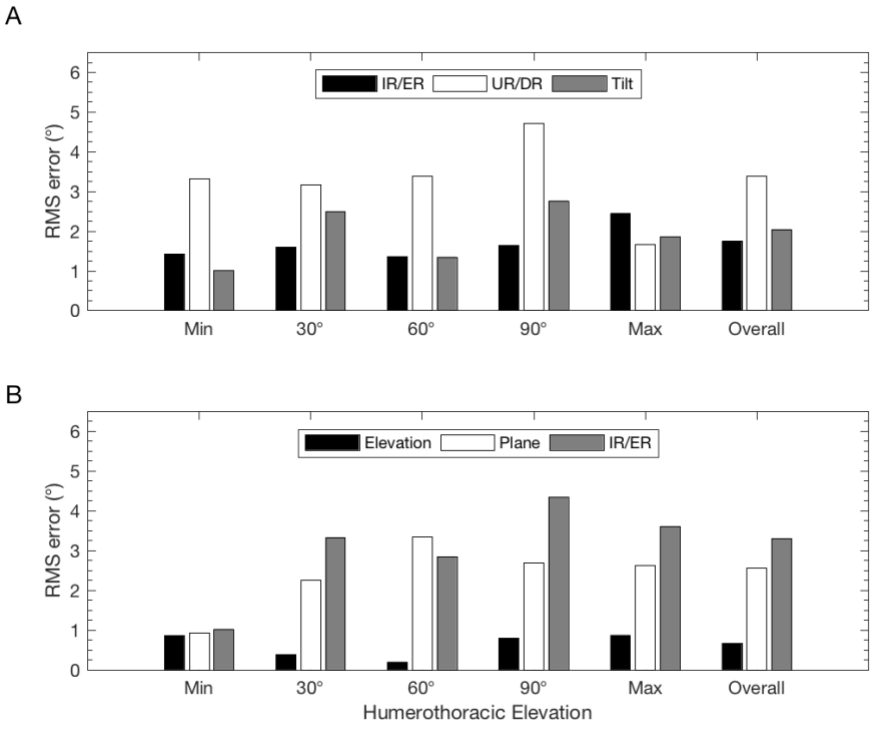

Figure 13: RMS errors for orientation of the acromioclavicular and glenohumeral joints across humerothoracic elevation angles. **A)** acromioclavicular and **B)** glenohumeral Abbreviations: IR = internal rotation, ER = external rotation, UR = upward rotation, DR = downward rotation.

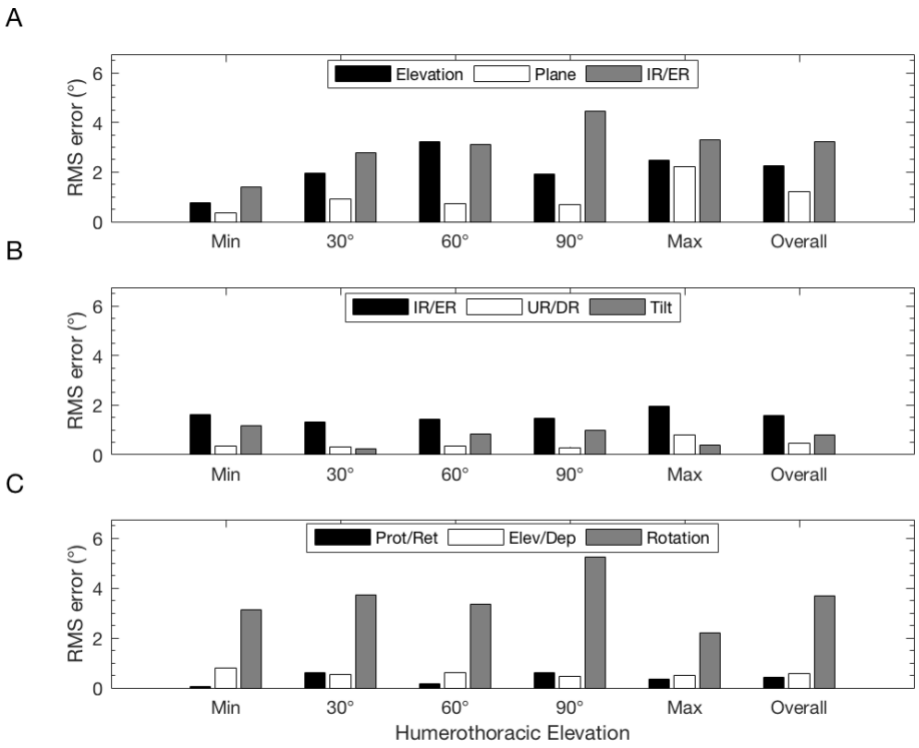

Figure 14: RMS errors representing the angular difference between the anatomical coordinate system from marker tracking and shape-matching for the humerus, scapula, and clavicle across humerothoracic elevation angles. **A)** humerus, **B)** scapula, and **C)** clavicle Abbreviations: IR = internal rotation, ER = external rotation, UR = upward rotation, DR = downward rotation, Prot = protraction, Ret = retraction, Elev = elevation, Dep = depression.

Chapter 4: The impact of decreased scapulothoracic upward rotation on subacromial proximities (Aim 2)

Many theories exist regarding the pathogenesis of rotator cuff disease. Abnormal scapular motion has long been considered a primary contributor. In particular, decreased scapulothoracic upward rotation is believed to increase risk for rotator cuff disease by reducing the magnitude of the subacromial space during arm motion. However, few studies have directly tested the movement-related mechanisms of rotator cuff disease. This gap in knowledge impacts our ability to maximize clinical outcomes by targeting treatment to the underlying cause. Therefore, the second aim of this thesis is to determine the impact of decreased scapulothoracic upward rotation on subacromial proximities.

Abstract

Study Design: Cross sectional observational study.

Background: Decreased scapulothoracic upward rotation has been theorized to increase an individual's risk for mechanical rotator cuff compression by reducing subacromial proximities. However, the impact of decreased scapulothoracic upward rotation on subacromial proximities has not been tested during dynamic *in vivo* shoulder motion.

Objectives: Determine the impact of decreased scapulothoracic upward rotation on subacromial proximities.

Methods: Shoulder kinematics were quantified in 40 participants classified as having high or low scapulothoracic upward rotation during scapular plane abduction using single-plane fluoroscopy and 2D/3D shape-matching. For each subject, 3D bone models of the humerus and scapula were reconstructed from MR images and animated with the subjects' glenohumeral kinematics. Subacromial proximities were calculated between the coracoacromial arch and rotator cuff insertion then normalized to the subjects' rotator cuff tendon thickness. The prevalence of contact between the coracoacromial arch and rotator cuff was also quantified. The effect of decreased scapulothoracic upward rotation on subacromial proximities was assessed using two-factor mixed-model ANOVAs.

Results: Subacromial proximities were generally smallest below 90° humerothoracic elevation. The difference between groups in normalized minimum distance was dependent on the angle of humerothoracic elevation ($p = 0.048$). With the arm at the side, the normalized minimum distance for participants in the low scapulothoracic upward rotation group was 34.8% smaller compared to those in the high upward rotation group (p

= 0.049). Contact between the coracoacromial arch and rotator cuff tendon occurred in 45% of subjects.

Conclusion: Decreased scapulothoracic upward rotation shifts the range of risk for subacromial rotator cuff compression to lower angles. However, the low prevalence of contact between the coracoacromial arch and rotator cuff tendon suggests subacromial compression may not be a common method for rotator cuff injury during unloaded humeral elevation in the scapular plane.

Introduction

Shoulder pain is a common condition for which patients often seek treatment (Feleus et al., 2008). The traditional approach for diagnosing shoulder pain involves attempting to identify the underlying pathoanatomic cause. The majority of patients with shoulder pain have evidence of degenerative rotator cuff disease (Freygant et al., 2014), yet simply identifying the rotator cuff as a potential source of pain proves insufficient to direct medical and rehabilitation treatment strategies (Braman et al., 2014; Ludewig et al., 2017; Ludewig et al., 2013; Schellingerhout et al., 2008). Indeed, randomized controlled trials of surgical and exercise interventions for individuals given a diagnosis of rotator cuff "impingement" or "tendonitis" often report an average improvement of only 50% in functional outcome measures (Camargo et al., 2015; Haahr et al., 2005; Struyf et al., 2013). This suggests current intervention strategies based on pathoanatomic diagnoses may be insufficient to maximize rehabilitation outcomes and patient quality of life.

Diagnosing musculoskeletal conditions based on movement impairments has been proposed to more directly link pathology with an underlying cause, and therefore diagnosis to treatment (Ludewig et al., 2017; Ludewig et al., 2013; Sahrmann et al., 2017). Numerous studies have shown that individuals with shoulder pain move differently than asymptomatic individuals, with the following potential movement-based subgroups identified: decreased scapulothoracic upward rotation (Endo et al., 2001; Lawrence et al., 2014a; Ludewig et al., 2000), increased scapulothoracic upward rotation (McClure et al., 2006; Sousa Cde et al., 2014), decreased scapulothoracic posterior tilt (Ludewig et al., 2000; Lukasiewicz et al., 1999), increased scapulothoracic posterior tilt

(McClure et al., 2006; Sousa Cde et al., 2014), and increased glenohumeral translations (Lawrence et al., 2014b). These movement-based subgroups may influence mechanisms of rotator cuff pathology in different ways. For example, it has long been hypothesized that a reduction in scapulothoracic upward rotation increases an individual's risk for subacromial rotator cuff compression (Ludewig et al., 2000), which occurs when the rotator cuff becomes compressed under the coracoacromial arch during shoulder movement (Neer, 1983). However, relatively few studies have investigated the impact of specific movement abnormalities on mechanisms of joint and soft tissue injury.

One study, by Karduna et al. (2000) utilized a cadaveric model to investigate the impact of reducing scapular upward rotation on subacromial proximities when the arm was positioned at 90° humerothoracic elevation and maximal internal rotation. The authors found that reducing scapular upward rotation increased subacromial proximities, however the angle of humerothoracic elevation suggests the rotator cuff insertions may have already cleared the acromion (Bey et al., 2007; Giphart et al., 2012; Lawrence et al., 2017). Seitz et al. (2012a) altered scapulothoracic position during a scapular assistance test and found an increase in scapulothoracic upward rotation and posterior tilt significantly increased acromiohumeral distance at 45° humerothoracic elevation. However, the study is limited by static arm positions and the use of a 2D ultrasonic measure of acromiohumeral distance.

The apparent conflict between the results reported by Karduna (2000) and Seitz (2012a) reflects the inherent complexity of studying the effect of scapulothoracic kinematics on subacromial proximities. Ultimately, subacromial proximities are

dependent upon glenohumeral relationships (i.e. kinematics and anatomy). When the effect of scapulothoracic kinematics on subacromial proximities are studied at particular angles of humerothoracic elevation, the influence of scapulohumeral rhythm (Inman et al., 1944) confounds the analysis. For example, if an individual is in decreased scapulothoracic upward rotation, this would coincide with increased glenohumeral elevation for a given angle of humerothoracic elevation compared to an individual in increased scapulothoracic upward rotation. Therefore, the impact of decreased scapulothoracic upward rotation on subacromial proximities likely depends on the angle of humerothoracic elevation at which the movement impairment is observed. Ultimately, there remains a critical need to identify whether abnormal shoulder movement contributes to the development of rotator cuff disease and if so, how, so that we may develop more targeted rehabilitation strategies and improve clinical outcomes.

The purpose of this study was to determine the impact of decreased scapulothoracic upward rotation on subacromial proximities. It was hypothesized that participants classified as having low scapulothoracic upward rotation would have significantly decreased subacromial proximities when the arm was at the side and at 30° humerothoracic elevation, and increased subacromial proximities at 60° and 90° humerothoracic elevation compared to participants classified as having high scapulothoracic upward rotation.

Methods

Study Participants

Two hundred ten individuals were recruited from the university community and local physical therapy clinics and screened for initial eligibility using REDCap electronic data capture tools hosted by the University of Minnesota (Harris et al., 2009) (**Appendix E**). Of these individuals, 82 met the initial eligibility criteria and underwent a clinical examination to finalize eligibility. This examination included a scapular movement screen, shoulder range of motion, strength, clinical special tests, and when indicated, a cervical spine screen (**Appendix E**). Sixty participants met the inclusion/exclusion criteria (**Table 5**) and proceeded to data collection. To ensure a broad distribution of scapulothoracic upward rotation and subacromial proximities, 30 of these participants were symptomatic with signs and symptoms consistent with a clinical diagnosis of "impingement syndrome" (age: 32.4 ± 8.8 years, 46.7% male, 40% tested on dominant side, BMI: 24.8 ± 4.1 kg/m^2), and the remaining had no history of pain in either shoulder (age: 32.7 ± 8.3 years, 46.7% male, 40% tested on dominant side, BMI: 23.9 ± 2.7 kg/m^2). Symptomatic and asymptomatic cohorts were matched based on age, gender, and the dominance of the side tested. Following inspection of their kinematic data, participants were classified as being in the low, mid, or high scapulothoracic upward rotation groups after quantifying and ranking their upward rotation at 30° humerothoracic elevation during the dynamic trial (described below). This angle corresponded to the approximate humerothoracic position at which subacromial proximities are generally smallest (Giphart et al., 2012; Lawrence et al., 2017). The 20 participants with the highest scapulothoracic upward rotation were assigned to the "high" group, while the 20 participants with the lowest scapulothoracic upward rotation were assigned to the "low"

group. Data for the mid scapular upward rotation group was not analyzed in this study. All participants completed the Disabilities of the Arm, Shoulder, and Hand (DASH) questionnaire (Hudak et al., 1996) (**Appendix E**), which is an objective measure of upper extremity function. Informed consent was obtained prior to initiation of data collection. The study protocol was approved by the Institutional Review Board and the All-University Radiation Protection Advisory Committee at the University of Minnesota.

Data Collection

Shoulder kinematic data were acquired using a Philips BV Pulsera mobile c-arm fluoroscopy system (99.5 cm source-to-image distance, 30 cm field-of-view, 1024×1024 image resolution) synced to a five-camera motion capture system (Vero cameras and Tracker Software; Vicon Motion Capture Systems; Hauppauge, NY) using MotionMonitor software (Innovative Sports Training, Inc.; Chicago, IL). A calibration cube with reflective and radiopaque markers was positioned in the combined imaging volume. The cube's pose was subsequently recorded by both data collection systems to establish a common global coordinate system. Reflective marker clusters were placed on the participants' thorax and humerus and their arbitrary reference frames were transformed into clinically meaningful coordinate systems by digitizing anatomical landmarks according to recommendations (Wu et al., 2005).

To ensure radiation protection safety, all female participants underwent a pregnancy test immediately prior to fluoroscopic data collection and all participants wore a lead apron and eye protection. Fluoroscopic images were acquired using high definition fluoroscopy (continuous x-ray mode) and the system's automatic kV/mA function.

Participants were positioned with their scapula approximately parallel with and as close as possible to the image intensifier. This position helped ensure scapular and humeral motion was as "in plane" as possible and reduced dose and image magnification. Fluoroscopic images and Vicon data were acquired simultaneously (25 Hz and 100 Hz, respectively) with the arm resting at the participant's side and during dynamic trials of scapular plane abduction. Prior to collecting the dynamic data, participants performed a series of practice trials to ensure proper pacing and maintaining contact with a guide pole placed 40° anterior to the coronal plane. Two trials of scapular plane abduction were acquired, each lasting approximately six seconds to complete the full cycle of arm raising and lowering.

Shoulder magnetic resonance (MR) scans were acquired using a 3T scanner (Siemens MAGNETOM Prisma, Siemens Healthcare; Erlangen, Germany) and shoulder coil array. The protocol utilized a T1-VIBE sequence specifically developed to produce 3D bone models with high geometric accuracy. Specific imaging parameters included: FOV=210×210×100 mm^3, resolution=0.8×0.8×0.7 mm, TR=7.16 ms, TE=2.66 ms, flip angle=10°, water excitation, 2D distortion correction, and a scan time of approximately 12 minutes. The field of view was defined to visualize the entire scapula and proximal humerus.

Data Processing

Three-dimensional bone models of the scapula and proximal humerus were created from the MR scans using Mimics software (Materialise NV; Leuven, Belgium). Anatomical coordinate systems were created by digitizing landmarks on the surface of

the 3D bone models. The scapular coordinate system was defined using published recommendations (Ludewig et al., 2010). The origin of the scapular coordinate system was placed at the centroid of the glenoid, which was defined as the geometric center of the glenoid rim. A modified humeral coordinate system was created because the medial and lateral epicondyle landmarks could not be visualized due to the MR field of view. Therefore, the humeral coordinate system was defined as follows: 1) the geometric center of the humeral head was defined as the center of a sphere fit to the articular surface using a least-squares algorithm; 2) the superior/inferior (Y) axis was defined as a vector connecting the geometric center of the humeral head with the center of a circle fit to the anatomical neck of the humeral shaft; 3) the anterior/posterior (X) axis was defined as an axis perpendicular to a plane created by the geometric center, the center of a circle fit to the anatomical neck of the humeral shaft, and the midpoint of the superior aspect of the biceps groove; 4) the medial/lateral (Z) axis was defined as being orthogonal to the superior/inferior and anterior/posterior axes. The origin of the humeral coordinate system was placed at the geometric center of the humeral head. Once 3D models were rendered, all data were blinded such that the knowledge of clinical presentation did not inadvertently bias kinematic descriptions (via shape-matching) or measures of rotator cuff thickness.

Fluoroscopic image calibration and undistortion were performed using XMALab software version 1.3.3 (Knorlein et al., 2016). To reduce data processing time, fluoroscopic images from the raising portion of the first trial were down-sampled to every 10° humerothoracic elevation based on Vicon data. Images and 3D bone models of the

humerus and scapula were imported into JointTrack, an open software for 2D/3D shape-matching (Mu, 2007). This process involves manually rotating and translating a 3D bone model until its projected contours align with the bone on the 2D fluoroscopic image. The data collection and processing protocol has been validated in our lab with RMS errors for glenohumeral joint orientation and position of 0.7-3.3° and 1.2-4.2 mm, respectively (Lawrence et al., 2018).

Glenohumeral kinematics were calculated as the humerus relative to the scapula from the shape-matched data using an X-Z'-Y'' rotation sequence (Phadke et al., 2011). Scapulothoracic and humerothoracic kinematics were calculated by relating the position and orientation of the scapula and humerus as quantified from shape-matching to that of the thorax, which was quantified using the Vicon cameras. This was made possible by co-calibrating the fluoroscopy and Vicon systems to produce a common global coordinate system from which to relate segmental motion. Scapulothoracic motion was described as the scapula moving relative to the thorax using a Y-X'-Z'' rotation sequence, and humerothoracic motion was described as the humerus moving relative to the thorax using an Y-X'-Y'' rotation sequence (Wu et al., 2005).

Two anatomical regions of interest were defined on each participant's 3D humeral model. First, the rotator cuff footprint (i.e. insertion site) was defined by triangulating the margins of the rotator cuff as visualized on each of the three MR image views (**Figure 31** and **Figure 32**). Second, the articular margin region of interest was defined as a 0.7 mm wide portion of the footprint along its medial-most aspect. This width was defined based on the resolution of the MR scan (0.7 mm). Each participant's rotator cuff thickness was

measured at the articular margin perpendicular to the footprint surface on the MR slice corresponding to the anterior/posterior midpoint of the footprint (**Figure 33** and **Figure 34**). Additionally, the acromion region of interest was defined on each participant's 3D scapular model. Finally, because the coracoacromial ligament could not be visualized on the MR images and reconstructed directly, a plane was fit between the anterior acromion and coracoid process based on anatomical descriptions (Edelson & Luchs, 1995).

Each participant's 3D humeral and scapular bone models were converted to surface meshes and animated based on their glenohumeral motion data using a custom MATLAB code (The Mathworks, Inc.; Natick, USA). Subacromial proximities were quantified at each position by calculating the Euclidean distance between pairwise sets of mesh vertices on the rotator cuff footprint and coracoacromial arch (i.e. acromion region of interest and coracoacromial ligament plane). Minimum distances were then normalized to the participant's rotator cuff thickness and expressed as percentages. From these normalized minimum distances, five primary dependent variables were calculated. First, a minimum distance was determined for each glenohumeral position based on the pairwise minimum distances between the coracoacromial arch and the articular margin region of interest. This constraint was added because the thickness of the rotator cuff was only quantified at the articular margin and cannot be assumed to be constant across its surface. Second, contact between the rotator cuff tendons and coracoacromial arch was assumed to occur when the normalized minimum distance was <120%. This cutoff was chosen as it allows for approximately 1 mm error in absolute minimum distance due to shape-matching. Third, the surface area of the rotator cuff footprint within 100% of the

tendon thickness was calculated by summing the surface area of each mesh face within the threshold. Fourth, the absolute minimum distance was calculated as the smallest minimum distance across the participant's full range of motion. Finally, the position of absolute minimum distance was defined as the humerothoracic elevation angle at which the absolute minimum distance occurred.

In addition to kinematics, scapular and humeral morphology have been hypothesized to impact an individual's risk for subacromial rotator cuff compression (Hughes et al., 2003; Kandemir et al., 2006; Neer, 1983). Therefore, several parameters were quantified on each participant's 3D bone models (acromial slope, glenoid inclination, glenoid version, critical shoulder angle, humeral head radius) and were considered potential covariates. Details of these calculations can be found in **Appendix C**.

Statistical Analysis

An *a priori* power analysis was performed to determine that 20 participants were needed per group to detect a 2-mm group difference in minimum distance using a standard deviation from unpublished data from our lab. An oversampling approach was utilized to increase the range of scapulothoracic upward rotation values and ensure a separation in mean scapulothoracic upward rotation between the low and high groups of at least 10°, which was considered clinically meaningful. A Monte Carlo simulation was performed to determine the amount of oversampling required using a probability distribution defined by previous studies (Ludewig et al., 2009a; McClure et al., 2001). The results indicated sixty total participants (20 participants per group) were necessary to

ensure a 10° difference in scapulothoracic upward rotation between the low and high groups.

Demographic data was compared between cohorts (symptomatic, asymptomatic) and scapulothoracic upward rotation groups (low, high) using two sample independent *t*-tests and Chi-square tests for continuous and categorical data, respectively. Data normality was tested prior to statistical analysis by assessing skewness, kurtosis, and Shapiro-Wilk statistics. The relationship between proximity measures and potential covariates were assessed using Pearson's correlation. Variables were retained as covariates if the absolute value of the correlation was ≥0.5.

Two-factor mixed-model ANOVAs with Toeplitz covariance structure were utilized to determine the effect of scapulothoracic upward rotation on normalized minimum distance and surface area of the footprint within the participants' rotator cuff thickness. The between-subject factor was scapulothoracic upward rotation group (low, high) and the within-subject factor was the angle of humerothoracic elevation. For the analysis of minimum distance, humerothoracic elevation angles included the arm resting at the side (i.e. minimum position), and 30°, 60°, and 90° during dynamic scapular plane abduction. However, only 30°, 60°, and 90° humerothoracic elevation were investigated for the analysis of surface area as only one participant had a surface area >0 mm^2 when the arm was at the side. The appropriate covariance structure with which to model the within-subject effects was determined by inspecting the covariance matrix of the within-subject factor and fit statistics of models using various covariance structures (Littell et al., 2000) (**Appendix C**). The two-factor interaction of group-by-angle was assessed first,

and the main effect of group was only considered in the absence of a significant interaction. The prevalence of contact between the rotator cuff and coracoacromial arch was compared between groups using Chi-square tests at the minimum position and at 30°, 60°, and 90° humerothoracic elevation. Comparison of the magnitude of the absolute minimum distance and position of absolute minimum distance between groups was performed using two-sample independent *t*-tests. Statistical analysis was performed in SAS 9.4 (The SAS Institute; Cary, NC) using an *a priori* type I error rate of 5%.

Results

Demographics

Participant demographic information based on scapulothoracic upward rotation classification is provided in **Table 6**. There was no significant difference in the proportion of asymptomatic and symptomatic participants between the high and low upward rotation groups ($p = 0.34$, $X^2 = 0.92$, $df = 1$; 50% asymptomatic in the high group, 35% asymptomatic in low group). However, the low upward rotation group had greater mass ($p = 0.02$, $t = -2.39$, $df = 38$; mean difference: 10.4 kg) and BMI ($p = 0.02$, $t = -2.42$, $df = 38$; mean difference: 2.6 kg/m^2). Clinical examination data is provided in **Appendix C.**

Covariate Analysis

No scapular or humeral morphology variable was moderately or highly correlated ($|r| \geq 0.5$) with either the normalized minimum distance (**Figure 39**-**Figure 43**) or the surface area of the footprint within 100% of the tendon thickness (**Figure 44**-**Figure 48**).

Further, the demographic variables by which the groups differed were not correlated with either the minimum distance (**Figure 49**-**Figure 54**) or the surface area (**Figure 55**-**Figure 60**). Therefore, no covariates were retained for the statistical analyses.

Kinematics

Descriptively, the low scapulothoracic upward rotation group was in decreased upward rotation throughout the dynamic trial compared to the high group (**Figure 15**), consistent with their group classification. Groups differed by 10.0° of upward rotation at the angle at which participants were classified (i.e. 30° humerothoracic elevation). Corresponding glenohumeral kinematics are presented in **Figure 66**.

Subacromial Proximities

Normalized minimum distance was generally smallest below 90° humerothoracic elevation in both groups. The difference between the high and low scapulothoracic upward rotation groups in normalized minimum distance was dependent on the angle of humerothoracic elevation (interaction: $p = 0.049$, $F = 2.71$, $df = 3,113$) (**Figure 16**). When the arm was at the side, participants in the low upward rotation group had significantly smaller normalized minimum distance ($p = 0.049$, $t = 1.99$, $df = 113$; mean difference: 34.8%). Groups were not different at any other angle of humerothoracic elevation ($p > 0.28$) (**Table 34**). Although not significant, participants in the high scapulothoracic upward rotation group tended to have smaller normalized minimum distances at 90º humerothoracic elevation ($p = 0.28$, $t = -1.08$, $df = 113$; mean difference: 18.7%).

Descriptively, the surface area of the footprint within 100% of the rotator cuff tendon thickness tended to be highest between 50-90° humerothoracic elevation in both scapulothoracic upward rotation groups. However, there was no difference between the high and low scapulothoracic upward rotation groups in the magnitude of surface area within 100% of the rotator cuff tendon thickness (p = 0.14, F = 2.00, df = 2,76) (**Figure 17**).

The prevalence of contact between the rotator cuff tendon and coracoacromial arch across humerothoracic elevation angles is presented in **Figure 18**. The highest prevalence occurred at 60° humerothoracic elevation, where 32.5% of participants were in contact with the coracoacromial arch. All participants had cleared the coracoacromial arch by 130° humerothoracic elevation. There was no significant difference between groups in the proportion of participants experiencing contact at any angle of humerothoracic elevation (p > 0.41). Overall, contact occurred in 45% of all participants without a significant difference between groups (p = 0.53, X^2 = 0.40, df = 1; 50% of participants in the low scapulothoracic upward rotation group, 40% of participants in the high scapulothoracic upward rotation group).

The absolute minimum distance occurred at an average humerothoracic elevation angle of 51.5° (±11.8°) in the low scapulothoracic upward rotation group and at 60.4° (±18.4°) in the high scapulothoracic upward rotation group (p = 0.07, t = -1.82, df = 38) (**Figure 19**). There was no difference between groups in the magnitude of the absolute minimum distance (p = 0.41, t = 0.83, df = 31.9; mean difference: 5.4%).

Discussion

During scapular plane abduction, subacromial proximities were generally smallest below 90° humerothoracic elevation. Although this finding is in contrast to the long held clinical belief that subacromial rotator cuff compression occurs above 80° humerothoracic elevation (Neer, 1972), it is largely consistent with other 3D studies (Bey et al., 2007; Giphart et al., 2012; Lawrence et al., 2017). However, small differences between studies exist in the upper and lower limits of the range of motion in which the smallest subacromial proximities occurred. These differences are likely a reflection of the different approaches used to define the rotator cuff insertion from which the subacromial proximities were measured. In the current study, the minimum distance calculation was constrained to the articular margin coinciding with where the rotator cuff thickness measure was taken. However, degenerative rotator cuff tears often originate in the portion of the tendon near or medial to the articular margin (Kim et al., 2010). Including this region of the rotator cuff tendon would have likely caused the lower limit of proximity to occur at an even lower angle of humerothoracic elevation (Lawrence et al., 2017). Furthermore, only measuring the proximities to the articular margin likely resulted in a lower upper-limit of the range of motion in which the rotator cuff insertion was within close proximity to the coracoacromial arch. This is because the articular margin region will clear the lateral acromion earlier in the range of motion compared to studies that included the entire footprint in the proximity calculations (Giphart et al., 2012; Lawrence et al., 2017). Despite these methodological differences, considerable evidence now exists (Bey et al., 2007; Giphart et al., 2012; Lawrence et al., 2017) suggesting subacromial

rotator cuff compression occurs at much lower angles in humerothoracic elevation than traditionally believed.

Although the minimum distance is the most widely used metric for quantifying subacromial proximities, multidimensional measures such as surface area may be more comprehensive. For example, surface area captures proximity to an entire surface whereas minimum distance is only a linear measure to a single point on the surface. The surface area metric extended the range of closest proximity to approximately 110° humerothoracic elevation. This higher upper limit was expected as proximities were calculated to the entire footprint, which extends more laterally than the articular margin and will therefore continue to approach the coracoacromial arch later in the range of motion. Further, the surface area calculation used in this study will likely result in an overestimation as it was quantified as the surface area within 100% rotator cuff tendon thickness, which was measured at the articular margin and likely becomes thinner more laterally along the insertion.

Despite the utility of a multi-dimensional metric such as surface area, few studies have used it to describe subacromial proximities. One study, by Flatow et al. (1994), utilized stereophotogrammetry to quantify subacromial proximity as surface areas in cadaveric specimens during passive simulated motion. Despite the differing methodologies, the authors found comparable results to the current study in that the range of highest surface area occurs between approximately 30° and 110° humerothoracic elevation. Ultimately however, direct measures of soft tissue deformation using finite element modeling may provide the best assessment of compression during arm

movement. Further work is required to develop these models and apply them towards movement-based clinical questions.

Clinically, the finding that subacromial proximities were smallest below 90° humerothoracic elevation may bring to question the source of pain during arm raising. This is because the predominant thought has been that subacromial compression provokes the pain that patients often feel near mid or at end range humerothoracic elevation. In light of the results of this study and others (Bey et al., 2007; Giphart et al., 2012; Lawrence et al., 2017), this explanation is no longer logical given the rotator cuff tendon has cleared the coracoacromial arch in most people by 90° humerothoracic elevation. However, it is possible that rotator cuff compression occurring at lower angles of humerothoracic elevation becomes symptomatic in mid ranges when the injured or irritated rotator cuff needs to produce more torque to overcome the larger moment arm. In contrast, symptoms above 90° humerothoracic elevation may be due to other mechanisms such as internal impingement, which occurs when the rotator cuff tendon becomes entrapped against the glenoid (Walch et al., 1992). This mechanism was found to occur in all participants in a modeling study during a simulated reaching task (Lawrence et al., 2016), suggesting it may be a common cause of symptoms at higher angles and an important mechanism for rotator cuff injury.

Interestingly, only 45% of participants in this study had a normalized minimum distance <120% during the motion suggesting contact between the rotator cuff tendon and the coracoacromial arch. This proportion seems surprisingly small given the presumption subacromial compression is a predominant cause of rotator cuff injury and shoulder pain

(Neer, 1983; Ostor et al., 2005). However, the relatively low prevalence is comparable to the findings of a previous study that reported contact between the supraspinatus tendon and coracoacromial arch occurred in only 50% of subject-specific anatomical models during a simulated functional reaching task (Lawrence et al., 2017). The slightly lower proportion of subjects in the current study may reflect the different methodological approaches between the studies. In particular, the study by Lawrence et al. simulated a functional reach task assuming the humeral head remained centered in the glenoid, which was defined by a circle fit to the inferior margin (Verstraeten et al., 2013). However, in the current study, subjects predominantly stayed an average of approximately 1.2 mm inferior, with some participants as much as 7 mm inferior (**Figure 61**). Presumably, this lower position of the humeral head in the glenoid would result in larger proximities and fewer incidences of contact. Together the findings of both studies suggest subacromial compression may not occur as often during unloaded scapular plane abduction as presumed. However, subacromial compression may still be a factor for the development of rotator cuff pathology in a subset of individuals and may be more prevalent during other functional motions such as reaching across the body, behind the back, or during fatiguing tasks. Further research is needed to identify the anatomical and kinematic factors that predispose individuals to this mechanism.

With regards to the effect of scapulothoracic upward rotation on subacromial proximities, our hypothesis was supported: a reduction in scapulothoracic upward rotation shifts the range of closest proximity to lower angles of humerothoracic elevation. This is evident primarily by the significant group-by-angle interaction for the normalized

minimum distance metric. In particular, decreased scapulothoracic upward rotation significantly decreased subacromial proximities when the arm was at the side (i.e. minimum position) and tended to increase subacromial proximities at 90º humerothoracic elevation. Given the mean rotator cuff thickness of 5.6 mm, the 35% group mean difference when the arm was at the side corresponds to an approximately 2.0 mm group difference in minimum distance, which is believed to be clinically meaningful.

The results relative to the position and magnitude of absolute minimum distance also provide evidence that a reduction in scapulothoracic upward rotation tends to shift the range of closest proximity to lower angles of humerothoracic elevation; however, it may not increase the amount of compression should it occur. Specifically, participants in the low scapulothoracic upward rotation group tended to be in closest proximity to the coracoacromial arch 9° lower in the range of motion than those in the high scapulothoracic upward rotation group. Although not statistically significant, it is likely the study was underpowered in this metric. A *post hoc* power analysis using a meaningful difference of 10° and the standard deviation found in this study confirms low power (51%) to detect a group difference and indicates 39 subjects would be needed to reach significance at 80% power.

A previous study by Karduna et al. (2000) likely observed the effects of the shift in the range of motion in which the smallest subacromial proximities occur. The researchers imposed changes in scapular upward rotation in cadaveric shoulder specimens when the arm was positioned at 90° humerothoracic elevation and found reducing scapular upward rotation increased subacromial proximities. Although the

authors concluded an increase in scapulothoracic upward rotation may be protective against subacromial rotator cuff compression, their conclusions should be interpreted relative to the findings of the current study. Likely what the authors observed was the same tendency of decreased scapulothoracic upward rotation to increase subacromial proximities at 90° humerothoracic elevation as was observed in the current study. However, 90° humerothoracic elevation is nearing the upper range of compression risk; therefore, the clinical relevance of this potential increase in subacromial proximities is unclear.

The shift in the range of closest proximity between the low and high scapulothoracic upward rotation groups can be explained by the inherent dependency of subacromial proximities on glenohumeral relationships and the influence of scapulohumeral rhythm, which describes the relative contribution of glenohumeral elevation and scapulothoracic upward rotation for producing net humerothoracic elevation (Inman et al., 1944). For a given angle of humerothoracic elevation, a reduction in scapulothoracic upward rotation must be accompanied by an increase in glenohumeral elevation. Therefore, at lower angles of humerothoracic elevation, a decrease in scapulothoracic upward rotation (or increase in glenohumeral elevation) will move the edge of the acromion downward and in closer proximity to the medial aspect of the rotator cuff insertion (**Figure 20A-B**). At higher angles of humerothoracic, an increase in scapulothoracic upward rotation will raise the acromial edge upward and back over the medial aspect of the rotator cuff insertion, thereby reducing proximities to this important area of the tendon (**Figure 20C**). However, a decrease in scapulothoracic upward rotation

will move the acromial edge downward, but the medial aspect of the rotator cuff insertion is no longer under it (**Figure 20D**).

In addition to scapulothoracic upward rotation, other kinematic variables may be impacting subacromial proximities. A more superior position of the humerus on the glenoid has also been theorized to cause subacromial rotator cuff compression (Deutsch et al., 1996). Therefore, it is possible the individuals in the low scapulothoracic upward rotation group were sitting lower in the glenoid, which would presumably increase subacromial space and confound the effect of the decreased upward rotation. To test this possibility, an exploratory two-factor mixed-model ANOVA was performed as described previously for the comparison of glenohumeral superior/inferior position normalized to the glenoid height. No group difference were found (interaction: $p = 0.26$, $F = 1.36$, $df = 3,113$; main effect: $p = 0.61$, $F = 0.26$, $df = 1,38$) (**Appendix C**) suggesting altered superior/inferior glenohumeral position did not likely confound the analysis of scapulothoracic upward rotation on subacromial proximities.

This study has several limitations that should be considered when interpreting the results. First, the use of a single fluoroscopic imaging system may result in increased out-of-plane errors (You et al., 2001). For the data collection setup employed for this study, out-of-plane position error will predominantly impact glenohumeral plane of elevation, axial rotation, and anterior/posterior position, and may impact subacromial proximities. However, a sensitivity analysis was performed using radiostereometric analysis as the gold standard to determine the extent to which shape-matching errors impacted minimum distances. The RMS error of this analysis was 1.5 mm (**Appendix B**). However, these

errors did not likely impact any statistical comparisons or interpretations given shape-matching was performed blinded to group membership and there is no reason to suspect errors will systematically differ between groups. Second, the coracoacromial ligament was modeled as a plane because it was not visible on the MR images from which 3D models are reconstructed. However, there was no substantial change in the results or conclusions when subacromial proximities were quantified to the acromion only (**Appendix C**). Third, the rotator cuff thickness was measured at the articular margin on a single MR image slice. Because it is not reasonable to assume the thickness of the rotator cuff is constant throughout its structure, we limited the minimum distance calculations to the articular margin to avoid over-representing proximities based on this metric. However, quantifying proximities to the entire rotator cuff would provide a more direct and comprehensive measure.

Ultimately the results of this study suggest subacromial proximities are smallest below 90° humerothoracic elevation. Decreased scapulothoracic upward rotation shifts the range of motion in which the rotator cuff insertion is closest to the coracoacromial arch to lower angles. Clinically, knowledge of the range of motion in which proximities are the smallest may help inform ergonomic tasks and exercise prescription to avoid prolonged and repeated exposures within this range.

Table 5: Study Inclusion and Exclusion Criteria

Symptomatic	Asymptomatic
Inclusion Criteria	
1. Age 21-60 years 2. Current shoulder joint pain of ≥4 weeks duration 3. Shoulder symptoms provoked during active motion 4. Ability to raise the arm ≥120° humerothoracic elevation	1. Age 21-60 years
Exclusion Criteria	
1. Shoulder symptoms reproduced during cervical spine screening 2. Radiating pain, numbness, or tingling in the upper extremity 3. ≥25% reduction in glenohumeral internal or external rotation range of motion compared to the contralateral side 4. Symptom onset following trauma 5. Positive apprehension test 6. History of shoulder surgery 7. History or presence of shoulder fracture, dislocation, separation, adhesive capsulitis, or rotator cuff tear on involved side 8. History or presence of scoliosis 9. Inflammatory joint disease 10. Known skin sensitivities or allergies to adhesives 11. Contraindications to MR imaging or radiation exposure	1. History of pain in either shoulder 2. Symptom provocation during clinical exam except during 1-2 provocation tests 3. ≥25% reduction in glenohumeral internal or external rotation range of motion compared to the contralateral side 4. Positive apprehension test 5. Radiating pain, numbness, or tingling in the upper extremity 6. History of shoulder fracture, dislocation, separation, adhesive capsulitis, or rotator cuff tear 7. History or presence of scoliosis 8. Inflammatory joint disease 9. Known skin sensitivities or allergies to adhesives 10. Contraindications to MR imaging or radiation exposure
Note: Provocation tests included Hawkins-Kennedy, Neer, Jobe, and resisted external rotation.	

Table 6: Participant Demographics by Scapulothoracic Upward Rotation Group

	High (n = 20)	**Low (n = 20)**	**Statistic**	**p-value**
Age (years)	32.9 ± 7.3	32.0 ± 8.7	$t_{38} = 0.35$	0.73
Gender (% male)	30%	55%	$X^2_1 = 2.56$	0.11
Dominance of the side tested (% dominant)	35%	50%	$X^2_1 = 0.92$	0.34
Height (cm)	170.0 ± 9.2	174.5 ± 6.9	$t_{38} = -1.76$	0.09
Mass (kg)	66.7 ± 14.3	77.1 ± 13.2	$t_{38} = -2.39$	0.02
BMI (kg/m^2)	22.9 ± 3.2	25.5 ± 3.6	$t_{38} = -2.42$	0.02
Group (% asymptomatic)	50%	35%	$X^2_1 = 0.92$	0.34
Rotator cuff tendon thickness (mm)	5.3 ± 1.2	5.6 ± 0.9	$t_{38} = -0.74$	0.47
Symptom duration (weeks)	31.0	40.0	$X^2_1 = 0.03$	0.85
NPRS past 7 days (0 – 100)				
Highest	45.0	51.0	$X^2_1 = 3.81$	0.05
Lowest	20.0	0.0	$X^2_1 = 1.58$	0.21
DASH (0 – 100)	3.4	12.1	$X^2_1 = 1.12$	0.29
Work subscale	0.0	0.0	$X^2_1 = 0.09$	0.76
Sport subscale	0.0	3.2	$X^2_1 = 0.02$	0.87

Notes: Groups were classified as having high or low upward rotation based on their scapulothoracic upward rotation magnitude at 30º humerothoracic elevation. Demographic data are presented as mean ± SD or proportions, as appropriate. Group comparisons were assessed using two-sample independent *t*-tests or Chi-square tests for continuous and binary data, respectively. Continuous data for symptom severity and dysfunction were highly skewed and are presented as the median, and group comparisons were assessed using Kruskal-Wallis test. Rotator cuff thickness was measured on the MR images at the articular margin on the image slice corresponding to the anterior/posterior midpoint of the rotator cuff insertion.

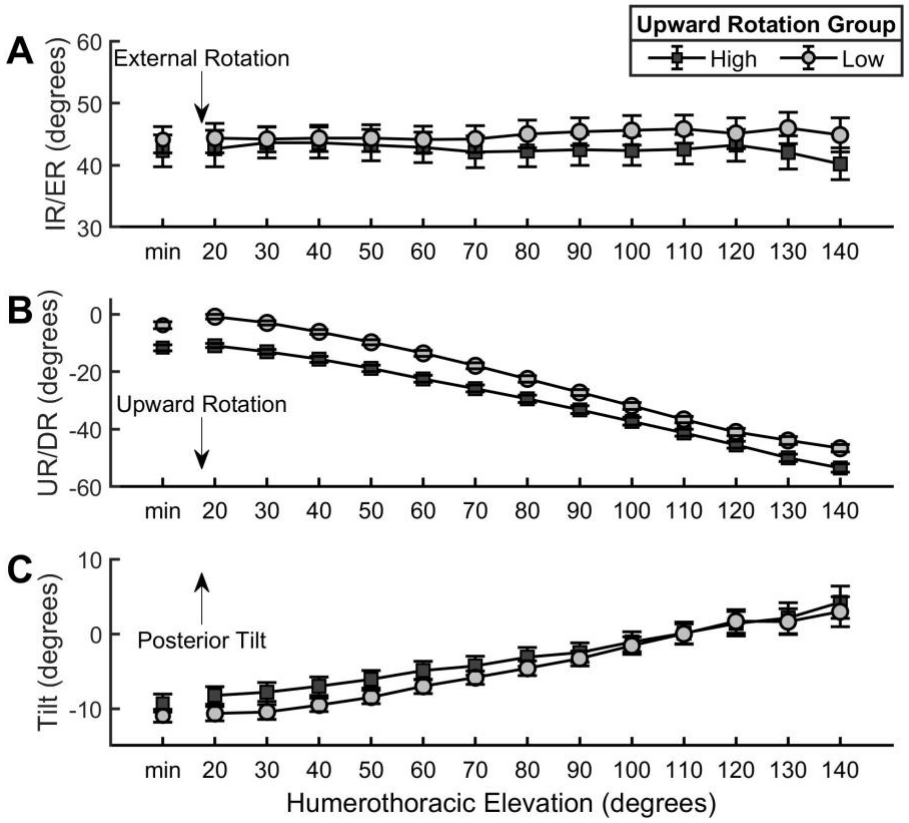

Figure 15: Scapulothoracic kinematic data for high and low scapulothoracic upward rotation groups. Data are reported descriptively as means and unpooled SEs for each angle/group. Abbreviations: IR=internal rotation, ER=external rotation, UR=upward rotation, DR=downward rotation.

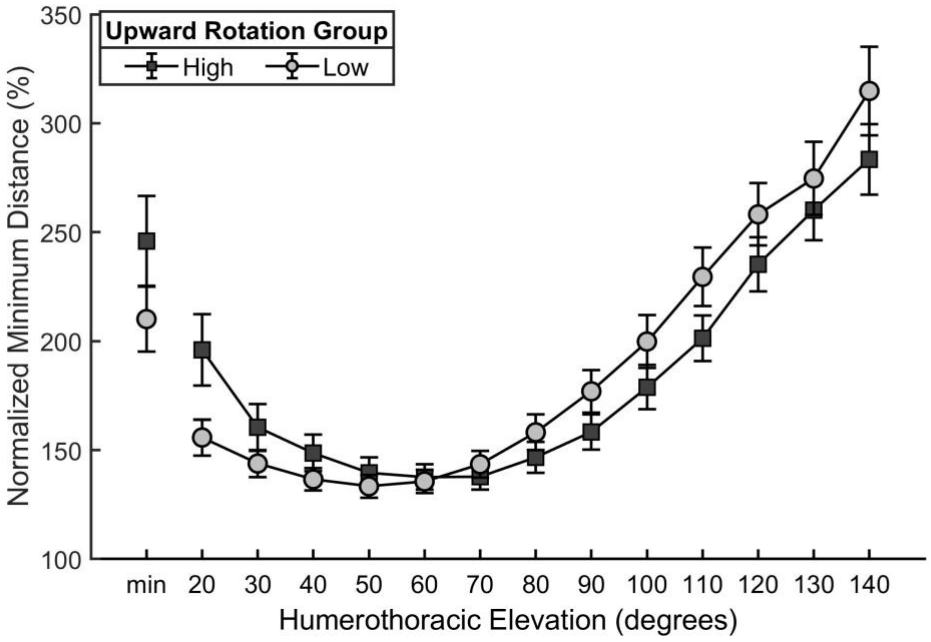

Figure 16: Normalized minimum distance between the coracoacromial arch and articular margin aspect of the rotator cuff insertion for the high and low scapulothoracic upward rotation groups. Minimum distances were normalized to the participant's rotator cuff tendon thickness and expressed as a percentage. Error bars represent the unpooled SE for each angle/group. Groups were compared statistically at the minimum, 30°, 60°, and 90° angles of humerothoracic elevation. Abbreviation: min = minimum.

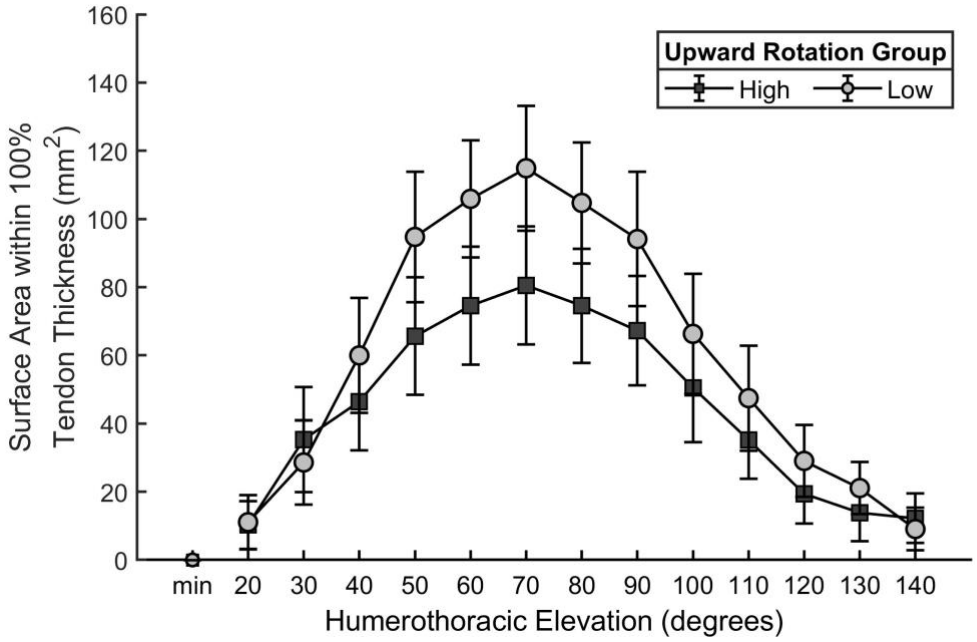

Figure 17: Surface area of the footprint within 100% of the rotator cuff tendon thickness for the high and low scapulothoracic upward rotation groups. Error bars represent the unpooled SE for each angle/group. Groups were compared statistically at the 30°, 60°, and 90° angles of humerothoracic elevation. Abbreviation: min = minimum.

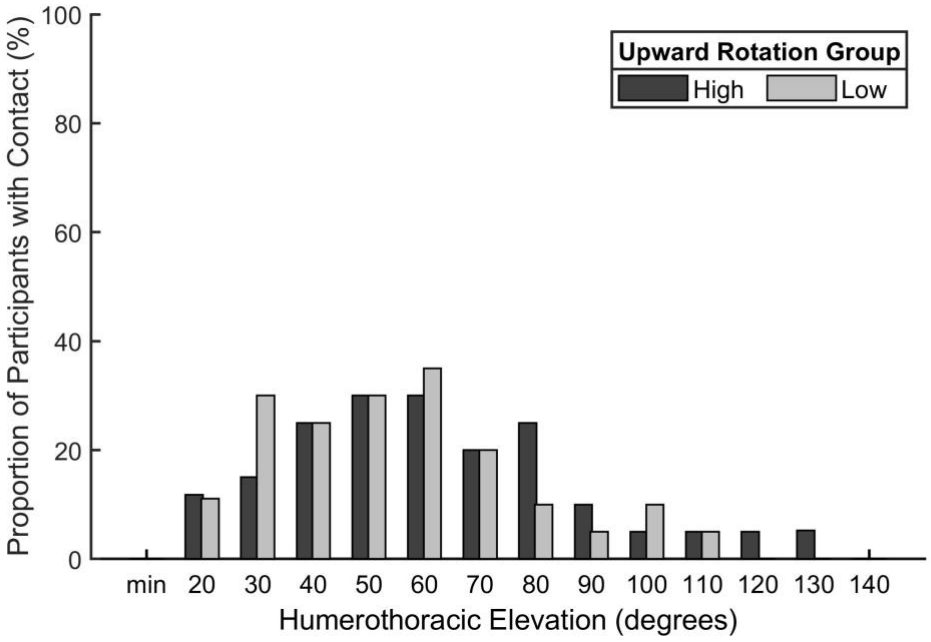

Figure 18: Proportion of participants with contact between the rotator cuff insertion and coracoacromial arch. Contact was defined as a normalize minimum distance <120%. Groups were compared statistically at the minimum, 30°, 60°, and 90° angles of humerothoracic elevation. Abbreviation: min = minimum.

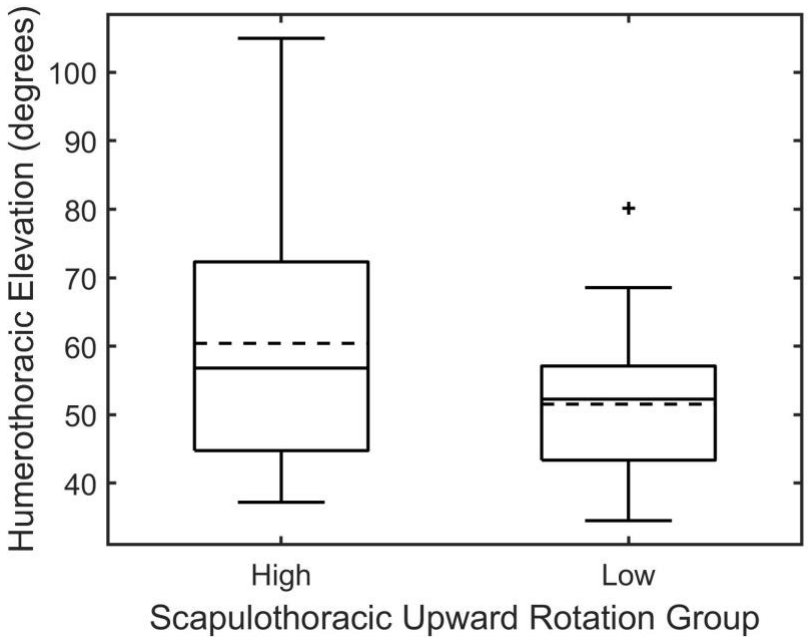

Figure 19: Distributions of the humerothoracic elevation angle at which the absolute minimum distance occurred for the high and low scapulothoracic upward rotation groups. The solid and dashed lines within each box represents the group median and mean, respectively. The boundaries of the box represent the 25th and 75th quartile. The whiskers represent the upper and lower adjacent values (i.e. the most extreme data points not considered outliers). Individual outliers are indicated by a '+' symbol.

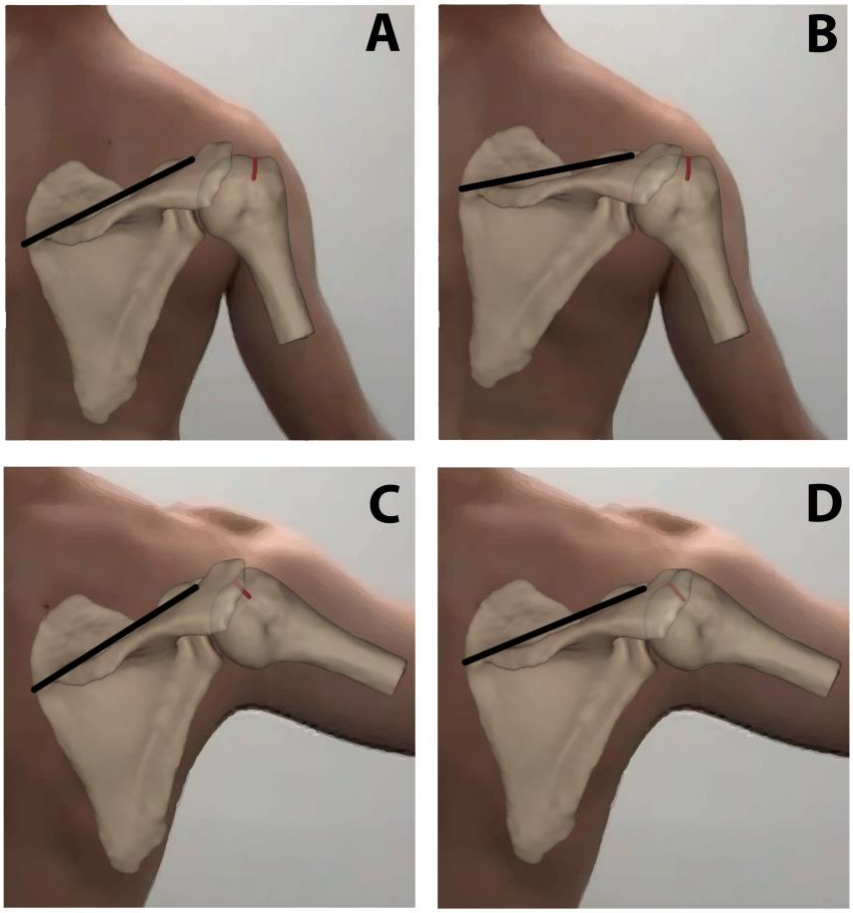

Figure 20: The effect of the magnitude of scapulothoracic upward rotation on the proximity of the acromial edge to the articular margin aspect of the rotator cuff insertion (red region on humeral head): **A**) Increased scapulothoracic upward rotation at a lower angle of humerothoracic elevation will move the acromial edge upward and away from the articular margin aspect of the rotator cuff insertion; **B**) Decreased scapulothoracic upward rotation at a lower angle of humerothoracic elevation will move the acromial edge downward and closer to the articular margin aspect of the rotator cuff insertion; **C**) Increased scapulothoracic upward rotation at a higher angle of humerothoracic elevation will raise the acromion upward, thereby moving the acromial edge back over the articular margin aspect of the rotator cuff insertion; and **D**) Decreased scapulothoracic upward rotation at a higher angle of humerothoracic elevation will move the acromial edge downward, but the articular margin aspect of the rotator cuff insertion has already cleared the acromion.

Chapter 5: Mechanical coupling of scapulothoracic upward rotation (Aim 3)

Scapulothoracic upward rotation is an important motion for overall shoulder function. Because of the complex anatomical configuration of the shoulder girdle, all scapulothoracic motion occurs due to coupled motion between the scapula and clavicle. Knowledge of these coupled mechanics is critical for understanding how normal and abnormal scapulothoracic motion occurs, which will help guide the diagnosis and treatment of individuals with shoulder pain. Therefore, the third aim of this thesis is to identify the kinematic mechanisms by which the sternoclavicular and acromioclavicular joints contribute to scapulothoracic upward rotation.

Abstract

Study Design: Cross sectional observational study

Background: Scapulothoracic upward rotation is an important motion of the shoulder complex allowing for increased functional range of motion and improved deltoid muscle function. However, the kinematic mechanisms producing scapulothoracic upward rotation remain unclear, thus limiting our understanding of normal and abnormal shoulder movement.

Objectives: Identify the kinematic mechanisms by which the sternoclavicular and acromioclavicular joints contribute to scapulothoracic upward rotation.

Methods: Sixty subjects were recruited for this study; 30 had current shoulder pain and 30 had no history of shoulder symptoms. Shoulder complex kinematics were quantified using single-plane fluoroscopy and 2D/3D shape-matching. Sternoclavicular, acromioclavicular, and scapulothoracic motion were described as helical displacements for 30° phases of humerothoracic elevation (30°-60°, 60°-90°, 90°-120°). Two coupling functions were derived to estimate scapulothoracic upward rotation from its component motions of acromioclavicular upward rotation, sternoclavicular posterior rotation, and sternoclavicular elevation as a function of the acromioclavicular internal rotation angle. The proportional contributions of the component motions were also calculated and compared across phases of humerothoracic elevation and group.

Results: Scapulothoracic upward rotation displacement can be estimated using the coupling functions derived. During the 30°-60° phase of humerothoracic elevation, acromioclavicular upward rotation accounted for 84.2% of the magnitude of

scapulothoracic upward rotation while sternoclavicular posterior rotation and elevation each accounted for <10%. During later phases, acromioclavicular upward rotation and sternoclavicular posterior rotation each accounted for 32-42%, while sternoclavicular elevation accounted for <11%.

Conclusion: Acromioclavicular upward rotation and sternoclavicular posterior rotation are the predominant component motions of scapulothoracic upward rotation. More research is needed to investigate how these coupling relationships influence muscle function and scapular dyskinesis.

Introduction

Optimal shoulder function depends on substantial and coordinated glenohumeral, sternoclavicular, acromioclavicular, and scapulothoracic motion. In particular, scapulothoracic upward rotation plays several critical roles in shoulder function including orienting the glenoid to promote glenohumeral joint congruency and maintaining deltoid muscle length to maximize contractile function (van der Helm, 1994; Voight & Thomson, 2000). Scapulothoracic upward rotation also increases overall shoulder functional range of motion during arm raising by accounting for approximately one-third of total humerothoracic motion via scapulohumeral rhythm (Inman et al., 1944; Ludewig et al., 2009a).

Due to its importance to shoulder function, scapulothoracic upward rotation position and/or motion are often examined clinically (Johnson et al., 2001; McClure et al., 2009). Altered scapulothoracic upward rotation has been found in various clinical presentations including adhesive capsulitis (Fayad et al., 2006; Rundquist, 2007; Vermeulen et al., 2002), rotator cuff tears (Mell et al., 2005), glenohumeral instability (Ogston et al., 2007; Struyf et al., 2013), and osteoarthritis (Braman et al., 2010; Fayad et al., 2006). When motions deemed "abnormal" are observed during a clinical examination, exercises are often prescribed to address impairments presumably underlying the abnormal motion, including scapulothoracic muscle function. However, like all scapulothoracic motions, upward rotation is produced through the complex interactions between sternoclavicular and acromioclavicular joint motion (Dvir et al., 1978; Inman et al., 1944; Teece et al., 2008). Given shoulder girdle muscles function through the

sternoclavicular and acromioclavicular joints to produce the observed scapulothoracic motion, understanding this complex interaction is crucial to diagnosing and treating shoulder motion abnormalities.

The interaction between sternoclavicular and acromioclavicular joint motion in producing scapulothoracic motion is sometimes termed "coupling" (Teece et al., 2008). Scapulothoracic upward rotation is believed to occur as a result of coupled motions between acromioclavicular upward rotation, sternoclavicular posterior rotation, and sternoclavicular elevation (Teece et al., 2008), which are collectively termed "component motions" (**Figure 21**). However, the relationships between these component motions are indirect due to the oblique orientation of the clavicular and scapular anatomical axes. Teece et al. (2008) proposed that scapulothoracic upward rotation is produced by these component motions as a function of the offset between the scapular and clavicular medial/lateral anatomical axes (i.e. the acromioclavicular internal rotation angle), which is approximately 60° (Ludewig et al., 2009a). However, this theory has not been directly tested in a data driven study. Thus, it remains unclear the extent to which these component motions contribute to scapulothoracic upward rotation, resulting in gaps in our understanding of how to identify and treat scapular movement dysfunctions in persons with shoulder pain.

A major barrier to understanding how the component motions contribute to scapulothoracic upward rotation has been the methodological challenges associated with quantifying clavicular kinematics. As a result, few studies have quantified sternoclavicular and acromioclavicular kinematics leaving the coupling relationships

untested. However, previous work by Lawrence et al. (2014a) provided construct validity to the coupling theory by showing differences in scapulothoracic upward rotation between symptomatic and asymptomatic subjects could be partially explained by concurrent differences in sternoclavicular and acromioclavicular motion. This was done using group means of shoulder complex kinematics in a relatively small sample of subjects due to the use of motion sensors fixed to transcortical bone pins. However, high between-subject variability in movement patterns limit the utility of using group means to rigorously test the coupling theory. Further, high between-subject variability also requires larger sample sizes to ensure representation of the broad spectrum of movement. Recent advances in the use of single-plane fluoroscopy and 2D/3D shape-matching allows for an accurate method for quantifying full shoulder complex kinematics (Lawrence et al., 2018). Importantly, the fluoroscopic approach is also non-invasive allowing for a larger sample of subjects to be tested.

The purpose of this study was to identify the kinematic mechanisms by which sternoclavicular and acromioclavicular joint motion contributes to scapulothoracic upward rotation through investigating the coupling theory proposed by Ludewig and colleagues (Teece et al., 2008) in a large sample of individuals with and without shoulder pain. It was hypothesized that acromioclavicular upward rotation would be the predominant component motion for producing scapulothoracic upward rotation.

Methods

Participants

Sixty participants were recruited from the university community and local physical therapy clinics. Of these participants, 30 had current shoulder symptoms consistent with a clinical diagnosis of "impingement syndrome" (Michener et al., 2009), and 30 had no history of shoulder pain. Symptomatic and asymptomatic participants were group matched for age, sex, and the dominance of the side tested. No specific group-related hypotheses were made; instead, individuals with and without shoulder pain were included to ensure a broad distribution of shoulder complex kinematics. Group demographic data are presented in **Table 7**. The study was approved by the Institutional Review Board and All-University Radiation Protection Advisory Committee at the University of Minnesota. All subjects provided written informed consent prior to data collection.

Data Collection

Shoulder complex kinematics were collected during dynamic scapular plane abduction by spatially and temporally syncing a single-plane fluoroscopy unit (Philips BV Pulsera; 99.5 cm source-to-image distance, 30 cm field-of-view, 1024×1024 image resolution) and a five-camera motion capture system (Vicon Motion Capture Systems; Hauppauge, NY) using MotionMonitor software (Innovative Sports Training, Inc.; Chicago, IL). Scapular and clavicular motion were tracked using the fluoroscopic imaging system, while trunk and humeral kinematics were simultaneously tracked using the camera system. Participants were seated and positioned to align their scapula approximately parallel to the image intensifier. Reflective marker clusters were placed on the participants' thorax and humerus and anatomical landmarks were digitized according

to published recommendations (Wu et al., 2005). Fluoroscopic images were acquired at 25 Hz using continuous x-ray mode and the system's automatic kV/mA function to minimize dose. Humeral plane of motion was controlled using a pole placed 40° anterior to the coronal plane.

Shoulder magnetic resonance (MR) scans were acquired using a Siemens MAGNETOM Prisma 3T scanner (Siemens Healthcare; Erlangen, Germany) with shoulder and flex coil arrays. A custom T1-VIBE sequence was developed to enhance bone edge contrast, with the following imaging parameters: FOV=210×210×100 mm, resolution=0.8×0.8×0.7 mm, TR=7.16 ms, TE=2.66 ms, flip angle=10°, water excitation, and 2D distortion correction. Separate scans were acquired for the glenohumeral (i.e. scapula and humerus) and clavicular regions with a total scan time of approximately 22 minutes.

Data Processing

Three-dimensional bone models of the scapula and clavicle were reconstructed from the MR scans using Mimics software (Materialise NV; Leuven, Belgium). The scapular coordinate system was defined by digitizing anatomical landmarks using published recommendations (Ludewig et al., 2010). The clavicular coordinate system was defined by digitizing the midpoints of the sternoclavicular and acromioclavicular joints and a point 5 cm superior to the bone's center of mass along the superior/inferior inertial axis. This arbitrary point was defined due to the lack of a third non-collinear point on the surface of the clavicle. The clavicular coordinate system was re-oriented during post-

processing by aligning its superior/inferior axis to that of the thorax when the subject was in a relaxed seated posture (Wu et al., 2005).

XMALab software version 1.3.3 (Knorlein et al., 2016) was used to calibrate the fluoroscopic image volume and correct for image distortion. Due to the extensive time required for data processing, the fluoroscopic frames corresponding to every 10° of humerothoracic elevation were identified based on camera data. The 3D bone models were then shape-matched to the fluoroscopic images on this subsample of frames using JointTrack software (Mu, 2007). Shape-matching is an extensive process that involves virtually rotating and translating the 3D bone model until the projected contours of the bones become aligned with their respective projections on the fluoroscopic images (**Figure 22**). Angular errors associated with shape-matching the scapula and clavicle using single-plane fluoroscopy have been established as 0.5-1.6° and 0.4-3.7°, respectively (Lawrence et al., 2018).

Sternoclavicular, acromioclavicular, and scapulothoracic kinematics were described in the following anatomically meaningful ways as: 1) joint positions at each angle of humerothoracic elevation; and 2) finite helical displacements (Spoor & Veldpaus, 1980) of the distal segment moving relative to the proximal segment for each 30° phase of humerothoracic elevation (i.e. 30°-60°, 60°-90°, 90°-120°). The total helical rotation was parsed into helical angles by projecting the orientation of the helical axis onto the coordinate system of the distal segment at the initial humerothoracic elevation position of the phase. For example, the motion of the acromioclavicular joint between 30° and 60° humerothoracic elevation describes the displacement of the scapular anatomical

axes relative to the clavicular anatomical axes, defined relative to the scapular anatomical axes at 30° humerothoracic elevation.

Deriving the Coupling Functions

Because of the oblique nature of the scapular and clavicular axes, scapulothoracic motion cannot be considered a simple summation of sternoclavicular and acromioclavicular motion (Pronk, 1991). Instead, the coupling function proposed by Ludewig and colleagues (Teece et al., 2008) suggests the complex relationships between scapular and clavicular kinematics can be best understood within the context of two theoretical configurations: if the scapular and clavicular medial/lateral axes were parallel and if they were perpendicular. Theoretically, if the acromioclavicular joint internal rotation angle was 0° (i.e. axes parallel) and no acromioclavicular motion occurred, scapulothoracic upward rotation would be produced by sternoclavicular elevation but not by sternoclavicular posterior rotation or retraction. Conversely, if the acromioclavicular joint internal rotation angle was 90° (i.e. axes perpendicular) and no acromioclavicular motion occurred, scapulothoracic upward rotation would be produced by sternoclavicular posterior rotation but not by sternoclavicular elevation or retraction. In reality, the acromioclavicular internal rotation angle is approximately 60° (Ludewig et al., 2009a). Therefore, the true relationship between clavicular and scapular motion behaves most like the perpendicular axis configuration (i.e. 67%, or 60°/90°) in which case sternoclavicular posterior rotation produces scapulothoracic upward rotation and behaves less like the parallel axis configuration (i.e. the remaining 33%) when sternoclavicular elevation produces scapulothoracic upward rotation (**Figure 23**).

To test the construct of the coupling theory, a coupling function was developed to estimate scapulothoracic upward rotation from the component motions for each phase of humerothoracic elevation (30°-60°, 60°-90°, 90°-120°) using the following equation and assuming a mean acromioclavicular internal rotation angle of 60° (Ludewig et al., 2009a):

$$\widehat{STur} = (33\% * SCelev) + (67\% * SCrot) + (100\% * ACur)$$

In this equation, $\widehat{STur}$ represents the estimated scapulothoracic upward rotation displacement and $SCelev$, $SCrot$, and $ACur$ are sternoclavicular elevation, sternoclavicular posterior rotation, and acromioclavicular upward rotation displacements, respectively. The constant (i.e. not subject-specific) weighting factors for the sternoclavicular component motions reflect the relationship described above. The weighting factor for acromioclavicular upward rotation is 100% as it reflects scapular motion relative to the clavicle, which should directly transfer to scapular motion relative to the thorax.

A second coupling function was also developed that, instead of assuming the acromioclavicular internal rotation angle is "average" and remains fixed at 60°, used each participant's mean acromioclavicular internal rotation angle for a given phase of humerothoracic elevation. For this function, the individual weighting factor for sternoclavicular elevation (ω_{SCelev}) and sternoclavicular posterior rotation (ω_{SCrot}) become a function of the mean acromioclavicular internal rotation angle ($ACir$) during the phase of humerothoracic elevation as follows:

$\omega_{SCelev} = \frac{90 - ACir}{90} \times 100\%$, which defines the extent to which the acromioclavicular internal rotation angle is coincident with the parallel axis configuration (i.e. 0°) and thus defines the magnitude of sternoclavicular elevation that contributes to scapulothoracic upward rotation.

$\omega_{SCrot} = \frac{ACir}{90} \times 100\%$, which defines the extent to which the acromioclavicular internal rotation angle is coincident with the perpendicular axis configuration (i.e. 90°) and thus defines the magnitude of sternoclavicular posterior rotation that contributes to scapulothoracic upward rotation.

Using these non-constant weighting factors, the subject-specific coupling function is defined as follows:

$$\widehat{STur} = (\omega_{SCelev} * SCelev) + (\omega_{SCrot} * SCrot) + (100\% * ACur)$$

The weighting factor for acromioclavicular upward rotation remains 100% as the motion directly transfers to scapulothoracic upward rotation regardless of the acromioclavicular internal rotation angle magnitude. From this equation and the non-constant weight factors, it can be seen that this question would provide the same result as the coupling function in Teece et al. (2008) (described above) if the mean acromioclavicular internal rotation angle for a participant was 60°.

Data Analysis

Descriptive statistics (mean and standard errors) were calculated for sternoclavicular elevation and posterior rotation, acromioclavicular upward rotation and internal rotation, and scapulothoracic upward rotation at 10° increments of

humerothoracic elevation. The accuracy of both coupling functions for estimating scapulothoracic upward rotation displacement was determined by calculating residual error (i.e. the difference between the estimated and actual scapulothoracic upward rotation displacement) for each phase. Bias error was calculated as the mean of the residual errors with a positive error indicating the coupling functions overestimated the actual scapulothoracic upward rotation displacement, and a negative error indicating the coupling functions underestimated the actual scapulothoracic upward rotation displacement. Root mean square (RMS) error was also calculated to reflect the average magnitude of the error between the estimated and actual scapulothoracic upward rotation displacements. The ability of each coupling function to predict the actual scapulothoracic upward rotation displacement was also described using r^2 statistics calculated using simple linear regression. Although this statistic does not necessarily reflect a measure of accuracy, it does provide an estimate of how much variance in the actual scapulothoracic upward rotation displacement can be explained by the coupling function.

To explore the proportional (i.e. relative) contributions of the component motions to scapulothoracic upward rotation, the product of each component motion and its weighting factor from the subject-specific coupling function was also expressed as a proportion of the actual scapulothoracic upward rotation displacement as follows:

$$P_{SCelev} = \frac{90 - ACir/_{90} * SCelev}{STur} * 100\%$$

$$P_{SCrot} = \frac{ACir/_{90} * SCrot}{STur} * 100\%$$

$$P_{ACur} = \frac{ACur}{STur} * 100\%$$

Additionally, the residual error in prediction was expressed as a proportion of the actual scapulothoracic upward rotation displacement. When summed for each subject, the proportional contributions of each component motion and residual error totaled 100%. Negative proportional contributions are possible and indicate the subject was moving in a way that retracted from scapulothoracic upward rotation (i.e. sternoclavicular anterior rotation, sternoclavicular depression, acromioclavicular downward rotation).

Differences across the range of motion in component motion proportional contributions were tested using two-factor mixed-model ANOVAs with a within-subject factor of humerothoracic elevation phase (30°-60°, 60°-90°, 90°-120°) and a between-subject factor of group (symptomatic, asymptomatic). The primary comparison of interest was the effect of humerothoracic elevation phase. The effect of group was included in the analysis to account for group differences should they exist. For each analysis, the appropriate covariance structure was determined by inspecting the covariance matrix of the within-subject factor (**Table 40**, **Table 42**, and **Table 44**) and fit statistics of models using various covariance structures (Littell et al., 2000) (**Table 41**, **Table 43**, and **Table 45**). The significance of two-factor interaction was assessed first, and main effects were only assessed in the absence of an interaction. All follow-up comparisons were performed using Tukey adjustments to protect for alpha inflation. Statistical analyses were performed in SAS 9.4 (The SAS Institute; Cary, NC) using an alpha level of 0.05.

Results

On average across the range of motion, participants underwent sternoclavicular elevation, sternoclavicular posterior rotation, acromioclavicular upward rotation,

scapulothoracic upward rotation, and a small amount of acromioclavicular internal rotation (**Figure 24**).

Coupling Functions Predicting Scapulothoracic Upward Rotation

Across all humerothoracic elevation phases, both coupling functions resulted in RMS errors of 1.2-2.8° and bias errors of -0.6° to -2.4° (**Table 8**). Further, the estimated scapulothoracic upward rotation calculated assuming a fixed 60° acromioclavicular internal rotation angle explained 80-90% of the variance in the actual scapulothoracic upward rotation ($p < 0.01$) (**Figure 25**). The estimated scapulothoracic upward rotation calculated using the subject-specific coupling function explained 79-90% of the variance in the actual scapulothoracic upward rotation ($p < 0.01$).

Proportional Contributions of Component Motions

Across all phases of humerothoracic elevation, acromioclavicular upward rotation contributed the most to scapulothoracic upward rotation (**Figure 26**). The magnitude of contribution depended on the phase of humerothoracic elevation (main effect of phase: $p < 0.01$, $F = 33.30$, $df = 2,115$). During the 30°-60° phase, acromioclavicular upward rotation was responsible for an average of 84.2% of the magnitude of scapulothoracic upward rotation. The proportional contribution decreased significantly to 42.3% for the 60°-90° phase ($p < 0.01$, $t = 6.58$, $df = 115$), where it remained unchanged (36.6%) for the 90°-120° phase ($p = 0.64$, $t = 0.90$, $df = 115$). The presence of symptoms did not significantly impact the proportional contribution of acromioclavicular upward rotation (main effect of group: $p = 0.09$, $F = 3.03$, $df = 1,58$) (**Figure 68A**).

Sternoclavicular posterior rotation was the secondary contributor to scapulothoracic upward rotation (**Figure 26**), and the magnitude of contribution depended on the phase of humerothoracic elevation (main effect of phase: $p < 0.01$, $F = 25.95$, $df = 2,115$). During the 30°-60° phase, sternoclavicular posterior rotation was responsible for an average of 2.8% of the magnitude of scapulothoracic upward rotation. The proportional contribution increased significantly to 32.2% for the 60°-90° phase ($p < 0.01$, $t = -6.04$, $df = 115$), where it remained unchanged (34.2%) for the 90°-120° phase ($p = 0.91$, $t = -0.40$, $df = 115$). The presence of symptoms did not significantly impact the proportional contribution of sternoclavicular posterior rotation (main effect of group: $p = 0.41$, $F = 0.68$, $df = 2,115$) (**Figure 68B**).

Sternoclavicular elevation consistently contributed minimally to scapulothoracic upward rotation (**Figure 26**). However, the magnitude of contribution depended on the phase of humerothoracic elevation (main effect of phase: $p = 0.02$, $F = 3.97$, $df = 2,115$). During the 30°-60° and 60°-90° phases, sternoclavicular elevation was responsible for an average of 8.3% and 8.6% of the magnitude of scapulothoracic upward rotation, respectively. During the 90°-120° phase, the contribution increased significantly to 10.7% ($p = 0.03$, $t = -2.63$, $df = 115$). The presence of symptoms did not significantly impact the proportional contribution of sternoclavicular elevation (main effect of group: $p = 0.08$, $F = 3.27$, $df = 2,115$) (**Figure 68C**).

Discussion

The results of the current study support the theory proposed by Ludewig and colleagues (Teece et al., 2008) that the sternoclavicular and acromioclavicular

contributions to scapulothoracic upward rotation can be simplified to three angular degrees of freedom: acromioclavicular upward rotation, sternoclavicular posterior rotation, and sternoclavicular elevation. The coupling functions derived for this study tended to underestimate the actual scapulothoracic upward rotation with errors increasing at higher phase of motion (**Figure 25** and **Table 8**). This is because the functions only account for the spatial offset between the clavicular and scapular coordinate systems in the transverse plane (i.e. acromioclavicular internal rotation angle), which appears to be a reasonable simplification at lower angles when the offset between the axes in the coronal and sagittal planes is small (i.e. small magnitudes of acromioclavicular upward rotation and posterior tilt). However, at higher angles of humerothoracic elevation, the scapular and clavicular axes become more oblique to one another necessitating a more complex coupling function model.

Despite the increased absolute errors at higher phases of humerothoracic elevation, the errors in estimating scapulothoracic upward rotation correspond to less than 20% of the actual scapulothoracic upward rotation motion. This suggests the coupling functions accurately described over 80% of scapulothoracic upward rotation motion. Additionally, the coupling functions explained a substantial portion of the variance in the actual scapulothoracic upward rotation (r^2 = 79-90%). Together these findings suggest the coupling functions have utility in simplifying the complex motion of scapulothoracic upward rotation into its component motions, which can be useful in developing kinematic and kinetic theories for explaining normal and abnormal scapulothoracic motion.

Given scapulothoracic upward rotation can be estimated from its component motions, the proportional contributions of the individual component motions can be explored. During the initial phase of humerothoracic elevation (i.e. 30°-60°), acromioclavicular upward rotation was the predominant component motion, accounting for an average of 84% of scapulothoracic upward rotation. Sternoclavicular posterior rotation and elevation can be considered accessory motions during this phase with a combined average contribution of only 10%. The relative dominance of acromioclavicular upward rotation and small contribution due to sternoclavicular posterior rotation during this initial phase suggests the scapula and clavicle are not yet fully coupled. In other words, motion of the scapula does not substantially transfer to the clavicle. This is likely due to the need to first take up slack in the acromioclavicular joint and coracoclavicular ligaments before motion can be transferred between bones through the acromioclavicular and coracoclavicular ligaments. Functionally, one potential benefit for not having the scapula fully coupled with the clavicle in the early phase of motion is that it may allow the scapula to seek conformity with the thorax by moving at the acromioclavicular joint in its other dimensions (i.e. tilt and internal rotation). Scapular conformity on the thorax helps create a functional "gliding plane" upon which the scapula may move, which may result in a more stable mechanism for the performance of upper extremity tasks (van der Helm, 1994).

The high proportional contribution from acromioclavicular upward rotation during the initial phase of humerothoracic elevation may also suggest a potential mechanical inefficiency for production of scapulothoracic motion. This is because the

serratus anterior and middle and lower trapezius would act primarily at the acromioclavicular joint to produce net scapulothoracic upward rotation and external rotation, respectively. Although the moment arms for these muscles are large when acting at the acromioclavicular joint, theoretically they become much larger when they act at the sternoclavicular joint (Veeger & van der Helm, 2007). A larger moment arm would allow for an even larger torque producing capability, making them more efficient at producing scapulothoracic upward rotation and external rotation. However, for the serratus anterior and middle and lower trapezius to act at the sternoclavicular joint, the clavicle and scapula need to move predominantly as one unit (i.e. through sternoclavicular posterior rotation), which does not appear to be occurring for most people during the initial phase of motion. Therefore, when the scapula and clavicle are not yet coupled in the initial phase, scapulothoracic muscle function may not be maximized.

During the final two phases of humerothoracic elevation (i.e. 60°-120°), acromioclavicular upward rotation continues to serve as the predominant component motion. However, the proportional contribution decreases to an average of 42% during the 60°-90° phase, and 37% during the 90°-120° phase. This reduction in the proportional contribution of acromioclavicular upward rotation coincides with an increased contribution from sternoclavicular posterior rotation, which now accounts for an average of 32-34% of scapulothoracic upward rotation motion. Sternoclavicular elevation remains an accessory motion accounting for less than 11% of scapulothoracic upward rotation.

The comparable contribution between acromioclavicular upward rotation and sternoclavicular posterior rotation after the initial phase suggests the scapula and clavicle

now function as a mechanism, but do not fully become a single "claviscapular link" as proposed by Dvir and Berme (1978). However, with the scapula and clavicle more coupled, the clavicle may be able to fulfill its role as a strut by supporting the upper limb on the thorax. This function may be especially critical in higher phases of motion because the total joint torque produced by muscles acting at the glenohumeral joint has been shown to be highest between 60-120° humerothoracic elevation (Yanagawa et al., 2008). The clavicle acting as a strut at higher angles may be especially important to support higher dynamic loads when the arm is overhead. The strut function may not be as critical during the initial phase of motion when the total joint torque produced by glenohumeral muscles is relatively less, which may explain why the clavicle and scapula do not need to be as coupled during that phase.

The increased proportional contribution from sternoclavicular posterior rotation during the 60°-90° and 90°-120° phases compared to the initial phase suggests the serratus anterior now acts, at least partially, at the sternoclavicular joint. The result is an increase in the moment arm for the muscle to theoretically increase its leverage to produce net scapulothoracic upward rotation and posterior tilt torque. However, this increase in mechanical efficiency of the serratus anterior would also coincide with an increased requirement for the counter-stabilizing action of the rhomboids and middle trapezius to prevent the scapula from excessively internally rotating and translating laterally around the thorax from the pull of the serratus anterior (Gupta & van der Helm, 2004; van der Helm, 1994). Therefore, it is possible the degree to which the scapula and clavicle are coupled may influence the magnitude of scapular "dyskinesia" observed. For

example, an individual with less coupling between the scapula and clavicle may be able to use lower rhomboid and middle trapezius muscle activation to maintain the scapula's position on the thorax compared to someone who is more coupled. This is because in the less coupled individual, the serratus anterior still predominantly acts at the acromioclavicular joint and has a lower overall torque generating capability, and therefore may require less rhomboid and middle trapezius muscle activation compared to a more coupled individual. Clinically, this may help explain the wide variation in scapulothoracic kinematics, particularly internal/external rotation, observed in both individuals with and without shoulder pain (Lawrence et al., 2014a; McClure et al., 2006; McClure et al., 2001).

The relative proportional contribution between acromioclavicular joint upward rotation and sternoclavicular posterior rotation may serve as a measure of "decoupling" in the shoulder complex. As such, this metric may have important implications for clinical decision making when examining patients post acromioclavicular separation. Current guidelines regarding whether to pursue surgical intervention are based on Rockwood's classification, which relies upon a series of static radiographs (Rockwood et al., 1996). However, this classification is limited by several factors that challenge its clinical utility. For example, radiographic projection error, patient position, and muscle activity may all impact the accuracy of accessing the magnitude of joint disruption (Tauber, 2013). But perhaps most importantly, there is an inherent challenge in diagnosing a musculoskeletal movement disorder using static radiographs. As such, a more objective measure of

identifying the degree to which the clavicle and scapula are decoupled could better guide treatment decisions and improve clinical outcomes.

Quantifying the proportional contribution between acromioclavicular upward rotation and sternoclavicular posterior rotation in individuals during the 60°-90° phase with acromioclavicular joint separation may be a means to identify who would benefit from surgical stabilization. Higher phases may be more sensitive to the presence of decoupling than the initial phase because motion of the scapula is at least partially transferred to the clavicle in most individuals, where this was not the case in the initial phase (**Figure 26**). Therefore, if an individual had an excessive proportional contribution from acromioclavicular upward rotation, this may suggest the acromioclavicular joint and coracoclavicular ligaments are no longer efficiently transmitting motion and surgical stabilization may be indicated.

The question then becomes what a reasonable cutoff is to define "excessive" acromioclavicular upward rotation in individuals post acromioclavicular separation. To fully answer this question, shoulder complex kinematics would need to be quantified using a large sample including individuals with a history of acromioclavicular joint separation. However, an estimate of this cutoff may be made by determining the acromioclavicular upward rotation proportional contribution magnitude that corresponds to 0% sternoclavicular posterior rotation proportional contribution. This was done on an exploratory basis with the data from this study using an equation developed through simple linear regression model for the 60°-90° phase of humerothoracic elevation. The results suggest that a proportional contribution from acromioclavicular upward rotation of

82% may serve as a conservative threshold for indicating decoupling has occurred (**Figure 27**). Any less acromioclavicular upward rotation proportional contribution suggests motion of the scapula is being transmitted, at least in part, to the clavicle. Future research is needed to more rigorously define a cutoff from which to base surgical decision making, as well as determine whether applying this cutoff improves surgical outcomes by targeting appropriate patients.

Another potential clinical implication of excessive decoupling between the scapula and clavicle is that the increased acromioclavicular upward rotation may result in increased shear stress at the acromioclavicular joint. Increased shear stress may create biomechanical changes in the articular cartilage which over time may predispose an individual to acromioclavicular joint osteoarthritis. This premise is supported by literature showing higher incidence of acromioclavicular osteoarthritis over the long term in individuals post Type III acromioclavicular joint separation (Cox, 1981; Taft et al., 1987). More research is needed to determine whether excess acromioclavicular upward rotation increases shear stresses, and subsequently whether increased acromioclavicular upward rotation is a risk factor for the development of acromioclavicular osteoarthritis.

An additional potential clinical implication of decoupling relates to when humerothoracic elevation is accomplished through increasing scapulothoracic upward rotation in individuals with decreased glenohumeral elevation such as in the case of massive rotator cuff tears (Mell et al., 2005), adhesive capsulitis (Fayad et al., 2006; Rundquist, 2007; Vermeulen et al., 2002), and glenohumeral osteoarthritis (Braman et al., 2010; Fayad et al., 2006). Generally, this is considered a positive compensatory strategy

to improve shoulder functional range of motion. However, given the theory that increased acromioclavicular upward rotation may predispose an individual to acromioclavicular osteoarthritis, the risk/benefit relationship of using the compensatory movement strategy may need to be considered. For chronic conditions such as massive rotator cuff tears and glenohumeral osteoarthritis, increasing humerothoracic elevation through increasing scapulothoracic upward rotation may still be considered a positive compensatory strategy to improve the patient's functional range of motion. However, for temporary conditions such as adhesive capsulitis, increasing acromioclavicular upward rotation as a short-term functional strategy may have potential unwanted long-term consequences such as acquired acromioclavicular joint laxity and osteoarthritis and may need to be considered judiciously. Further, exercises that aim to stretch the glenohumeral joint by maximizing passive humerothoracic elevation but do not involve stabilizing the scapula (e.g. wand exercises) may be counter-productive for the long-term health of the acromioclavicular joint. Instead, focusing manual and exercise interventions at stretching the glenohumeral joint without requiring excessive acromioclavicular compensatory motion may be indicated.

Across all phases of humerothoracic elevation, high variability between subjects exists in the proportional contribution of each component motion. This variability can be seen using parallel coordinates plots which show the proportional contribution of each component motion (across the x-axis) with each subject represented as a single line (**Figure 28**). The shared y-axis represents the magnitude of the proportional contribution. This type of visualization allows the between-subject variance within each variable to be

appreciated as well as the relationship between adjacent variables (via line slope). Using this method of visualizing the multidimensional data, the between-subject variability appears to be the highest in the 30°-60° phase of humerothoracic elevation, particularly for acromioclavicular upward rotation and sternoclavicular posterior rotation. This may reflect differing magnitudes of coupling seen during this phase, potentially from between-subject variability in initial alignment or differing laxity in the acromioclavicular and coracoclavicular ligaments. The magnitude of the between-subject variation in both sternoclavicular posterior rotation and acromioclavicular upward rotation appears to decrease for higher phases of humerothoracic elevation, suggesting the shoulder complex mechanism becomes more constrained at higher elevation angles.

The proportional contribution due to sternoclavicular elevation consistently contributes only a small amount to scapulothoracic upward rotation (**Figure 26**) and with comparatively small between-subject variability (**Figure 28)**. This finding may suggest shoulder shrugging (through increasing sternoclavicular elevation) which is often seen in individuals with massive rotator cuff tears and glenohumeral hypomobility, may not be an optimal compensatory strategy to increase scapulothoracic upward rotation. This is also supported by the generally low magnitudes of sternoclavicular elevation displacements during arm raising found in this study and others (Lawrence et al., 2014a; Ludewig et al., 2009a; McClure et al., 2006).

This study has methodological limitations that are important to consider when interpreting the results. First, the shape and position of the clavicle relative to the imaging plane often make it challenging to shape-match, especially at lower angles of elevation.

Initial validation work found RMS errors for shape-matching clavicle axial rotation position of 3.7° corresponding to RMS errors in acromioclavicular upward rotation of 3.4° (Lawrence et al., 2018). Therefore, it is possible shape-matching errors added irrelevant variance which confounded descriptions of the underlying mechanics and may have resulted in smaller sternoclavicular posterior rotation displacements than those reported by previous studies (Lawrence et al., 2014a; Ludewig et al., 2009a). If sternoclavicular posterior rotation displacement was in fact under-estimated, this would result in an underestimation of its proportional contribution and an overestimation of acromioclavicular proportional contribution.

Second, the approach used in this study can only account for the kinematic mechanisms related to scapulothoracic upward rotation. Other sternoclavicular, acromioclavicular, and scapulothoracic rotations also serve important roles in shoulder function. Additional work is needed to investigate how scapulothoracic anterior/posterior tilt and internal/external rotation are produced as scapular dyskinesias are often seen in combination (Kibler et al., 2002). Future studies are also needed to translate this kinematic knowledge into kinetics where muscle function (and potentially dysfunction) can be studied, which will have a more direct impact on exercise recommendations.

Third, the average participant age was relatively young at 33 years. However, the age range spanned from 22 to 55 years old helping capture age-related movement variability. Future studies should investigate whether coupling relationships are age-dependent and related to the development of degenerative pathology such as osteoarthritis and rotator cuff disease.

Finally, the motion performed in this study was controlled to the scapular plane. The proportional contributions of the component motions will likely change if the motion is performed in other planes due to the altered acromioclavicular internal rotation angle as the arm is brought across the body or behind the back. The subject-specific coupling function may still be useful as the acromioclavicular internal rotation angle will increase or decrease to reflect the different planar motions (Ludewig et al., 2009a). However, the coupling function assuming 60° acromioclavicular internal rotation may no longer be appropriate.

Despite the complex anatomical and kinematic relationships of the shoulder complex, scapulothoracic upward rotation can be reliably estimated from the component motions of acromioclavicular upward rotation, sternoclavicular posterior rotation, and sternoclavicular elevation as a function of the acromioclavicular internal rotation position. Acromioclavicular upward rotation and sternoclavicular posterior rotation are the predominant component motions of scapulothoracic upward rotation, with a combined contribution of at least 70%. More research is needed to investigate how these coupling relationships influence muscle function and scapular dyskinesia.

Table 7: Participant Demographics by Group

	Asymptomatic (n=30)	**Symptomatic (n=30)**	**Statistic**	**p-value**
Age (years)	32.7 ± 8.3	32.4 ± 8.8	$t_{58} = 0.12$	0.90
Sex (% male)	46.7%	46.7%	$X^2_1 = 0.0$	1.0
Dominance of the side tested (% dominant)	40.0%	40.0%	$X^2_1 = 0.0$	1.0
Height (cm)	173.1 ± 8.5	170.9 ± 7.8	$t_{58} = 1.01$	0.32
Mass (kg)	72.1 ± 12.5	72.9 ± 15.6	$t_{58} = -0.23$	0.82
BMI (kg/m^2)	23.9 ± 2.7	24.8 ± 4.1	$t_{50.6} = -0.98$	0.33
Symptom duration (weeks)	0.0 ± 0.0	108.2 ± 240.0	NC	NC
NPRS (0 – 100)				
Highest past 7 days	0.0 ± 0.0	49.6 ± 16.9	NC	NC
Lowest past 7 days	0.0 ± 0.0	14.1 ± 17.2	NC	NC
DASH (0 – 100)	0.7 ± 1.8	15.3 ± 8.1	$t_{31.9} = -9.59$	<0.01
Work subscale	0.2 ± 1.2	9.0 ± 14.5	$t_{26.4} = -3.13$	<0.01
Sport subscale	2.1 ± 6.5	25.8 ± 28.1	$t_{16.7} = -3.25$	<0.01

Notes: Demographic data are presented as mean ± SD or proportions, as appropriate. Symptom duration presented as median due to skewed distribution. Group comparisons were assessed using two-sample independent *t*-tests or Chi-square tests for continuous and binary data, respectively. Abbreviations: BMI = body mass index; NPRS = numeric pain rating scale; DASH = Disabilities of the Arm, Shoulder, and Hand; NC = not computed due to no data in the asymptomatic group.

Table 8: Results for Estimating Scapulothoracic Upward Rotation using the Coupling Function

	Humerothoracic Elevation Phase		
	30°-60° (n=60)	**60°-90° (n=60)**	**90°-120° (n=59)**
Coupling function			
RMS error	1.2°	2.5°	2.8°
Bias error	-0.6°	-2.1°	-2.4°
r^2	0.90 (<0.01)	0.80 (<0.01)	0.88 (<0.01)
Subject-specific coupling function			
RMS error	1.2°	2.5°	2.8°
Bias error	-0.6°	-2.1°	-2.4°
r^2	0.88 (<0.01)	0.79 (<0.01)	0.90 (<0.01)

Notes: The formula for the coupling function is based on the theory proposed in Teece et al. (2008) and assumes a fixed acromioclavicular internal rotation angle (60°). The equation for the subject-specific coupling function uses the subjects' mean acromioclavicular internal rotation angle during the phase of humerothoracic elevation. Negative bias indicates an under-estimation of scapulothoracic upward rotation displacement. R-squared statistics expressed as a magnitude and associated p-value. Abbreviations: RMS = root mean square.

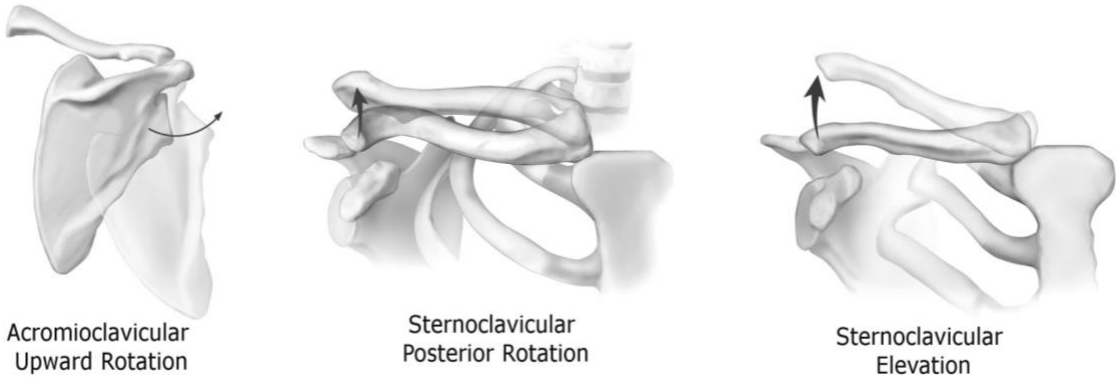

Figure 21: The component motions of scapulothoracic upward rotation. Figure modified and used with permission from Ludewig et al. (2009a).

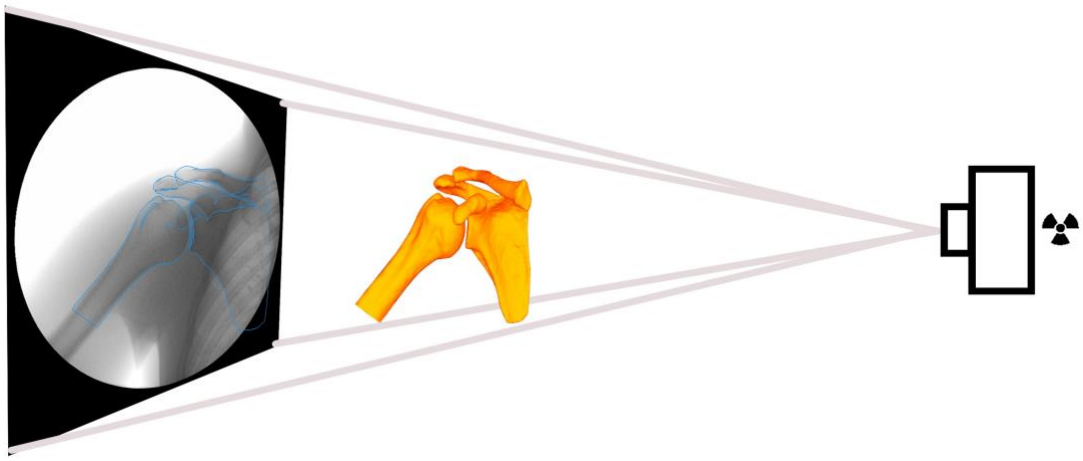

Figure 22: The shoulder complex shape-matched for one fluoroscopic frame. Shape-matching was performed by virtually rotating and translating the 3D bone model within JointTrack software until the projected contours of the bones (blue line) become aligned with their respective projections on the fluoroscopic image.

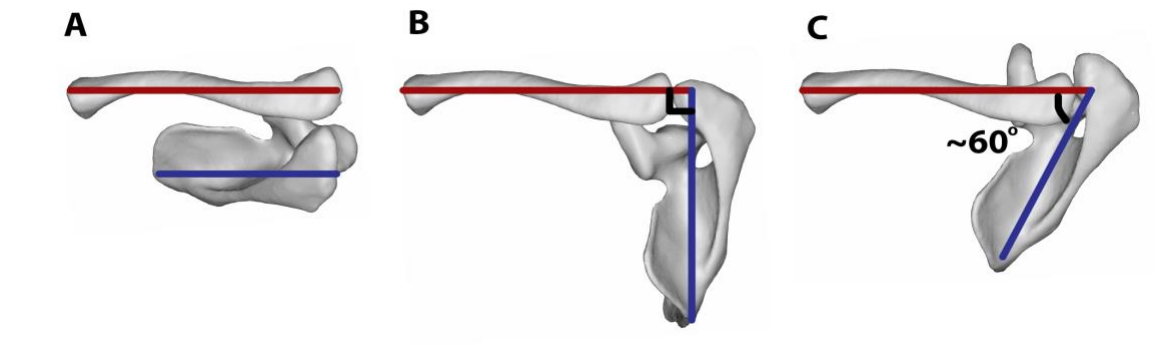

Figure 23: Relationship between acromioclavicular joint axes and coupled mechanics of the clavicle and scapula. The red line represents the clavicle medial/lateral axis, while the blue line represents the scapular medial/lateral axis. **A)** Theoretical relationship in which axes are parallel; therefore, only sternoclavicular elevation produces scapulothoracic upward rotation. **B)** Theoretical relationship in which axes are perpendicular; therefore, only sternoclavicular posterior rotation produces scapulothoracic upward rotation. **C)** Average physiological relationship with acromioclavicular internal rotation angle of approximately 60°, where both sternoclavicular posterior rotation and elevation will contribute to scapulothoracic upward rotation.

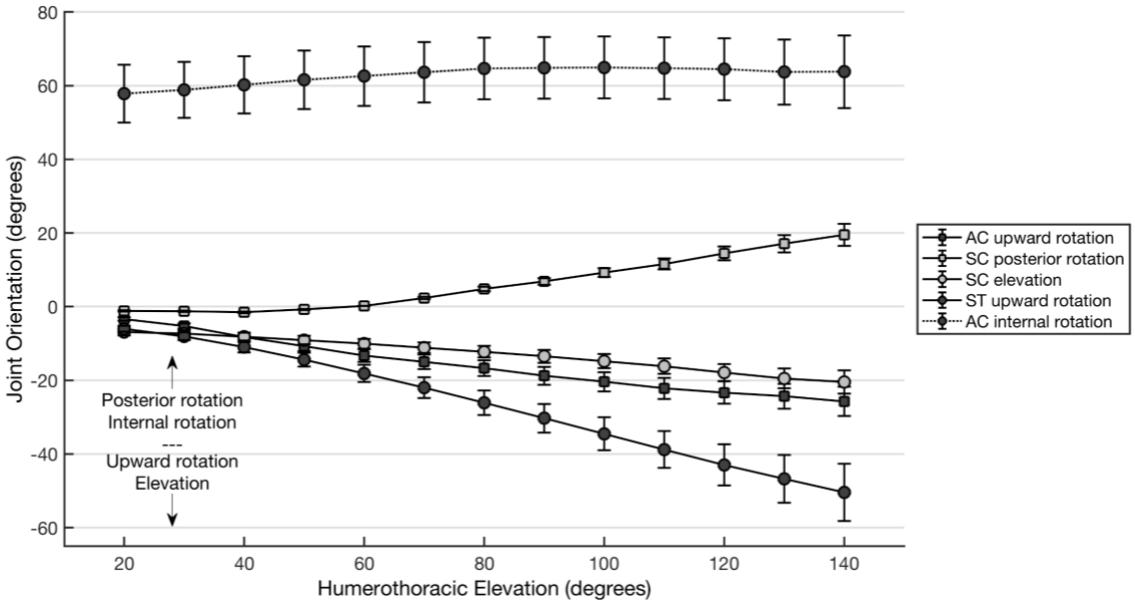

Figure 24: Angular position across angles of humerothoracic elevation for acromioclavicular upward rotation, sternoclavicular posterior rotation, sternoclavicular elevation, scapulothoracic upward rotation, and acromioclavicular internal rotation. Data is presented as the mean and unpooled SE. Abbreviations: AC = acromioclavicular; SC = sternoclavicular; ST = scapulothoracic.

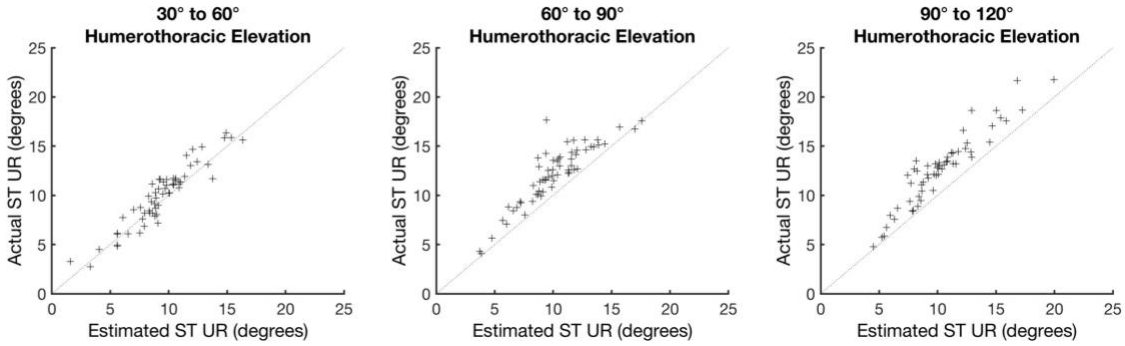

Figure 25: Results of the subject-specific coupling function for estimating scapulothoracic upward rotation displacement from the component motions of sternoclavicular posterior rotation, acromioclavicular upward rotation, and sternoclavicular elevation displacements across phases of humerothoracic elevation (30°-60°, 60°-90°, 90°-120°). Abbreviations: ST = scapulothoracic; UR = upward rotation.

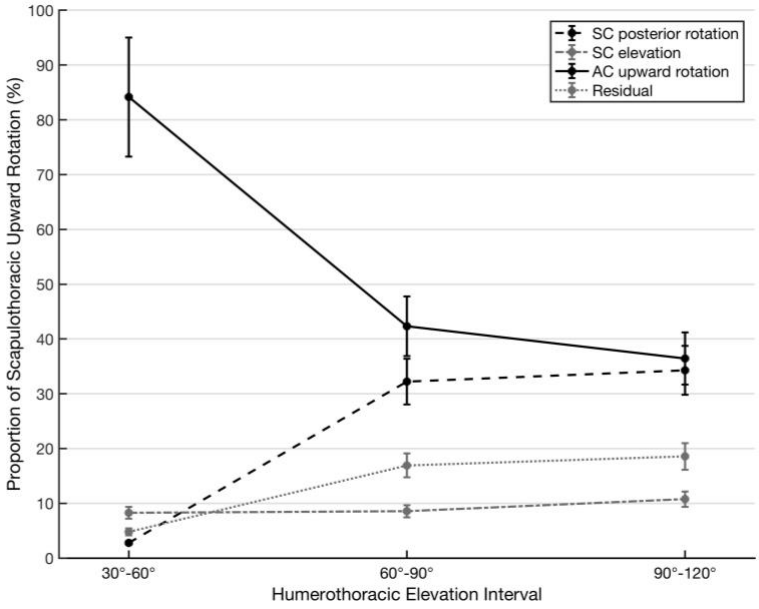

Figure 26: Proportional contributions of sternoclavicular posterior rotation, sternoclavicular elevation, and acromioclavicular upward rotation to scapulothoracic upward rotation across phases of humerothoracic elevation (30°-60°, 60°-90°, 90°-120°) based on the subject-specific coupling function. The mean residual error in prediction is also presented as a proportion of scapulothoracic upward rotation. Abbreviations: AC = acromioclavicular; SC = sternoclavicular.

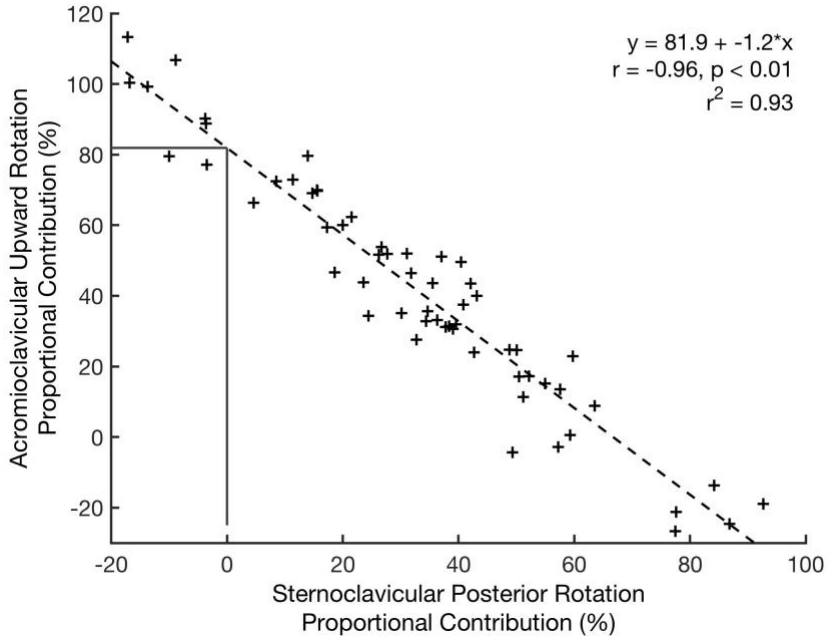

Figure 27: The relationship between acromioclavicular upward rotation and sternoclavicular posterior rotation proportional contributions to scapulothoracic upward rotation as calculated using the subject-specific coupling function during the 60°-90° phase. The intercept from the regression equation (81.9%, denoted by horizontal reference line) provides an estimate of the acromioclavicular upward rotation proportional contribution that corresponds to 0% contribution of sternoclavicular posterior rotation, which may be useful for defining "decoupling".

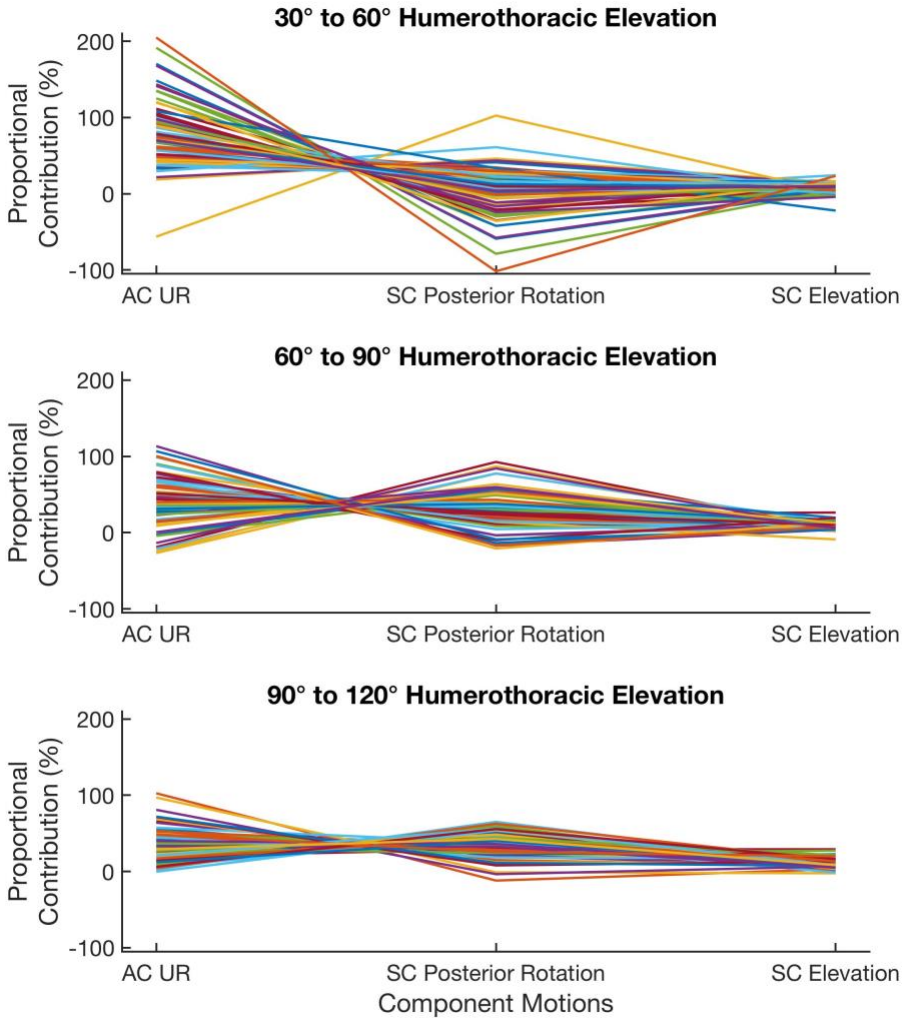

Figure 28: Parallel coordinates plots showing the proportional contribution of each component motion (across x-axis) for each phase of humerothoracic elevation. Each subject is represented as a single line. The shared y-axis represents the magnitude of the proportional contribution of the component motions to scapulothoracic upward rotation. Abbreviations: AC = acromioclavicular; SC = sternoclavicular; UR = upward rotation.

Chapter 6: Conclusion

This thesis sought to advance the understanding of the movement-related pathogenesis of rotator cuff disease. This effort is important because relatively few studies have investigated the impact of specific movement abnormalities on measures of joint and soft tissue injury mechanisms. The results of the studies contained within this thesis suggest: 1) single-plane fluoroscopy and 2D/3D shape-matching can accurately track shoulder complex kinematics during static trials; 2) the impact of scapulothoracic upward rotation on subacromial space is more complex than traditionally believed; and 3) acromioclavicular upward rotation and sternoclavicular posterior rotation are the predominant contributors to scapulothoracic upward rotation. As is often the case in research, the process of exploring and interpreting these findings created many more questions than answers and serves as a foundation upon which future research may be based.

Validation of single-plane fluoroscopy and 2D/3D shape-matching for quantifying shoulder complex kinematics (Aim 1)

Single-plane fluoroscopy and 2D/3D shape-matching can accurately track shoulder complex kinematics during static positions. In general, RMS errors were less than 3° for tracking acromioclavicular and glenohumeral joint orientations. Additionally, RMS errors for joint position were <1.8 mm except for anterior/posterior glenohumeral position. These errors constitute good improvement over traditional surface based measures (Hamming et al., 2012; Karduna et al., 2001; Ludewig et al., 2002), and do not require invasive methods such as transcortical bone pins (Lawrence et al., 2014a;

Lawrence et al., 2014b; Ludewig et al., 2009a; McClure et al., 2001) allowing for larger sample sizes.

Importantly, the use of fluoroscopy allows for the direct visualization of movement, which can provide insight into subtle movement patterns that may not be captured by traditional methods of tracking kinematics. For example, rapid downward rotation of the scapula during the lowering phase is often observed clinically (Kibler et al., 2013; McClure et al., 2009) and is thought to be evidence of impaired motor control. However, this theory is difficult to test using surface-based motion sensors due to skin motion artifact. The rapid downward rotation was often seen anecdotally in participants using fluoroscopy, which offered a new theory that the motion may be compensatory in nature in response to the need to control excessive glenohumeral translations. For example, if an individual had glenohumeral laxity, dynamic control of these translations may be difficult during dynamic tasks. During lowering of the arm, locking humeral motion to the scapula may potentially be a means of reducing translations but results in the rapid downward rotation we observe clinically and on fluoroscopy. More research is needed to investigate the implications of these presumed movement "impairments", and other kinematic descriptions (e.g. acceleration) may be important to characterize these movements.

Although the study described in Chapter 3 used well-established methods of validating fluoroscopy with radiostereometric analysis, the study has several limitations when being used to support the accuracy of our protocol used in the *in vivo* studies (Chapters 4 and 5). A primary limitation is that the validation was performed during

static trials due to the inability to sync the fluoroscopic systems. This may limit the generalizability to dynamic trials where motion blur may occur depending on the balance between the speed of movement and the frame rate and pulse width of the acquisition (Ellingson et al., 2016). However, comparison of the results of the current study to previous studies of dynamic glenohumeral motion (Matsuki et al., 2012; Zhu et al., 2012) suggest the addition of movement does not substantially increase errors over the underlying error due to using a single fluoroscopic plane.

A second key limitation was the resolution of the CT scan, which may have impacted the accuracy of the gold standard. This was because the entire specimen was imaged in a single scan resulting in lower resolution than if the shoulders were scanned independently. The primary consequence is the reduced precision with which the beads were digitized, which may have increased the error in defining the coordinate systems used as the gold standard. In the future, scanning each shoulder individually will maximize the resolution for a given anatomical region improving our ability to more accurately describe kinematic tracking errors.

Another key limitation of the study was the use of CT-based bone models for shape-matching while MR-based models were used for the *in vivo* analyses. The concern related to this limitation is that MR-based bone models may provide lower geometric accuracy than CT-based models for several reasons. First, MR imaging provides lower contrast, which can impact the ability to accurately segment the margins of the bones and subsequently impact shape-matching (Moro-oka et al., 2007). Second, MR imaging introduces spatial distortions which increase with higher magnet strength (Moro-oka et

al., 2007). The current study used a 3T scanner and spatial distortions were often observed on the distal shaft of the humerus. When distortions were observed, the 3D humeral bone models where cropped. However, this reduced the contours available for shape-matching. Third, the acquisition time of the MR introduces the potential for motion artifact. Anecdotally, segmentation of the clavicle was particularly challenging due to breathing artifact and a lower signal to noise ratio likely due to the difficulty conforming the flex coil to the subject's upper thorax.

Despite the potential limitations associated with using MR-based bone models, previous studies investigating the geometric accuracy of using MR for reconstructing 3D models of long bones reports generally <0.25 mm error (Moro-oka et al., 2007; Rathnayaka et al., 2012). However, these errors have not been quantified for the shoulder complex. Recent unpublished work in our lab has shown that MR-based bone models result in only small increases in RMS errors (<1°, <1 mm) for automated biplane tracking (Akbari-Shandiz et al., 2018). While a similar study has not been performed for single-plane tracking, it is likely the primary source of error continues to be the single plane and not the geometric accuracy of the bone models. Importantly, the need to quantify soft tissue parameters in the current study necessitated the use of MR-derived bone models. Further, the use of MR-based bone models also reduced the risk to the subject consistent with the ALARA (as low as reasonably achievable) principle for minimizing radiation exposure.

The use of a clinical fluoroscopy unit was associated with both benefits and technical challenges. The primary benefit was the existing FDA approval, which

accelerated support from regulatory committees for the proposed research. In contrast, the primary technical challenge was the inability to change the pre-programmed factory settings to improve image quality. Clinical image acquisition is not often focused on gross movement across the field of view. Therefore, the factory settings are not optimized for precisely tracking dynamic human movement. The motions studied during the *in vivo* analyses (Chapters 4 and 5) were performed at a rate of approximately 50°/second and captured during continuous x-ray exposure at a rate of 25 Hz. Although the frame rate used as generally high enough to minimize motion blur for this relatively slow trial, the continuous exposure may have increased the amount of blur present (Ellingson et al., 2016) and increased the dose to the subject. However, short-duration pulsed acquisition on the c-arm was not feasible due to the factory settings designed for clinical purposes. Specifically, the shortest pulsed exposure available for the data capture settings was 13 ms, which would have reduced the frame rate to 12 Hz. These acquisition parameters would have resulted is approximately 50% fewer images and therefore analyzable data. Although data from the *in vivo* analyses (i.e. Chapters 4 and 5) was down-sampled to every 10° humerothoracic elevation to reduce data processing time, future studies may benefit from advances in automated tracking to analyze all frames and investigate subtle motion deviations that are often visible. For example, subtle superior glenohumeral translation and/or scapulothoracic downward rotation at the onset of motion may be important movement impairments to investigate but require analyzing more frames than the subset used for the current study.

Despite its challenges in a research setting, the major benefit of using a clinical fluoroscopy unit in the current study is the potential integration into clinical practice. Current clinical methods of quantifying shoulder complex kinematics (e.g. visual assessment or inclinometer) may not be accurate enough to detect subtle alterations in motion (Johnson et al., 2001). A more accurate method may help in the diagnosis and treatment of mechanical shoulder pain. However, 2D/3D shape-matching even with the use of a clinical system requires substantial time commitment to process and analyze the data. Future work aimed at developing automated algorithms for shape-matching and generation of the 3D bone models is critical to ensure the clinical translation of this measurement approach.

The accuracy of single-plane fluoroscopy and 2D/3D shape-matching was sufficient to quantify subacromial proximities. Importantly, the errors in quantifying subacromial space did not likely impact the magnitude of any group differences because shape-matching was performed blinded and there is no known reason to believe one group was more susceptible to errors than another. However, errors in quantifying subacromial space due to shape-matching may have introduced irrelevant variance that may have increased variability in the proximity metrics, and thereby reduced power to detect group differences as described in Chapter 4. Future studies investigating the relationship between shoulder motion and mechanisms of pathology may benefit from the higher accuracy of biplane fluoroscopy and from higher level modeling such as finite element analyses.

The impact of decreased scapulothoracic upward rotation on subacromial proximities (Aim 2)

The results of the second study contained within this thesis support the hypothesis that decreased scapulothoracic upward rotation creates a shift in the range of smallest proximity between the low and high scapulothoracic upward rotation groups. As a whole, the impact of scapulothoracic upward rotation on subacromial space is more complex than traditionally believed. Clinically, the finding of a shift suggests the implications of decreased scapulothoracic upward rotation on subacromial proximities may need to be interpreted within the context of the humerothoracic elevation range in which the movement impairment is observed.

The impact of scapulothoracic upward rotation on subacromial space becomes more complex when data from the participants in the mid scapulothoracic upward rotation group are considered. It is possible that comparing the subacromial proximities in the two groups at the tails of the scapulothoracic upward rotation distribution may introduce a confounding factor. This is because neither group's kinematics may be considered a control for the other as both represent "extreme" motion. To investigate this possibility, an exploratory two-factor mixed-model ANOVA was performed to compare all three scapulothoracic upward rotation groups (low, mid, high) across the four angles of humerothoracic elevation (minimum, 30°, 60°, and 90°). Although no effect involving group was significant (interaction: $p = 0.16$, $F = 1.57$, $df = 6,137$; main effect of group: $p = 0.53$, $F = 0.64$, $df = 2,57$), participants in the mid scapulothoracic upward rotation group tended to have higher normalized minimum distance than both the low and high groups (**Figure 29**). In particular, participants in the mid scapulothoracic upward rotation

group had 40.2% larger normalized minimum distance than those in the low subgroup when the arm was at the side, and 37.7% larger normalized minimum distance at 30° humerothoracic elevation. Although not statistically significant, both magnitudes exceed our hypothesized threshold of clinical meaningfulness (35%). Further, participants in the mid scapulothoracic upward rotation group had 21.1% larger normalized minimum distance than those in the high subgroup at 30° humerothoracic elevation.

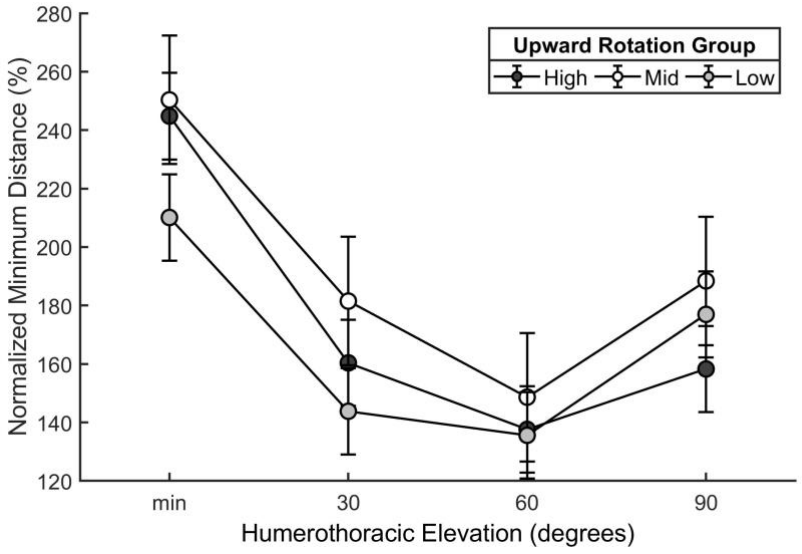

Figure 29: Normalized minimum distance between the coracoacromial arch and articular margin aspect of the rotator cuff insertion for all scapulothoracic upward rotation groups. Abbreviation: min = minimum

The finding that participants in both high and mid scapulothoracic upward rotation groups tended to have higher subacromial proximities than those in the low group may have important implications for the development of a movement-based diagnostic classification system. Within this framework, some extreme joint positions may not necessarily be considered “bad” or “good” but may depend on the context in which it is observed. For example, increased scapulothoracic upward rotation may offer

some protection for subacromial compression at lower angles of humerothoracic elevation but may reduce subacromial proximities at higher angles. This may be an important consideration for ergonomic design and matching workers to job tasks.

In the current study, the mid group differed from the low group in scapulothoracic upward rotation by approximately 5° until 50° humerothoracic elevation (**Figure 30**). This suggests a 5° deviation in scapulothoracic upward rotation from "average" may reduce the subacromial space, but the range in which this reduction occurs may depend on the direction of the deviation as previously described. The challenge clinically is to be able to accurately quantify scapulothoracic upward rotation to identify which patients present with more extreme motion. More research is needed to establish normative data and to improve clinical measures for scapulothoracic upward rotation so that deviations from "average" may be reliably and accurately identified.

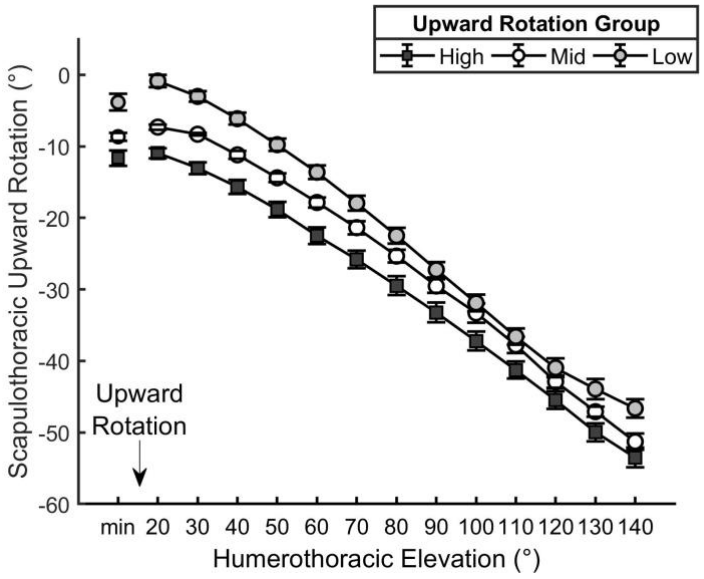

Figure 30: Scapulothoracic upward rotation magnitudes across humerothoracic elevation for all three scapulothoracic upward rotation groups.

Mechanical coupling of scapulothoracic upward rotation (Aim 3)

Understanding the coupling relationships amongst the joints of the shoulder complex forms the foundation from which we can understand how normal and abnormal motion are produced. The results of the third study contained within this thesis build upon classic studies that proposed theories regarding the structure and function of the shoulder complex (Bagg & Forrest, 1988; Dvir et al., 1978; Inman et al., 1944; van der Helm, 1994; van der Helm et al., 1995). These early studies sought to understand shoulder motion primarily through the use of 2D measures such as radiographs. Although exploratory in nature, the current study is an important addition to this foundational work as it accurately quantified full shoulder complex kinematics in three-dimensions.

A key limitation to this study is that it only investigated the coupling relationships related to scapulothoracic upward rotation. Scapulothoracic posterior tilt and internal rotation also play important roles in shoulder function by helping the scapula seek conformity with the thorax and improve the effectiveness of the gliding plane by reducing the available degrees of freedom (van der Helm, 1994). Furthermore, the question of coupling relationships is inherently a multivariate one due to the oblique nature of the clavicular and scapular axes. For example, sternoclavicular posterior rotation was found to be a predominant component motion of scapulothoracic upward rotation but likely also plays an important role in producing posterior tilt (Teece et al., 2008). Future studies are needed to investigate the coupling relationships for scapulothoracic posterior tilt and internal rotation, and how these relationships interrelate.

This work will be especially important as muscles function in three dimensions and scapular dyskinesia are often seen in combination (Kibler et al., 2002).

An important factor in estimating kinetics from kinematics is an accurate representation of the axis of rotation. Early work proposed various theories on the location and orientation of the scapulothoracic axis of rotation during humeral elevation (Bagg et al., 1988; Dvir et al., 1978; Poppen et al., 1976). Poppen and Walker (1976) observed the axis of rotation was initially located lateral to the scapular body but shifted superior and medially as the arm was elevated. Conversely, Dvir and Berme (1978) and Bagg and Forrest (1988) proposed similar theories that the axis of rotation was oriented anteriorly/posteriorly near the root of the scapular spine during lower angles of elevation and shifted to the acromioclavicular joint towards the end of motion. These conflicting theories are likely due to projection errors associated with quantifying 3D kinematics from 2D radiographs.

A helical axis may offer the most precise method for describing a joint's axis of rotation. An exploratory analysis was performed using the data from the current study to visualize the scapulothoracic helical axis and test these early theories regarding the location and orientation of the axis of rotation. However, helical axis calculations are highly sensitive to noise and kinematics are often filtered prior to analysis (Woltring et al., 1985). Given the extensive data processing time required for this study, kinematic data was down-sampled to every 10º humerothoracic elevation, which precluded the ability to filter the data. Furthermore, finite helical axis calculations are sensitive to small total rotations (Spoor et al., 1980), which are often present at the sternoclavicular and

acromioclavicular joint. Future studies that track shoulder complex kinematics at a high sampling rate and use an instantaneous helical axis calculation will be an important step in understanding muscle function by establishing the scapulothoracic axis of rotation.

Summary

The shoulder is a complex system that serves an important function for facilitating upper limb function. Investigating these complex relationships requires highly accurate methods of quantifying shoulder kinematics. Single-plane fluoroscopy and 2D/3D shape-matching provides sufficient accuracy to address many clinical questions related to shoulder motion and how it relates to potential mechanisms of rotator cuff injury. The impact of abnormal scapulothoracic motion on subacromial proximities is more complex than traditionally believed but emphasizes the need for accurate methods of measuring human motion in the clinic. More research is needed to investigate the impact of abnormal scapulothoracic kinematics on other mechanisms of soft tissue injury (i.e. internal impingement, labral tears) and identify the underlying kinematic and kinetic mechanisms of scapulothoracic motion.

Bibliography

AHRQ. (1996-2006). *Agency for Healthcare Research and Quality Medical Expenditures Panel Survey*.

Akbari-Shandiz, M., Lawrence, R. L., Ellingson, A. M., Zhao, K. D., & Ludewig, P. M. (2018). MRI vs. CT-based 3D-2D auto-registration accuracy for quantifying shoulder motion using biplane fluoroscopy. *J Biomech*, (under review).

An, K. N., Browne, A. O., Korinek, S., Tanaka, S., & Morrey, B. F. (1991). Three-dimensional kinematics of glenohumeral elevation. *J Orthop Res, 9*(1), 143-149. doi:10.1002/jor.1100090117

Anderst, W., Zauel, R., Bishop, J., Demps, E., & Tashman, S. (2009). Validation of three-dimensional model-based tibio-femoral tracking during running. *Med Eng Phys, 31*(1), 10-16. doi:10.1016/j.medengphy.2008.03.003

Auerbach, B. M., & Raxter, M. H. (2008). Patterns of clavicular bilateral asymmetry in relation to the humerus: variation among humans. *J Hum Evol, 54*(5), 663-674. doi:10.1016/j.jhevol.2007.10.002

Bagg, S. D., & Forrest, W. J. (1988). A biomechanical analysis of scapular rotation during arm abduction in the scapular plane. *Am J Phys Med Rehabil, 67*(6), 238-245.

Balke, M., Schmidt, C., Dedy, N., Banerjee, M., Bouillon, B., & Liem, D. (2013). Correlation of acromial morphology with impingement syndrome and rotator cuff tears. *Acta Orthop, 84*(2), 178-183. doi:10.3109/17453674.2013.773413

Beard, D. J., Rees, J. L., Cook, J. A., Rombach, I., Cooper, C., Merritt, N., . . . Group, C. S. (2017). Arthroscopic subacromial decompression for subacromial shoulder pain (CSAW): a multicentre, pragmatic, parallel group, placebo-controlled, three-group, randomised surgical trial. *Lancet, 391*(10118), 329-338. doi:10.1016/S0140-6736(17)32457-1

Bey, M. J., Brock, S. K., Beierwaltes, W. N., Zauel, R., Kolowich, P. A., & Lock, T. R. (2007). In vivo measurement of subacromial space width during shoulder elevation: technique and preliminary results in patients following unilateral

rotator cuff repair. *Clin Biomech (Bristol, Avon), 22*(7), 767-773. doi:10.1016/j.clinbiomech.2007.04.006

Bey, M. J., Zauel, R., Brock, S. K., & Tashman, S. (2006). Validation of a new model-based tracking technique for measuring three-dimensional, in vivo glenohumeral joint kinematics. *J Biomech Eng, 128*(4), 604-609. doi:10.1115/1.2206199

Bigliani, L. U., Ticker, J. B., Flatow, E. L., Soslowsky, L. J., & Mow, V. C. (1991). The relationship of acromial architecture to rotator cuff disease. *Clin Sports Med, 10*(4), 823-838.

Bishop, J. L., Kline, S. K., Aalderink, K. J., Zauel, R., & Bey, M. J. (2009). Glenoid inclination: in vivo measures in rotator cuff tear patients and associations with superior glenohumeral joint translation. *J Shoulder Elbow Surg, 18*(2), 231-236. doi:10.1016/j.jse.2008.08.002

Brainerd, E. L., Baier, D. B., Gatesy, S. M., Hedrick, T. L., Metzger, K. A., Gilbert, S. L., & Crisco, J. J. (2010). X-ray reconstruction of moving morphology (XROMM): precision, accuracy and applications in comparative biomechanics research. *J Exp Zool A Ecol Genet Physiol, 313*(5), 262-279. doi:10.1002/jez.589

Braman, J. P., Engel, S. C., Laprade, R. F., & Ludewig, P. M. (2009). In vivo assessment of scapulohumeral rhythm during unconstrained overhead reaching in asymptomatic subjects. *J Shoulder Elbow Surg, 18*(6), 960-967. doi:10.1016/j.jse.2009.02.001

Braman, J. P., Thomas, B. M., Laprade, R. F., Phadke, V., & Ludewig, P. M. (2010). Three-dimensional in vivo kinematics of an osteoarthritic shoulder before and after total shoulder arthroplasty. *Knee Surg Sports Traumatol Arthrosc, 18*(12), 1774-1778. doi:10.1007/s00167-010-1167-4

Braman, J. P., Zhao, K. D., Lawrence, R. L., Harrison, A. K., & Ludewig, P. M. (2014). Shoulder impingement revisited: evolution of diagnostic understanding in orthopedic surgery and physical therapy. *Med Biol Eng Comput, 52*(3), 211-219. doi:10.1007/s11517-013-1074-1

Brossmann, J., Preidler, K. W., Pedowitz, R. A., White, L. M., Trudell, D., & Resnick, D. (1996). Shoulder impingement syndrome: influence of shoulder position on

rotator cuff impingement--an anatomic study. *AJR Am J Roentgenol, 167*(6), 1511-1515. doi:10.2214/ajr.167.6.8956588

Burns, W. C., 2nd, & Whipple, T. L. (1993). Anatomic relationships in the shoulder impingement syndrome. *Clin Orthop Relat Res*(294), 96-102.

Caldwell, C., Sahrmann, S., & Van Dillen, L. (2007). Use of a movement system impairment diagnosis for physical therapy in the management of a patient with shoulder pain. *J Orthop Sports Phys Ther, 37*(9), 551-563. doi:10.2519/jospt.2007.2283

Camargo, P. R., Alburquerque-Sendin, F., Avila, M. A., Haik, M. N., Vieira, A., & Salvini, T. F. (2015). Effects of stretching and strengthening exercises, with and without manual therapy, on scapular kinematics, function, and pain in individuals with shoulder impingement: A randomized controlled trial. *J Orthop Sports Phys Ther, 45*(12), 984-997. doi:10.2519/jospt.2015.5939

Cohen, J., & Cohen, J. (2003). *Applied multiple regression/correlation analysis for the behavioral sciences* (3rd ed.). Mahwah, N.J.: L. Erlbaum Associates.

Cotton, R. E., & Rideout, D. F. (1964). Tears of the humeral rotator cuff: a radiological and pathological necropsy survey. *J Bone Joint Surg Br, 46*, 314-328.

Cox, J. S. (1981). The fate of the acromioclavicular joint in athletic injuries. *Am J Sports Med, 9*(1), 50-53. doi:10.1177/036354658100900111

Daruwalla, Z. J., Courtis, P., Fitzpatrick, C., Fitzpatrick, D., & Mullett, H. (2010). Anatomic variation of the clavicle: A novel three-dimensional study. *Clin Anat, 23*(2), 199-209. doi:10.1002/ca.20924

Deutsch, A., Altchek, D. W., Schwartz, E., Otis, J. C., & Warren, R. F. (1996). Radiologic measurement of superior displacement of the humeral head in the impingement syndrome. *J Shoulder Elbow Surg, 5*(3), 186-193.

Dogan, M., Cay, N., Tosun, O., Karaoglanoglu, M., & Bozkurt, M. (2012). Glenoid axis is not related with rotator cuff tears--a magnetic resonance imaging comparative study. *Int Orthop, 36*(3), 595-598. doi:10.1007/s00264-011-1356-x

Dvir, Z., & Berme, N. (1978). The shoulder complex in elevation of the arm: a mechanism approach. *J Biomech, 11*(5), 219-225.

Ebaugh, D. D., McClure, P. W., & Karduna, A. R. (2005). Three-dimensional scapulothoracic motion during active and passive arm elevation. *Clin Biomech (Bristol, Avon), 20*(7), 700-709. doi:10.1016/j.clinbiomech.2005.03.008

Edelson, J. G., & Luchs, J. (1995). Aspects of coracoacromial ligament anatomy of interest to the arthroscopic surgeon. *Arthroscopy, 11*(6), 715-719.

Ellingson, A. M., Mozingo, J. D., Magnuson, D. J., Pagnano, M. W., & Zhao, K. D. (2016). Characterizing fluoroscopy based kinematic accuracy as a function of pulse width and velocity. *J Biomech, 49*(15), 3741-3745. doi:10.1016/j.jbiomech.2016.09.044

Endo, K., Ikata, T., Katoh, S., & Takeda, Y. (2001). Radiographic assessment of scapular rotational tilt in chronic shoulder impingement syndrome. *J Orthop Sci, 6*(1), 3-10.

Epstein, R. E., Schweitzer, M. E., Frieman, B. G., Fenlin, J. M., Jr., & Mitchell, D. G. (1993). Hooked acromion: prevalence on MR images of painful shoulders. *Radiology, 187*(2), 479-481. doi:10.1148/radiology.187.2.8475294

Farley, T. E., Neumann, C. H., Steinbach, L. S., & Petersen, S. A. (1994). The coracoacromial arch: MR evaluation and correlation with rotator cuff pathology. *Skeletal Radiol, 23*(8), 641-645.

Fayad, F., Hoffmann, G., Hanneton, S., Yazbeck, C., Lefevre-Colau, M. M., Poiraudeau, S., . . . Roby-Brami, A. (2006). 3-D scapular kinematics during arm elevation: effect of motion velocity. *Clin Biomech (Bristol, Avon), 21*(9), 932-941. doi:10.1016/j.clinbiomech.2006.04.015

Feleus, A., Bierma-Zeinstra, S. M., Miedema, H. S., Bernsen, R. M., Verhaar, J. A., & Koes, B. W. (2008). Incidence of non-traumatic complaints of arm, neck and shoulder in general practice. *Man Ther, 13*(5), 426-433. doi:10.1016/j.math.2007.05.010

Flatow, E. L., Soslowsky, L. J., Ticker, J. B., Pawluk, R. J., Hepler, M., Ark, J., . . . Bigliani, L. U. (1994). Excursion of the rotator cuff under the acromion. Patterns of subacromial contact. *Am J Sports Med, 22*(6), 779-788. doi:10.1177/036354659402200609

Freygant, M., Dziurzynska-Bialek, E., Guz, W., Samojedny, A., Golofit, A., Kostkiewicz, A., & Terpin, K. (2014). Magnetic resonance imaging of rotator cuff tears in shoulder impingement syndrome. *Pol J Radiol, 79*, 391-397. doi:10.12659/PJR.890541

Fukuda, T. Y., Melo, W. P., Zaffalon, B. M., Rossetto, F. M., Magalhaes, E., Bryk, F. F., & Martin, R. L. (2012). Hip posterolateral musculature strengthening in sedentary women with patellofemoral pain syndrome: a randomized controlled clinical trial with 1-year follow-up. *J Orthop Sports Phys Ther, 42*(10), 823-830. doi:10.2519/jospt.2012.4184

Fukuta, S., Kuge, A., & Korai, F. (2009). Clinical significance of meniscal abnormalities on magnetic resonance imaging in an older population. *Knee, 16*(3), 187-190. doi:10.1016/j.knee.2008.11.006

Giphart, J. E., Brunkhorst, J. P., Horn, N. H., Shelburne, K. B., Torry, M. R., & Millett, P. J. (2013). Effect of plane of arm elevation on glenohumeral kinematics: a normative biplane fluoroscopy study. *J Bone Joint Surg Am, 95*(3), 238-245. doi:10.2106/JBJS.J.01875

Giphart, J. E., van der Meijden, O. A., & Millett, P. J. (2012). The effects of arm elevation on the 3-dimensional acromiohumeral distance: a biplane fluoroscopy study with normative data. *J Shoulder Elbow Surg, 21*(11), 1593-1600. doi:10.1016/j.jse.2011.11.023

Gold, G. E., Pappas, G. P., Blemker, S. S., Whalen, S. T., Campbell, G., McAdams, T. A., & Beaulieu, C. F. (2007). Abduction and external rotation in shoulder impingement: an open MR study on healthy volunteers initial experience. *Radiology, 244*(3), 815-822. doi:10.1148/radiol.2443060998

Graichen, H., Bonel, H., Stammberger, T., Englmeier, K. H., Reiser, M., & Eckstein, F. (1999a). Subacromial space width changes during abduction and rotation--a 3-D MR imaging study. *Surg Radiol Anat, 21*(1), 59-64.

Graichen, H., Bonel, H., Stammberger, T., Haubner, M., Rohrer, H., Englmeier, K. H., . . . Eckstein, F. (1999b). Three-dimensional analysis of the width of the subacromial space in healthy subjects and patients with impingement syndrome. *AJR Am J Roentgenol, 172*(4), 1081-1086. doi:10.2214/ajr.172.4.10587151

Gupta, S., & van der Helm, F. C. (2004). Load transfer across the scapula during humeral abduction. *J Biomech, 37*(7), 1001-1009. doi:10.1016/j.jbiomech.2003.11.025

Haahr, J. P., Ostergaard, S., Dalsgaard, J., Norup, K., Frost, P., Lausen, S., . . . Andersen, J. H. (2005). Exercises versus arthroscopic decompression in patients with subacromial impingement: a randomised, controlled study in 90 cases with a one year follow up. *Ann Rheum Dis, 64*(5), 760-764. doi:10.1136/ard.2004.021188

Hallstrom, E., & Karrholm, J. (2009). Shoulder rhythm in patients with impingement and in controls: dynamic RSA during active and passive abduction. *Acta Orthop, 80*(4), 456-464. doi:10.3109/17453670903153543

Hamming, D., Braman, J. P., Phadke, V., LaPrade, R. F., & Ludewig, P. M. (2012). The accuracy of measuring glenohumeral motion with a surface humeral cuff. *J Biomech, 45*(7), 1161-1168. doi:10.1016/j.jbiomech.2012.02.003

Harris, P. A., Taylor, R., Thielke, R., Payne, J., Gonzalez, N., & Conde, J. G. (2009). Research electronic data capture (REDCap)--a metadata-driven methodology and workflow process for providing translational research informatics support. *J Biomed Inform, 42*(2), 377-381. doi:10.1016/j.jbi.2008.08.010

Health, N. I. f. O. S. a. (1997). *Musculoskeletal disorders and workplace factors: A Critical review of epidemiologic evidence for work-related musculoskeletal disorders of the neck, upper extremity, and low back.* (97-141(3):1-7). Cincinnati, OH.

Hebert, L. J., Moffet, H., Dufour, M., & Moisan, C. (2003). Acromiohumeral distance in a seated position in persons with impingement syndrome. *J Magn Reson Imaging, 18*(1), 72-79. doi:10.1002/jmri.10327

Hebert, L. J., Moffet, H., McFadyen, B. J., & Dionne, C. E. (2002). Scapular behavior in shoulder impingement syndrome. *Arch Phys Med Rehabil, 83*(1), 60-69.

Hegedus, E. J., Goode, A. P., Cook, C. E., Michener, L., Myer, C. A., Myer, D. M., & Wright, A. A. (2012). Which physical examination tests provide clinicians with the most value when examining the shoulder? Update of a systematic review with meta-analysis of individual tests. *Br J Sports Med, 46*(14), 964-978. doi:10.1136/bjsports-2012-091066

Hudak, P. L., Amadio, P. C., & Bombardier, C. (1996). Development of an upper extremity outcome measure: the DASH (disabilities of the arm, shoulder and hand) [corrected]. The Upper Extremity Collaborative Group (UECG). *Am J Ind Med, 29*(6), 602-608. doi:10.1002/(SICI)1097-0274(199606)29:6<602::AID-AJIM4>3.0.CO;2-L

Hughes, R. E., Bryant, C. R., Hall, J. M., Wening, J., Huston, L. J., Kuhn, J. E., . . . Blasier, R. B. (2003). Glenoid inclination is associated with full-thickness rotator cuff tears. *Clin Orthop Relat Res*(407), 86-91.

Inman, V. T., Saunders, M., & Abbott, L. C. (1944). Observations of the function of the shoulder joint. *J Bone Joint Surg Am, 26*(1), 1-30.

Ishimoto, Y., Yoshimura, N., Muraki, S., Yamada, H., Nagata, K., Hashizume, H., . . . Yoshida, M. (2013). Associations between radiographic lumbar spinal stenosis and clinical symptoms in the general population: the Wakayama Spine Study. *Osteoarthritis Cartilage, 21*(6), 783-788. doi:10.1016/j.joca.2013.02.656

Jacobson, A., Gilot, G. J., Hamilton, M. A., Greene, A., Flurin, P. H., Wright, T. W., . . . Roche, C. P. (2015). Glenohumeral Anatomic Study. A Comparison of Male and Female Shoulders with Similar Average Age and BMI. *Bull Hosp Jt Dis (2013), 73 Suppl 1*, S68-78.

Johnson, M. P., McClure, P. W., & Karduna, A. R. (2001). New method to assess scapular upward rotation in subjects with shoulder pathology. *J Orthop Sports Phys Ther, 31*(2), 81-89. doi:10.2519/jospt.2001.31.2.81

Kandemir, U., Allaire, R. B., Jolly, J. T., Debski, R. E., & McMahon, P. J. (2006). The relationship between the orientation of the glenoid and tears of the rotator cuff. *J Bone Joint Surg Br, 88*(8), 1105-1109. doi:10.1302/0301-620X.88B8.17732

Karduna, A. R., McClure, P. W., & Michener, L. A. (2000). Scapular kinematics: effects of altering the Euler angle sequence of rotations. *J Biomech, 33*(9), 1063-1068.

Karduna, A. R., McClure, P. W., Michener, L. A., & Sennett, B. (2001). Dynamic measurements of three-dimensional scapular kinematics: a validation study. *J Biomech Eng, 123*(2), 184-190.

Ketola, S., Lehtinen, J., Arnala, I., Nissinen, M., Westenius, H., Sintonen, H., . . . Rousi, T. (2009). Does arthroscopic acromioplasty provide any additional value in the treatment of shoulder impingement syndrome?: a two-year randomised controlled trial. *J Bone Joint Surg Br, 91*(10), 1326-1334. doi:10.1302/0301-620X.91B10.22094

Kibler, W. B., Ludewig, P. M., McClure, P. W., Michener, L. A., Bak, K., & Sciascia, A. D. (2013). Clinical implications of scapular dyskinesis in shoulder injury: the 2013 consensus statement from the 'Scapular Summit'. *Br J Sports Med, 47*(14), 877-885. doi:10.1136/bjsports-2013-092425

Kibler, W. B., & McMullen, J. (2003). Scapular dyskinesis and its relation to shoulder pain. *J Am Acad Orthop Surg, 11*(2), 142-151.

Kibler, W. B., Uhl, T. L., Maddux, J. W., Brooks, P. V., Zeller, B., & McMullen, J. (2002). Qualitative clinical evaluation of scapular dysfunction: a reliability study. *J Shoulder Elbow Surg, 11*(6), 550-556. doi:10.1067/mse.2002.126766

Kim, H. M., Dahiya, N., Teefey, S. A., Middleton, W. D., Stobbs, G., Steger-May, K., . . . Keener, J. D. (2010). Location and initiation of degenerative rotator cuff tears: an analysis of three hundred and sixty shoulders. *J Bone Joint Surg Am, 92*(5), 1088-1096. doi:10.2106/JBJS.I.00686

Knorlein, B. J., Baier, D. B., Gatesy, S. M., Laurence-Chasen, J. D., & Brainerd, E. L. (2016). Validation of XMALab software for marker-based XROMM. *J Exp Biol, 219*(Pt 23), 3701-3711. doi:10.1242/jeb.145383

Kon, Y., Nishinaka, N., Gamada, K., Tsutsui, H., & Banks, S. A. (2008). The influence of handheld weight on the scapulohumeral rhythm. *J Shoulder Elbow Surg, 17*(6), 943-946. doi:10.1016/j.jse.2008.05.047

Lawrence, R. L., Braman, J. P., LaPrade, R. F., & Ludewig, P. M. (2014a). Comparison of 3-dimensional shoulder complex kinematics in individuals with and without shoulder pain, part 1: sternoclavicular, acromioclavicular, and scapulothoracic

joints. *J Orthop Sports Phys Ther, 44*(9), 636-645, A631-638. doi:10.2519/jospt.2014.5339

Lawrence, R. L., Braman, J. P., Staker, J. L., LaPrade, R. F., & Ludewig, P. M. (2014b). Comparison of 3-dimensional shoulder complex kinematics in individuals with and without shoulder pain, part 2: glenohumeral joint. *J Orthop Sports Phys Ther, 44*(9), 646-655, B641-643. doi:10.2519/jospt.2014.5556

Lawrence, R. L., Ellingson, A. M., & Ludewig, P. M. (2018). Validation of single-plane fluoroscopy and 2D/3D shape-matching for quantifying shoulder complex kinematics. *Med Eng Phys, 52*, 69-75. doi:10.1016/j.medengphy.2017.11.005

Lawrence, R. L., Schlangen, D. M., Schneider, K. A., Schoenecker, J., Senger, A. L., Starr, W. C., . . . Ludewig, P. M. (2017). Effect of glenohumeral elevation on subacromial supraspinatus compression risk during simulated reaching. *J Orthop Res, 35*(10), 2329-2337. doi:10.1002/jor.23515

Lawrence, R. L., Staker, J. L., Braman, J. P., & Ludewig, P. M. (2016). *Mechanical internal impingement of the supraspinatus tendon during a simulated reaching task.* Paper presented at the 11th Conference of the International Shoulder Group, Winterthur, Switzerland.

Littell, R. C., Pendergast, J., & Natarajan, R. (2000). Modelling covariance structure in the analysis of repeated measures data. *Stat Med, 19*(13), 1793-1819.

Ludewig, P. M., Behrens, S. A., Meyer, S. M., Spoden, S. M., & Wilson, L. A. (2004). Three-dimensional clavicular motion during arm elevation: reliability and descriptive data. *J Orthop Sports Phys Ther, 34*(3), 140-149. doi:10.2519/jospt.2004.34.3.140

Ludewig, P. M., & Borstad, J. D. (2003). Effects of a home exercise programme on shoulder pain and functional status in construction workers. *Occup Environ Med, 60*(11), 841-849.

Ludewig, P. M., & Braman, J. P. (2011). Shoulder impingement: biomechanical considerations in rehabilitation. *Man Ther, 16*(1), 33-39. doi:10.1016/j.math.2010.08.004

Ludewig, P. M., & Cook, T. M. (2000). Alterations in shoulder kinematics and associated muscle activity in people with symptoms of shoulder impingement. *Phys Ther, 80*(3), 276-291.

Ludewig, P. M., Cook, T. M., & Nawoczenski, D. A. (1996). Three-dimensional scapular orientation and muscle activity at selected positions of humeral elevation. *J Orthop Sports Phys Ther, 24*(2), 57-65. doi:10.2519/jospt.1996.24.2.57

Ludewig, P. M., Cook, T. M., & Shields, R. K. (2002). Comparison of surface sensor and bone-fixed measurement of humeral motion. *Journal of Applied Biomechanics, 18*, 163-170.

Ludewig, P. M., Hassett, D. R., Laprade, R. F., Camargo, P. R., & Braman, J. P. (2010). Comparison of scapular local coordinate systems. *Clin Biomech (Bristol, Avon), 25*(5), 415-421. doi:10.1016/j.clinbiomech.2010.01.015

Ludewig, P. M., Kamonseki, D. H., Staker, J. L., Lawrence, R. L., Camargo, P. R., & Braman, J. P. (2017). Changing Our Diagnostic Paradigm: Movement System Diagnostic Classification. *Int J Sports Phys Ther, 12*(6), 884-893.

Ludewig, P. M., Lawrence, R. L., & Braman, J. P. (2013). What's in a name? Using movement system diagnoses versus pathoanatomic diagnoses. *J Orthop Sports Phys Ther, 43*(5), 280-283. doi:10.2519/jospt.2013.0104

Ludewig, P. M., Phadke, V., Braman, J. P., Hassett, D. R., Cieminski, C. J., & LaPrade, R. F. (2009a). Motion of the shoulder complex during multiplanar humeral elevation. *J Bone Joint Surg Am, 91*(2), 378-389. doi:10.2106/JBJS.G.01483

Ludewig, P. M., & Reynolds, J. F. (2009b). The association of scapular kinematics and glenohumeral joint pathologies. *J Orthop Sports Phys Ther, 39*(2), 90-104. doi:10.2519/jospt.2009.2808

Lukasiewicz, A. C., McClure, P., Michener, L., Pratt, N., & Sennett, B. (1999). Comparison of 3-dimensional scapular position and orientation between subjects with and without shoulder impingement. *J Orthop Sports Phys Ther, 29*(10), 574-583; discussion 584-576. doi:10.2519/jospt.1999.29.10.574

Matsuki, K., Matsuki, K. O., Mu, S., Kenmoku, T., Yamaguchi, S., Ochiai, N., . . . Banks, S. A. (2014). In vivo 3D analysis of clavicular kinematics during scapular plane abduction: comparison of dominant and non-dominant shoulders. *Gait Posture, 39*(1), 625-627. doi:10.1016/j.gaitpost.2013.06.021

Matsuki, K., Matsuki, K. O., Mu, S., Yamaguchi, S., Ochiai, N., Sasho, T., . . . Banks, S. A. (2011). In vivo 3-dimensional analysis of scapular kinematics: comparison of dominant and nondominant shoulders. *J Shoulder Elbow Surg, 20*(4), 659-665. doi:10.1016/j.jse.2010.09.012

Matsuki, K., Matsuki, K. O., Yamaguchi, S., Ochiai, N., Sasho, T., Sugaya, H., . . . Banks, S. A. (2012). Dynamic in vivo glenohumeral kinematics during scapular plane abduction in healthy shoulders. *J Orthop Sports Phys Ther, 42*(2), 96-104. doi:10.2519/jospt.2012.3584

McClure, P. W., Michener, L. A., & Karduna, A. R. (2006). Shoulder function and 3-dimensional scapular kinematics in people with and without shoulder impingement syndrome. *Phys Ther, 86*(8), 1075-1090.

McClure, P. W., Michener, L. A., Sennett, B. J., & Karduna, A. R. (2001). Direct 3-dimensional measurement of scapular kinematics during dynamic movements in vivo. *J Shoulder Elbow Surg, 10*(3), 269-277. doi:10.1067/mse.2001.112954

McClure, P. W., Tate, A. R., Kareha, S., Irwin, D., & Zlupko, E. (2009). A clinical method for identifying scapular dyskinesis, part 1: reliability. *J Athl Train, 44*(2), 160-164. doi:10.4085/1062-6050-44.2.160

Mell, A. G., LaScalza, S., Guffey, P., Ray, J., Maciejewski, M., Carpenter, J. E., & Hughes, R. E. (2005). Effect of rotator cuff pathology on shoulder rhythm. *J Shoulder Elbow Surg, 14*(1 Suppl S), 58S-64S. doi:10.1016/j.jse.2004.09.018

Michener, L. A., McClure, P. W., & Karduna, A. R. (2003). Anatomical and biomechanical mechanisms of subacromial impingement syndrome. *Clin Biomech (Bristol, Avon), 18*(5), 369-379.

Michener, L. A., Walsworth, M. K., Doukas, W. C., & Murphy, K. P. (2009). Reliability and diagnostic accuracy of 5 physical examination tests and combination of tests for subacromial impingement. *Arch Phys Med Rehabil, 90*(11), 1898-1903. doi:10.1016/j.apmr.2009.05.015

Miranda, D. L., Schwartz, J. B., Loomis, A. C., Brainerd, E. L., Fleming, B. C., & Crisco, J. J. (2011). Static and dynamic error of a biplanar videoradiography system using marker-based and markerless tracking techniques. *J Biomech Eng, 133*(12), 121002. doi:10.1115/1.4005471

Moor, B. K., Bouaicha, S., Rothenfluh, D. A., Sukthankar, A., & Gerber, C. (2013). Is there an association between the individual anatomy of the scapula and the development of rotator cuff tears or osteoarthritis of the glenohumeral joint?: A radiological study of the critical shoulder angle. *Bone Joint J, 95-B*(7), 935-941. doi:10.1302/0301-620X.95B7.31028

Moor, B. K., Wieser, K., Slankamenac, K., Gerber, C., & Bouaicha, S. (2014). Relationship of individual scapular anatomy and degenerative rotator cuff tears. *J Shoulder Elbow Surg, 23*(4), 536-541. doi:10.1016/j.jse.2013.11.008

Moro-oka, T. A., Hamai, S., Miura, H., Shimoto, T., Higaki, H., Fregly, B. J., . . . Banks, S. A. (2007). Can magnetic resonance imaging-derived bone models be used for accurate motion measurement with single-plane three-dimensional shape registration? *J Orthop Res, 25*(7), 867-872. doi:10.1002/jor.20355

Mu, S. (2007). *JointTrack: An open-source, easily expandable program for skeletal kinematic measurement using model-image registration.* (MS), University of Florida, Gainesville, FL.

Neer, C. S., 2nd. (1972). Anterior acromioplasty for the chronic impingement syndrome in the shoulder: a preliminary report. *J Bone Joint Surg Am, 54*(1), 41-50.

Neer, C. S., 2nd. (1983). Impingement lesions. *Clin Orthop Relat Res*(173), 70-77.

Nishinaka, N., Tsutsui, H., Mihara, K., Suzuki, K., Makiuchi, D., Kon, Y., . . . Banks, S. A. (2008). Determination of in vivo glenohumeral translation using fluoroscopy and shape-matching techniques. *J Shoulder Elbow Surg, 17*(2), 319-322. doi:10.1016/j.jse.2007.05.018

Ogston, J. B., & Ludewig, P. M. (2007). Differences in 3-dimensional shoulder kinematics between persons with multidirectional instability and asymptomatic controls. *Am J Sports Med, 35*(8), 1361-1370. doi:10.1177/0363546507300820

Ostor, A. J., Richards, C. A., Prevost, A. T., Speed, C. A., & Hazleman, B. L. (2005). Diagnosis and relation to general health of shoulder disorders presenting to primary care. *Rheumatology (Oxford), 44*(6), 800-805. doi:10.1093/rheumatology/keh598

Pandey, V., Vijayan, D., Tapashetti, S., Agarwal, L., Kamath, A., Acharya, K., . . . Willems, W. J. (2016). Does scapular morphology affect the integrity of the rotator cuff? *J Shoulder Elbow Surg, 25*(3), 413-421. doi:10.1016/j.jse.2015.09.016

Pellegrini, A., Pegreffi, F., Paladini, P., Verdano, M. A., Ceccarelli, F., & Porcellini, G. (2012). Prevalence of shoulder discomfort in paraplegic subjects. *Acta Biomed, 83*(3), 177-182.

Peltz, C. D., Divine, G., Drake, A., Ramo, N. L., Zauel, R., Moutzouros, V., & Bey, M. J. (2015). Associations between in-vivo glenohumeral joint motion and morphology. *J Biomech, 48*(12), 3252-3257. doi:10.1016/j.jbiomech.2015.06.030

Phadke, V., Braman, J. P., LaPrade, R. F., & Ludewig, P. M. (2011). Comparison of glenohumeral motion using different rotation sequences. *J Biomech, 44*(4), 700-705. doi:10.1016/j.jbiomech.2010.10.042

Picavet, H. S., & Schouten, J. S. (2003). Musculoskeletal pain in the Netherlands: prevalences, consequences and risk groups, the DMC(3)-study. *Pain, 102*(1-2), 167-178.

Poppen, N. K., & Walker, P. S. (1976). Normal and abnormal motion of the shoulder. *J Bone Joint Surg Am, 58*(2), 195-201.

Pronk, G. M. (1991). *The shoulder girdle analysed and modelled kinematically.* (PhD), Delft University of Technology, Delft, Netherlands.

Pronk, G. M., van der Helm, F. C., & Rozendaal, L. A. (1993). Interaction between the joints in the shoulder mechanism: the function of the costoclavicular, conoid and trapezoid ligaments. *Proc Inst Mech Eng H, 207*(4), 219-229. doi:10.1243/PIME_PROC_1993_207_300_02

Rathnayaka, K., Momot, K. I., Noser, H., Volp, A., Schuetz, M. A., Sahama, T., & Schmutz, B. (2012). Quantification of the accuracy of MRI generated 3D models of long bones compared to CT generated 3D models. *Med Eng Phys, 34*(3), 357-363. doi:10.1016/j.medengphy.2011.07.027

Reinold, M. M., Escamilla, R. F., & Wilk, K. E. (2009). Current concepts in the scientific and clinical rationale behind exercises for glenohumeral and scapulothoracic musculature. *J Orthop Sports Phys Ther, 39*(2), 105-117. doi:10.2519/jospt.2009.2835

Rockwood, C. A., Williams, G. R., & Young, D. C. (1996). Acromioclavicular injuries. In C. A. Rockwood, D. P. Green, R. W. Bucholz, & J. D. Heckman (Eds.), *Fractures in Adults* (4th ed., Vol. I, pp. 1341–1413). Philadelphia, PA: Lippincott-Raven.

Roe, Y., Bautz-Holter, E., Juel, N. G., & Soberg, H. L. (2013). Identification of relevant International Classification of Functioning, Disability and Health categories in patients with shoulder pain: a cross-sectional study. *J Rehabil Med, 45*(7), 662-669. doi:10.2340/16501977-1159

Rundquist, P. J. (2007). Alterations in scapular kinematics in subjects with idiopathic loss of shoulder range of motion. *J Orthop Sports Phys Ther, 37*(1), 19-25. doi:10.2519/jospt.2007.2121

Sahara, W., Sugamoto, K., Murai, M., Tanaka, H., & Yoshikawa, H. (2006). 3D kinematic analysis of the acromioclavicular joint during arm abduction using vertically open MRI. *J Orthop Res, 24*(9), 1823-1831. doi:10.1002/jor.20208

Sahara, W., Sugamoto, K., Murai, M., & Yoshikawa, H. (2007). Three-dimensional clavicular and acromioclavicular rotations during arm abduction using vertically open MRI. *J Orthop Res, 25*(9), 1243-1249. doi:10.1002/jor.20407

Sahrmann, S., Azevedo, D. C., & Dillen, L. V. (2017). Diagnosis and treatment of movement system impairment syndromes. *Braz J Phys Ther, 21*(6), 391-399. doi:10.1016/j.bjpt.2017.08.001

Schellingerhout, J. M., Verhagen, A. P., Thomas, S., & Koes, B. W. (2008). Lack of uniformity in diagnostic labeling of shoulder pain: time for a different approach. *Man Ther, 13*(6), 478-483. doi:10.1016/j.math.2008.04.005

Seitz, A. L., McClure, P. W., Finucane, S., Boardman, N. D., 3rd, & Michener, L. A. (2011). Mechanisms of rotator cuff tendinopathy: intrinsic, extrinsic, or both? *Clin Biomech (Bristol, Avon), 26*(1), 1-12. doi:10.1016/j.clinbiomech.2010.08.001

Seitz, A. L., McClure, P. W., Finucane, S., Ketchum, J. M., Walsworth, M. K., Boardman, N. D., & Michener, L. A. (2012a). The scapular assistance test results in changes in scapular position and subacromial space but not rotator cuff strength in subacromial impingement. *J Orthop Sports Phys Ther, 42*(5), 400-412. doi:10.2519/jospt.2012.3579

Seitz, A. L., McClure, P. W., Lynch, S. S., Ketchum, J. M., & Michener, L. A. (2012b). Effects of scapular dyskinesis and scapular assistance test on subacromial space during static arm elevation. *J Shoulder Elbow Surg, 21*(5), 631-640. doi:10.1016/j.jse.2011.01.008

Sher, J. S., Uribe, J. W., Posada, A., Murphy, B. J., & Zlatkin, M. B. (1995). Abnormal findings on magnetic resonance images of asymptomatic shoulders. *J Bone Joint Surg Am, 77*(1), 10-15.

Silva, R. T., Hartmann, L. G., Laurino, C. F., & Bilo, J. P. (2010). Clinical and ultrasonographic correlation between scapular dyskinesia and subacromial space measurement among junior elite tennis players. *Br J Sports Med, 44*(6), 407-410. doi:10.1136/bjsm.2008.046284

Sousa Cde, O., Camargo, P. R., Ribeiro, I. L., Reiff, R. B., Michener, L. A., & Salvini, T. F. (2014). Motion of the shoulder complex in individuals with isolated acromioclavicular osteoarthritis and associated with rotator cuff dysfunction: part 1 - Three-dimensional shoulder kinematics. *J Electromyogr Kinesiol, 24*(4), 520-530. doi:10.1016/j.jelekin.2014.04.015

Spiegl, U. J., Horan, M. P., Smith, S. W., Ho, C. P., & Millett, P. J. (2016). The critical shoulder angle is associated with rotator cuff tears and shoulder osteoarthritis and is better assessed with radiographs over MRI. *Knee Surg Sports Traumatol Arthrosc, 24*(7), 2244-2251. doi:10.1007/s00167-015-3587-7

Spoor, C. W., & Veldpaus, F. E. (1980). Rigid body motion calculated from spatial co-ordinates of markers. *J Biomech, 13*(4), 391-393.

Struyf, F., Nijs, J., Mollekens, S., Jeurissen, I., Truijen, S., Mottram, S., & Meeusen, R. (2013). Scapular-focused treatment in patients with shoulder impingement syndrome: a randomized clinical trial. *Clin Rheumatol, 32*(1), 73-85. doi:10.1007/s10067-012-2093-2

Taft, T. N., Wilson, F. C., & Oglesby, J. W. (1987). Dislocation of the acromioclavicular joint. An end-result study. *J Bone Joint Surg Am, 69*(7), 1045-1051.

Tasaki, A., Nimura, A., Nozaki, T., Yamakawa, A., Niitsu, M., Morita, W., . . . Akita, K. (2015). Quantitative and qualitative analyses of subacromial impingement by kinematic open MRI. *Knee Surg Sports Traumatol Arthrosc, 23*(5), 1489-1497. doi:10.1007/s00167-014-2876-x

Tashman, S., & Anderst, W. (2003). In-vivo measurement of dynamic joint motion using high speed biplane radiography and CT: application to canine ACL deficiency. *J Biomech Eng, 125*(2), 238-245.

Tate, A. R., McClure, P., Kareha, S., Irwin, D., & Barbe, M. F. (2009). A clinical method for identifying scapular dyskinesis, part 2: validity. *J Athl Train, 44*(2), 165-173. doi:10.4085/1062-6050-44.2.165

Tauber, M. (2013). Management of acute acromioclavicular joint dislocations: current concepts. *Arch Orthop Trauma Surg, 133*(7), 985-995. doi:10.1007/s00402-013-1748-z

Teece, R. M., Lunden, J. B., Lloyd, A. S., Kaiser, A. P., Cieminski, C. J., & Ludewig, P. M. (2008). Three-dimensional acromioclavicular joint motions during elevation of the arm. *J Orthop Sports Phys Ther, 38*(4), 181-190. doi:10.2519/jospt.2008.2386

Tetreault, P., Krueger, A., Zurakowski, D., & Gerber, C. (2004). Glenoid version and rotator cuff tears. *J Orthop Res, 22*(1), 202-207. doi:10.1016/S0736-0266(03)00116-5

Thompson, M. D., Landin, D., & Page, P. A. (2011). Dynamic acromiohumeral interval changes in baseball players during scaption exercises. *J Shoulder Elbow Surg, 20*(2), 251-258. doi:10.1016/j.jse.2010.07.012

Tokgoz, N., Kanatli, U., Voyvoda, N. K., Gultekin, S., Bolukbasi, S., & Tali, E. T. (2007). The relationship of glenoid and humeral version with supraspinatus tendon tears. *Skeletal Radiol, 36*(6), 509-514. doi:10.1007/s00256-007-0290-x

van der Helm, F. C. (1994). Analysis of the kinematic and dynamic behavior of the shoulder mechanism. *J Biomech, 27*(5), 527-550.

van der Helm, F. C., & Pronk, G. M. (1995). Three-dimensional recording and description of motions of the shoulder mechanism. *J Biomech Eng, 117*(1), 27-40.

Veeger, H. E., & van der Helm, F. C. (2007). Shoulder function: the perfect compromise between mobility and stability. *J Biomech, 40*(10), 2119-2129. doi:10.1016/j.jbiomech.2006.10.016

Vermeulen, H. M., Stokdijk, M., Eilers, P. H., Meskers, C. G., Rozing, P. M., & Vliet Vlieland, T. P. (2002). Measurement of three dimensional shoulder movement patterns with an electromagnetic tracking device in patients with a frozen shoulder. *Ann Rheum Dis, 61*(2), 115-120.

Verstraeten, T. R., Deschepper, E., Jacxsens, M., Walravens, S., De Coninck, B., Pouliart, N., & De Wilde, L. F. (2013). Determination of a reference system for the three-dimensional study of the glenohumeral relationship. *Skeletal Radiol, 42*(8), 1061-1071. doi:10.1007/s00256-013-1572-0

Vitale, M. A., Arons, R. R., Hurwitz, S., Ahmad, C. S., & Levine, W. N. (2010). The rising incidence of acromioplasty. *J Bone Joint Surg Am, 92*(9), 1842-1850. doi:10.2106/JBJS.I.01003

Voight, M. L., & Thomson, B. C. (2000). The role of the scapula in the rehabilitation of shoulder injuries. *J Athl Train, 35*(3), 364-372.

Walch, G., Boileau, P., Noel, E., & Donell, S. T. (1992). Impingement of the deep surface of the supraspinatus tendon on the posterosuperior glenoid rim: An arthroscopic study. *J Shoulder Elbow Surg, 1*(5), 238-245. doi:10.1016/S1058-2746(09)80065-7

Woltring, H. J., Huiskes, R., de Lange, A., & Veldpaus, F. E. (1985). Finite centroid and helical axis estimation from noisy landmark measurements in the study of human joint kinematics. *J Biomech, 18*(5), 379-389.

Wong, A. S., Gallo, L., Kuhn, J. E., Carpenter, J. E., & Hughes, R. E. (2003). The effect of glenoid inclination on superior humeral head migration. *J Shoulder Elbow Surg, 12*(4), 360-364. doi:10.1016/mse.2003.S1058274603000260

Wu, G., van der Helm, F. C., Veeger, H. E., Makhsous, M., Van Roy, P., Anglin, C., . . . International Society of, B. (2005). ISB recommendation on definitions of joint coordinate systems of various joints for the reporting of human joint motion--Part II: shoulder, elbow, wrist and hand. *J Biomech, 38*(5), 981-992.

Yanagawa, T., Goodwin, C. J., Shelburne, K. B., Giphart, J. E., Torry, M. R., & Pandy, M. G. (2008). Contributions of the individual muscles of the shoulder to glenohumeral joint stability during abduction. *J Biomech Eng, 130*(2), 021024. doi:10.1115/1.2903422

You, B. M., Siy, P., Anderst, W., & Tashman, S. (2001). In vivo measurement of 3-D skeletal kinematics from sequences of biplane radiographs: application to knee kinematics. *IEEE Trans Med Imaging, 20*(6), 514-525. doi:10.1109/42.929617

Zatsiorsky, V. M. (1998). *Kinematics of Human Motion* (1st Ed.): Human Kinetics.

Zhu, Z., Massimini, D. F., Wang, G., Warner, J. J., & Li, G. (2012). The accuracy and repeatability of an automatic 2D-3D fluoroscopic image-model registration technique for determining shoulder joint kinematics. *Med Eng Phys, 34*(9), 1303-1309. doi:10.1016/j.medengphy.2011.12.021

Appendices

Appendix A: Literature Review Summary Tables

Table 9: Summary of Scapulothoracic Kinematic Studies in Asymptomatic Subjects during Scapular Plane Abduction

Study	Methods	Subjects	Range	Angular Position	Initial Position	Final Position	Change in Position
Ludewig 1996	- Electromagnetic digitizer (static) - New ISB	- N=25 - 11 M, 14 F, 26±5 yrs.	0°-140°	IR/ER	33°	20°	-13°
				UR/DR	-2°	-36°	-34°
				AT/PT	-8°	7°	15°
McClure 2001	- Electromagnetic sensors attached to bone pins - Old ISB	- N=8 - 5 M, 3 F, 33 yrs.	30°-120°	IR/ER*	36°	29°	-7°
				UR/DR*	-19°	-50°	-31°
				AT/PT*	5°	15°	10°
Ludewig 2000	- Electromagnetic surface sensors - Old ISB	- N=26 - 26 M, 40±13 yrs. - Overhead workers	40°-120°	IR/ER*	40°	47°	7°
				UR/DR	-17°	-41°	-24°
				AT/PT*	-10°	-8°	2°
Ebaugh 2005	- Electromagnetic surface sensors with scapular tracker - Old ISB	- N=20 - 10 M, 10 F, 23 yrs.	Min-120°	IR/ER	45°	42°	-3°
				UR/DR	-29°	-67°	-38°
				AT/PT	0°	1°	1°
McClure 2006	- Electromagnetic surface sensors - Old ISB	- N=45 - 24 M, 21 F, 44±12 yrs.	Min-120°	IR/ER*	37°	35°	-2°
				UR/DR*	-18°	-50°	-32°
				AT/PT*	0°	4°	4°
Ludewig 2009	- Electromagnetic sensors attached to bone pins - Old ISB	- N=12 - 7 M, 5 F, 29±7 yrs.	30°-120°	IR/ER	39°	37°	-2°
				UR/DR	-16°	-44°	-28°
				AT/PT	-11°	3°	14°

Notes: Positive rotations: IR, DR, and PT. Abbreviations: ISB = International Society of Biomechanics, SAB = scapular plane abduction, IR = internal rotation, ER = external rotation, DR = downward rotation, UR = upward rotation, PT = posterior tilt, AT = anterior tilt. *Data estimated from plots

Table 10: Summary of Glenohumeral Kinematic Studies in Asymptomatic Subjects during Scapular Plane Abduction

Study	Methods	Subjects	Range	Angular Position	Initial Position	Final Position	Change in Position
Ludewig 2009	- Electromagnetic sensors attached to bone pins - Old ISB - XZ'Y"	- N=12 - 7 M, 5 F, 29±7 yrs.	30°-120°	Abduction	-14°	-77°	-63°
				Plane of elevation	6°	5°	-1°
				IR/ER	-50°	-62°	-12°
Matsuki 2012	- Single-plane fluoro with 2D/3D shape-matching - Glenoid LCS - Biceps LCS - ZX'Y"	- N=12 - 12 M, 32 yrs.	30°-120°	IR/ER*	-97°	-93°	4°
Giphart 2013	- Biplane fluoro with 2D/3D shape-matching - New ISB for scapula - Biceps LCS - YX'Y"	- N=13	30°-120°	Abduction*	-18°	80°	-62°
				Plane of elevation*	8°	-8°	-16°
				IR/ER*	25°	20°	-5°

Notes: Positive rotations: adduction, posterior plane of elevation, and IR. Abbreviations: ISB = International Society of Biomechanics, LCS = local coordinate system, SAB = scapular plane abduction, IR = internal rotation, ER = external rotation. *Data estimated from plots

Table 11: Summary of Sternoclavicular Kinematic Studies during Scapular Plane Abduction

Study	Methods	Subjects	Range	Angular Position	Initial Position	Final Position	Change in Position
Inman 1944	- Bone pin inserted into the clavicle	- Presumably 1 male subject - Age unknown	30°-120°	Axial rotation*	0°	15°	15°
McClure 2001	- Electromagnetic sensors attached to bone pins - Motion tracked as scapular position	- N=8 - 5 M, 3 F, 33 yrs.	30°-120°	Prot/Ret*	-19°	-30°	-11°
				Elev/Dep*	-2°	-9°	-7°
Fung 2001	- Bone fixed electromagnetic sensors - Glenoid LCS - ISB for humerus and clavicle	- N=5 - Cadaveric specimen - 76±7 yrs.	30°-120°	Prot/Ret*	-18°	-31°	-13°
				Elev/Dep*	-4°	-11°	-7°
				Axial rotation*	4°	14°	10°
Ludewig 2004	- Electromagnetic surface sensors - ISB	- N=30 - 14 M, 16 F, 27±5 yrs.	Rest-110°	Prot/Ret*	-18°	-26°	-8°
				Elev/Dep	-2°	-11°	-9°
				Axial rotation	1°	18°	17°
Ebaugh 2005	- Electromagnetic surface sensors with scapular tracker - Motion tracked as scapular position	- N=20 - 10 M, 10 F, 23 yrs.	Min-120°	Prot/Ret	-21°	-34°	-13°
				Elev/Dep	-6°	-19°	-13°
McClure 2006	- Electromagnetic surface sensors - Motion tracked as scapular position	- N=45 - 24 M, 21 F, 44±12 yrs.	Min-120°	Prot/Ret*	-20°	-30°	-10°
				Elev/Dep*	-3°	-14°	-11°
Sahara 2007	- Static MR scan - Glenoid LCS - Clavicle expressed relative to lung	- N=14 - 14 M, 24 yrs.	30°-120° (abduction)	Prot/Ret*	-32°	-50°	-18°
				Elev/Dep*	-7°	-14°	-7°
				Axial rotation*	4°	22°	18°
Ludewig 2009	- Electromagnetic sensors attached to bone pins - ISB	- N=12 - 7 M, 5 F, 29±7 yrs.	30°-120°	Prot/Ret*	-25°	-36°	-11°
				Elev/Dep	-12°	-17°	-5°
				Axial rotation	2°	24°	22°

Notes: Positive rotations: protraction, depression, posterior axial rotation. Abbreviations: ISB = International Society of Biomechanics, LCS = local coordinate system, SAB = scapular plane abduction, Prot = protraction, Ret = retraction, Elev = elevation, Dep = depression. *Data estimated from plots

Table 12: Summary of Acromioclavicular Kinematic Studies during Scapular Plane Abduction

Study	Methods	Subjects	Range	Angular Position	Initial Position	Final Position	Change in Position
Inman 1944	- Static radiographs	- Presumably 1 male subject - Age unknown	30°-120° (abduction)	UR/DR*	-5°	-35°	-30°
Sahara 2007	- Static MR - Glenoid LCS - Clavicle expressed relative to lung	- N=14 - 14 M, 24 yrs.	30°-120° (abduction)	IR/ER*	66°	73°	7°
				UR/DR*	10°	-2°	-12°
				AT/PT*	-14°	-4°	10°
Teece 2008	- Electromagnetic surface sensors - Old ISB	- *In vivo* - N=30 - 16 M, 14 F, 25±4 yrs.	30°-90°	IR/ER*	66°	70°	4°
				UR/DR*	-14°	-21°	-7°
				AT/PT*	-2°	1°	3°
	- Electromagnetic sensors attached to bone pins - Old ISB	- *In vitro* - N=8, 63 yrs.	30°-90°	IR/ER	67°	70°	3°
				UR/DR	-4°	-9°	-5°
				AT/PT	0°	13°	13°
Ludewig 2009	- Electromagnetic sensors attached to bone pins - Old ISB	- N=12 - 7 M, 5 F, 29±7 yrs.	30°-120°	IR/ER	59°	64°	5°
				UR/DR	-9°	-16°	-7°
				AT/PT	-2°	11°	13°

Notes: Positive rotations: IR, DR, PT. Abbreviations: ISB = International Society of Biomechanics, LCS = local coordinate system, SAB = scapular plane abduction, IR = internal rotation, ER = external rotation, DR = downward rotation, UR = upward rotation, PT = posterior tilt, AT = anterior tilt.
*Data estimated from plots

Table 13: Summary of Studies Comparing Scapulothoracic Kinematics between Symptomatic and Asymptomatic Subjects

Study	Methods	Subjects	Comparisons	Statistical Differences
Lukasiewicz 1999	- Electromagnetic digitizer (static) - Projection angles	Asymptomatic (N=20) 8 M, 12 F, 34±8 yrs. Symptomatic (N=17) 12 M, 5 F, 46±11 yrs. Duration: not specified	SAB Rest, 90°, max	Side-to-side comparisons* PT (90°, max): -8° Between-group comparisons* PT (90°, max): -10°
Ludewig 2000	- Electromagnetic surface sensors - Old ISB - Construction workers	Asymptomatic (N=26) 26 M, 40±13 yrs. Symptomatic (N=26) 26 M, 40±12 yrs. Duration: 5.5 yrs.	SAB 60°, 90°, 120°	UR (60°): -4° PT (120°): -6° IR (loaded): +5°
Endo 2001	- Static AP radiographs - Projection angles on scapula - Side-to-side comparisons	Symptomatic (N=27) 14 M, 13 F, 57 yrs. Duration: "chronic"	Abduction 0°, 45°, 90°	UR (90°): -4° PT (45°): -3° PT (90°): -5°
McClure 2006	- Electromagnetic surface sensors - Sternoclavicular motion tracked as scapular position - Old ISB	Asymptomatic (N=45) 24 M, 21 F, 44±12 yrs. Symptomatic (N=45) 24 M, 21 F, 45±13 yrs. Duration: >4 wks.	SAB 60°, 90°, 120°	SAB UR (90°): +4° PT (120°): +3°
Lawrence 2014	- Electromagnetic sensors attached to bone pins - Old ISB	Asymptomatic (N=12) 7 M, 5 F, 29±7 yrs. Symptomatic (N=10); 5 M, 5 F, 36±13 yrs. Duration: 10±8 yrs.	SAB 30°, 60°, 90°, 120°	SAB UR (30°): -7° UR (60°): -3°
Sousa 2014	- Electromagnetic surface sensors - Old ISB	Asymptomatic (N=26) 13M, 13 F, 46±9 yrs. Symptomatic (N=25) 13 M, 12 F, 48±9 yrs. Duration: >6 mo.	SAB 30°, 60°, 90°	SAB UR: +3-4°

Notes: Negative values for mean difference indicate symptomatic shoulders have decreased angular value compared to asymptomatic shoulders. Abbreviations: ISB = International Society of Biomechanics, SAB = scapular plane abduction, UR = upward rotation, PT = posterior tilt, IR = internal rotation. *Data estimated from plots

Table 14: Summary of Studies Comparing Glenohumeral Kinematics between Symptomatic and Asymptomatic Subjects

Study	Methods	Subjects	Comparisons	Statistical Differences
Ludewig 2000	- Electromagnetic surface sensors - Old ISB - Construction workers	Asymptomatic (N=26) 26 M, 40±13 yrs. Symptomatic (N=26) 26 M, 40±12 yrs. Duration: 5.5 yrs.	SAB 60°, 90°, 120°	No group differences
Hallström 2006	- Dynamic biplane radiostereometry - Coordinate systems not related to anatomy - Rotation sequence: abduction/adduction, IR/ER, flexion/extension	Asymptomatic (N=12) 8 M, 4 F, 32 yrs. Symptomatic (N=25) 16 M, 9 F, 51 yrs. Duration: >18 mo.	Abduction	No group differences
Lawrence 2014	- Electromagnetic sensors attached to bone pins - Old ISB	Asymptomatic (N=12) 7 M, 5 F, 29±7 yrs. Symptomatic (N=10) 5 M, 5 F, 36±13 yrs. Duration: 10±8 yrs.	Abduction, flexion, SAB 30°, 60°, 90°, 120°	SAB Elevation (30°): +7° Elevation (60°): +6°

Notes: Positive values for mean difference indicate symptomatic shoulders have increased angular value compared to asymptomatic shoulders.
Abbreviations: ISB = International Society of Biomechanics, SAB = scapular plane abduction, IR = internal rotation, ER = external rotation.

Table 15: Summary of Studies Comparing Sternoclavicular and Acromioclavicular Kinematics between Symptomatic and Asymptomatic Subjects

Study	Methods	Subjects	Comparisons	Statistical Differences
McClure 2006	- Electromagnetic surface sensors - Sternoclavicular motion tracked as scapular position - Old ISB	Asymptomatic (N=45) 24 M, 21 F, 44±12 yrs. Symptomatic (N=45) 24 M, 21 F, 45±13 yrs. Duration: varied	Flexion, SAB 60°, 90°, 120°	Flexion SC elevation (90°): +3° SC elevation (120°): +3° SAB SC retraction (120°): +3°
Lawrence 2014	- Electromagnetic sensors attached to bone pins - Old ISB	Asymptomatic (N=12) 7 M, 5 F, 29±7 yrs. Symptomatic (N=10) 5 M, 5 F, 36±13 yrs. Duration: 10±8 yrs.	Abduction, flexion, SAB 30°, 60°, 90°, 120°	Abduction SC posterior rotation: -5° Flexion SC posterior rotation: -6° SAB SC elevation (30° raising): -5° SC posterior rotation: -5°
Sousa 2014	- Electromagnetic surface sensors - Old ISB	Asymptomatic (N=26) 13M, 13 F, 46±9 yrs. Symptomatic (N=25) 13 M, 12 F, 48±9 yrs. Duration: >6 mo.	Flexion and SAB 30°, 60°, 90°	Flexion (lowering) SC retraction: -4° Flexion (raising) AC posterior tilt: +5° SAB (lowering) AC upward rotation: -6°

Notes: Negative values for mean difference indicate symptomatic shoulders have decreased angular value compared to asymptomatic shoulders.
Abbreviations: ISB = International Society of Biomechanics, SAB = scapular plane abduction, SC = sternoclavicular, AC = acromioclavicular.

Table 16: Summary of Studies of Subacromial Space during Simulated Scapular Plane Abduction in Cadaveric Shoulder Specimen

Study	Methods	Subjects	Motions Studied	Angle of Absolute Minimum Distance	Absolute Minimum Distance (mean ± SD)	Range of Rotator Cuff Risk
Two-Dimensional Studies						
Burns and Whipple 1993	- Photography and video - Static positioning of simulated glenohumeral motion	Fresh-frozen cadaveric shoulders (N=5) Age: >50 yrs.	SAB[a]: 0°-90° in 15° increments	Not described	Not described	67-135°*
Brossman 1996	- Static MR images and radiographs	Fresh cadaveric shoulder specimen (N=3) Age range: 70-80 yrs.	SAB[a]: 60°, 90°	Not described	Not described	60° and 90°
			Flexion[a]: 0°, 60°, 90°	Not described	Not described	60° and 90°
Other Methodologies						
Flatow 1994	- Stereo-photogrammetry (3D) and radiographs (2D) - Static positioning of simulated glenohumeral motion	Fresh-frozen cadaveric shoulders (N=9) Mean age: 73 yrs.	SAB: 0° to 180° in 30° increments	120°	4.8 ± 2.5 mm	<90°

Notes: All angles are humerothoracic elevation. Abbreviation: SAB = scapular plane abduction. *Glenohumeral elevation angle.

Table 17: Summary of Studies of Subacromial Space during Humeral Elevation in Asymptomatic Subjects

Study	Methods	Subjects	Motions Studied	Angle of Absolute Minimum Distance (mean ± SD)	Absolute Minimum Distance (mean ± SD)	Range of Rotator Cuff Risk
Two-Dimensional Studies						
Thompson 2011	- Single-plane fluoroscopy and static motion	College baseball players (N=16) Age: 20±1 yrs.	SAB: 0°, 30°, 45°, 60°, 75°	45°	5.2 ± 2.1 mm (to humerus)	Not described
Tasaki 2014	- Kinematic MR images	N=20 Mean age: 37 yrs.	SAB: 30° to max	93.5° ± 14.6°	1.6 ± 1.2 mm (to rotator cuff)	Not described
Three-Dimensional Studies						
Graichen 1999	- Bone models reconstructed from static MR images	N=12 Age range: 23-35 yrs.	SAB: 30°, 60°, 90°, 120°, 150°	120°	3.9 ± 1.8 mm (to humerus)	30°-90°
Giphart 2012	- Dynamic bi-plane fluoroscopy and 2D/3D shape-matching	N=8, 8 M Age: 30±7 yrs.	SAB: 20°-150°	83° ± 13°	2.6 ± 0.8 mm (to humerus)	34°-72°
			Flexion: 20°-150°	97° ± 23°	1.8 ± 1.2 mm (to humerus)	36°-65°

Notes: All angles are humerothoracic elevation. Abbreviation: SAB = scapular plane abduction, GH = glenohumeral, HT = humerothoracic.

Table 18: Summary of Studies of Comparing Subacromial Space between Asymptomatic Subjects and Clinical Populations

Study	Methods	Subjects	Motions Studied	Angle of Absolute Minimum Distance	Mean Difference in Absolute Minimum Distance	Significant Group Difference in Minimum Distances
Two-Dimensional Studies						
Hébert 2003	- Static MR images in upright seated posture	Symptomatic impingement (N=41) 44±9 yrs. Asymptomatic contralateral shoulders (N=30)	Flexion: rest, 50°, 70°, 90°, 110°, 130°	110°	-1.3 mm	70-130°: -1.1 to -1.3 mm*
			Abduction: rest, 70°, 80°, 90°, 110°	110°	-1.2 mm	80-110°: -1 to -1.2 mm*
Silva 2010	- Static ultrasound	Asymptomatic junior elite tennis players with/without dyskinesia (age: 15 years)	Abduction: 0° and 60° with IR	60°	Not reported	-0.5 mm†
Seitz 2012	- Static ultrasound	Asymptomatic (N=20) Symptomatic (N=20) Scapular dyskinesia Pooled mean age: 27±6 yrs.	SAB: rest, 45° and 90°	45°	-0.4 mm	None
Three-Dimensional Studies						
Graichen 1999	- Bone models reconstructed from static MR images - Side-to-side comparison	Symptomatic (N=10) Age: 39-64 yrs. Stage I impingement (N=6)	SAB: 30°, 90°	90°	-0.7 mm*	None
		Full thickness rotator cuff tear (N=3)		90°	-0.25 mm*	30°: -1.75 mm* 90°: -0.75 mm*
		Acromioclavicular joint arthritis (N=1)		Not reported	Not reported	Not reported
Bey 2007	- Dynamic bi-plane fluoroscopy and 2D/3D shape-matching	N=11; 63±11 yrs. 12-16 wks. after repair of isolated full-thickness supraspinatus tear and acromioplasty	Abduction: 15° increments from 15° to 105°‡	90°c	+1.1 mm*	15°-120°‡: +0.6 mm
Lawrence 2017	- 3D anatomical models reconstructed from MR images - Simulated using mean kinematics of asymptomatic subjects during functional reach	Asymptomatic (N=10) Age: 38.5 ± 12.8 yrs. Symptomatic (N=10) 43.0 ± 11.8 yrs.	Functional reaching task	Not reported	Not reported	None

Notes: All angles are humerothoracic elevation. Negative values for mean difference in absolute minimum distance indicate symptomatic shoulders have smaller distances.
Abbreviations: SAB = scapular plane abduction. *Estimated from plots. †Change in acromiohumeral distance between 0° and 60°. ‡Glenohumeral elevation angle.

Appendix B: Additional Descriptions and Analyses for Aim 1

Shape-Matching Errors for Angular Displacement and Glenohumeral Translations

In addition to the bone and joint orientation and position errors due to shape-matching described in Chapter 3, errors in glenohumeral translation (**Table 19**) and acromioclavicular (**Table 20**) and glenohumeral joint angular displacement (**Table 21**) were quantified between successive humerothoracic elevation positions.

Glenohumeral translation was calculated as the difference between the glenohumeral position at time 2 relative to its position at time 1. The angular displacement errors were of particular interest as sternoclavicular, acromioclavicular, and scapulothoracic angular displacement will be variables of interest in Aim 3 (i.e. Chapter 5). Displacements were calculated as the distal segment moving relative to the proximal segment between increments of humerothoracic elevation and described in the reference frame of the distal segment at the initial position (i.e. local displacement) (Zatsiorsky, 1998). Angular displacements of the acromiohumeral joint were described using a Y-X'-Z'' rotation sequence (Wu et al., 2005), whereas angular displacements of the glenohumeral joint were described using a X-Z'-Y'' rotation sequence (Phadke et al., 2011).

Table 19: Shape-Matching Errors for Glenohumeral Joint Translation

Phase	Anterior/ Posterior	Superior/ Inferior	Medial/ Lateral
Min to 30°	4.4 (-0.4 ± 5.4)	0.5 (0.4 ± 0.3)	1.7 (0.5 ± 2.0)
30° to 60°	3.1 (-1.8 ± 2.9)	0.7 (0.2 ± 0.8)	0.7 (0.0 ± 0.8)
60° to 90°	2.9 (-2.0 ± 2.5)	0.5 (-0.1 ± 0.6)	1.1 (0.3 ± 1.3)
90° to Max	1.4 (0.5 ± 1.4)	0.6 (0.2 ± 0.6)	0.7 (0.1 ± 0.8)
Overall	3.0 (-0.9 ± 3.0)	0.6 (0.2 ± 0.6)	1.1 (0.2 ± 1.1)

Notes: Data presented as RMS error (bias ± precision). All values are in mm.

Table 20: Shape-Matching Errors for Acromioclavicular Joint Angular Displacement

Phase	Internal Rotation	Upward Rotation	Tilt
Min to 30°	2.1 (0.6 ± 3.4)	4.1 (2.6 ± 3.9)	2.4 (-1.2 ± 2.5)
30° to 60°	2.6 (-0.7 ± 2.9)	2.8 (-0.5 ± 3.2)	1.5 (0.3 ± 1.8)
60° to 90°	2.6 (0.9 ± 2.8)	3.0 (-0.6 ± 3.4)	2.4 (1.0 ± 2.5)
90° to Max	1.6 (-0.8 ± 1.6)	4.2 (-0.3 ± 4.8)	2.3 (-0.6 ± 2.5)
Overall	2.4 (0.0 ± 2.5)	3.5 (0.2 ± 3.7)	2.2 (0.0 ± 2.2)

Notes: Data presented as RMS error (bias ± precision). All values are in degrees.

Table 21: Shape-Matching Errors for Glenohumeral Joint Angular Displacement

Phase	Elevation	Plane of Elevation	Axial Rotation
Min to 30°	2.2 (-0.1 ± 2.7)	0.8 (0.6 ± 0.5)	4.2 (0.1 ± 5.1)
30° to 60°	4.3 (-0.1 ± 5.0)	2.1 (-0.7 ± 2.3)	3.2 (0.5 ± 3.7)
60° to 90°	1.9 (-1.0 ± 1.8)	0.6 (0.0 ± 0.7)	5.2 (-3.3 ± 4.6)
90° to Max	2.1 (0.6 ± 2.3)	2.2 (-0.1 ± 2.5)	3.4 (0.1 ± 3.9)
Overall	2.8 (-0.2 ± 2.9)	1.6 (-0.1 ± 1.7)	4.1 (-0.7 ± 4.1)

Notes: Data presented as RMS error (bias ± precision). All values are in degrees.

Monte Carlo Simulation for Determining the Relative Impact of Marker Digitizing Errors on Error Attributed to Shape-Matching

An inherent assumption of radiostereometric analysis (RSA) is that the tantalum beads can be tracked accurately in 3D space. This assumption was tested by digitizing beads embedded in an acrylic validation object as reported in Chapter 3. Although the RMS error due to marker digitization for describing the relative orientation between arbitrary coordinate systems was only 0.2°, it remains unclear the extent to which errors in digitizing beads under *in vitro* conditions confounded the description of the bead-based coordinate systems that ultimately represent the gold standard. Of particular interest was the potential impact of errors from digitizing the three nearly collinear beads in the clavicle on the description of clavicular kinematics.

To investigate the impact of bead digitization errors on defining the gold standard kinematics, a Monte Carlo simulation was performed for each specimen using the following approach. First, a Gaussian sampling distribution was defined using the bias and precision from relative marker cluster position as described in the marker tracking validation in Chapter 3 (bias ± precision: 0.11 ± 0.21 mm). This step results in a distribution of errors expected along each coordinate axis due to bead digitization.

Second, three errors (e_x, e_y, e_z) were randomly sampled from the distribution for each bead and applied to the originally digitized bead coordinates:

$$X' = X + e_x$$

$$Y' = Y + e_y$$

$$Z' = Z + e_z$$

Where *X*, *Y*, and *Z* are the originally digitized bead coordinates, e_x, e_y, e_z are the randomly sampled errors, and *X', Y',* and *Z'* are the new bead coordinates with the randomly sampled error. This step was repeated for each segment (i.e. clavicle, humerus, scapula) and resulted in new bead coordinates for each bead on each segment.

Third, a new bead-based coordinate system was calculated in the same manner as the originally digitized coordinate system. Fourth, each segments' new bead-based coordinate system was transformed into anatomical coordinate systems in the same manner as the original bead-based coordinate system. Fifth, the angular displacement between the original and new anatomical coordinate systems was calculated for each segment, and the difference in angular orientation was calculated for the acromioclavicular and glenohumeral joints. Sixth, the process was repeated 10,000 times to obtain a stable estimate of the errors once aggregated.

Finally, overall RMS errors were calculated for joint (glenohumeral and acromioclavicular) and bone (clavicle, humerus, scapula) orientation. Segmental and joint position was not calculated as it would be dependent upon tracking a single point. Ultimately, this analysis provides a description of the extent to which each segment axis is sensitive to errors in digitization, and how these errors impact the gold standard description of joint kinematics.

Comparison of errors due to digitization from the simulation and errors attributed to shape-matching (Chapter 3) are presented in **Table 22** for bone orientation and **Table 23** for joint orientation. For the clavicle, axial rotation appears the most sensitive to digitization errors, which is also reflected in the higher errors in shape-matching

compared to other rotations. This suggests a portion of the error attributed to shape-matching for clavicular axial rotation may be due to digitization errors. By comparison, retraction and elevation appear less sensitive to digitization errors. For the scapula, all three rotations appear to be minimally impacted by digitization errors. This suggests the higher error in scapular internal rotation attributed to shape-matching may be due to the out-of-plane position and not digitization error. Finally, for the humerus, axial rotation is the most sensitive to digitization errors, which is also reflected in the higher errors in shape-matching compared to other rotations. Errors due to digitization for humeral plane of elevation are relatively small, suggesting the errors attributed to shape-matching may also be due to the out-of-plane position and the difficulty shape-matching the humerus' cylindrical shape.

Table 22: Bone Orientation Errors Attributed to Marker Digitization and Shape-Matching

	Digitization	**Shape-Matching**
Clavicle		
Retraction	0.2°	0.4°
Elevation	0.3°	0.6°
Axial rotation	1.2°	3.7°
Scapula		
Internal rotation	0.2°	1.6°
Upward rotation	0.3°	0.5°
Tilt	0.2°	0.8°
Humerus		
Elevation	0.3°	2.3°
Plane of elevation	0.2°	1.2°
Axial rotation	0.9°	3.2°

Note: Errors are expressed as RMS.

Given clavicle axial rotation was most sensitive to digitization error, it is not surprising that acromioclavicular upward rotation is also most sensitive to digitization

error. For the glenohumeral joint, the error attributed to shape-matching axial rotation and plane of elevation appear to be primarily due to the out-of-plane nature of the motion and the difficulty shape-matching the humerus.

Table 23: Joint Orientation Errors Attributed to Marker Digitization and Shape-Matching

	Digitization	Shape-Matching
Acromioclavicular		
Internal rotation	0.3°	1.8°
Upward rotation	1.3°	3.4°
Tilt	0.4°	2.0°
Glenohumeral		
Elevation	0.4°	0.7°
Plane of elevation	0.3°	2.6°
Axial rotation	0.9°	3.3°

Note: Errors are expressed as RMS.

Sensitivity Analysis to Determine the Effect of Shape-Matching Errors on Proximity Parameters

A sensitivity analysis was performed to determine how errors in shape-matching impact the calculation of minimum distance. In particular, out-of-plane position errors are generally high for shape-matching single-plane fluoroscopic images, and these errors may impact minimum distance calculations. Given the data collection setup employed for this thesis, out-of-plane position error will predominantly impact glenohumeral anterior/posterior position, plane of elevation, and axial rotation. To investigate the sensitivity of the minimum distance calculation to shape-matching errors, modeling was performed on each specimen using their individual glenohumeral kinematics from: 1) marker tracking (i.e. RSA), 2) shape-matching (i.e. unconstrained), and 3) shape-matching assuming the humeral head remains centered anterior/posterior in the glenoid

(i.e. constrained). Errors between marker-tracking and both shape-matching conditions were described as root mean square (RMS), bias, and precision. Paired *t*-tests were performed to determine whether the minimum distance errors were significantly different between conditions.

Errors for calculating minimum distance based on constrained and unconstrained kinematics are shown in **Table 24**. Unconstrained kinematics resulted in lower RMS errors and precision than constraining the humeral anterior/posterior position to the center of the glenoid. However, the unconstrained method resulted in higher bias error.

Table 24: Errors in Methods for Modeling Glenohumeral Kinematics for Quantifying Subacromial Minimum Distance

Error Statistic	Unconstrained	Constrained
RMS	1.5 mm	1.8 mm
Bias	0.6 mm	0.3 mm
Precision	1.4 mm	1.8 mm

Notes: Unconstrained refers to glenohumeral kinematics from original shape-matching, while constrained refers to glenohumeral kinematics assuming the humerus remains centered anteroposteriorly in the glenoid.

When compared statistically, both methods of modeling the kinematics were not significantly different than marker tracking (unconstrained: p = 0.09, t =1.79, df = 18; constrained: p = 0.49, t = 0.70, df = 18). Although insignificant, the lower p-value for the unconstrained method is the result of a larger mean difference (i.e. bias) and a smaller standard deviation (i.e. precision). Further, no difference was found between shape-matching methods (p = 0.55, t = -0.61, df = 18). Given there was no difference between modeling using constrained and unconstrained kinematics on the calculation of minimum distance, it was decided to proceed using the unconstrained approach as it would not

presume the humerus remains centered in the glenoid when anterior/posterior translations are known to occur during humeral elevation (Lawrence et al., 2014b; Ludewig et al., 2000).

Appendix C: Additional Descriptions and Analyses for Aim 2

Additional Descriptions of Methods for Determining Rotator Cuff Insertion and Thickness

Identification of Rotator Cuff Insertion Region of Interest

The rotator cuff insertion region of interest was identified on MR images within Mimics software following 3D model reconstruction by fitting two polyplanes to the humeral head model. The first polyplane defined the articular margin and extended anteriorly from the biceps groove to the posterior aspect of the humeral head (**Figure 31A**). The second polyplane defined the anterior, lateral, and posterior margins of the rotator cuff insertion (**Figure 31B**). Initial guesses were made of the location of both polyplanes based on the margins of the superior facet of the greater tuberosity on the 3D humeral model. Once defined, the polyplanes' locations were iteratively refined by scrolling through the MR slices and triangulating the visual margin of the rotator cuff soft tissue based on the coronal, sagittal, and transverse plane MR views (**Figure 32**). This process was repeated until the margins of the rotator cuff on the MR were as close as possible with the margins of the footprint on the 3D bone model. Once defined, these planes were used to define and isolate (i.e. cut) the rotator cuff insertion region of interest from the 3D humeral model.

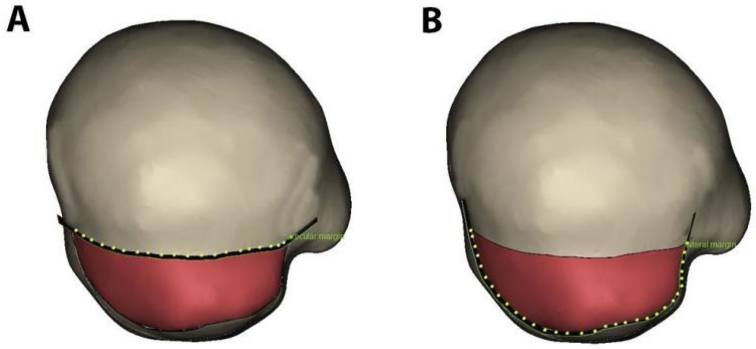

Figure 31: Definition of polyplanes at rotator cuff insertion margins. **A)** The articular margin polyplane follows inflection between the superior facet and articular surface and extended anteriorly from the biceps groove to the posterior aspect of the humeral head; **B)** A polyplane representing the initial guess of the anterior, lateral, and posterior margins of the rotator cuff insertion based on the contours of the superior facet.

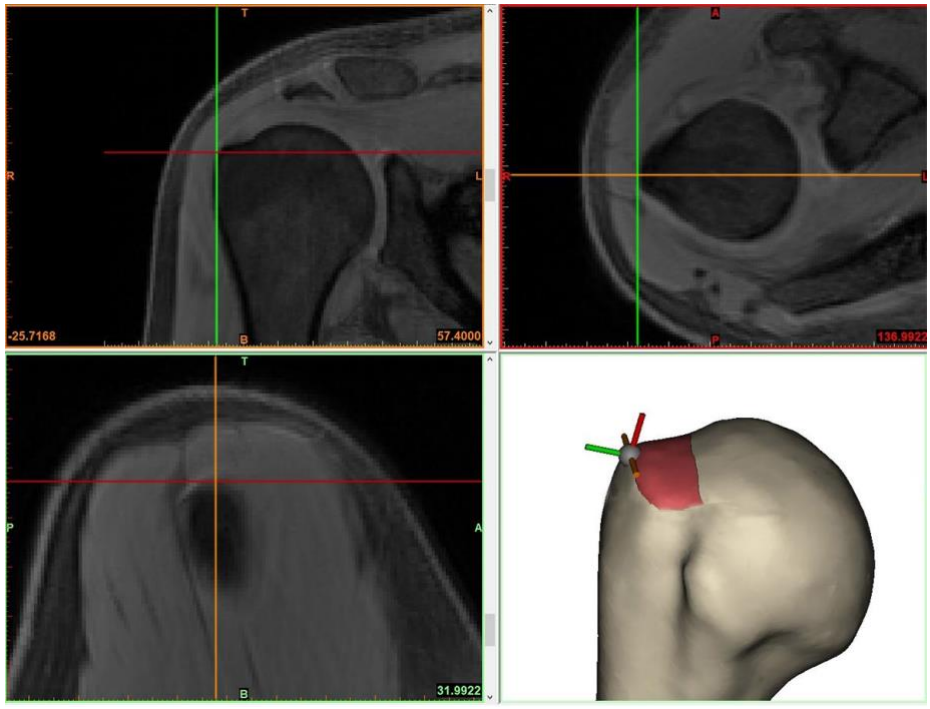

Figure 32: Identification of rotator cuff insertion region of interest. The crosshairs on the three MR views indicates the 2D location of the reference marker (ball with crosshairs) on the 3D humeral model. The margin of the rotator cuff insertion was identified by scrolling through the slices of each MR view and ensuring the margins of the insertion as seen on the MR images are consistent between the reference maker and insertion region of interest (red surface) on the 3D model.

Identification of Articular Margin Region of Interest

Following identification of the rotator cuff insertion margins, the articular surface polyplane was duplicated and translated 0.7 mm laterally (**Figure 33**). This width was chosen as it was the resolution of the MR scan. Once defined, these planes were used to define and isolate (i.e. cut) the articular margin region of interest from the 3D humeral model.

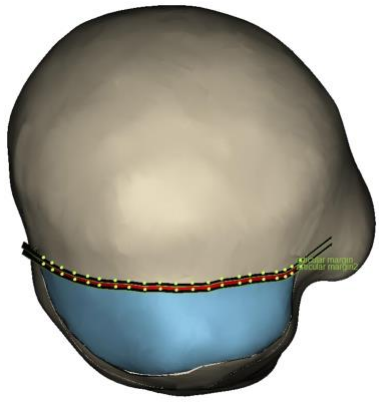

Figure 33: Definition of the articular margin region of interest (red) from the rotator cuff insertion region of interest (blue and red). The articular margin region of interest was defined by duplicating the articular margin polyplane and translating it 0.7 mm laterally.

Measurement of Rotator Cuff Thickness

The anterior and posterior margins of the rotator cuff insertion region of interest were digitized on the humeral 3D model. The sagittal MR slice corresponding to the midpoint between these landmarks was identified for the thickness measurement. A reference line was drawn on the 2D sagittal MR image slice extending from the articular margin to the lateral aspect of the rotator cuff insertion (**Figure 34**). A second line was drawn perpendicular to the first, and the rotator cuff thickness measurement was taken along this line (**Figure 34**).

Figure 34: Measurement of rotator cuff thickness. Two reference lines were drawn (red), which included a line connecting the medial and lateral margins of the insertion and its perpendicular. The rotator cuff thickness was measured from the surface of the humeral head along the perpendicular (blue lines).

Calculation of Morphology Parameters

Several scapular morphological parameters were calculated as potential covariates for the investigation of scapulothoracic upward rotation on subacromial space. In total, five parameters were calculated for each subject: acromial slope, glenoid inclination, glenoid version, critical shoulder angle, and the radius of the humeral head. Details of these calculations are provided below. The descriptions of acromial slope, glenoid inclination, and glenoid version were made relative to the orientation of the scapular anatomical coordinate system, which was defined based on published recommendations (Ludewig et al., 2010)

Acromial Slope

Acromial slope represents the angulation of the undersurface of the acromion (**Figure 35**). To perform this calculation, the undersurface of the acromion was manually identified in 3-Matic software (Materialise NV; Leuven, Belgium) and converted to a point cloud. A plane was fit to the point cloud using a principal components analysis. This approach was chosen as is capable of accounting for the multi-dimensional nature of the anatomical point cloud and is not constrained to the orientation of the reference coordinate system as is a least squares approach. The principal axis representing the plane's normal vector was defined as a unit vector and transformed into the scapular anatomical coordinate system. Acromial slope was calculated as the angle between the plane's normal vector and the scapular Y (i.e. superior/inferior) axis after being projected onto the scapular XY (i.e. sagittal) plane. Calculations performed on left-sided scapula were converted to right-sided equivalence by negating the X (i.e. anterior/posterior) component:

$$\text{Lateral acromial slope (right)} = \tan^{-1}\left(\frac{V_x\hat{\imath}}{-V_y\hat{\jmath}}\right)$$

$$\text{Lateral acromial slope (left)} = \tan^{-1}\left(\frac{-V_x\hat{\imath}}{-V_y\hat{\jmath}}\right)$$

Where $\bar{V}$ is the normal vector of the plane fit to the undersurface of the acromion represented relative to the scapular anatomical coordinate system, and *i* and *j* are its unit vector components.

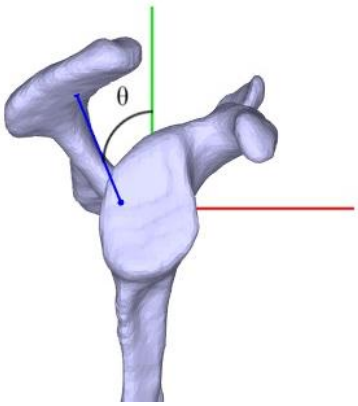

Figure 35: Lateral acromial slope (θ) was calculated as the angle between a vector normal to the undersurface of the acromion (blue) and the scapular Y axis (green) after being projected onto the scapula's XY (i.e. sagittal) planes.

Glenoid Inclination

Glenoid inclination represents the angulation of the glenoid in the superior/inferior direction (**Figure 36**). To perform this calculation, the glenoid rim was manually identified in 3-Matic software (Materialise NV; Leuven, Belgium) and converted to a point cloud. A plane was fit to the point cloud using a principal components analysis. The superior/inferior principal axis of the glenoid was defined as a unit vector and transformed into the scapular anatomical coordinate system. Glenoid inclination was calculated as the angle between the glenoid's superior/inferior principal axis and the scapular Y (i.e. superior/inferior) axis after being projected onto the scapular YZ (i.e. coronal) plane. Glenoid inclination was described as a positive magnitude and declination was described as a negative magnitude:

$$\text{Glenoid inclination} = 0° - \tan^{-1}\left(\frac{V_z\hat{k}}{V_y\hat{j}}\right)$$

Where $\bar{V}$ is the superior/inferior principal axis of the glenoid represented relative to the scapular anatomical coordinate system, and *j* and *k* are its unit vector components.

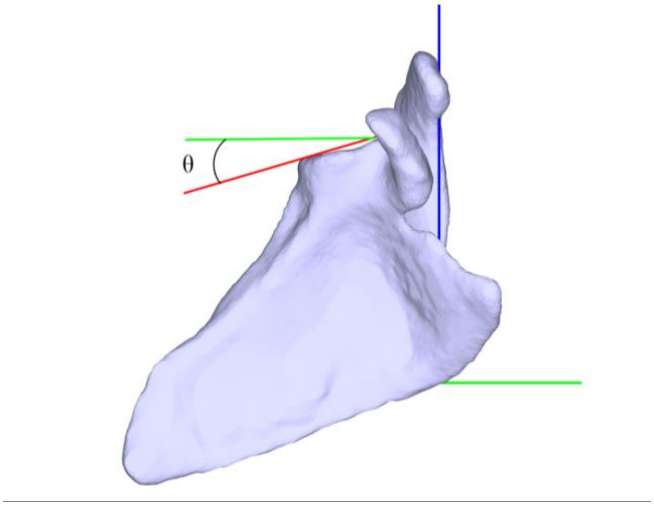

Figure 36: Glenoid inclination (θ) was calculated as the angle between the glenoid's superior/inferior principal axis (red) and the scapular Y axis (green) after being projected onto the scapular YZ (i.e. coronal) plane.

Glenoid Version

Glenoid version represents the angulation of the glenoid in the anterior/posterior direction (**Figure 37**). The anterior/posterior principal axis of the glenoid was defined as a unit vector and transformed into the scapular anatomical coordinate system. Glenoid version was calculated as the angle between the anterior/posterior principal axis and the scapular X (i.e. anterior/posterior) axis after being projected onto the scapular XZ (i.e. transverse) plane. Glenoid anteversion was described as a positive magnitude and retroversion being described as a negative magnitude:

$$\text{Glenoid version (right)} = 0° - \tan^{-1}\left(\frac{V_z\hat{k}}{V_x\hat{\imath}}\right)$$

$$\text{Glenoid version (left)} = \tan^{-1}\left(\frac{V_z\hat{k}}{V_x\hat{\imath}}\right)$$

Where $\bar{V}$ is the anterior/posterior principal axis of the glenoid represented relative to the scapular anatomical coordinate system, and *i* and *k* are its unit vector components.

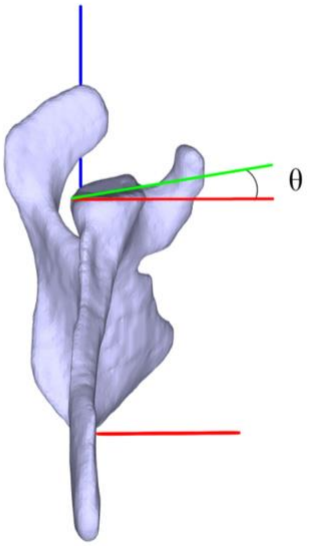

Figure 37: Glenoid version (θ) was calculated as the angle between the anterior/posterior principal axis (green) and the scapular X axis (red) after being projected onto the scapula's XZ (i.e. transverse) plane.

Critical Shoulder Angle

The critical shoulder angle represents the laterality of the acromion relative to the inclination of the glenoid (**Figure 38**). To perform this calculation, the acromion and glenoid rim were converted into point clouds with the coordinates transformed into the scapular coordinate system. The lateral-most point of the acromion was then identified as the point coordinate with the maximum magnitude in the $+Z$ direction. A similar approach was used to identify the inferior-most point on the glenoid rim. A vector was created between these two points (pointing superolaterally) and converted to a unit vector

represented in the scapular coordinate system. The critical shoulder angle was calculated as the 3D angle between this vector and the superior/inferior principal axis of the glenoid:

$$\text{CSA} = \hat{A} \cdot \hat{B}$$

Where $\hat{A}$ is the unit vector representation of the lateral-most point on the acromion relative to the inferior-most point on the glenoid, and $\hat{B}$ is the superior/inferior principal axis of the glenoid represented relative to the scapular anatomical coordinate system.

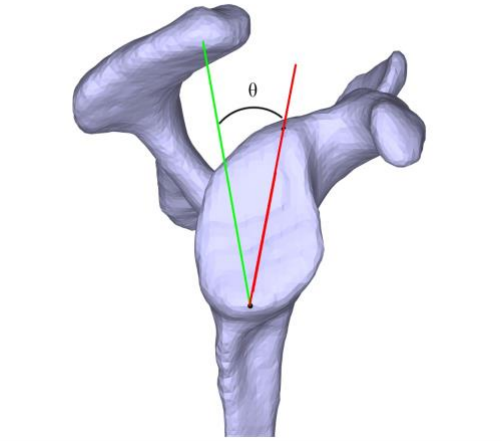

Figure 38: The critical shoulder angle (θ) was calculated as the 3D angle between this lateral acromion/inferior glenoid vector (green) and the superior/inferior principal axis of the glenoid (red).

Determination of Covariance Structure for Mixed Models

Utilization of mixed models requires specification of a covariance structure with which to model the within-subject (i.e. repeated) factor. This specification accounts for the presence and type (i.e. structure) of relationship between the levels of the within-subject factor. With repeated measures analyses, these levels cannot be assumed to be independent, which is a general assumption of traditional ANOVA analyses.

For the current study, the covariance structure chosen to specify the relationship between the levels of the repeated factor (i.e. humerothoracic elevation angle) was chosen by inspecting covariance and correlation values across the pairwise time points, and by comparing the fit statistics from models fit with different covariance structures (Littell et al., 2000). For the analyses of both normalized minimum distance and surface area, inspecting the covariance and correlation matrix suggests a decay is present across adjacent levels of humerothoracic elevation (**Table 25** and **Table 27**). This suggests first order autoregressive or Toeplitz covariance structures may be most appropriate. However, the magnitude does not fully decay to zero for levels furthest apart (i.e. arm at side and 90º for normalized minimum distance, 30º and 90º for surface area) suggesting Toeplitz may be most appropriate. Inspection of the fit statistics (**Table 26** and **Table 28**) confirms a Toeplitz structure is most appropriate and was chosen to model the covariance for the analysis of normalized minimum distance and surface area.

Normalized Minimum Distance

Table 25: Covariance and Correlations for Normalized Minimum Distance to Coracoacromial Arch (log transformed)

	Arm at side	**30º**	**60º**	**90º**
Arm at side	6358.2 (1.0)	2603.5 (0.81)	1242.9 (0.63)	1045.4 (0.32)
30º	--	1594.7 (1.0)	542.2 (0.55)	207.3 (0.13)
60º	--	--	601.6 (1.00)	716.5 (0.72)
90º	--	--	--	1645.3 (1.00)

Note: Data presented as pairwise variance/covariance (correlation).

Table 26: Fit Statistics for Models with Different Covariance Structures for Normalized Minimum Distance to Coracoacromial Arch (log transformed)

Covariance Structure	AIC	AICC	BIC
Variance Components	1633.9	1633.9	1635.9
Compound Symmetry	1602.2	1602.3	1605.6
Autoregressive (1st order)	1577.8	1577.9	1581.1
Toeplitz	1576.5	1576.8	1583.2

Note: Smaller fit statistics indicate better model fit.

Surface Area

Table 27: Covariance and Correlations for Surface Area of the Footprint within 100% of the Rotator Cuff Tendon Thickness

	30º	60º	90º
30º	3803.4 (1.00)	2416.9 (0.50)	1203.5 (0.24)
60º	--	6040.4 (1.00)	4895.2 (0.78)
90º	--	--	6486.8 (1.00)

Note: Data presented as pairwise variance/covariance (correlation).

Table 28: Fit Statistics for Models with Different Covariance Structures for Surface Area of the Footprint within 100% of the Rotator Cuff Tendon Thickness

Covariance Structure	AIC	AICC	BIC
Variance Components	1323.9	1324.0	1325.6
Compound Symmetry	1296.1	1296.3	1299.5
Autoregressive (AR-1)	1282.5	1282.6	1285.8
Toeplitz	1279.9	1280.1	1285.0

Note: Smaller fit statistics indicate better model fit.

Summary of Clinical Examination Findings

Below are tables summarizing the clinical presentation of the symptomatic participants (**Table 29**), the results of the scapular movement examination by symptom group (asymptomatic, symptomatic) (**Table 30**) and by scapulothoracic upward rotation group (**Table 31**), and other clinical examination findings by symptom group

(asymptomatic, symptomatic) (**Table 32**) and by scapulothoracic upward rotation group (**Table 33**).

Table 29: Clinical Presentation in Symptomatic Participants (n = 24)

Characteristic	Responses
Symptom duration (weeks)*	36.0
Symptoms disturb sleep (% yes)	58.3%
Receiving treatment (% yes)	8.3%
Location of symptoms	
Front of shoulder joint	54.2%
Back of shoulder joint	25.0%
Side of shoulder joint	25.0%
Deep in shoulder joint	54.2%
Shoulder blade area	13.0%
Symptom quality	
Loss of motion	16.7%
Instability	29.2%
Weakness	25.0%
Stiffness	29.2%
Pain	95.8%
NPRS (0-100)	
Best in last week*	10.0
Worst in last week*	50.0
Symptom temporality	
Intermittent	70.8%
Constant	29.2%

Notes: Percentages for location of symptoms and quality of symptoms may not sum to 100% as some participants may have responded affirmatively to multiple options. *Indicates data presented as median due to skewed distribution.

Table 30: Scapular Movement Examination Results by Symptom Group

	Asymptomatic (n = 25)	Symptomatic (n = 24)	Statistic	p-value
Unloaded Flexion				
Positive test	40.0%	87.5%	$X^2_1 = 11.9$	<0.01
Shrug	0.0%	0.0%	$X^2_1 = 0.0$*	1.00
Dumping	0.0%	16.7%	$X^2_1 = 4.5$*	0.05
Medial border winging	12.0%	25.0%	$X^2_1 = 1.4$*	0.29
Inferior border winging	32.0%	83.3%	$X^2_1 = 13.2$	<0.01
Unloaded Abduction				
Positive test	52.0%	79.2%	$X^2_1 = 4.0$	0.05
Shrug	4.0%	25.0%	$X^2_1 = 4.4$*	0.05
Dumping	24.0%	58.3%	$X^2_1 = 6.0$	0.01
Medial border winging	12.0%	29.2%	$X^2_1 = 2.2$*	0.17
Inferior border winging	32.0%	41.7%	$X^2_1 = 0.5$	0.48
Loaded Flexion				
Positive test	64.0%	91.7%	$X^2_1 = 5.4$	0.02
Shrug	4.0%	8.3%	$X^2_1 = 0.4$*	0.61
Dumping	4.0%	37.5%	$X^2_1 = 8.5$*	<0.01
Medial border winging	12.0%	33.3%	$X^2_1 = 3.2$	0.07
Inferior border winging	56.0%	83.3%	$X^2_1 = 4.3$	0.04
Loaded Abduction				
Positive test	40.0%	91.7%	$X^2_1 = 14.4$	<0.01
Shrug	20.0%	50.0%	$X^2_1 = 4.9$	0.03
Dumping	8.0%	58.3%	$X^2_1 = 14.1$	<0.01
Medial border winging	20.0%	37.5%	$X^2_1 = 1.8$	0.18
Inferior border winging	24.0%	50.0%	$X^2_1 = 3.6$	0.06

Notes: Data presented as proportions for the side tested only. A positive test indicates the participant had at least one finding (i.e. subtle or obvious for at least one deviation). Data for specific deviations (i.e. shrug, dumping, etc.) presented as proportions of participants with a positive finding (i.e. subtle or obvious). Proportions may not sum to 100% as some participants may have had positive findings for multiple deviations. *Indicates Fisher's Exact Tests was used due to low expected counts.

Table 31: Scapular Movement Examination Results by Scapulothoracic Upward Rotation Group

	High (n = 20)	Low (n = 20)	Statistic	p-value
Unloaded Flexion				
Positive test	45.0%	90.0%	$X^2_1 = 9.2$	<0.01
Shrug	0.0%	0.0%	$X^2_1 = 0.0$*	1.00
Dumping	5.0%	15.0%	$X^2_1 = 1.1$*	0.61
Medial border winging	5.0%	25.0%	$X^2_1 = 3.1$*	0.18
Inferior border winging	45.0%	85.0%	$X^2_1 = 7.0$	<0.01
Unloaded Abduction				
Positive test	50.0%	80.0%	$X^2_1 = 4.0$	0.05
Shrug	5.0%	25.0%	$X^2_1 = 3.1$*	0.18
Dumping	30.0%	50.0%	$X^2_1 = 1.7$	0.20
Medial border winging	15.0%	20.0%	$X^2_1 = 0.2$*	1.00
Inferior border winging	25.0%	55.0%	$X^2_1 = 3.8$	0.05
Loaded Flexion				
Positive test	65.0%	90.0%	$X^2_1 = 3.6$*	0.13
Shrug	5.0%	10.0%	$X^2_1 = 0.4$*	1.00
Dumping	15.0%	25.0%	$X^2_1 = 0.6$*	0.69
Medial border winging	20.0%	15.0%	$X^2_1 = 0.2$*	1.00
Inferior border winging	60.0%	85.0%	$X^2_1 = 3.1$	0.08
Loaded Abduction				
Positive test	60.0%	80.0%	$X^2_1 = 1.9$	0.17
Shrug	35.0%	40.0%	$X^2_1 = 0.1$	0.74
Dumping	20.0%	45.0%	$X^2_1 = 2.8$	0.09
Medial border winging	20.0%	35.0%	$X^2_1 = 1.1$	0.29
Inferior border winging	30.0%	55.0%	$X^2_1 = 2.6$	0.11

Notes: Data presented as proportions for the side tested only. A positive test indicates the participant had at least one finding (i.e. subtle or obvious for at least one deviation). Data for specific deviations (i.e. shrug, dumping, etc.) presented as proportions of participants with a positive finding (i.e. subtle or obvious). Proportions may not sum to 100% as some participants may have had positive findings for multiple deviations. *Indicates Fisher's Exact Tests was used due to low expected counts.

Table 32: Clinical Examination Results by Symptom Group

	Asymptomatic (n = 25)	Symptomatic (n = 24)	Statistic	p-value
Posture				
Within normal limits	44.0%	41.7%	$X^2_1 = 0.0$	0.87
Forward head	44.0%	29.2%	$X^2_1 = 1.2$	0.28
Rounded shoulders	24.0%	41.7%	$X^2_1 = 1.7$	0.19
Range of Motion				
Scapular plane abduction	162.8° ± 7.0°	161.0° ± 6.8°	$t_{47} = 0.9$	0.35
External rotation	90.3° ± 8.8°	88.8° ± 9.2°	$t_{47} = 0.6$	0.58
Internal Rotation	62.0° ± 10.2°	57.1° ± 11.0°	$t_{47} = 1.6$	0.11
Total arc of motion	152.3° ± 13.3°	146.0° ± 14.4°	$t_{47} = 1.6$	0.12
Special Tests				
Provocation tests positive†	0.0	3.0	$X^2_1 = 38.8$	<0.01
Scapular assistance test	0.0%	79.2%	$X^2_1 = 38.3$	<0.01
Hawkins-Kennedy	4.0%	62.5%	$X^2_1 = 19.1$	<0.01
Jobe	0.0%	70.8%	$X^2_1 = 27.1$	<0.01
Neer	4.0%	62.5%	$X^2_1 = 19.1$	<0.01
Resisted external rotation	0.0%	66.7%	$X^2_1 = 24.7$	<0.01
Biceps load II	0.0%	4.2%	$X^2_1 = 1.1$	0.49
Sulcus	8.0%	8.3%	$X^2_1 = 0.0$*	1.00

Notes: Data presented for the side tested only. Continuous data presented as mean ± SD and statistically assessed using an independent two-sample *t*-test. Categorical data presented as proportions and statistically assessed using Chi-square tests. Proportions may not sum to 100% as some participants may have had positive findings for multiple options within an assessment. Provocation tests positive represents the number of tests positive from the following: Hawkins-Kennedy, Jobe, Neer, and resisted external rotation. †Indicates data presented as median due to highly non-normal data in asymptomatic group, data tested statistically with Kruskal-Wallis test. *Indicates Fisher's Exact Tests was used due to low expected counts.

Table 33: Clinical Examination Results by Scapulothoracic Upward Rotation Group

	High (n = 20)	Low (n = 20)	Statistic	p-value
Posture				
Within normal limits	60.0%	40.0%	$X^2_1 = 1.6$	0.21
Forward head	20.0%	45.0%	$X^2_1 = 2.8$	0.09
Rounded shoulders	30.0%	35.0%	$X^2_1 = 0.1$	0.74
Range of Motion				
Scapular plane abduction	161.8° ± 7.0°	162.1° ± 6.8°	$t_{38} = -0.1$	0.91
External rotation	88.5° ± 7.0°	89.7° ± 10.6°	$t_{38} = -0.4$	0.67
Internal Rotation	59.5° ± 12.3°	56.9° ± 8.3°	$t_{38} = 0.8$	0.45
Total arc of motion	147.9° ± 13.3°	146.6° ± 14.2°	$t_{38} = 0.3$	0.76
Special Tests				
Provocation tests positive	1.4 ± 1.6	1.7 ± 1.6	$t_{38} = -0.6$	0.56
Scapular assistance test	45.0%	45.0%	$X^2_2 = 0.9$	0.64
Hawkins-Kennedy	40.0%	35.0%	$X^2_1 = 0.1$	0.74
Jobe	30.0%	50.0%	$X^2_1 = 1.7$	0.20
Neer	35.0%	45.0%	$X^2_1 = 0.4$	0.52
Resisted external rotation	35.0%	40.0%	$X^2_1 = 0.1$	0.74
Biceps load II	0.0%	5.0%	$X^2_1 = 1.0$*	1.00
Sulcus	10.0%	0.0%	$X^2_1 = 2.1$*	0.49

Notes: Data presented for the side tested only. Continuous data presented as mean ± SD and statistically assessed using an independent two-sample *t*-test. Categorical data presented as proportions and statistically assessed using Chi-square tests. Proportions may not sum to 100% as some participants may have had positive findings for multiple options within an assessment. Provocation tests positive represents the number of tests positive from the following: Hawkins-Kennedy, Jobe, Neer, and resisted external rotation. *Indicates Fisher's Exact Tests was used due to low expected counts. NC = not computed due to no data in the high group.

Correlations Between Proximity Variables and Morphology

In addition to kinematics, scapular and humeral morphology parameters have been hypothesized to impact an individual's risk for subacromial rotator cuff compression (Hughes et al., 2003; Kandemir et al., 2006; Neer, 1983). To determine whether morphology variables should be added to the mixed model as covariates, Pearson's correlations were calculated with subacromial proximity variables (i.e. normalized minimum distance and surface area) at each angle of humerothoracic elevation assessed statistically. Variables were retained as a covariate if the magnitude of the correlation was ≥ 0.5.

Normalized Minimum Distance

Below are scatter plots and correlation statistics for the relationship between morphology variables and the normalized minimum distance at the humerothoracic angles analyzed statistically (arm at side, 30°, 60°, and 90°).

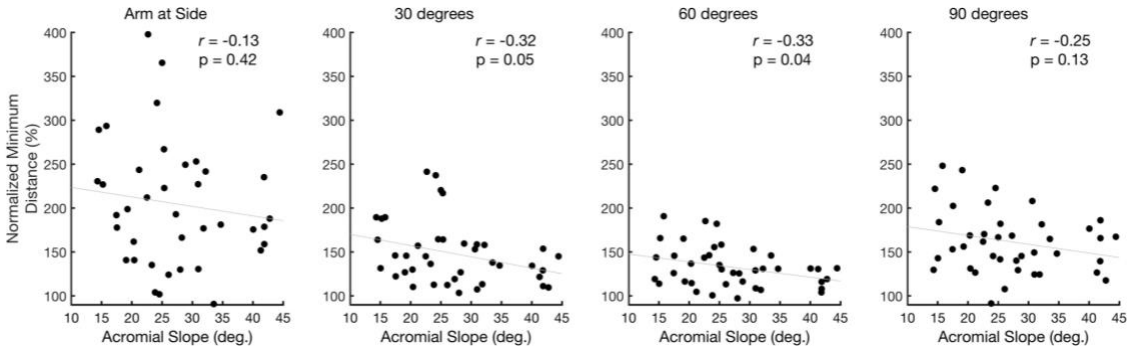

Figure 39: The relationship between acromial slope and normalized minimum distance at each angle of humerothoracic elevation analyzed statistically.

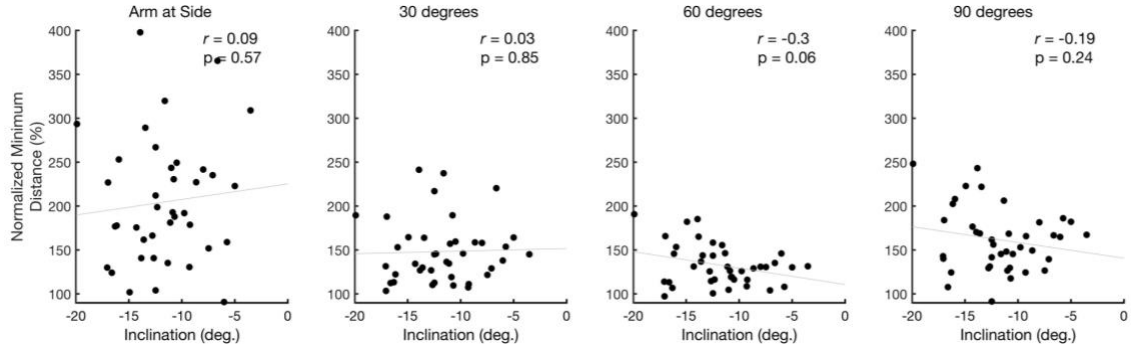

Figure 40: The relationship between glenoid inclination and normalized minimum distance at each angle of humerothoracic elevation analyzed statistically. Positive values indicate inclination, negative values indicate declination.

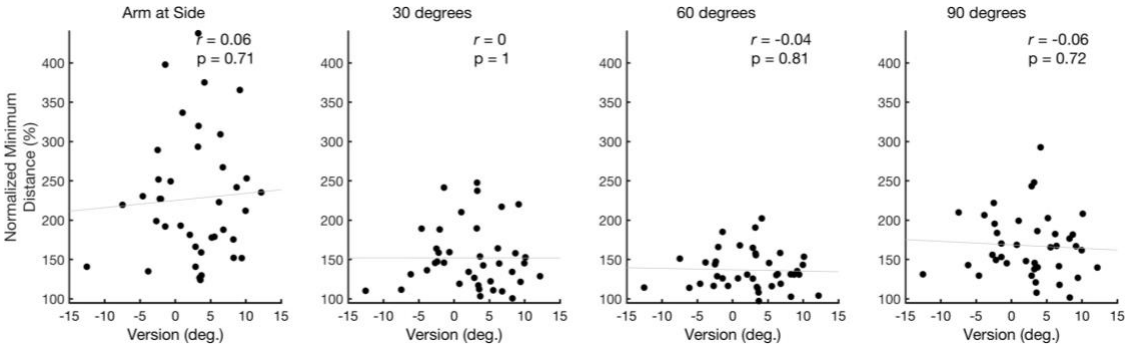

Figure 41: The relationship between glenoid version and normalized minimum distance at each angle of humerothoracic elevation analyzed statistically. Positive values indicate anteversion, negative values indicate retroversion.

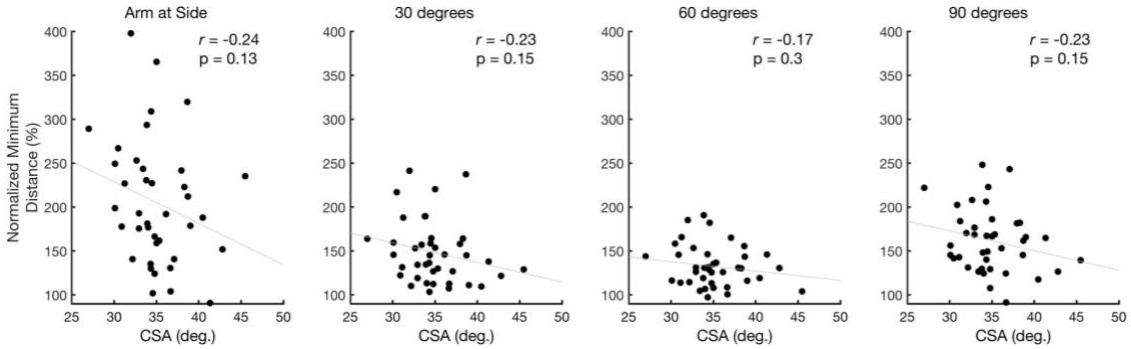

Figure 42: The relationship between critical shoulder angle and normalized minimum distance at each angle of humerothoracic elevation analyzed statistically.

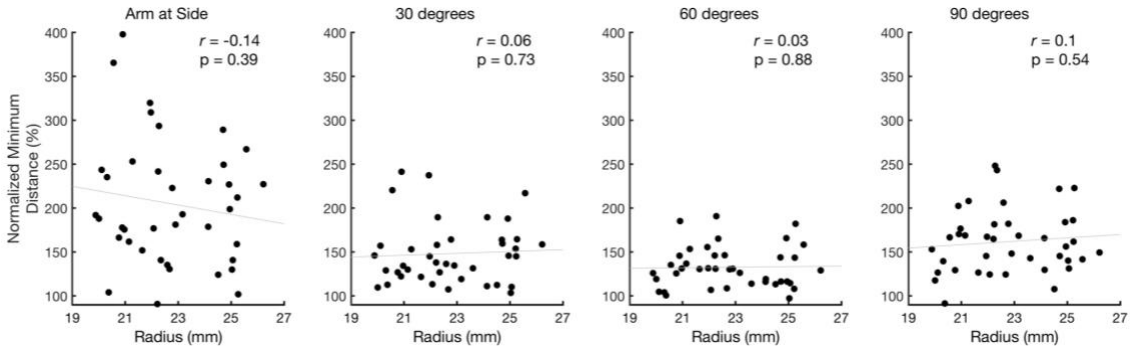

Figure 43: The relationship between humeral head radius and normalized minimum distance at each angle of humerothoracic elevation analyzed statistically.

Surface Area

Below are scatter plots and correlation statistics for the relationship between morphology variables and the surface area of the footprint within 100% of the tendon thickness at the humerothoracic angles analyzed statistically (30°, 60°, and 90°).

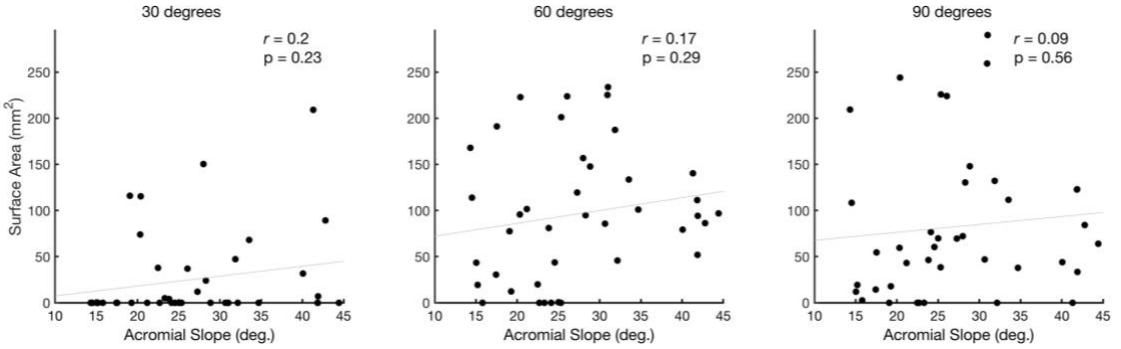

Figure 44: The relationship between acromial slope and the surface area within 100% of the rotator cuff tendon thickness at each angle of humerothoracic elevation analyzed statistically.

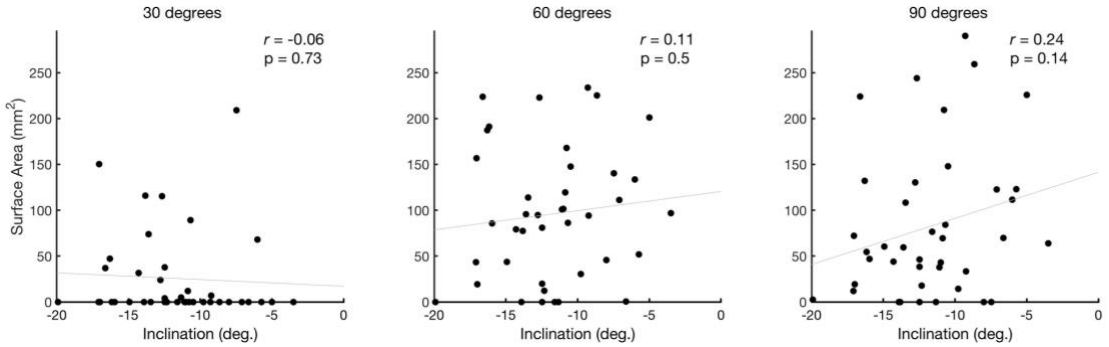

Figure 45: The relationship between glenoid inclination and the surface area within 100% of the rotator cuff tendon thickness at each angle of humerothoracic elevation analyzed statistically. Positive values indicate inclination, negative values indicate declination.

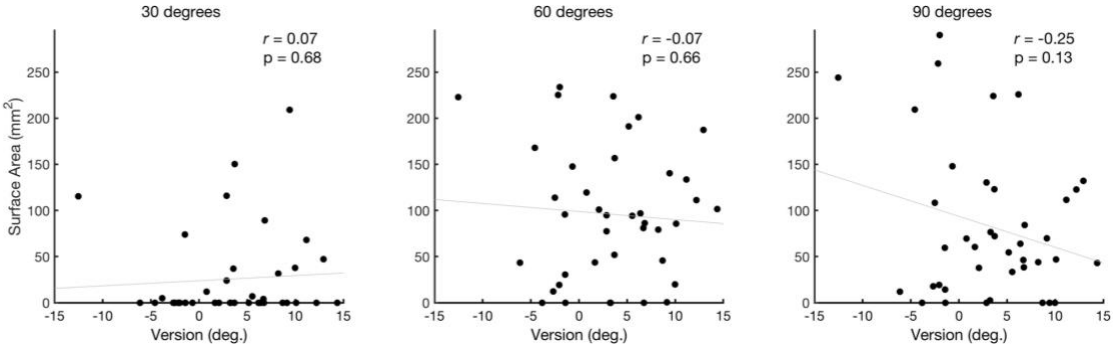

Figure 46: The relationship between glenoid version and the surface area within 100% of the rotator cuff tendon thickness at each angle of humerothoracic elevation analyzed statistically. Positive values indicate anteversion, negative values indicate retroversion.

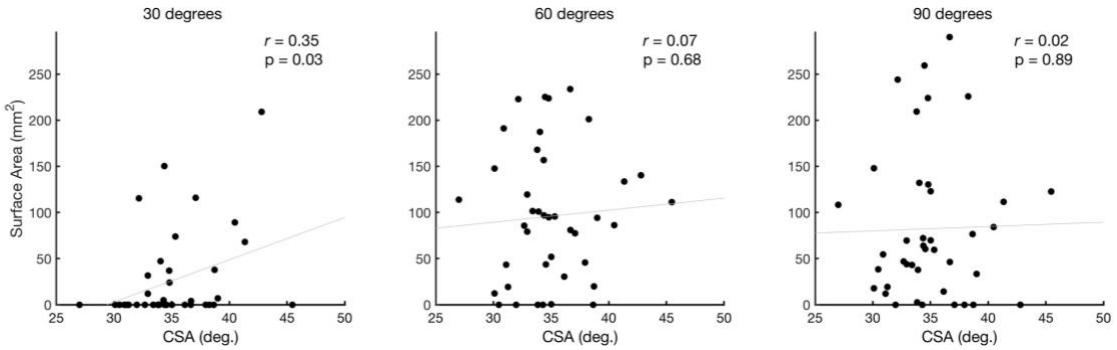

Figure 47: The relationship between critical shoulder angle and the surface area within 100% of the rotator cuff tendon thickness at each angle of humerothoracic elevation analyzed statistically.

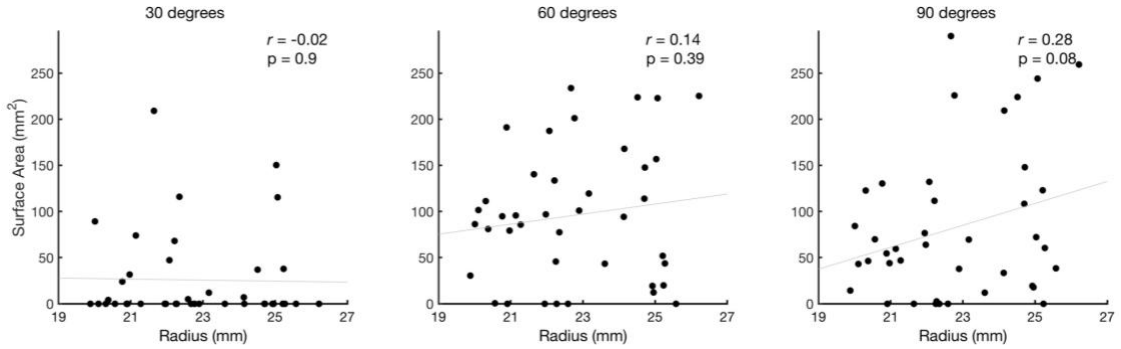

Figure 48: The relationship between the humeral head radius and surface area within 100% of the rotator cuff tendon thickness at each angle of humerothoracic elevation analyzed statistically.

Correlations Between Proximity Variables and Participant Demographics

Asymptomatic and symptomatic groups were matched based on age, gender, and dominance of the side tested as it is possible these factors could also influence subacromial proximities. However, once subjects were classified into the scapulothoracic upward rotation groups, it was not guaranteed demographic variables would remain matched between groups. Therefore, Pearson's (or Spearman's when appropriate) correlations were calculated between demographic and subacromial proximity variables (i.e. normalized minimum distance and surface area) at each angle of humerothoracic elevation assessed statistically. Variables were retained as a covariate if the magnitude of the correlation was ≥ 0.5.

Normalized Minimum Distance

Below are scatter plots and correlation statistics for the relationship between participant demographic variables and the normalized minimum distance at the humerothoracic angles analyzed statistically (arm at side, 30°, 60°, and 90°).

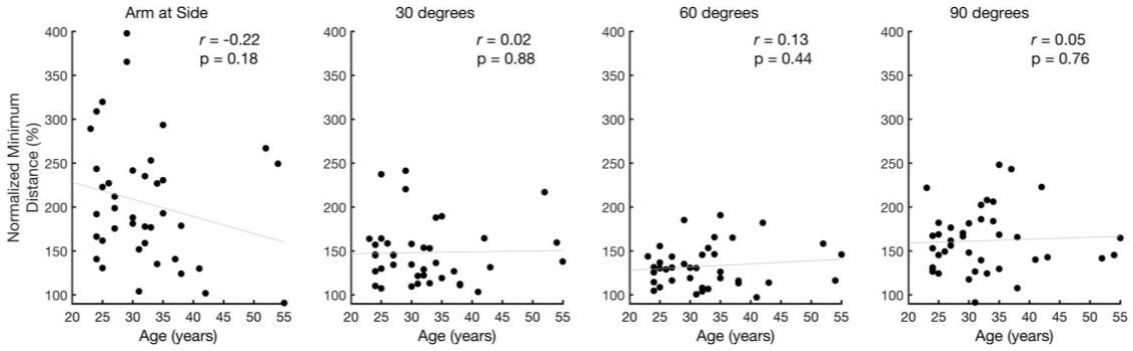

Figure 49: The relationship between age and normalized minimum distance at each angle of humerothoracic elevation analyzed statistically.

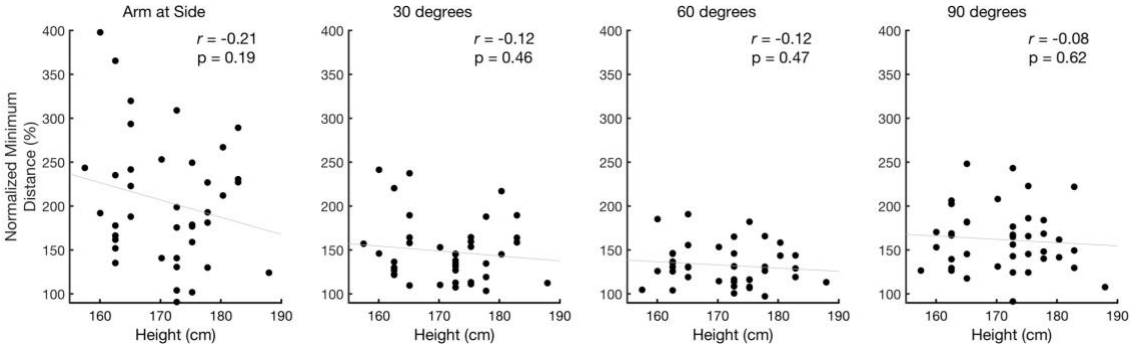

Figure 50: The relationship between height and normalized minimum distance at each angle of humerothoracic elevation analyzed statistically.

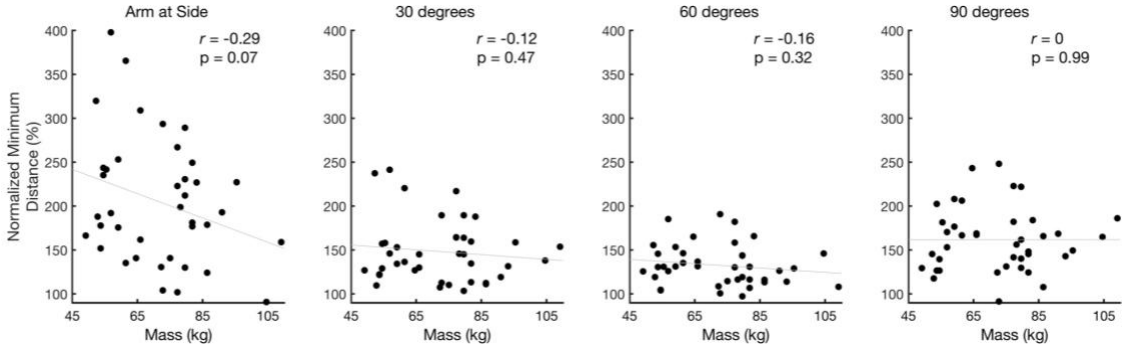

Figure 51: The relationship between mass and normalized minimum distance at each angle of humerothoracic elevation analyzed statistically.

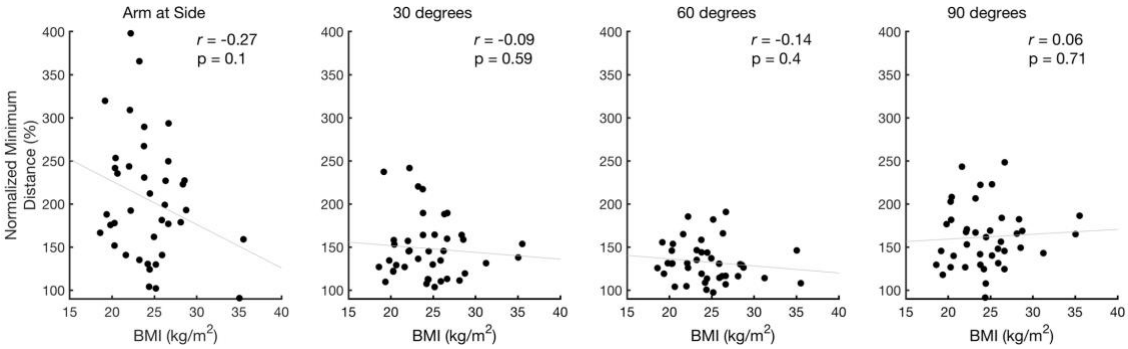

Figure 52: The relationship between BMI and normalized minimum distance at each angle of humerothoracic elevation analyzed statistically.

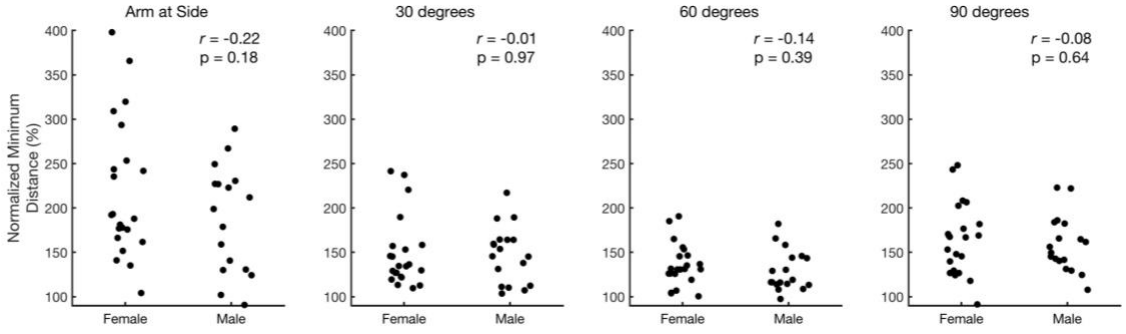

Figure 53: The relationship between gender and normalized minimum distance at each angle of humerothoracic elevation analyzed statistically.

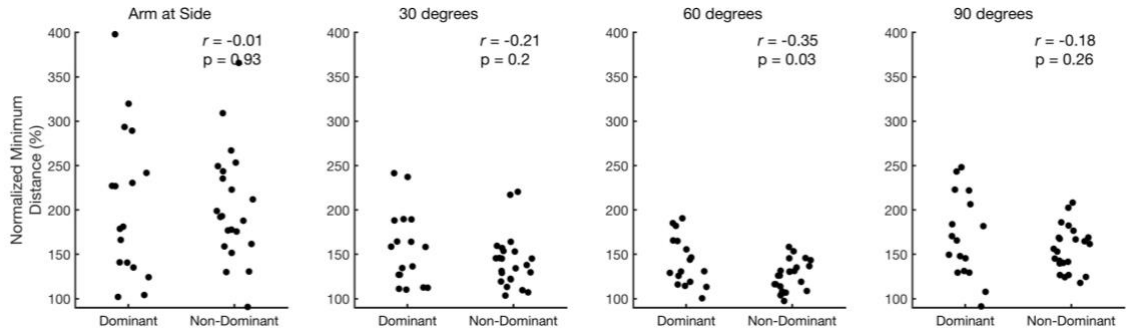

Figure 54: The relationship between the dominance of the side tested and normalized minimum distance at each angle of humerothoracic elevation analyzed statistically.

Surface Area

Below are scatter plots and correlation statistics for the relationship between participant demographics and the surface area of the footprint within 100% of the tendon thickness at the humerothoracic angles analyzed statistically (30°, 60°, and 90°).

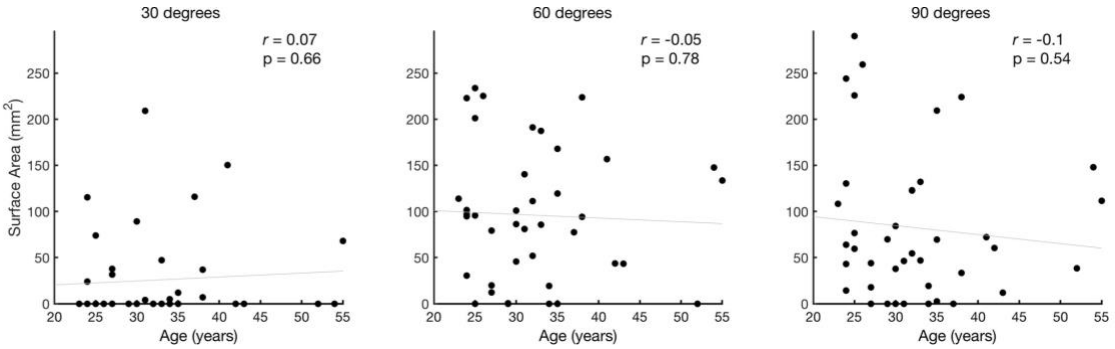

Figure 55: The relationship between age and the surface area within 100% of the rotator cuff tendon thickness at each angle of humerothoracic elevation analyzed statistically.

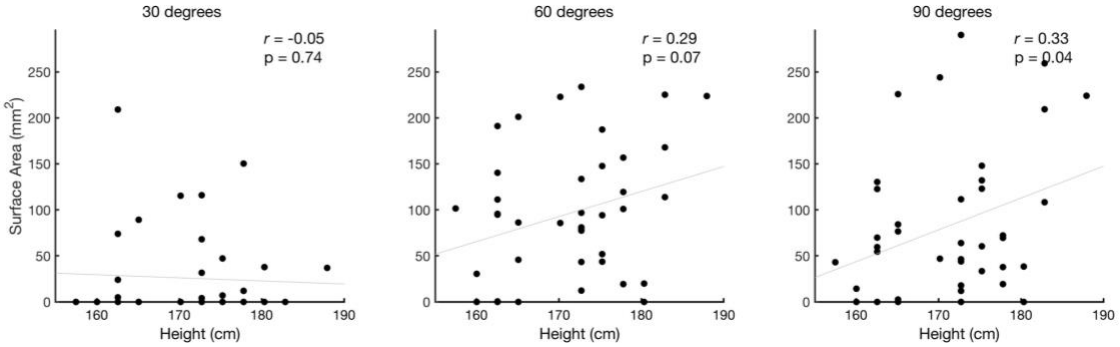

Figure 56: The relationship between height and the surface area within 100% of the rotator cuff tendon thickness at each angle of humerothoracic elevation analyzed statistically.

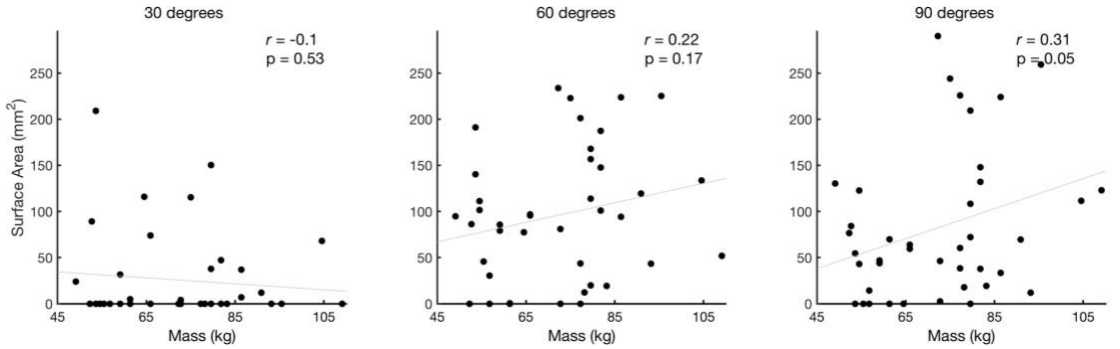

Figure 57: The relationship between mass and the surface area within 100% of the rotator cuff tendon thickness at each angle of humerothoracic elevation analyzed statistically.

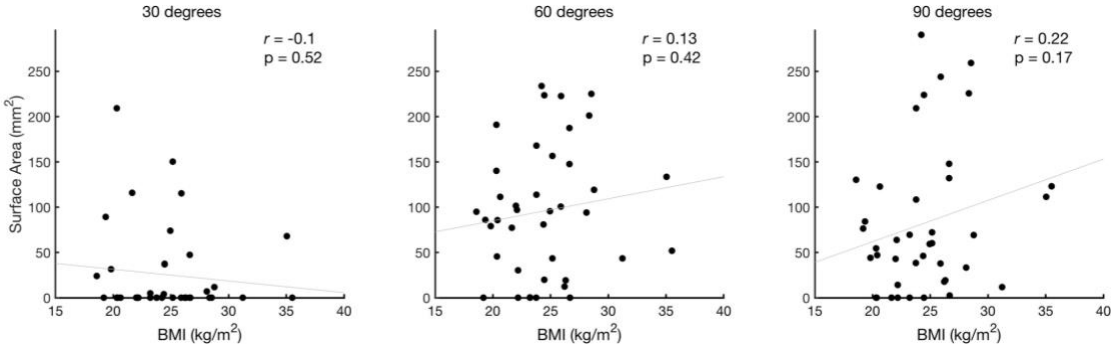

Figure 58: The relationship between BMI and the surface area within 100% of the rotator cuff tendon thickness at each angle of humerothoracic elevation analyzed statistically.

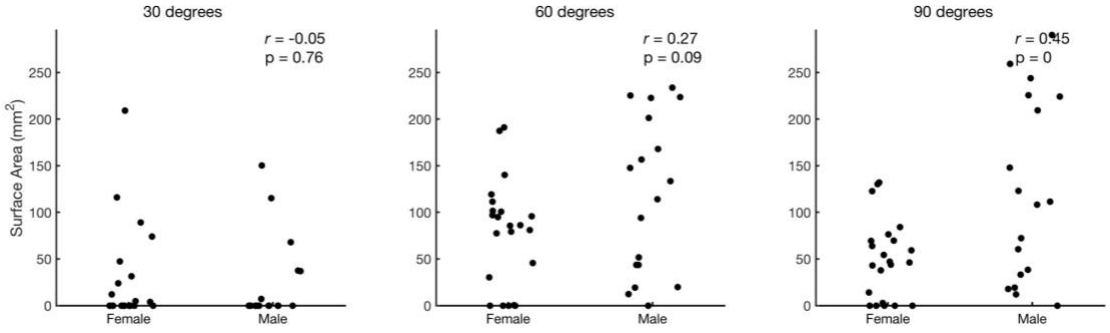

Figure 59: The relationship between gender and the surface area within 100% of the rotator cuff tendon thickness at each angle of humerothoracic elevation analyzed statistically.

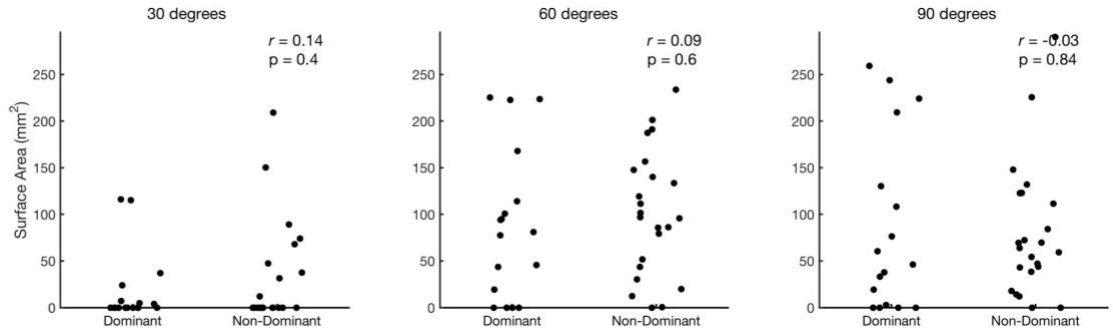

Figure 60: The relationship between the dominance of the side tested and the surface area within 100% of the rotator cuff tendon thickness at each angle of humerothoracic elevation analyzed statistically.

Pairwise Comparisons for Follow-up of Group-by-Angle Interaction for Normalized Minimum Distance

A two-factor mixed-model ANOVA was performed to assess for group differences in normalized minimum distance, which were log transformed to correct for skewness. The model was performed using a Toeplitz covariance structure with a between-subject factor of group (low and high scapulothoracic upward rotation), and a within-subject factor of humerothoracic elevation position (arm at side, 30º, 60º, 90º). The group-by-position interaction was significant at p = 0.049 (F = 2.71, df = 3,113).

Table 34 provides the pairwise comparisons to follow up the significant group-by-angle interaction for minimum distance.

Table 34: Pairwise Comparisons of Normalized Minimum Distance between Scapular Upward Rotation Groups

Position	High Group	Low Group	Mean Difference	Statistic	p-value
Arm at side	244.9	210.1	34.8	$t_{113} = 1.99$	0.049
30º	160.4	143.8	16.6	$t_{113} = 0.95$	0.34
60º	137.6	135.6	2.0	$t_{113} = 0.12$	0.91
90º	158.3	177.0	-18.7	$t_{113} = -1.08$	0.28

Analysis of Glenohumeral Superior/Inferior Positions Across Scapular Plane Abduction

Glenohumeral position data was calculated such that it represented the geometric center of the humeral head relative to the geometric center of the glenoid. However, this data was transformed such that the humeral head center could be represented relative to a circle fit to the inferior glenoid margin to allow comparison with data from Lawrence et al. (Lawrence et al., 2017). This study calculated subacromial proximities directly to the supraspinatus tendon by imposing average kinematics onto subject-specific anatomical models with the important assumption that the humeral head remained centered in the glenoid. **Figure 61** shows the distribution of the superior/inferior glenohumeral position in all participants in the current study at each humerothoracic elevation position (center of humeral head relative to center of inferior glenoid).

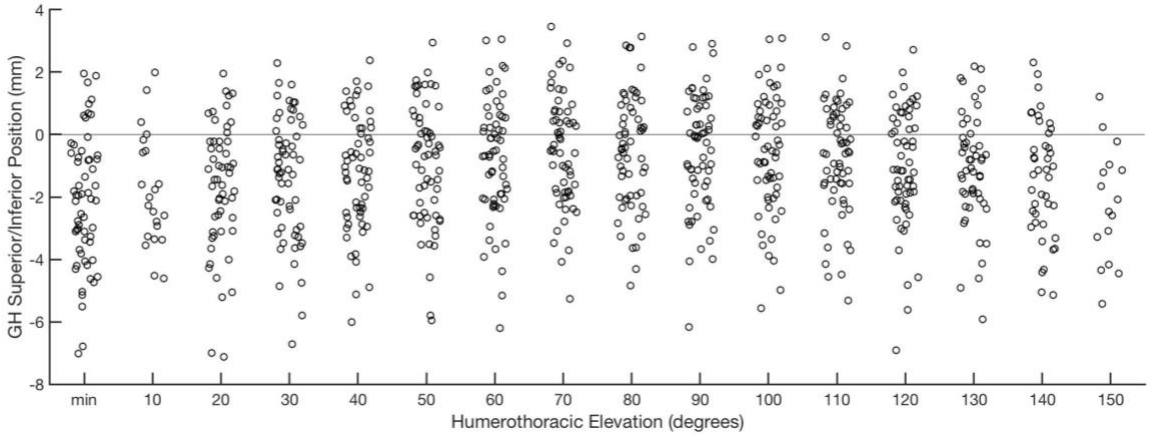

Figure 61: Glenohumeral superior/inferior positions across scapular plane abduction. Glenohumeral position defined as the center of the humeral head relative to the center of the inferior glenoid. The reference line at 0 mm indicates the center of the humeral head is aligned with the center of a circle fit to the inferior glenoid as in (Lawrence et al., 2017). Abbreviations: min = arm at the side.

It is possible the superior/inferior glenohumeral position confounded the analysis of subacromial proximities. Therefore, superior/inferior glenohumeral position was compared between scapulothoracic upward rotation groups using a two-factor mixed-model ANOVA. The covariance structure chosen to specify the relationship amongst the levels of the repeated factor (i.e. humerothoracic elevation angle) was chosen by inspecting covariance and correlation values and by comparing the fit statistics from models fit with different covariance structures (Littell et al., 2000). It appears a decay is generally present in the covariance and correlation matrix across adjacent levels of humerothoracic elevation (**Table 35**). This suggests a first order autoregressive or Toeplitz covariance structure may be most appropriate. However, the magnitude does not fully decay to zero for the levels furthest apart (i.e. arm at side and 90°) suggesting Toeplitz may be most appropriate. Inspection of the fit statistics (**Table 36**) confirms both

a first order autoregressive and Toeplitz appear to produce the best model fit, with autoregressive performing slightly better although not likely to substantially alter the conclusions compared to those obtained from Toeplitz. Ultimately, a first order autoregressive was chosen to model the covariance for the analysis of glenohumeral superior/inferior position.

Table 35: Covariance and Correlations for Glenohumeral Superior/Inferior Position

	Arm at side	**30º**	**60º**	**90º**
Arm at side	39.8 (1.0)	22.5 (0.74)	20.1 (0.64)	21.6 (0.70)
30º	--	24.1 (1.0)	21.5 (0.88)	20.5 (0.83)
60º	--	--	24.7 (1.00)	22.8 (0.92)
90º	--	--	--	24.9 (1.00)
Note: Data presented as pairwise variance/covariance (correlation).				

Table 36: Fit Statistics for Models with Different Covariance Structures for Glenohumeral Superior/Inferior Position

Covariance Structure	**AIC**	**AICC**	**BIC**
Variance Components	961.7	961.7	963.4
Compound Symmetry	844.1	844.2	847.4
Autoregressive (1st order)	829.6	829.6	832.9
Toeplitz	830.2	830.4	836.9
Note: Smaller fit statistics indicate better model fit.			

Groups were not found to be significantly different in glenohumeral superior/inferior position (interaction: p = 0.26, F = 1.36, df = 3,113; main effect: p = 0.61, F = 0.26, df = 1,38) (**Figure 62**).

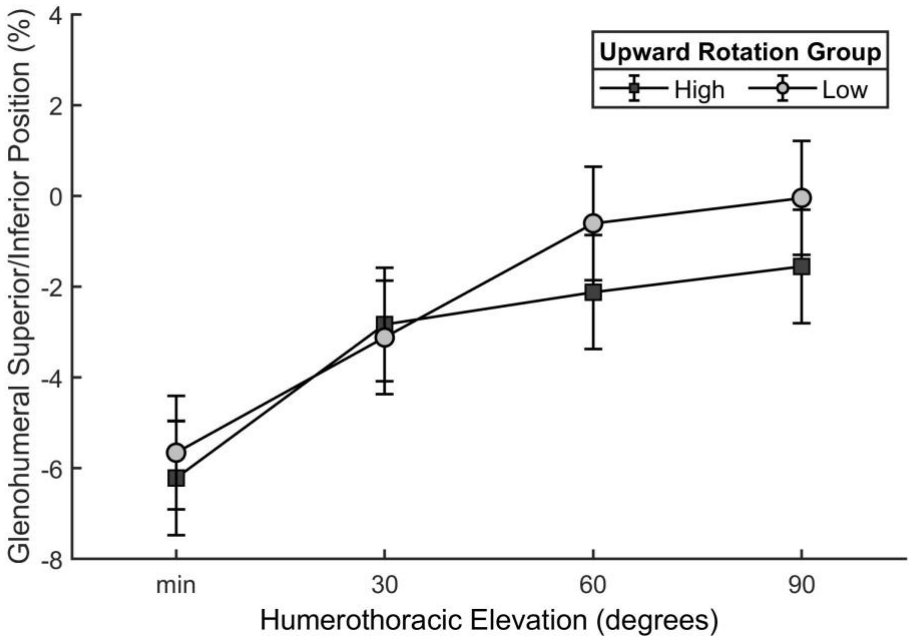

Figure 62: Group comparison of glenohumeral superior/inferior position. Position normalized to the glenoid height and expressed as a percentage.

Exploratory Analysis Investigating the Impact of Modeling the Coracoacromial Ligament as a Plane on Subacromial Proximity Calculations

The coracoacromial ligament was constructed as a plane fit between the coracoid process and anterior acromion based on anatomical descriptions (Edelson et al., 1995) because it could not be visualized and therefore reconstructed from the MR scan. Consequently, it is possible representing the coracoacromial ligament in this manner could have impacted the description of subacromial proximities. To investigate this, minimum distances were calculated between the articular margin and acromion only (i.e. removing the coracoacromial ligament plane from the analysis). A separate two-factor mixed-model ANOVA was performed with group as the between-subject factor (high and low scapulothoracic upward rotation) and humerothoracic elevation angle as the within-

subject factor (arm at side, 30°, 60°, 90°). The results indicate that, although the group mean differences have changed slightly, modeling the coracoacromial ligament did not impact the interpretation of the results particularly in the range of motion in which subacromial proximities are smallest (i.e. below 90°). Using either approach, it is concluded that there is no difference between groups at any angle of humerothoracic elevation (**Table 37** and **Figure 63**).

Table 37: Results of Two-Factor Mixed Model ANOVA for Normalized Minimum Distance to the Acromion

Effect	Statistic	p-value
Group main effect	$F_{1,38} = 0.43$	0.51
Position main effect	$F_{3,113} = 47.47$	<0.01
Group-by-position interaction	$F_{3,113} = 0.95$	0.42

Note: Model was fit using log transformed normalized minimum distance and a Toeplitz covariance structure. There are two levels for the group independent variable (high/low scapulothoracic upward rotation) and 4 levels for the humerothoracic elevation position independent variable (minimum, 30°, 60°, 90°).

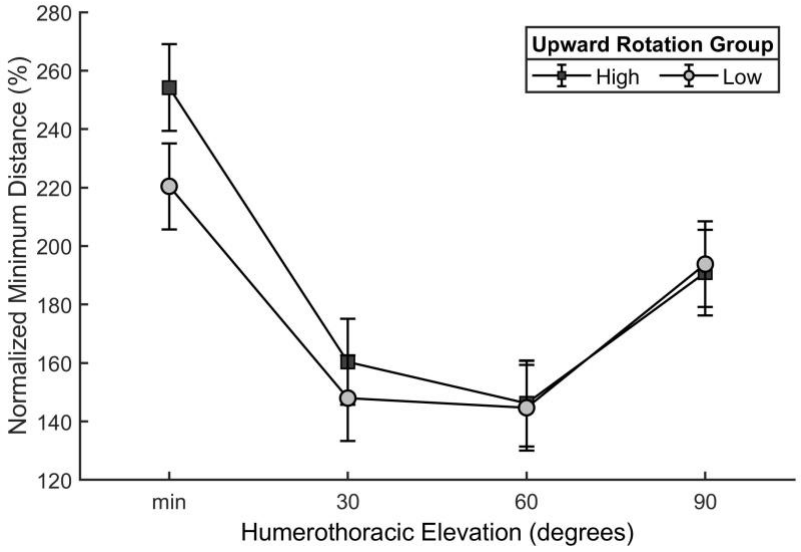

Figure 63: Group comparison of normalized minimum distance between the acromion and articular margin. Magnitudes of normalized minimum distance have been back-transformed and are reported as geometric means and 95% confidence intervals.

Shoulder Complex Kinematics by Scapulothoracic Upward Rotation Groups

Figure 64, **Figure 65**, and **Figure 66** provide descriptive statistics for shoulder complex kinematics by scapulothoracic upward rotation group.

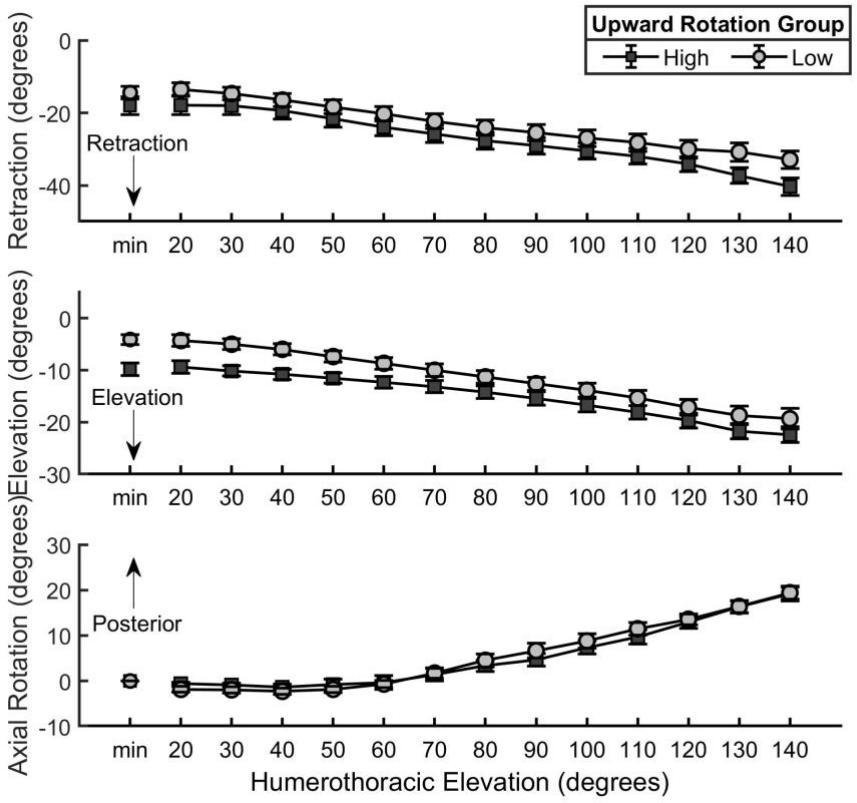

Figure 64: Sternoclavicular kinematic descriptive data for high and low scapulothoracic upward rotation groups. Data are reported descriptively as means and unpooled SEs for each angle/group.

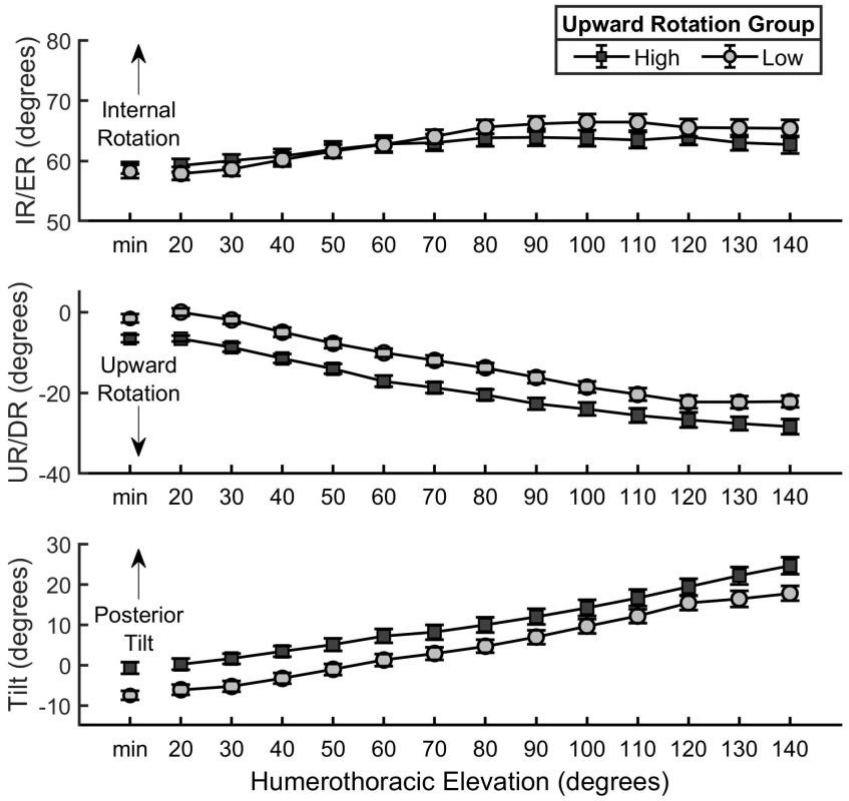

Figure 65: Acromioclavicular kinematic descriptive data for high and low scapulothoracic upward rotation groups. Data are reported descriptively as means and unpooled SEs for each angle/group. Abbreviations: IR/ER = internal/external rotation; UR/DR = upward/downward rotation.

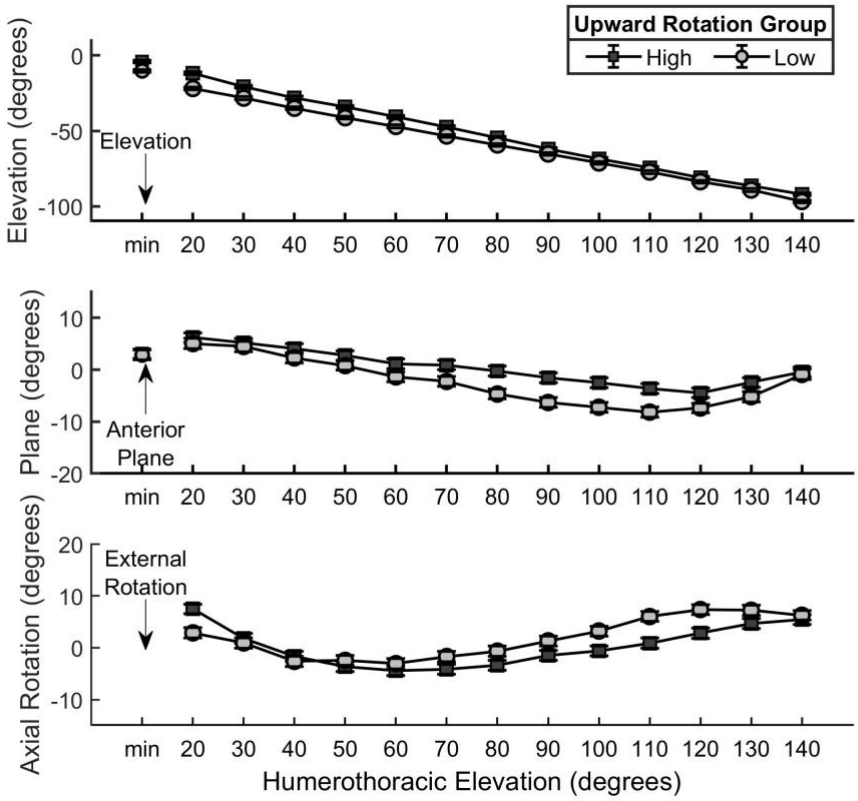

Figure 66: Glenohumeral kinematic descriptive data for high and low scapulothoracic upward rotation groups. Data are reported descriptively as means and unpooled SEs for each angle/group.

A Priori Analysis not Included in Chapter 4

Hypothesis 2.4: Of the component motions of scapulothoracic upward rotation, acromioclavicular upward rotation will be the strongest predictor of absolute minimum subacromial distance magnitude.

An initial multiple regression analysis was run for model diagnostics using data from the 49 subjects analyzed in Aim 2. Data were assessed using Cook's D, DFFITS, DFBETAS, and outlier and leverage statistics. Following model diagnostics, multiple regression analyses were performed with data from 45 subjects.

The results of the multiple regression analysis are presented in **Table 38**. The overall R^2 for the model was very low (0.03, adjusted R^2 = -0.04), which is consistent with the generally very low bivariate r^2 values. In considering the analysis *post hoc*, it was realized the hypothesis was not prudent primarily because the kinematic predictors contain significant variability and are likely confounded by the large variance in the humerothoracic elevation angle at which the absolute minimum distance occurred **Figure 19**. However, a similar analysis performed at a specified angle of humerothoracic elevation (30°) yielded a similarly low adjusted model R^2 (-0.02, p = 0.55). Together these analyses suggest a low relationship between normalized minimum distance and the component motions of scapulothoracic upward rotation. Upon exploring the data more, this conclusion is not surprising given the very low correlation between the magnitude of the absolute minimum distance and the magnitude of scapulothoracic upward rotation position for the position of absolute minimum distance (r = -0.02, p = 0.92). High variability is also visible in this relationship **Figure 67**, again likely reflecting the large variance in the humerothoracic elevation angle at which the absolute minimum distance occurred.

Table 38: Results of Multiple Regression Analyses for Predicting the Magnitude of Absolute Minimum Distance from Scapulothoracic Upward Rotation Component Motions

Effect	R^2	Regression Coefficient	p-value
Sternoclavicular posterior rotation	0.00	-0.14 (-0.04)	0.80
Sternoclavicular elevation	0.00	-0.07 (-0.02)	0.89
Acromioclavicular upward rotation	0.02	-0.42 (-0.16)	0.31
Intercept	N/A	119.7 (0)	<0.01
Overall Model	-0.04	N/A	0.70

Notes: Outcome: magnitude of absolute minimum distance; Predictors: sternoclavicular posterior rotation, sternoclavicular upward rotation, and acromioclavicular upward rotation at position of absolute minimum distance. Regression coefficients for the predictors presented as non-standardized (standardized). R^2 for overall model expressed as adjusted R^2. R^2 for individual predictors expressed as squared semi-partial correlations. N/A indicates the statistic is not appropriate for the specific effect.

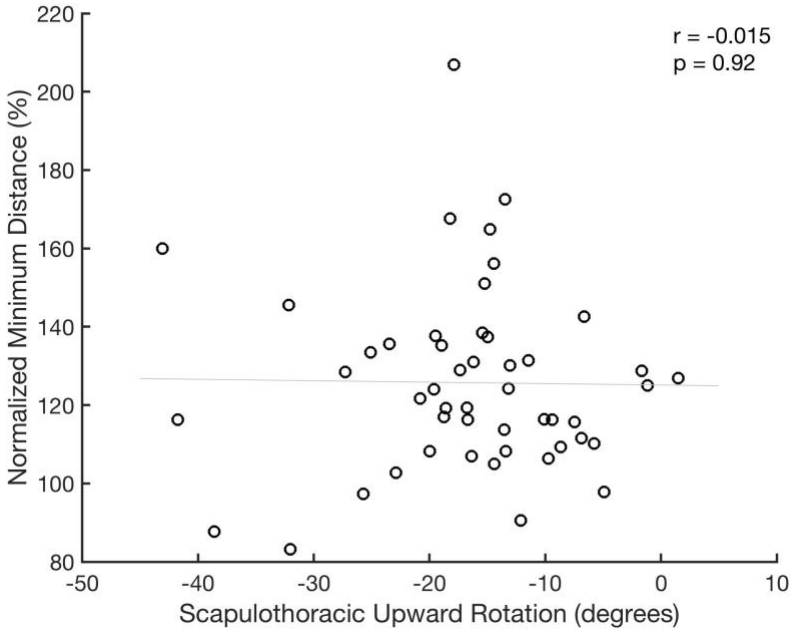

Figure 67: Relationship between normalized minimum distance and scapulothoracic upward rotation at the absolute minimum distance.

Collectively these findings and those reported in Chapter 4 suggest the magnitude of the absolute minimum distance may not be influenced by kinematic factors. Instead, it may be primarily influenced by anatomical factors, whereas the range of motion in which the absolute minimum distance occurs may be primarily influenced by kinematics factors. To explore this possibility, bivariate correlations were calculated between the magnitude of the absolute minimum distance and the morphology parameters described in **Appendix C**. The results of this analysis are provided in **Table 39**. The findings support the hypothesis stated above, suggesting the magnitude of the absolute minimum distance may be more related to morphology than kinematics. In particular, critical shoulder angle, glenoid inclination, and acromial slope had the strongest relationship with the magnitude of the absolute minimum distance. For both critical shoulder angle and glenoid inclination, the results suggest an increasing positive magnitude (i.e. inclination and increased critical shoulder angle) are mildly although significantly associated with a smaller absolute minimum distance (critical shoulder angle: r = -0.33, p = 0.02; glenoid inclination: r = -0.31, p = 0.03). The modest correlation between critical shoulder angle and absolute minimum distance is consistent with a growing body of evidence suggesting the metric may be an important factor in the pathogenesis of rotator cuff disease (Moor et al., 2013; Moor et al., 2014; Spiegl et al., 2016).

Table 39: Relationship between Morphology Parameters and the Magnitude of the Absolute Minimum Distance

Morphology Parameter	***r***	***r*²**	**p-value**
Acromial slope	-0.28	0.08	0.06
Glenoid inclination	-0.31	0.10	0.03
Glenoid version	-0.14	0.02	0.32
Critical shoulder angle	-0.33	0.11	0.02
Humeral head radius	0.05	0.00	0.71

Notes: Increasing acromial slope indicates sloped acromion (i.e. 0º indicates flat), positive inclination indicates inclination, and positive version indicates anteversion.

The negative correlation for acromial slope (r = -0.28) suggests a larger angle is mildly although significantly associated with a smaller absolute minimum distance. This supports the theory that a sloped acromion may increase an individual's risk for rotator cuff compression and injury (Balke et al., 2013; Bigliani et al., 1991; Epstein et al., 1993; Neer, 1972). However, findings related to this theory are often mixed (Bigliani et al., 1991; Epstein et al., 1993; Farley et al., 1994; Pandey et al., 2016).

It is important to note, however, that the way acromial slope was quantified in the current study is different than what has been traditionally described. Bigliani originally defined acromial slope based on lateral radiographs as the angle between two lines; the first between the anterior-most point and the midpoint along the undersurface of the acromion, and the second between the posterior-most point and the midpoint along the undersurface of the acromion (Bigliani et al., 1991). This metric provides an estimate of the curvature within the lateral acromion, and in particular the presence of any spurs along the anterior-inferior surface. Conversely, acromial slope in the current study was defined using a plane fit to the entire undersurface of the acromion. Therefore, the degree

to which the acromion is hooked may not be reflected in the magnitude of acromial slope because the impact of the points that define the lateral acromion may be reduced by the mass of points describing the more medial aspects. Further, the plane's normal vector was related to an extrinsic vector (i.e. the scapular coordinate system) as opposed to an intrinsic aspect of the acromion itself as in Bigliani (1991). Therefore, it is possible these metrics are describing different underlying morphological constructs that may require additional studies to fully explore. In general, the relationship between morphology, kinematics, and the mechanisms of rotator cuff injury is an important future area of research to explore what is likely a very complex interaction of variables.

Appendix D: Additional Descriptions and Analyses for Aim 3

Determination of Covariance Structure for Mixed Models

For the analysis of component motion proportional contributions, the covariance structure to specify the relationship amongst the levels of the repeated factor (i.e. humerothoracic elevation phase) was chosen by inspecting covariance and correlation values and by comparing the fit statistics from models fit with different covariance structures (Littell et al., 2000). This process was performed for each mixed-model analysis of the component motion proportional contributions as described below.

Sternoclavicular Posterior Rotation

Inspecting the covariance and correlation magnitudes indicates a lack of overall structure with very low correlations (**Table 40**). This suggests a variance components structure may be most appropriate (Littell et al., 2000) for modeling sternoclavicular posterior rotation proportional contributions, which is confirmed based on fit statistics (**Table 41**).

Table 40: Covariance and Correlations for Sternoclavicular Posterior Rotation Proportional Contribution

	30° to 60°	**60° to 90°**	**90° to 120°**
30° to 60°	1145.3 (1.0)	201.5 (0.23)	-53.2 (-0.09)
60° to 90°	--	700.4 (1.0)	-31.0 (-0.07)
90° to 120°	--	--	280.6 (1.00)

Note: Data presented as pairwise variance/covariance (correlation).

Table 41: Fit Statistics for Models with Different Covariance Structures for Sternoclavicular Posterior Rotation Proportional Contribution

Covariance Structure	AIC	AICC	BIC
Variance Components	1649.8	1649.8	1651.9
Compound Symmetry	1651.2	1651.3	1655.4
Autoregressive (1st order)	1649.8	1649.9	1654.0
Toeplitz	1651.2	1651.3	1657.5

Note: Smaller fit statistics indicate better model fit.

Sternoclavicular Elevation

Inspecting the covariance and correlation magnitudes suggests a decay is present across adjacent levels of humerothoracic elevation (**Table 42**); therefore, either an autoregressive or Toeplitz structure may be appropriate (Littell et al., 2000). Inspection of the fit statistics (**Table 43**) confirms a first order autoregressive structure is most appropriate and was chosen to model the covariance for the analysis of sternoclavicular posterior rotation proportional contribution.

Table 42: Covariance and Correlations for Sternoclavicular Elevation Proportional Contribution

	30° to 60°	60° to 90°	90° to 120°
30° to 60°	53.1 (1.0)	18.9 (0.50)	8.2 (0.17)
60° to 90°	--	26.9 (1.0)	18.9 (0.56)
90° to 120°	--	--	42.6 (1.00)

Note: Data presented as pairwise variance/covariance (correlation).

Table 43: Fit Statistics for Models with Different Covariance Structures for Sternoclavicular Elevation Proportional Contribution

Covariance Structure	AIC	AICC	BIC
Variance Components	1151.4	1151.4	1153.5
Compound Symmetry	1133.5	1133.6	1137.7
Autoregressive (1st order)	1122.1	1122.1	1126.2
Toeplitz	1123.3	1123.4	1129.6

Note: Smaller fit statistics indicate better model fit.

Acromioclavicular Upward Rotation

Inspecting the covariance and correlation magnitudes indicates a lack of overall structure with very low correlations (**Table 44**). This suggests a variance components structure may be most appropriate (Littell et al., 2000) for modeling acromioclavicular upward rotation proportional contributions, which is confirmed based on fit statistics (**Table 45**).

Table 44: Covariance and Correlations for Acromioclavicular Upward Rotation Proportional Contribution

	30° to 60°	60° to 90°	90° to 120°
30° to 60°	1995.0 (1.0)	288.0 (0.19)	-79.0 (-0.08)
60° to 90°	--	1139.4 (1.0)	-65.1 (-0.08)
90° to 120°	--	--	510.1 (1.00)

Note: Data presented as pairwise variance/covariance (correlation).

Table 45: Fit Statistics for Models with Different Covariance Structures for Acromioclavicular Upward Rotation Proportional Contribution

Covariance Structure	AIC	AICC	BIC
Variance Components	1741.6	1741.6	1743.7
Compound Symmetry	1743.5	1743.6	1747.7
Autoregressive (1st order)	1742.7	1742.8	1746.9
Toeplitz	1744.1	1744.2	1750.3

Note: Smaller fit statistics indicate better model fit.

Details of the Group Comparisons for Proportional Contributions of Component Motions to Scapulothoracic Upward Rotation

There was no significant group difference (i.e. main effect) for any component motion proportional contribution (**Table 46** and **Figure 68**).

Table 46: Results of Two-Factor Mixed Model ANOVAs for Component Motion Proportional Contributions

	Statistic	p-value
Sternoclavicular Posterior Rotation		
Group main effect	$F_{1,58} = 0.68$	0.41
Phase main effect	$F_{2,115} = 25.95$	<0.01
Group-by-phase interaction	$F_{2,115} = 0.98$	0.38
Sternoclavicular Elevation		
Group main effect	$F_{1,58} = 3.27$	0.08
Phase main effect	$F_{2,115} = 3.97$	0.02
Group-by-phase interaction	$F_{2,115} = 0.45$	0.64
Acromioclavicular Upward Rotation		
Group main effect	$F_{1,58} = 3.03$	0.09
Phase main effect	$F_{2,115} = 33.30$	<0.01
Group-by-phase interaction	$F_{2,115} = 0.50$	0.61

Notes: There are two levels for the group independent variable (asymptomatic/symptomatic) and three levels for the humerothoracic elevation phase independent variable (30° to 60°, 60° to 90°, and 90° to 120°).

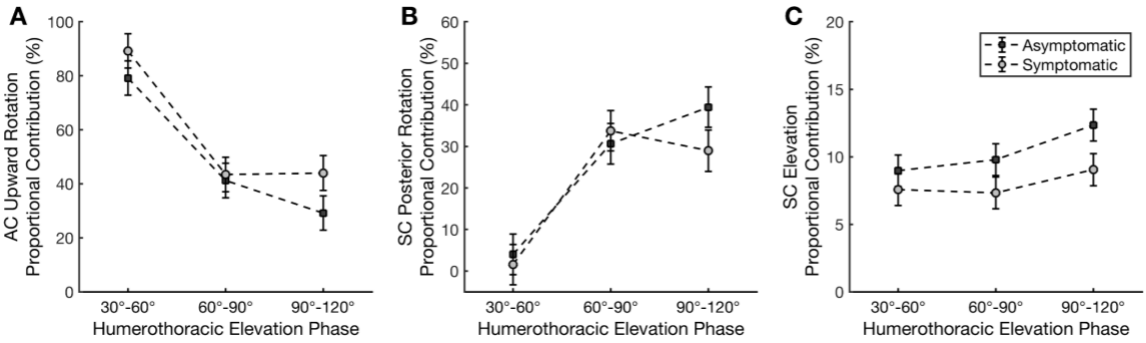

Figure 68: The proportional contribution of scapulothoracic upward rotation component motions in symptomatic and asymptomatic individuals across phases of humerothoracic elevation (30°-60°, 60°-90°, 90°-120°). **A)** acromioclavicular upward rotation; **B)** sternoclavicular posterior rotation; and **C)** sternoclavicular elevation. Note the different y-axis scales across the subplots. Abbreviations: AC = acromioclavicular, SC = sternoclavicular.

A Priori Analyses Not Included in Chapter 5

Two analyses planned *a priori* were not included in Chapter 5. The details of the analysis and results are described below.

Hypothesis 3.1: Compared to the high scapulothoracic upward rotation group, the low scapulothoracic upward rotation group will be in decreased acromioclavicular upward rotation, sternoclavicular posterior rotation, and sternoclavicular elevation at the same angles of humerothoracic elevation at which the groups differ in scapulothoracic upward rotation.

Scapulothoracic upward rotation, acromioclavicular upward rotation, sternoclavicular elevation and posterior rotation, and scapulothoracic upward rotation positions were calculated at every 10° increment of humerothoracic elevation. Two-factor mixed-model ANOVAs were performed with between-subject factor of scapulothoracic upward rotation group (high, low) and within-subject factor of humerothoracic elevation angle (minimum, 30°, 60°, 90°). Humerothoracic elevation angles were reduced to three levels (30°, 60°, 90°) for the comparison of sternoclavicular posterior rotation as there is no between-subject variance for the minimum position due to the need to align the clavicular vertical axis to that of the thorax (Wu et al., 2005). The appropriate covariance structure was determined by inspecting the covariance matrix of the within-subject factor and fit statistics of models using various covariance structures (Littell et al., 2000). The significance of the two-factor interaction was assessed first. The significance of the main effects was only assessed in the absence of a significant interaction.

At all angles assesses statistically, participants in the low scapulothoracic upward rotation group were in less scapulothoracic upward rotation than participants in the high scapulothoracic upward rotation group, however, the magnitude of the difference depended on the angle of humerothoracic elevation (interaction: $p = 0.04$, $F = 2.79$, $df = 3,113$) (**Figure 15B**). Specifically, the low scapulothoracic upward rotation group were in 7.9°, 10.0°, 8.9°, and 6.0° less scapulothoracic upward rotation at the minimum, 30°, 60°, and 90° humerothoracic elevation positions, respectively (minimum: $p < 0.01$, $t = -5.07$, $df = 113$; 30°: $p < 0.01$, $t = -6.44$, $df = 113$; 60°: $p < 0.01$, $t = -5.69$, $df = 113$; and 90°: $p < 0.01$, $t = -3.83$, $df = 113$).

Participants in the low scapulothoracic upward rotation group were consistently in an average of 4.4° less sternoclavicular elevation than participants in the high scapulothoracic upward rotation group (main effect of group: $p = 0.01$, $F = 7.82$, $df = 1,38$) (**Figure 69A**). Additionally, participants in the low scapulothoracic upward rotation group were consistently in an average of 6.4° less acromioclavicular upward rotation across all angles of humerothoracic elevation than participants in the high scapulothoracic upward rotation group (main effect of group: $p < 0.01$, $F = 21.18$, $df = 1,38$) (**Figure 69B**). Groups were not significant different in the magnitude of sternoclavicular posterior rotation at any angle of humerothoracic elevation (interaction: $p = 0.36$, $F = 1.03$, $df = 2,76$; main effect: $p = 0.86$, $F = 0.03$, $df = 1,38$) (**Figure 69C**).

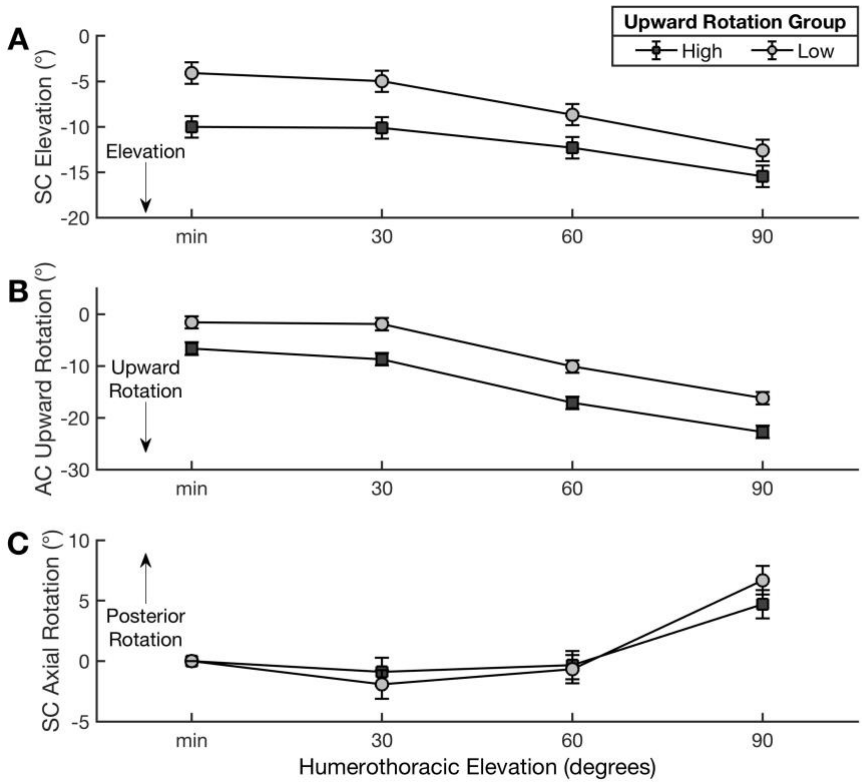

Figure 69: Comparison of scapulothoracic upward rotation component motions between high and low scapulothoracic upward rotation groups across angles of humerothoracic elevation: **A)** sternoclavicular elevation; **B)** acromioclavicular upward rotation; and **C)** sternoclavicular posterior rotation. Abbreviations: AC = acromioclavicular, SC = sternoclavicular.

Hypothesis 3.2: Acromioclavicular upward rotation and sternoclavicular posterior rotation angular displacement will be the strongest predictors of scapulothoracic upward rotation angular displacement.

Acromioclavicular, sternoclavicular, and scapulothoracic joint positions were calculated at every 30° increment of humerothoracic elevation for all 60 subjects. Transformation matrices were calculated as the displacement of the distal segment moving relative to the proximal segment between 30° increments of humerothoracic elevation and described in the reference frame of the distal segment at the initial position. The position and orientation of a helical axis was determined using a finite calculation (Spoor et al., 1980). Helical angles were then calculated by projecting the helical axis onto the reference frame of the distal segment at the initial position. Multiple regression analyses were used to determine the relationship between scapulothoracic upward rotation displacement (response) and acromioclavicular upward rotation, sternoclavicular posterior rotation, and sternoclavicular elevation angular displacement (predictors) at each humerothoracic elevation phase (30°-60°, 60°-90°, 90°-120°).

Initial multiple regression analyses were run for model diagnostics using data from all 60 subjects. Data were assessed using Cook's D, DFFITS, DFBETAS, and outlier and leverage statistics. Following model diagnostics, multiple regression analyses were performed with data from 57 subjects. Separate analyses were performed for each humerothoracic elevation phase (30°-60°, 60°-90°, 90°-120°). Squared bivariate and semi-partial (i.e. part) correlations were also calculated to assess the unadjusted and

adjusted relationship with each predictor and scapulothoracic upward rotation displacement, respectively.

The results of the bivariate correlation and multiple regression analyses are presented in (**Table 47**). The results suggest all component motions are significantly associated with scapulothoracic upward rotation displacement across all phases of humerothoracic elevation. In particular, sternoclavicular elevation is the component motion with the strongest relationship with scapulothoracic upward rotation displacement (r^2 = 0.27-0.53). Likewise, sternoclavicular posterior rotation and acromioclavicular upward rotation have weaker relationships with scapulothoracic upward rotation displacement (r^2 = 0.08-0.28 and r^2 = 0.09-0.11, respectively), despite the statistical significance. These findings are in conflict with the predominant belief (and supporting evidence from Chapter 5) that sternoclavicular elevation is the least important component motion and highlight a limitation of correlations (especially bivariate) when investigating complex causative hypotheses.

Table 47: Results of Multiple Regression Analyses for Predicting Scapulothoracic Upward Rotation Displacement from Component Motion Displacements

	Humerothoracic Elevation Phase		
	30° to 60°	**60° to 90°**	**90° to 120°**
Sternoclavicular posterior rotation			
Coefficients	-0.84 (-1.08)	-0.87 (-1.35)	-0.95 (-0.99)
Squared semi-partial correlation	0.39 (<0.01)	0.59 (<0.01)	0.58 (<0.01)
Squared bivariate correlation	0.10 (0.02)	0.08 (0.03)	0.28 (<0.01)
Type I Sums of Squares	50.4	37.9	159.6
Type III Sums of Squares	193.2	271.6	338.0
Sternoclavicular elevation			
Coefficients	0.51 (0.35)	0.40 (0.29)	0.29 (0.24)
Squared semi-partial correlation	0.09 (<0.01)	0.08 (<0.01)	0.05 (<0.01)
Squared bivariate correlation	0.53 (<0.01)	0.27 (<0.01)	0.30 (<0.01)
Type I Sums of Squares	260.8	125.3	176.8
Type III Sums of Squares	46.4	34.7	27.6
Acromioclavicular upward rotation			
Coefficients	0.99 (1.10)	1.02 (1.37)	0.99 (0.85)
Squared semi-partial correlation	0.41 (<0.01)	0.62 (<0.01)	0.41 (<0.01)
Squared bivariate correlation	0.11 (0.01)	0.09 (0.03)	0.11 (0.01)
Type I Sums of Squares	55.6	40.0	62.4
Type III Sums of Squares	201.0	286.5	238.7
Intercept			
Coefficient	-0.19	-0.65	-0.83
Overall model			
Significance	< 0.01	< 0.01	< 0.01
R^2	0.97	0.93	0.93

Notes: Outcome: scapulothoracic upward rotation displacement; Predictors: sternoclavicular posterior rotation, sternoclavicular upward rotation, and acromioclavicular upward rotation displacement. Regression coefficients for the predictors presented as non-standardized (standardized). Squared part and bivariate correlations presented as statistic (p-value). R^2 for overall model expressed as adjusted R^2.

When considered together in multiple regression models for each humerothoracic elevation phase, the linear combination of component motions (i.e. sternoclavicular posterior rotation, acromioclavicular upward rotation, and sternoclavicular elevation) account for 93-97% of the variance in scapulothoracic upward rotation displacement. Compared to the bivariate relationships, a shift is observed in the relative importance of the individual predictors (**Table 47**). In particular, sternoclavicular posterior rotation and

acromioclavicular upward rotation emerge as the strongest predictors of scapulothoracic upward rotation across all humerothoracic elevation phases. This suggests the presence of suppression in the multiple regression model. Additional evidence suggesting suppression effects in the model includes the Type III Sums of Squares for sternoclavicular posterior rotation and acromioclavicular upward rotation being higher than their respective Type I Sums of Squares. This suggests an individual predictor (i.e. sternoclavicular posterior rotation or acromioclavicular upward rotation) accounts for more variance above and beyond that of the combined effect of the other predictors (Type III Sums of Squares) than it does alone (Type I Sums of Squares). Finally, increment multiple regression model building in which pairs of predictors are included further suggests suppression only occurs when sternoclavicular posterior rotation and acromioclavicular upward rotation are included in the same model.

Suppression in multiple regression is a paradoxical phenomenon in which the influence of an individual predictor is inflated due to the presence of another predictor in the model. This typically occurs when a predictor has a weak relationship with the outcome but a strong relationship with another predictor (Cohen & Cohen, 2003). For the case of the component motions predicting scapulothoracic upward rotation displacement, the suppressor effect is due to the presence of both sternoclavicular posterior rotation and acromioclavicular upward rotation in the model. When included in a multiple regression model together, sternoclavicular posterior rotation and acromioclavicular upward rotation suppress the irrelevant variance in each other making them both appear more important to the prediction of scapulothoracic upward rotation (or have a stronger relationship) than

they would have alone. This results in an increase in the variable's regression coefficient, squared semi-partial correlation, and the overall model fit (i.e. R^2).

The practical implications of suppression are not well understood and may depend on whether a regression model is used for prediction or explanation of multivariate relationships. In the case of explanation which was the goal of the proposed analysis, inference should be made with caution unless the cause of the suppression is known. For the current study, it is believed the cause of the suppression between sternoclavicular posterior rotation and acromioclavicular upward rotation is related to shape-matching error. Errors in quantifying acromioclavicular upward rotation should be related to sternoclavicular posterior rotation as they both depend on the accuracy of shape-matching the clavicle, and in particular its axial rotation. Of the acromioclavicular joint angular displacements, upward rotation was the most prone to shape-matching errors (RMS error = 3.5°) (**Table 20**), which was likely due to the error in shape-matching clavicle axial rotation (RMS error = 3.7°). Therefore, it is possible shape-matching errors added irrelevant variance to the measurement of sternoclavicular posterior rotation and acromioclavicular upward rotation displacement that reduce the bivariate correlations with scapulothoracic upward rotation. Further, the bivariate correlation between sternoclavicular posterior rotation and acromioclavicular upward rotation remains relatively unaffected because the error is shared and therefore can continue to explain variance in each other. Once all three variables are included in the same multiple regression model, this shared variance is suppressed, thereby increasing the regression

coefficients and squared semi-partial correlations of sternoclavicular posterior rotation and acromioclavicular upward rotation.

Ultimately, this analysis was deferred from being included in Chapter 5 as it cannot directly investigate the purpose of Aim 3, which was to identify the mechanisms by which sternoclavicular and acromioclavicular joint motion contributes to scapulothoracic upward rotation. The coupling theory suggests component motions *cause* or, in the case of sternoclavicular posterior rotation, *allow* scapulothoracic upward rotation to occur. Regression analysis can provide estimates of relationships, which are necessary but not sufficient to infer causation. However, the prediction equations developed from the multiple regression provide a means to estimate scapulothoracic upward rotation displacement directly from the data as opposed to a predefined coupling function as was done in Chapter 5. Importantly, the weights applied to each of the component motions in the coupling function only account for the offset between the clavicular and scapular axes in the transverse plane, whereas the weights calculated from the regression equation are not limited in this manner. Therefore, direct comparison between analyses (i.e. coupling function and multiple regression models) will be confounded.

Appendix E: Data Collection Documents

Online Screening Tool Distributed using REDCap

This form was available as an internet link to individuals interested in participating in the study. It primarily asked question to determine initial eligibility.

Potential Research Participant Questionnaire

Thank you for your interest in participating as a research subject in our shoulder study. Please answer the following questions to help us determine your elgibility for current or future shoulder studies. The answers to these questions will be kept confidential.

There will be no compensation provided for completion of this survey. However, eligible subjects will be compensated at the conclusion of the study.

Thank you!

Demographic Information

First Name	_____
Last Name	_____
Date of Birth	_____ (Example 03-16-1954)
Age	_____
Gender	◯ Male ◯ Female
Height (in inches)	_____
Weight (in lbs)	_____
Are you left handed or right handed?	◯ Left ◯ Right

Contact Information

Email Address	_____
Phone number	_____
How do you prefer to be contacted?	◯ Email ◯ Phone ◯ No preference

Occupational and Recreational Activities

What is your occupation?	_____
Does your job involve regular lifting of more than a few pounds?	◯ Yes ◯ No
Please estimate the average amount you are required to lift in pounds:	_____

www.projectredcap.org REDCap

How frequently?

- ◯ less than 5 times per hour
- ◯ greater than 5 times per hour

Do you participate in any recreational activities?

- ◯ Yes
- ◯ No

Please describe the activities and their frequency:
(For example: Soccer, 3 times each week for 1 hour)

_____

Shoulder Health

Have you ever had shoulder symptoms that have lasted longer than one week?

- ◯ Yes
- ◯ No

Are you currently experiencing shoulder symptoms on a regular basis?

- ◯ Yes
- ◯ No

Are you willing to serve as a healthy, comparison subject for our study?

- ◯ Yes
- ◯ No

How long have you been experiencing these symptoms?

- ◯ Less than 4 weeks
- ◯ 1-6 months
- ◯ 6 months to a year
- ◯ 1-2 years
- ◯ More than 2 years

Duration of Symptoms (in weeks)

_____

Do you believe your current shoulder symptoms started with a particular event/activity?

- ◯ Yes
- ◯ No

Please briefly describe the event/activity that you believe is/was associated with your shoulder symptoms

_____

What motions or activities aggravate your symptoms?

_____

Once your symptoms become aggravated by an activity or movement, how long does it take to return to its usual intensity?

- ◯ Immediately
- ◯ Within 5 minutes
- ◯ Within an hour
- ◯ Within several hours
- ◯ More than a day

What motions or activities reduce or relieve your symptoms?

_____

In which shoulder do you have symptoms?

- ◯ Right
- ◯ Left
- ◯ Both

Which shoulder is worse?

- ◯ Right
- ◯ Left
- ◯ Equal

Where are you shoulder symptoms located?

- ☐ Front of shoulder joint
- ☐ Back of shoulder joint
- ☐ Deep in shoulder joint
- ☐ Side of shoulder joint
- ☐ Shoulder blade
- ☐ other

(Select all that apply)

Please describe your symptoms:

- ☐ Loss of motion
- ☐ Instability
- ☐ Weakness
- ☐ Stiffness
- ☐ Pain
- ☐ Numbness or tingling
- ☐ Other

(Select all that apply)

Please describe your symptoms as best you can

_____

What type of pain?

- ☐ Aching
- ☐ Burning
- ☐ Stabbing
- ☐ Sharp
- ☐ Dull
- ☐ other

Are you able to raise your arm above shoulder height?

- ◯ Yes
- ◯ No

What is the highest level of your pain in the last week?

0 50 100

(Place a mark on the scale above)

What is the lowest level of your pain in the last week?

0 50 100

(Place a mark on the scale above)

Are your symptoms constant or intermittent?

- ◯ Constant
- ◯ Intermittent

Do you have any difficulty sleeping because of your shoulder symptoms?

- ◯ Yes
- ◯ No

Do you ever experience popping, clicking, catching, or clunking in your shoulder?

- ◯ Yes
- ◯ No

Is the popping, clicking, catching, or clunking painful?

- ◯ Yes
- ◯ No

Have you ever had a shoulder dislocation or separation?

- ◯ Yes
- ◯ No

Are you currently receiving any treatments or therapies for your shoulder(s)?

- ◯ Yes
- ◯ No

What treatments are you receiving or performing?

_____

Have you received a diagnosis related to your shoulder(s)?

- ◯ Yes
- ◯ No

What was the diagnosis related to your shoulder symptoms?

- ☐ Rotator cuff tear
- ☐ Impingement
- ☐ Adhesive capsulitis
- ☐ Arthritis
- ☐ Shoulder instability or dislocation/subluxation
- ☐ Cervical disk herniation
- ☐ Other

(click all that apply)

Please give the diagnosis

_____

Are you currently experiencing neck (cervical) symptoms?

- ◯ Yes
- ◯ No

Where are your neck symptoms located?

- ☐ Back of the head
- ☐ Side of the neck
- ☐ Upper shoulder
- ☐ Between shoulder blades
- ☐ Down the arm
- ☐ Around the chest
- ☐ other

Do you feel your neck and shoulder symptoms are related?

- ◯ Yes
- ◯ No

How are your shoulder and neck symptoms related?

- ☐ Symptoms start in the neck and eventually shoulder pain starts or gets worse
- ☐ Symptoms start in the shoulder and eventually neck pain starts or gets worse
- ☐ Symptoms usually occur at the same time
- ☐ None of these answers fit my symptoms

Please describe how you feel your neck and shoulder symptoms are related

_____

Are you taking any oral medications or topical substances for your symptoms?

- ◯ Yes
- ◯ No

Please list the medications/supplements/substances you are utilizing for your symptoms.

_____

Have you ever had shoulder surgery?

- ◯ Yes
- ◯ No

Please provide a brief description of the surgery performed

_____

Do you currently have or have you ever had a shoulder fracture?

- ☐ Upper arm (humerus)
- ☐ Collarbone (clavicle)
- ☐ Shoulder blade (scapula)
- ☐ Other shoulder fracture
- ☐ I have not had a shoulder fracture

Have you ever had any x-rays, CT scans, MRIs, or any other medical imaging performed on your shoulder?

- ◯ Yes
- ◯ No

Do you have any other problems with your shoulder, elbow wrist or hand that has not been addressed with the previous questions?

- ◯ Yes
- ◯ No

Please describe these problems

_____

General Health

Have you ever been diagnosed with rheumatoid arthritis?	◯ Yes ◯ No
Have you ever been diagnosed with scoliosis?	◯ Yes ◯ No
Do you smoke?	◯ Yes ◯ No
How many cigarettes per day?	_____
Have you had any episodes of skin sensitivity or irritations?	◯ Yes ◯ No
Have you ever experienced a skin reaction to tape or adhesives (e.g. Band-Aids)?	◯ Yes ◯ No
Have you ever fainted?	◯ Yes ◯ No

Screening Questions for Magnetic Resonance Imaging (MRI)

Have you ever experienced claustrophobia?	◯ Yes ◯ No
Are you sensitive to loud noises?	◯ Yes ◯ No
Do you have any of the following?	☐ Cardiac pacemaker ☐ Aortic clip ☐ Internal pacing wires ☐ Swan-Ganz catheter ☐ Aneurysm clips ☐ Heart valve prosthesis ☐ Neurostimulator or DBS device ☐ Metal rods in bones ☐ Harrington rods (spine) ☐ Metal or wire mesh implants ☐ Bone growth/fusion stimulator ☐ Insulin pump or infusion device ☐ Carotid artery vascular clamp ☐ Implanted cardiac defibrillator ☐ Cochlear, otologic, or ear implant ☐ Intravascular stents, filters or coils ☐ Vascular access port and/or catheter ☐ Shunt (spinal or intraventricular) ☐ Any type of prosthesis (eye, penile, etc.) ☐ Electrodes (on body, head, or brain) ☐ Artificial limb or joint replacement ☐ Bone/joint pin, screw, nail, wire, plate ☐ Wire sutures, staples, or suture anchors ☐ Any implant held in place by a magnet ☐ Any metal fragments in your body ☐ I don't have any of these.

Screening Questions for Fluoroscopy

Are you currently pregnant or is there a possibility that you could be pregnant?	◯ Yes ◯ No
Have you had a recent CT scan or radiation therapy?	◯ Yes ◯ No

Thank you for your willingness to fill out the questionnaire and participate in this study. Research personnel will contact you once your questionnaire is reviewed. If you are found to meet the study's eligibility criteria, you will be invited to participate in the study. If you agree, the study will require 2-3 visits totaling approximately 3 hours. Participants that complete the study will receive a $50 gift card.

Please indicate below which days of the week and which times (morning or afternoon) you are most available to participate in this study.

	Monday	Tuesday	Wednesday	Thursday	Friday
Morning	☐	☐	☐	☐	☐
Afternoon	☐	☐	☐	☐	☐

Clinical Examination Form

This form guided the clinical examination process to determine official study eligibility.

Clinical examination

Postural Assessment

Scoliosis screen	◯ Positive ◯ Negative
Posture	☐ WNL ☐ Forward head ☐ Rounded shoulders

Cervical Screen

Was cervical screen performed?	◯ Yes ◯ No

Cervical ROM

	WNL	Restricted	Neck symptoms	Shoulder symptoms
Extension	☐	☐	☐	☐
Flexion	☐	☐	☐	☐
R rotation	☐	☐	☐	☐
L rotation	☐	☐	☐	☐
R SB	☐	☐	☐	☐
L SB	☐	☐	☐	☐

Cervical OP

	Negative	Neck symptoms	Shoulder symptoms	Not tested
Extension	☐	☐	☐	☐
Flexion	☐	☐	☐	☐
R rotation	☐	☐	☐	☐
L rotation	☐	☐	☐	☐
R SB	☐	☐	☐	☐
L SB	☐	☐	☐	☐

www.projectredcap.org REDCap

Cervical Special Tests

	Positive	Negative	Not tested
Spurlings	○	○	○
Compression	○	○	○
Distraction	○	○	○
ULTT	○	○	○

Dyskinesia Screen - Unloaded Flexion

	WNL	Subtle	Obvious
R - Shrug	○	○	○
R - Dumping	○	○	○
R - Medial border winging	○	○	○
R - Inferior border winging	○	○	○
L - Shrug	○	○	○
L - Dumping	○	○	○
L - Medial border winging	○	○	○
L - Inferior border winging	○	○	○

Pain during unloaded flexion?
○ Yes
○ No

Dyskinesia Screen - Unloaded Abduction

	WNL	Subtle	Obvious
R - Shrug	○	○	○
R - Dumping	○	○	○
R - Medial border winging	○	○	○
R - Inferior border winging	○	○	○
L - Shrug	○	○	○
L - Dumping	○	○	○
L - Medial border winging	○	○	○
L - Inferior border winging	○	○	○

Pain during unloaded abduction?
○ Yes
○ No

Dyskinesia Screen - Loaded Flexion

	WNL	Subtle	Obvious
R - Shrug	○	○	○
R - Dumping	○	○	○
R - Medial Border Winging	○	○	○
R - Inferior Border Winging	○	○	○
L - Shrug	○	○	○
L - Dumping	○	○	○
L - Medial Border Winging	○	○	○
L - Inferior Border Winging	○	○	○

Pain during loaded flexion? ○ Yes ○ No

Weight used for Flexion Loaded _____

Dyskinesia Screen - Loaded Abduction

	WNL	Subtle	Obvious
R - Shrug	○	○	○
R - Dumping	○	○	○
R - Medial border winging	○	○	○
R - Inferior border winging	○	○	○
L - Shrug	○	○	○
L - Dumping	○	○	○
L - Medial border winging	○	○	○
L - Inferior border winging	○	○	○

Pain during loaded abduction? ○ Yes ○ No

Weight used for Abduction Loaded _____

Scapular Position at Rest (inclinometer)

R Trial 1 _____

R Trial 2 _____

Mean R _____

L Trial 1 _____

L Trial 2 _____

Mean L _____

Scapular Position at 30 degree HT Elevation (inclinometer)

R Trial 1 _____

R Trial 2 _____

R Mean _____

L Trial 1 _____

L Trial 2 _____

L Mean _____

Shoulder AROM

R SAB _____

R SAB Pain Provocation? ○ Yes ○ No

L SAB _____

L SAB Pain Provocation? ○ Yes ○ No

Shoulder PROM

R ER _____ (At 90 degrees ABD)

R IR _____

L ER _____ (At 90 degrees ABD)

L IR _____

R SAB _____ (If limited AROM)

L SAB _____ (If limited AROM)

Resistance Testing

	3-/5	3/5	3+/5	4-/5	4/5	4+/5	5/5	Painful?
R - SAB	○	○	○	○	○	○	○	○
R - ER	○	○	○	○	○	○	○	○
R - IR	○	○	○	○	○	○	○	○
R - LT	○	○	○	○	○	○	○	○
R - SA	○	○	○	○	○	○	○	○
L - SAB	○	○	○	○	○	○	○	○
L - ER	○	○	○	○	○	○	○	○
L - IR	○	○	○	○	○	○	○	○
L - LT	○	○	○	○	○	○	○	○
L - SA	○	○	○	○	○	○	○	○

Shoulder Special Tests

	Positive	Negative	Not tested
R - Scapular Assistant Test	○	○	○
R - Hawkin's-Kennedy	○	○	○
R - Neer	○	○	○
R - Jobe	○	○	○
R - Resisted ER	○	○	○
R - ERLS	○	○	○
R - Biceps Load II	○	○	○
R - Apprehension	○	○	○
R - Sulcus	○	○	○
L - Scapular Assistant Test	○	○	○
L - Hawkin's-Kennedy	○	○	○
L - Neer	○	○	○
L - Jobe	○	○	○
L - Resisted ER	○	○	○
L - ERLS	○	○	○
L - Apprehension	○	○	○
L - Sulcus	○	○	○
L - Biceps Load II	○	○	○

Scapular Assistant Test: motions facilitated on R

- ☐ Upward rotation
- ☐ Posterior tilt
- ☐ External rotation

Scapular Assistant Test: motions facilitated on L

- ☐ Upward rotation
- ☐ Posterior tilt
- ☐ External rotation

Disabilities of the Arm Shoulder and Hand (DASH) Questionnaire

This questionnaire was used to objectively measure upper extremity function.

DISABILITIES OF THE ARM, SHOULDER AND HAND

THE **DASH**

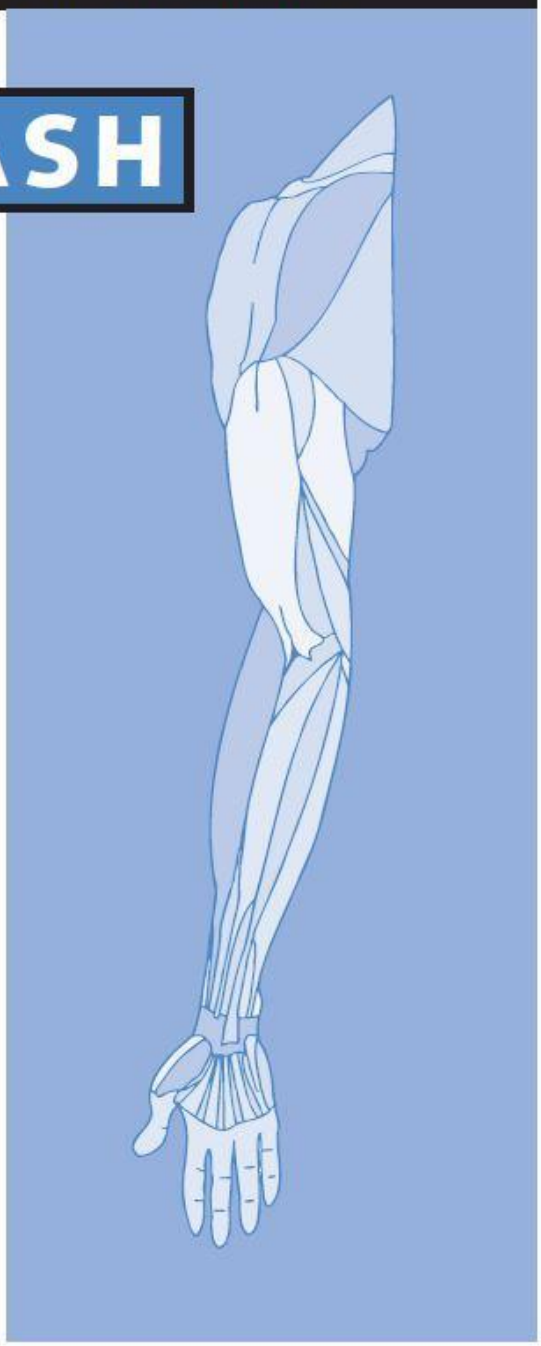

INSTRUCTIONS

This questionnaire asks about your symptoms as well as your ability to perform certain activities.

Please answer *every question*, based on your condition in the last week, by circling the appropriate number.

If you did not have the opportunity to perform an activity in the past week, please make your *best estimate* on which response would be the most accurate.

It doesn't matter which hand or arm you use to perform the activity; please answer based on your ability regardless of how you perform the task.

Disabilities of the Arm, Shoulder and Hand

Please rate your ability to do the following activities in the last week by circling the number below the appropriate response.

	NO DIFFICULTY	MILD DIFFICULTY	MODERATE DIFFICULTY	SEVERE DIFFICULTY	UNABLE
1. Open a tight or new jar.	1	2	3	4	5
2. Write.	1	2	3	4	5
3. Turn a key.	1	2	3	4	5
4. Prepare a meal.	1	2	3	4	5
5. Push open a heavy door.	1	2	3	4	5
6. Place an object on a shelf above your head.	1	2	3	4	5
7. Do heavy household chores (e.g., wash walls, wash floors).	1	2	3	4	5
8. Garden or do yard work.	1	2	3	4	5
9. Make a bed.	1	2	3	4	5
10. Carry a shopping bag or briefcase.	1	2	3	4	5
11. Carry a heavy object (over 10 lbs).	1	2	3	4	5
12. Change a lightbulb overhead.	1	2	3	4	5
13. Wash or blow dry your hair.	1	2	3	4	5
14. Wash your back.	1	2	3	4	5
15. Put on a pullover sweater.	1	2	3	4	5
16. Use a knife to cut food.	1	2	3	4	5
17. Recreational activities which require little effort (e.g., cardplaying, knitting, etc.).	1	2	3	4	5
18. Recreational activities in which you take some force or impact through your arm, shoulder or hand (e.g., golf, hammering, tennis, etc.).	1	2	3	4	5
19. Recreational activities in which you move your arm freely (e.g., playing frisbee, badminton, etc.).	1	2	3	4	5
20. Manage transportation needs (getting from one place to another).	1	2	3	4	5
21. Sexual activities.	1	2	3	4	5

DISABILITIES OF THE ARM, SHOULDER AND HAND

	NOT AT ALL	SLIGHTLY	MODERATELY	QUITE A BIT	EXTREMELY
22. During the past week, *to what extent* has your arm, shoulder or hand problem interfered with your normal social activities with family, friends, neighbours or groups? *(circle number)*	1	2	3	4	5

	NOT LIMITED AT ALL	SLIGHTLY LIMITED	MODERATELY LIMITED	VERY LIMITED	UNABLE
23. During the past week, were you limited in your work or other regular daily activities as a result of your arm, shoulder or hand problem? *(circle number)*	1	2	3	4	5

Please rate the severity of the following symptoms in the last week. *(circle number)*

	NONE	MILD	MODERATE	SEVERE	EXTREME
24. Arm, shoulder or hand pain.	1	2	3	4	5
25. Arm, shoulder or hand pain when you performed any specific activity.	1	2	3	4	5
26. Tingling (pins and needles) in your arm, shoulder or hand.	1	2	3	4	5
27. Weakness in your arm, shoulder or hand.	1	2	3	4	5
28. Stiffness in your arm, shoulder or hand.	1	2	3	4	5

	NO DIFFICULTY	MILD DIFFICULTY	MODERATE DIFFICULTY	SEVERE DIFFICULTY	SO MUCH DIFFICULTY THAT I CAN'T SLEEP
29. During the past week, how much difficulty have you had sleeping because of the pain in your arm, shoulder or hand? *(circle number)*	1	2	3	4	5

	STRONGLY DISAGREE	DISAGREE	NEITHER AGREE NOR DISAGREE	AGREE	STRONGLY AGREE
30. I feel less capable, less confident or less useful because of my arm, shoulder or hand problem. *(circle number)*	1	2	3	4	5

DASH DISABILITY/SYMPTOM SCORE = $\left[\left(\frac{\text{sum of n responses}}{n}\right) - 1\right] \times 25$, where n is equal to the number of completed responses.

A DASH score may <u>not</u> be calculated if there are greater than 3 missing items.

\

DISABILITIES OF THE ARM, SHOULDER AND HAND

WORK MODULE (OPTIONAL)

The following questions ask about the impact of your arm, shoulder or hand problem on your ability to work (including home-making if that is your main work role).

Please indicate what your job/work is: _____

❒ I do not work. (You may skip this section.)

Please circle the number that best describes your physical ability in the past week. Did you have any difficulty:

	NO DIFFICULTY	MILD DIFFICULTY	MODERATE DIFFICULTY	SEVERE DIFFICULTY	UNABLE
1. using your usual technique for your work?	1	2	3	4	5
2. doing your usual work because of arm, shoulder or hand pain?	1	2	3	4	5
3. doing your work as well as you would like?	1	2	3	4	5
4. spending your usual amount of time doing your work?	1	2	3	4	5

SPORTS/PERFORMING ARTS MODULE (OPTIONAL)

The following questions relate to the impact of your arm, shoulder or hand problem on playing *your musical instrument or sport or both*. If you play more than one sport or instrument (or play both), please answer with respect to that activity which is most important to you.

Please indicate the sport or instrument which is most important to you: _____

❑ I do not play a sport or an instrument. (You may skip this section.)

Please circle the number that best describes your physical ability in the past week. Did you have any difficulty:

	NO DIFFICULTY	MILD DIFFICULTY	MODERATE DIFFICULTY	SEVERE DIFFICULTY	UNABLE
1. using your usual technique for playing your instrument or sport?	1	2	3	4	5
2. playing your musical instrument or sport because of arm, shoulder or hand pain?	1	2	3	4	5
3. playing your musical instrument or sport as well as you would like?	1	2	3	4	5
4. spending your usual amount of time practising or playing your instrument or sport?	1	2	3	4	5

SCORING THE OPTIONAL MODULES: Add up assigned values for each response; divide by 4 (number of items); subtract 1; multiply by 25.
An optional module score may <u>not</u> be calculated if there are any missing items.

Institute for Work & Health | Research Excellence Advancing Employee Health